Interference Mitigation in Multicell Networks

Von der Fakultät für Elektrotechnik und Informationstechnik
der Rheinisch–Westfälischen Technischen Hochschule Aachen
zur Erlangung des akademischen Grades
eines Doktors der Ingenieurwissenschaften
genehmigte Dissertation

vorgelegt von
Diplom–Ingenieur Guido Dartmann
aus Münster, Deutschland

Berichter: Universitätsprofessor Dr.-Ing. Gerd Ascheid
Universitätsprofessor Dr. Petri Mähönen

Tag der mündlichen Prüfung: 02.10.2013

Abstract

This thesis investigates the theoretical and algorithmic framework for intercell interference mitigation in multicell networks based on transmitter optimization. A problem in multiuser multicell communication systems is the unfair distribution of the achievable data rate. By the exchange of channel state information (CSI) and cooperation among base station antenna arrays max–min fairness can be achieved in the network. Especially in multicell networks, the CSI is out-dated very rapidly. Consequently, fast algorithms are required for the optimization.

The theory of the unicast max–min beamforming problem (MBP) in a single base station scenario with a single sum power constraint is well understood. Low complexity algorithms based on uplink–downlink duality exist. This thesis extends the duality framework of the single base station scenario to the multicell scenario where multiple heterogeneous power constraints are practically more relevant. Based on this duality, an algorithm with low complexity is developed. For the more general case of a multicast MBP, a dual problem, which can be solved efficiently, does not exists. However, this thesis presents an equivalent quasi-convex form of the multicast MBP for a special case of long-term CSI which is practically relevant. In addition to the quasi-convex form, a dual problem is also presented. While strong duality is not given in general, a duality-based algorithm finds near optimal solutions with better performance than conventional solutions based on convex relaxation.

Based on Multicast Beamforming, this work finally presented an adaptive approach for the global adjustment of the cell pattern of a multicellular network using globally available long-term channel statistics of users. Additionally, users in the network are selected based on instantaneous but local channel statistics.

A problem of unicast max–min beamforming (MBF) is a decreased sum rate performance in some cases. One reason is interference due to beam collisions. A formulation of an optimization problem to avoid these collisions is derived and its $\mathcal{NP}$-hardness is proved. Furthermore, this thesis presents several methods with polynomial complexity to find near optimal solutions for this problem. Another reason for an impairment of the sum rate in MMF systems are strongly shadowed users. To improve the sum rate of the MMF system, this thesis presents a solution based on one-way half-duplex relays.

Contents

Chapter 1

Introduction

In the field of wireless communication enormous progress has taken place in the last two decades. The development began in the early 90s with the 2nd generation of mobile communication called Global System for Mobile Communications (GSM), which was the first standardized wireless communication system. Due to a constantly growing number of subscribers, already at the end of the 90s, the transition to the next generation mobile communication system, called Universal Mobile Telecommunications System (UMTS), was initiated. At the beginning of this century the number of subscribers reached its maximum in developed countries.

Although the number of subscribers reached its maximum, the recent years have shown an enormous demand in data rate through wireless communication channels. Although the first wireless communication standards like GSM are primarily developed for mobile phoning, the demand in data rate for video or other multimedia applications and internet access grows dramatically, e.g., due to the development of smart phones.

The achievable rate in wireless systems is naturally limited by bandwidth; consequently, it is an expensive and limited resource in wireless systems. An efficient utilization of this resource is, therefore, very important. A measure for an efficient utilization of the bandwidth (spectrum) is the spectral efficiency [55].

Wireless networks are usually composed of so-called cells. Each cell covers an area with multiple subscribers.[1] The users within the cell are served by one or multiple (BS) antenna arrays. The resources, e.g., bandwidth or spatial resources, are limited. Consequently, resources must be reused. However, reusing resources in cellular networks results in interference among different sites which becomes a performance limiting factor. Interference concerns in particular users far away from their serving BS in the cell edge region. Cell edge users receive signals with a low power. Additionally, the received signal power of other BSs (interference power) is comparatively high. A performance measure determining the quality of the downlink signal received by users is the signal-to-interference-plus-noise ratio (SINR). The SINR is the ratio of the power of the useful signal divided by the power of the signals received from interfering BSs plus the noise power. In a cell, an unfair distribution of the SINRs arises if the interference of adjacent cells (intercell interference) can not be mitigated. Figure 1.1a depicts the SINR as a function of the location. Close to the cell center, the users will have a high SINR (red color). However, in the cell edge region (blue color) the SINR is very low. In addition to intercell interference also intracell interference can be regarded: users inside a cell are separated by orthogonal or semi-orthogonal

[1] Subscriber in a wireless network are often simply termed as user.

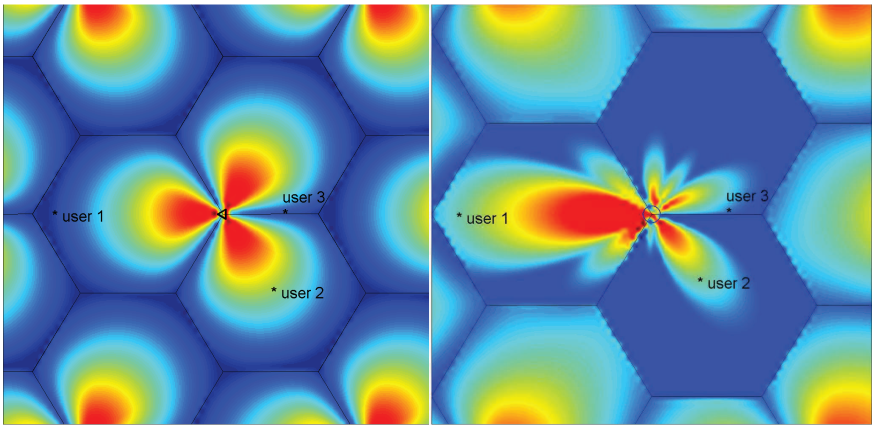

(a) Omnidirectional transmission. (b) Beamforming.

Figure 1.1: SINR as a function of the location. Warm colors (red/yellow) indicate high SINR, cold colors (green/blue) indicate low SINR.

resources. In the case of semi-orthogonal separation, intracell interference occurs as a performance limiting factor. To simplify the investigation in a multicell network, this thesis only focuses on intercell interference. Intracell interference is avoided by orthogonal frequency resources.

Increasing the spectral efficiency by reusing resources or using so-called semi-orthogonal resources results in interference. An unfair distribution of the performance among the users can be the consequence. Cooperative and adaptive technologies are required to mitigate interference.

Interference can be avoided by a smart assignment of temporal, frequency, orthogonal codes, or spatial resources. The first three resources are particularly considered in the wireless communication standards of the second and third generation. GSM considers frequency division multiple access (FDMA) to separate users by orthogonal frequency resources. Intercell interference is avoided by using different frequency bands in adjacent cells. Consequently, a low spectral efficiency was the result. The third generation uses orthogonal codes for a separation of users. However, the number of orthogonal codes is limited as well. In upcoming standards, a combination of different dimensions (frequency or time) is considered. The usage of multiple antennas in so-called antenna arrays at the BSs allows the exploitation of an additional dimension: the spatial domain. The ongoing standardizations Long-Term Evolution (LTE) and LTE advanced allow the usage of antenna arrays. So-called smart antennas allow the focusing of the transmit power in dedicated directions. This concept is called beamforming and enables separation of users in the spatial domain. Figure 1.1b shows the SINR as function of the location in the case of beamforming. Now user 1 and user 3 can achieve a higher SINR. Beamforming can be also categorized in orthogonal and semi-orthogonal approaches. Orthogonal beamforming results in a complete interference free transmission. However, as in other approaches, the orthogonal spatial directions are a limited resource. Semi-orthogonal beamforming is more flexible and enables other objective functions as max–min fairness or sum rate maximization. Interference mitigation with semi-orthogonal beamforming in a small domain, e.g., among a BS and multiple users, was deeply investigated in the last 15 years, e.g., [10]. This scenario is often termed as broadcast channel and is well understood. The goal for semi-orthogonal beamforming in a broadcast scenario is the mitigation of intracell interference. Different objective functions are possible: A famous approach is the minimization of the total transmit power where each user is guaranteed a so-called quality-of-service (QoS) SINR. However, the amplifiers of antenna arrays have power constraints. These constraints are given due to regulations or due to technical constraints. Therefore, the so-called max–min approach is practically more relevant. In this approach the BS is subject to a total power constraint and it is desired to maximize the SINR of the weakest users.

Furthermore, current wireless networks are heterogeneous because they consist of multiple, different BSs with different power constraints. An optimization of these heterogeneous networks based on beamforming is more complex due to heterogeneous power constraints.

1.1 Scope of the Thesis

Max-min fairness is important in wireless systems. In particular, in modern wireless networks, due to multiple wireless multimedia applications, customers desire a sufficient data rate at each location. By reason of the previous mentioned causes especially intercell interference leads to an unfair distribution of the SINR and, therefore, of the available data rates. A necessary technological step in wireless networks is cooperation among different stations, cells, or users. Cooperative multicell transmission enables mitigation of intercell interference and, therefore, fairness in multicell networks. This thesis aims to answer several questions emerging in this new field of research.

First of all, the downlink transmission can be separated into two different schemes:

- In a downlink unicast transmission, each user gets different contents.
- In a downlink multicast transmission several users, belonging to the same multicast group, receive the same content.

This thesis presents findings in both areas. Furthermore, the following key issues should be considered in the context of intercell interference mitigation:

- Heterogeneous power constraints
- Complexity and optimality of algorithms
- CSI assumptions
- Sum rate performance vs. max–min fairness

1.1.1 Heterogeneous Power Constraints

Beamforming algorithms and methods regarding the single cell unicast/broadcast scenario are well understood. However, a simple migration to a scenario with coordination is not straightforward. For example, in a heterogeneous multicell network each station, or each antenna is subject to a power constraint. Methods or algorithms regarding the unicast/broadcast[2] scenario consider a sum power constraint which is reasonable if only one BS is optimized. In a multicell network such an approach will lead to a network-wide power constraint which is practically not relevant.

1.1.2 Complexity and Optimality of Algorithms

Unicast max–min fair beamforming is a complex and non-convex optimization problem [54]. However, if a sum power constraint is given, efficient methods exist. A low complexity and fast converging algorithm becomes even more relevant in multicell scenarios, where the channel state information must be updated among multiple BSs. In optimization theory, a promising approach for those fast algorithms is based on the so-called uplink–downlink duality.

Furthermore, an optimization problem can be efficiently solved if it is quasi-convex or convex. The max–min beamforming problem with a sum power constraint has a dual problem which can be solved efficiently base on an eigenvalue decomposition. The question arises: Is there also a dual problem in the case of heterogeneous power constraints, e.g., per BS array power constraints, in the multicell scenario?

In addition to the complexity of the algorithms for the unicast max–min beamforming problem, the solution itself is not perfectly characterized. If a sum power constraint is used, a balanced SINR[3] among all jointly active users can be achieved. The question arises: Is this also always given in the case of per-station power constraints?

Another question regards the assignment of BSs to users. Distributed antenna arrays can increase the coverage of the BS. However, then an optimal assignment of antenna arrays to users must be determined. Does there exists a simple algorithm which jointly finds the beamforming weights and assignments of BSs to users?

1.1.3 CSI Assumptions

Multicell beamforming requires the channel state information of multiple BSs. Optimization approaches for the unicast/broadcast scenario are based on instantaneous channels. This is reasonable in this small scenario but challenging in a multicell scenario, due to the required frequent update of the instantaneous channel state information (CSI). The CSI must be transferred to a central unit or exchanged among all base stations. Consequently a very fast backhaul network is required if instantaneous CSI is used.

[2] Unicast/broadcast terms the information theoretic broadcast scenario which is different to the multicast/broadcast scenario where the same content is transmitted to multiple users.

[3] Balanced SINR means the SINR of all jointly scheduled users is equal.

Therefore, this thesis regards optimization based on the channel statistics in the form of spatial correlation information. This so-called long-term CSI is valid over the stationary interval of the channel which is much longer compared to the instantaneous CSI. In the case of instantaneous CSI, several equivalent quasi-convex forms are known but this equivalence is not given for long-term CSI in the form of spatial correlation knowledge.

1.1.4 Sum Rate Performance vs. Max–Min Fairness

Unicast max–min fair beamforming can achieve a balanced SINR among all jointly active users. However max–min fairness has the disadvantage that bad conditions for one users can decrease the performance of all jointly active users. For example, a beam collision can decrease the SINR of all jointly served users in the network. The question arises: Are there low complex solutions to avoid beam collisions and can an optimal solution be achieved with an polynomial algorithm? In addition to beam collisions shadowed users can decrease the performance of all jointly served users. Are there simple and low-cost possibilities to avoid shadowing and to increase the coverage in a multicell network with beamforming?

In future wireless networks, besides conventional unicast transmission, multicast services are considered as well. Famous examples are digital audio broadcasting (DAB) [49] and digital video broadcasting (DVB) [50]. The multicast beamforming can also be used for unicast transmission. For example the sector pattern of a cell can be adapted with multicast beamforming based on the spatial correlation information of all users inside this cell. The multicast max–min beamforming problem is $\mathcal{NP}$-hard in general. However, for special instances an equivalent quasi-convex form of the problem might exist. Furthermore, an unanswered question is, whether there exists a dual problem similar to the unicast case, or are there also further equivalent quasi-convex forms?

1.2 Structure of the Thesis

The questions of the previous section should be answered in a structured way. For a better understanding some fundamentals are required. Chapter 2 briefly illustrates the multicell scenario and introduces the data and signal models used in this thesis.

Several findings of this thesis are based on optimization theory. Chapter 3 presents a summary of all applied optimization theory. The theory of convex optimization is well known and several tutorials and textbooks exist. However, several findings of non-convex optimization problems are distributed in several mathematical publications. Chapter 3, therefore, concentrates on some new approaches regarding non-convex problems, such as quasi-convex or fractional programs.

The thesis is separated in two parts: The main part of this thesis considers unicast beamforming schemes and consists of the Chapters 4 5 and 6. The second part of the thesis focuses on multicast beamforming and consists of the Chapters 7 and 8.

The first chapter of each part presents basic theories and the last chapter presents applications.

Chapter 4 answers several questions regarding the theory of the unicast max–min beamforming problem. In particular, this chapter introduces a novel duality framework for the unicast max–min beamforming problem in heterogeneous networks with multiple power constraints. Based on the duality framework a low complexity algorithm with a fast convergence is derived and its near optimality is shown by numerical results.

Chapter 5 considers the beam collision problem which is one difficulty of the max–min fairness approach. To avoid beam collisions, this chapter defines the multicell beamscheduling problem and proves the $\mathcal{NP}$-hardness of the problem in the general N-cell scenario. In the $N \leq 2$-cell scenario this problem is proved to be optimally solvable with a polynomial time algorithm. Furthermore, several heuristics providing near optimal solutions for the general $N \geq 2$-cell are presented.

Chapter 6 presents a different approach to avoid a low balanced SINR in max–min fair systems. This Chapter considers relays to serve small cells which increases the coverage and, therefore, improves the performance of shadowed users in the network. If max–min fairness among the users is desired all users can gain from an improvement of a single link. Several beamforming and scheduling approaches for these heterogeneous networks are presented.

The second part only considers multicast beamforming and begins with Chapter 7. This chapter answers several questions regarding the theory of the multicast beamforming problem. An equivalent quasi-convex form for the case of long-term CSI in the form of Hermitian positive semidefinite Toeplitz matrix is presented. In addition to this equivalent quasi-convex form, this chapter presents a novel duality framework for the multicast beamforming problem similar to the duality framework of the unicast case. Based on this theory this chapter presents a low complexity algorithm which finds near optimal solutions.

Chapter 8 shows a practically relevant application of the multicast beamforming problem in a multicell scenario with a unicast transmission. Each base station optimizes the beamforming vector to cover all users inside a cell (multicast). Then, one of these users is scheduled based on local channel quality information. Hence, actually a unicast transmission is realized. This so-called sector pattern adaptation scheme results an adaptation of the sector pattern based on the available spatial correlation information of all active users in a network. Due to these low fluctuations of the beams this technique can be combined with channel aware scheduling methods. Furthermore, this chapter compares different unicast beamscheduling approaches with sector pattern adaptation and channel aware scheduling methods in a joint scenario.

Finally, Chapter 9 gives an overall summary of this thesis by answering the questions of Section 1.1.

1.3 Author's Contributions

This thesis is written as a monograph but it is based on the previous made publications:

- Chapter 4 is based on the previously published articles [37, 41].
- Chapter 5 is based on the previously published article [42].
- Chapter 6 is based on the previously published articles [46, 47].
- Chapter 7 is based on the previously published articles [35, 43].
- Chapter 8 is based in parts on the previously published articles [44, 45].

In addition to the above listed publictions, until April 2013, the author published the following publications [32–34, 36, 38–40].

1.4 Copyright

1.5 Notation

The main notations are given in the following table. Further details regarding the notations are presented in the glossary.

Table 1.1: Overview of the notations

$\mathbf{a}$	vector
$\mathbf{A}$	matrix
$[\mathbf{a}]_n$	nth element of a vector
$[\mathbf{A}]_{n,m}$	element with indices n, m of a matrix $\mathbf{A}$
$[\mathbf{A}]_{:,m}$	mth column vector of a matrix $\mathbf{A}$
$[\mathbf{A}]_{m,:}$	mth row vector of a matrix $\mathbf{A}$
$\mathbf{A}^H$	conjugate transpose of a matrix $\mathbf{A}$
$\mathbf{a}_k^t$	t and k denote indexes of vector
$\mathbf{I}_N$	identity matrix of dimension $N \times N$
$\lvert\mathcal{S}\rvert$	cardinality of a set $\mathcal{S}$
$\mathrm{diag}(\mathbf{A}_1, \ldots, \mathbf{A}_N)$	block-diagonal matrix of matrices $\mathbf{A}_i$ and $i = 1, \ldots, N$
$\succcurlyeq$	matrix inequality on a cone of nonnegative definite matrices
$\mathrm{Tr}(\mathbf{A})$	trace operation on a square matrix $\mathbf{A}$
LCM	lowest common multiple

Chapter 2

Scenario

2.1 Network Layout

A frequency reuse-1 factor is used in future wireless multicell networks to increase the spectral efficiency. As a performance limiting factor, intercell interference occurs in these networks. Especially cell edge users suffer from interference of adjacent BSs. Therefore, smarter technologies, e.g., beamforming or multiuser scheduling are required to mitigate interference. Interference can be mitigated locally at each BS or, more promisingly, globally by intercell interference coordination among different BSs. Figure 2.1 depicts an example of a multicell network. A set $\mathcal{S} = \{1, 2, 3, 4\}$ of $N = 4$ BSs transmit to a set $\mathcal{U} = \{1, 2, 3, 6, 8\}$ of $M = 6$ scheduled users. In this example BS $c = 1$ serves user $i = 1$. This link is marked by red color. All other links (blue) cause interference for user $i = 1$.

This section introduces the multicell multiuser scenario of this thesis which is focused on the downlink transmission from multiple BSs to multiple users. During the entire thesis the following assumptions are made:

- The multicell network uses frequency reuse-1 factor.
- Only downlink beamforming is investigated.
- The antennas at the BS arrays[1] are correlated.
- A multiple input single output (MISO) system is regarded. The BS has $N_A > 1$ antenna elements and each user is equipped with a single antenna.
- All channels are assumed to be constant over the regarded time slot [151].
- Long-term channel state information of all links is perfectly known and stationary over multiple time slots.
- The complex noise n_i is circularly symmetric Gaussian with zero-mean and a variance $\sigma_i^2 > 0$ and the system is interference dominated.
- In all simulation results the system is interference limited (dominated). This is a reasonable assumption especially for cell edge users.

[1] BS and BS array are often used in the same context. Note a BS may have multiple antenna arrays. Then BS array is the correct term.

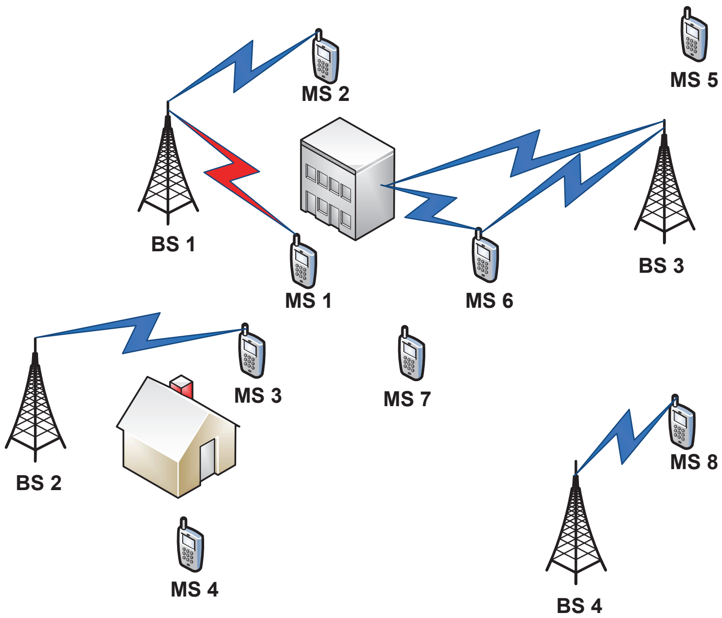

Figure 2.1: Example of a wireless network with 4 BSs and 8 mobile stations (MSs).

The received signal over the wireless channel is modeled by a summation of multiple path components caused by multiple reflections [7]. The result is a frequency selective channel. Multicarrier systems like orthogonal frequency division multiplexing (OFDM) [126] transform a frequency dispersive channel in multiple frequency flat channels [151]. Furthermore, these parallel frequency flat sub-channels are orthogonal[2], therefore, intra-cell interference can be avoided by a smart assignment of these orthogonal channels[3] to users. However, the number of carriers is limited and in a network with a frequency reuse-1, therefore, these carriers are reused in adjacent cells. Intercell interference is the result and especially cell edge users suffer interference. An unfair distribution of the achievable rate [151] of each user is the result.

A promising technology to mitigate interference is the use of multiple antennas at the BSs. A system with multiple antennas at the transmitter and a single antenna at the receiver is called MISO system. Using multiple antennas, each BS can focus the transmit signal in the desired direction, hence, unnecessary interference in other directions is avoided. A combination of MISO and OFDM is called MISO-OFDM [51, 105, 113, 138] and is depicted in Figure 2.2. Assuming there are M_C carriers, the transmit signal $s_i(m)$ transmitted from BS array $c(i)$ to user i on a carrier m is weighted by weights (beamforming weights), e.g. $\omega_{c(i)}(n, m)$. Each weighted signal is transmitted over an orthogonal channel $h_{c,i}(n, m)$ to the user. Let $\mathbf{h}_{c,i}(m) = [h_{c,i}(1, m), \ldots, h_{c,i}(N_A, m)] \in \mathbb{C}^{N_A \times 1}$ be the channel vector for the mth sub-

[2] assuming a perfect synchronization
[3] Each sub-channel is assigned to carrier.

carrier between BS c and user i and let $\boldsymbol{\omega}_c(m) = [\omega_c(1,m),\ldots,\omega_c(N_A,m)] \in \mathbb{C}^{N_A\times 1}$ be the precoding vector for the mth subcarrier, the received signal at user i on subcarrier m is:

$$r_{i,m} = \sum_{c=1}^{N} \mathbf{h}_{c,i}^{H}(m)\boldsymbol{\omega}_c(m)s_i(m) + n_i, \tag{2.1}$$

This thesis is focused on intercell interference. To simplify the signal model and for better presentation of the effects on intercell interference, intracell interference is eliminated by orthogonal subchannels. Intercell interference occurs by reusing the same subchannel in an adjacent cells. To simplify the notation in this thesis, the subchannel index m will be dropped from now on.

Definition 1. *The base band [151] channel vector between a BS c and a user i is presented by the vector* $\mathbf{h}_{c,i} = [h_{c,i}(1),\ldots,h_{c,i}(N_A)] \in \mathbb{C}^{N_A\times 1}$.

Given the definition of the channel vector $\mathbf{h}_{c,i}^{H} \in \mathbb{C}^{N_A\times 1}$, a user i receives the signals (desired signal and interference) of N BS arrays:

$$r_i = \sum_{c=1}^{N} \mathbf{h}_{c,i}^{H}\boldsymbol{\omega}_c s_i + n_i, \tag{2.2}$$

where n_i denotes additive noise with $\sigma_i^2 = \mathbb{E}\{|n_i|^2\} > 0$ and s_c is the symbol transmitted from BS array c.

2.2 CSI Assumption

In a system with a large number of subcarriers, transmit beamforming on each subcarrier independently results in a huge amount of required channel feedback [105]. Furthermore, in fast fading scenarios, an accurate knowledge is difficult to obtain even in a local (single cell) scenario [9]. In multicell scenarios with a centralized coordination an accurate knowledge of the instantaneous channel is even more challenging. A fast backhaul network is required then, otherwise the CSI is outdated at the network coordinating unit.

Due to the above mentioned reasons it is justified to use the so-called spatial correlation matrices of the channels. The spatial correlation matrices are also-called long-term CSI in this thesis. Assuming correlated antennas at each BS array, the long-term spatial correlation matrix is given by

$$\hat{\mathbf{R}}_{c,i} = \mathbb{E}_{\mathcal{H}}\{\mathbf{h}_{c,i}\mathbf{h}_{c,i}^{H}\}. \tag{2.3}$$

where $\mathbb{E}_{\mathcal{H}}\{\ \}$ denotes the expectation over the channel realizations $\mathcal{H}$. In time division duplex (TDD) systems the spatial correlation can be simply estimated from the uplink signal, since uplink and downlink share the same carrier frequencies. In frequency division duplex (FDD) systems, uplink and downlink are on separate carrier frequencies, therefore, estimation of the spatial correlation matrix is more challeng-

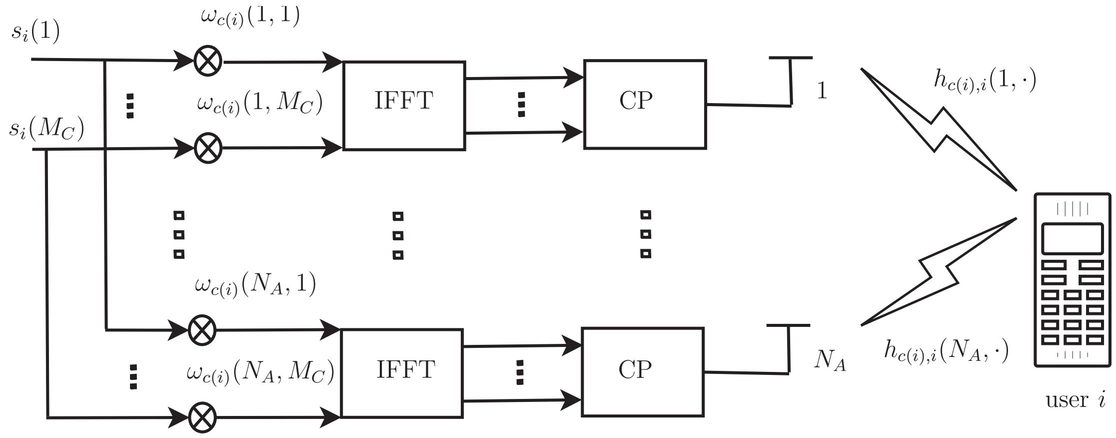

Figure 2.2: Blockdiagram of a MISO-OFDM system similar to [26].

ing. The user might estimate the downlink correlation and feed it back to the BS. A consequence would be an increased uplink load. However, in the literature, various methods are investigated to estimate the downlink correlation without explicit user feedback [74,80,81,104].

A special role have uniform linear arrays (ULAs). Considering a ULA with N_A antenna elements and an antenna spacing δ (and $d = \delta/\lambda$, where λ denotes the wave length) at the BS and letting $\mathbf{R}_{c,i} = \hat{\mathbf{R}}_{c,i}/\sigma_i^2$ and $\sigma_i^2 > 0$, the spatial correlation matrix is given by a Toeplitz matrix and can be decomposed as follows [1]:

$$\mathbf{R}_{c,i} = \mathbf{A}(\boldsymbol{\theta}_{c,i})\mathbf{P}_{c,i}\mathbf{A}(\boldsymbol{\theta}_{c,i})^H. \tag{2.4}$$

Using this notation, the spatial correlation is observed as a combination of N_P uncorrelated waves with directions of arrival given by $\boldsymbol{\theta}_{c,i} = [\theta_{c,i,1}, \dots, \theta_{c,i,N_P}]$ and path powers given by $\mathbf{P}_{c,i} = \text{diag}(q_{c,i,1}, \dots, q_{c,i,N_P}) \in \mathbb{R}^{N_P \times N_P}$. The matrix $\mathbf{A}(\boldsymbol{\theta}_{c,i}) = [\mathbf{a}(\theta_{c,i,1}), \dots, \mathbf{a}(\theta_{c,i,N_p})] \in \mathbb{C}^{N_A \times N_p}$ is a Vandermonde matrix containing the steering vectors:

$$\mathbf{a}(\theta_{c,i,p}) = [1, \exp(\zeta \sin(\theta_{c,i,p})), \dots, \exp(\zeta(N_A - 1)\sin(\theta_{c,i,p}))]^T, \ \zeta = j2\pi d. \tag{2.5}$$

The formulation of (2.4) can be rewritten as:

$$\mathbf{R}_{c,i} = \mathbf{A}(\boldsymbol{\theta}_{c,i})\mathbf{P}_{c,i}\mathbf{A}(\boldsymbol{\theta}_{c,i})^H = \sum_{p=1}^{N_P} q_{c,i,p}\mathbf{a}(\theta_{c,i,p})\mathbf{a}(\theta_{c,i,p})^H \tag{2.6}$$

with $\sum_{p=1}^{N_P} q_{c,i,p} = 1$. The matrix in (2.4) is a Hermitian positive semidefinite Toeplitz matrix which is a reasonable assumption if ULAs are used at the BSs [53,104]. Toeplitz matrices can be estimated perfectly when an infinite number of pilot sequences is given. Different methods exist to approximate the Toeplitz matrices, e.g., the method in [132].

Chapter 3

Optimization Theory

This Chapter summarizes theorems and fundamentals of optimization theory applied in the rest of this thesis. This chapter investigates constrained continuous problems.

Optimization theory is a broad topic and can be categorized in theory for convex and non-convex optimization problems. Section 3.2 summarizes several fundamentals of convex optimization theory. Convex problems have the advantage that an efficient algorithm can find a globally optimal solution. Section 3.3 gives a short summary for non-convex optimization problems. Non-convex problems do not have a unique optimal value in general. A polynomial algorithm will usually find only locally optimal solutions. Some non-convex problems are even $\mathcal{NP}$-hard. However, for some special non-convex problems an efficient algorithm can find a global optimal value. Examples for these problems are quasi-convex problems and some generalized fractional programs.

Beside the categorization in convexity and non-convexity, optimization problems are often categorized into continuous and discrete problems. The later ones appear in this thesis in the context of scheduling problems presented in Chapter 5. Some heuristics for the optimization of assignment problems are very useful for scheduling problems in the field of wireless communications.

In any optimization problem, the variables $\boldsymbol{x}$ can be defined over an Euclidian space denoted by $\mathbb{E}^n$. This Euclidian space can either be the space of real numbers $\mathbb{R}$ or the space of complex numbers $\mathbb{C}$ [108]. This thesis considers multiple optimization problems with complex or real variables; hence; the general Euclidian space is used in this section to broadern the scope of the theory.

The objective functions of this thesis are bounded $-\infty < f(\boldsymbol{x}) < \infty$ and the domain of the variables $\mathcal{X} \subset \mathbb{E}^n$ is assumed to be a closed set, hence, the objective function can attain its optimum and $\min_{\boldsymbol{x}\in\mathcal{X}} f(\boldsymbol{x})$ or $\max_{\boldsymbol{x}\in\mathcal{X}} f(\boldsymbol{x})$ can be used instead of $\inf_{\boldsymbol{x}\in\mathcal{X}} f(\boldsymbol{x})$ or $\sup_{\boldsymbol{x}\in\mathcal{X}} f(\boldsymbol{x})$. This is a valid assumption if the objective function is the, e.g., minimum signal-to-interference-plus-noise ratio (SINR) and the transmit power is limited.

3.1 Complex–Real Isomorphism

Various optimization problems of this thesis are based on complex valued optimization variables $\boldsymbol{X} \in \mathbb{C}^{n\times n}$. However, in multiple books about optimization theory, real variables $\boldsymbol{Y} \in \mathbb{R}^{n\times n}$ are used to simplify the investigations.

These complex variables can be transformed to real variables in a straight-forward way:

Definition 2. *Let $\boldsymbol{X} \in \mathbb{C}^{n\times n}$ be a complex valued matrix, the corresponding real vector $\boldsymbol{Y} \in \mathbb{R}^{2n\times 2n}$ can be obtained by the transformation [16]:*

$$\mathbf{Y} = \begin{bmatrix} \mathrm{Re}(\mathbf{X}) & -\mathrm{Im}(\mathbf{X}) \\ \mathrm{Im}(\mathbf{X}) & \mathrm{Re}(\mathbf{X}) \end{bmatrix} \tag{3.1}$$

If the variables are given by complex vectors $\boldsymbol{x} \in \mathbb{C}^n$, the following transformation to real vectors $\boldsymbol{y} \in \mathbb{R}^{2n}$ can be used.

Definition 3. *Let $\boldsymbol{x} \in \mathbb{C}^n$ be a complex valued vector, the corresponding real vector $\boldsymbol{y} \in \mathbb{R}^{2n}$ can be obtained by the transformation [16]:*

$$\boldsymbol{y} = \begin{bmatrix} \mathrm{Re}(\boldsymbol{x}) \\ \mathrm{Im}(\boldsymbol{x}) \end{bmatrix} \tag{3.2}$$

Theorem 1. *The transformation* (3.1) *is an isomorphism between a subspace of $\mathbb{R}^{2n\times 2n}$ and $\mathbb{C}^{n\times n}$.*

Proof. A proof is presented in [123]. □

Isomorphism is a useful property in mathematics. Two isomorphic objects have the same properties. If there exists an isomorphism between a "new" field of mathematics and a very well understood field of mathematics, then this isomorphism allows to apply many available methods, theorems, and algorithms of the well understood field of mathematics in the "new" field of mathematics.

The isomorphic transformation (3.1) preserves any operation as, addition, subtraction, multiplication, and inversion [16]. If $\mathbf{X}$ is Hermitian, then $\mathbf{Y}$ is symmetric and if $\mathbf{X}$ is positive semidefinite, the same holds for $\mathbf{Y}$.

This thesis often presents vector–matrix–vector products as $\boldsymbol{x}^H\boldsymbol{X}\boldsymbol{x}$ with $\boldsymbol{x} \in \mathbb{C}^n$ and $\boldsymbol{X} \in \mathbb{C}^{n\times n}$. Let $\boldsymbol{y} \in \mathbb{R}^{2n}$ and $\boldsymbol{Y} \in \mathbb{R}^{2n\times 2n}$, with Definitions 2 and 3 and Theorem 1, $\boldsymbol{x}^H\mathbf{X}\boldsymbol{x} = \boldsymbol{y}^T\mathbf{Y}\boldsymbol{y}$ holds.

3.2 Convex Optimization

Convex optimization problems have the elegant property that an efficient algorithm can find the global optimum if its domain is a closed convex set [15]. A convex maximization problem consists of a concave objective function and convex constraints. A concave function is formally defined by the following Definition:

Definition 4. *A function $f : \mathcal{X} \subset \mathbb{E}^n \to \mathbb{R}$ is concave if the domain $\mathcal{X}$ of f is a convex set, and if for all $\boldsymbol{x}, \boldsymbol{y} \in \mathcal{X}$, and for all $\theta \in [0, 1]$*

$$f(\theta\boldsymbol{x} + (1-\theta)\boldsymbol{y}) \geq \theta f(\boldsymbol{x}) + (1-\theta)f(\boldsymbol{y}) \tag{3.3}$$

holds.

Correspondingly, a convex function is defined by:

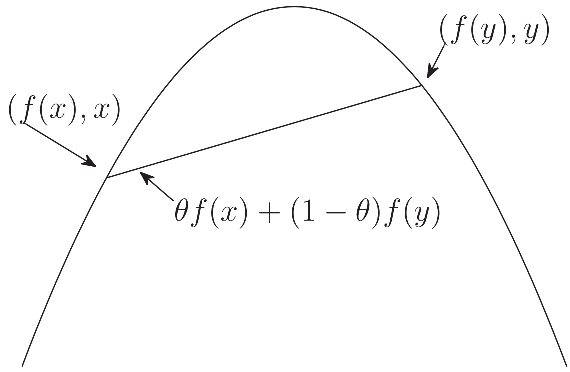

Figure 3.1: Example of a concave function.

Definition 5. *[15] A function $f : \mathcal{X} \subset \mathbb{E}^n \to \mathbb{R}$ is convex if the domain $\mathcal{X}$ of f is a convex set, and if for all $\boldsymbol{x}, \boldsymbol{y} \in \mathcal{X}$, and for all $\theta \in [0, 1]$*

$$f(\theta \boldsymbol{x} + (1-\theta)\boldsymbol{y}) \leq \theta f(\boldsymbol{x}) + (1-\theta) f(\boldsymbol{y}) \tag{3.4}$$

holds.

Definition 4 is illustrated in Figure 3.1. The figure shows an example of a concave function, where any line segment between two points of this function is below the function. Such a function has a unique global maximum value.

Definition 6. *Let $\mathcal{X}$ be a closed convex set of $\mathbb{E}^n$ and $f : \mathcal{X} \subset \mathbb{E}^n \to \mathbb{R}$ be a concave function, and all $g_i : \mathcal{X} \subset \mathbb{E}^n \to \mathbb{R}\ \forall i = 1, \ldots, m$, be convex functions, a convex maximization problem with the optimization variable $\boldsymbol{x} \in \mathcal{X} \subset \mathbb{E}^n$ in its standard form is given by*

$$\begin{aligned} t_0 = &\max_{x \in \mathcal{X}} f(\boldsymbol{x}) \\ &\text{s.t. } g_i(\boldsymbol{x}) \leq 0\ \forall i = 1, \ldots, m. \end{aligned} \tag{3.5}$$

Definition 7. *[15] Let $\mathcal{X}$ be a closed set of $\mathbb{E}^n$ and $f : \mathcal{X} \subset \mathbb{E}^n \to \mathbb{R}$ be a convex function, and all $g_i : \mathcal{X} \subset \mathbb{E}^n \to \mathbb{R}\ \forall i = 1, \ldots, m$, be convex functions, a convex minimization problem with the optimization variable $\boldsymbol{x} \in \mathcal{X} \subset \mathbb{E}^n$ in its standard form is given by*

$$\begin{aligned} t_0 = &\min_{x \in \mathcal{X}} f(\boldsymbol{x}) \\ &\text{s.t. } g_i(\boldsymbol{x}) \leq 0\ \forall i = 1, \ldots, m. \end{aligned} \tag{3.6}$$

Throughout this thesis the domain dom() of an optimization problem is defined as:

$$\mathcal{X} = \text{dom}(f) \cap \bigcap_{i=1}^{m} \text{dom}(g_i). \tag{3.7}$$

Furthermore, the domain $\mathcal{X}$ is assumed to be non-empty, closed, and convex. The following part of this section presents a compact summary of well known convex optimization programs, as linear programming, semidefinite programming, and second order cone programming. These problems also appear in this thesis in different chapters. A linear problem is a special convex problem where the objective function and the constraint functions are all linear functions.

Definition 8. *[15] **(Linear Program)** A convex optimization problem according to Definition 6 or 7 is called a linear program (LP) if the objective function $f(\boldsymbol{x}) = \boldsymbol{f}^T\boldsymbol{x}$ is a linear function with $\boldsymbol{f} \in \mathbb{R}^n$ and the constraints are affine functions $g_i(\boldsymbol{x}) = \boldsymbol{g}_i^T\boldsymbol{x} + d_i$ with vectors $\boldsymbol{g}_i \in \mathbb{R}^n$ and constants $b_i \in \mathbb{R}\ \forall i = 1, \ldots, m$.*

The feasible set of a linear program is a polyhedron and the optimum, if it exists, is attained at a vertex of this polyhedron. An efficient algorithm can find this optimal solution in polynomial time. Linear programs appear in this thesis in the context of power control problems, e.g, the multicast power control problem in Chapter 7. Definition 8 holds for maximization problems as well as for minimization problems. A generalization is a so-called second order cone problem.

Definition 9. *[15] **(Second Order Cone Program)** A convex optimization problem according to Definition 6 or 7 is called a second order cone problem (SOCP) if the objective function $f(\boldsymbol{x}) = \boldsymbol{f}^T\boldsymbol{x}$ is a linear function with $\boldsymbol{f} \in \mathbb{R}^n$ and the constraint functions $g_i(\boldsymbol{x}) = ||\mathbf{A}_i\boldsymbol{x} + \boldsymbol{b}_i|| - \boldsymbol{c}_i^T\boldsymbol{x} - d_i$, with vectors $\boldsymbol{c}_i \in \mathbb{R}^n$, $\boldsymbol{b}_i \in \mathbb{R}^n$, matrices $\mathbf{A}_i \in \mathbb{R}^{m\times n}$, and constants $d_i \in \mathbb{R}\ \forall i = 1, \ldots, m$, implying second order cone constraints.*

Second order cone problems appear in this thesis in Section 4.3.3. The most general form of a convex optimization problem in this thesis is given by a semidefinite program. A semidefinite program is defined in this thesis on Hermitian positive semidefinite matrices. The set of Hermitian positive semidefinite matrices $\mathcal{P} = \{\mathbf{X} \in \mathbb{C}^{n\times n} \mid \mathbf{X} = \mathbf{X}^H \succeq 0\}$ is convex.

Definition 10. *[15] **(Semidefinite Program)** Let $\boldsymbol{x} = \mathrm{vec}(\mathbf{X})$[1] and $\mathbf{X} \in \mathcal{P}$, a convex optimization problem according to Definition 6 or 7 is called a semidefinite program (SDP) if the objective function $f(\boldsymbol{x}) = \mathrm{Tr}\{\mathbf{C}\mathbf{X}\}$ is a general linear function with $\mathbf{C} \in \mathbb{R}^{n\times n}$ and the constraint functions are given by $g_i(\boldsymbol{x}) = \mathrm{Tr}\{\mathbf{A}_i\mathbf{X}\} - d_i$, with symmetric matrices $\mathbf{A}_i \in \mathbb{R}^{n\times n}$ and constants $d_i \in \mathbb{R}\ \forall i = 1, \ldots, m$.*

SDPs are a well known method to solve beamforming problems. Several nonconvex beamforming problems can be relaxed to SDPs. In this thesis SDPs are used in several sections, e.g., Section 4.3.1.

3.2.1 Lagrange Duality

Several technical problems are difficult to solve in the primal representation. Multiple problems appear non-convex in the primal representation. However, all problems can be relaxed to a so-called Lagrangian dual problem which is convex in the Lagrangian dual variables. Hence, such a dual problem can be efficiently solved.

However, a Lagrangian dual problem provides only a lower bound, if the primal problem is a minimization problem, or an upper bound, if the original problem is

[1] $\mathrm{vec}(\mathbf{X})$ denotes the vectorized version of a matrix $\mathbf{X}$ given by the stacked column vectors.

a maximization problem. In special cases, e.g., if the primal problem is convex and strictly feasible, the value of a Lagrangian dual solution is equal to the value of the primal solution.

In most optimization problems, the constraints cause difficulties in solving the primal problem. These constraints are weighted by Lagrangian dual variables and subtracted from the objective function in the case of a maximization problem. Hence, the concept of Lagrangian duality can be understood as a relaxation.

In what follows, the primal problems (3.5) and (3.6) can also be non-convex. The theory of Lagrangian duality is well known and summarized in [15]. Some of these definitions and Lemmas are introduced here for the minimization as well as for maximization.

Definition 11. *The Lagrangian* $L : \mathcal{X} \subset \mathbb{E}^n \times \mathbb{R}^m \to \mathbb{R}$ *of a maximization problem* (3.5) *defined as: Let* $\boldsymbol{\mu} \in \mathbb{R}^m_+$ *be the vector of so-called Lagrangian dual variables, and let* $\mathbf{g}(\boldsymbol{x}) = [g_1(\boldsymbol{x}), \ldots, g_m(\boldsymbol{x})]^T$ *denote the vector of the constraints functions, the Lagrangian is given by*

$$L(\boldsymbol{x}, \boldsymbol{\mu}) = f(\boldsymbol{x}) - \boldsymbol{\mu}^T \mathbf{g}(\boldsymbol{x}). \tag{3.8}$$

The Lagrangian dual function is then given by

$$l(\boldsymbol{\mu}) = \sup_{x \in \mathcal{X}} L(\boldsymbol{x}, \boldsymbol{\mu}). \tag{3.9}$$

Lemma 1. *The Lagrangian dual function* $l(\boldsymbol{\mu})$ *is an upper bound of the primal problem* (3.5).

Proof. Let $\boldsymbol{x}^*$ be feasible in (3.5), obviously $f(\boldsymbol{x}^*) \leq L(\boldsymbol{x}^*, \boldsymbol{\mu})$. Consequently, $f(\boldsymbol{x}^*) \leq L(\boldsymbol{x}^*, \boldsymbol{\mu}) \leq \sup_{x \in \mathcal{X}} L(\boldsymbol{x}, \boldsymbol{\mu}) = l(\boldsymbol{\mu})$ holds. □

The Lagrangian dual problem of the primal maximization problem aims to find the tightest of these upper bounds:

Definition 12. *Let* $\boldsymbol{\mu} \in \mathbb{R}^n_+$*, the Lagrangian dual problem is defined as* $d = \min_{\boldsymbol{\mu}} l(\boldsymbol{\mu})$.

In general, so-called weak duality $d \geq t_0$ holds [15].

Definition 13. *The Lagrangian* $L : \mathbb{E}^n \times \mathbb{R}^m \to \mathbb{R}$ *of a minimization problem* (3.6) *is defined as: Let* $\boldsymbol{\mu} \in \mathbb{R}^m_+$ *be the vector of so-called Lagrangian dual variables, and let* $\mathbf{g}(\boldsymbol{x}) = [g_1(\boldsymbol{x}), \ldots, g_m(\boldsymbol{x})]^T$ *denote the vector of the constraints functions, the Lagrangian is given by*

$$L(\boldsymbol{x}, \boldsymbol{\mu}) = f(\boldsymbol{x}) + \boldsymbol{\mu}^T \mathbf{g}(\boldsymbol{x}). \tag{3.10}$$

The Lagrangian dual problem is then given by

$$l(\boldsymbol{\mu}) = \inf_{x \in \mathcal{X}} L(\boldsymbol{x}, \boldsymbol{\mu}). \tag{3.11}$$

Lemma 2. *The Lagrangian dual function* $l(\boldsymbol{\mu})$ *is a lower bound of the primal problem* (3.6).

Proof. Let $\boldsymbol{x}^*$ be feasible in (3.6), obviously $f(\boldsymbol{x}^*) \geq L(\boldsymbol{x}^*, \boldsymbol{\mu})$. Consequently, $f(\boldsymbol{x}^*) \geq L(\boldsymbol{x}^*, \boldsymbol{\mu}) \geq \inf_{x \in \mathcal{X}} L(\boldsymbol{x}, \boldsymbol{\mu}) = l(\boldsymbol{\mu})$ holds. □

The Lagrangian dual problem of the primal minimization problem aims to find the tightest of these lower bounds:

Definition 14. *Let $\boldsymbol{\mu} \in \mathbb{R}_{+}^{n}$, the Lagrangian dual problem is defined as $d = \max_{\boldsymbol{\mu}} l(\boldsymbol{\mu})$.*

In the case of a minimization, weak duality $d \leq t_0$ holds.

Given special conditions (Slater conditions) even so-called strong duality $d = t_0$ holds. This is satisfied if, e.g., the primal problem is convex. In addition, strong duality is even given for some special non-convex problems.

The concept of Lagrangian duality is used in this thesis in several sections, e.g, in Chapter 4. The concept of Lagrangian duality is extended in Section 3.3.2 to a more general duality concept, termed surrogate duality. Surrogate duality yields tighter bounds compared to the Lagrangian duality.

3.2.2 Convex Optimization with Finite Autocorrelation Sequences

Several non-convex optimization problems can be solved with an equivalent convex problem. The optimization variables are replaced by new optimization variables allowing an equivalent convex representation of the original non-convex problem.

Variables of some non-convex optimization problems can be sometimes represented as finite autocorrelation sequences (FASs). A representation of the original problem by using FASs leads to an equivalent convex problem. The idea of convex optimization with FASs is introduced in the work [4] and is based on the following definitions [4]:

Definition 15. *[4] $\mathbf{E}^k$ denotes the kth power of the matrix $\mathbf{E}$ where $\mathbf{E}$ has zero entries except on the 1st lower subdiagonal where it has only ones.*

In [4] the following definition is introduced:

Definition 16. *With the shift matrix $\mathbf{E}^k$, the autocorrelation sequence is defined by*

$$x(k) = \boldsymbol{u}^H \mathbf{E}^k \boldsymbol{u} = \mathrm{Tr}\{\mathbf{E}^k \boldsymbol{u}\boldsymbol{u}^H\}, \tag{3.12}$$

$k \in \{0, \ldots, n-1\}$ with vectors $\boldsymbol{u} \in \mathbb{C}^{n \times 1}$. The matrix $\mathbf{E}^k$ has zeros everywhere, except on the k-th subdiagonal.

Equation (3.12) is non-convex because of the rank-1 $\boldsymbol{U} = \boldsymbol{u}\boldsymbol{u}^H$ constraint. Remarkably, the same set as in the definition of the FAS given by (3.12) can be described with a relaxed rank-1 constraint.

Lemma 3. *[4] Using some positive semidefinite matrix $\mathbf{U} \succeq 0$ such that*

$$\hat{x}(k) = \mathrm{Tr}\{\mathbf{E}^k \boldsymbol{U}\}, \;\; k = 0, ..., n-1, \tag{3.13}$$

the above equation describes the same set as

$$x(k) = \boldsymbol{u}^H \mathbf{E}^k \boldsymbol{u} = \mathrm{Tr}\{\mathbf{E}^k \boldsymbol{u}\boldsymbol{u}^H\}.$$

Proof. The proof is presented in [4, Appendix A]. □

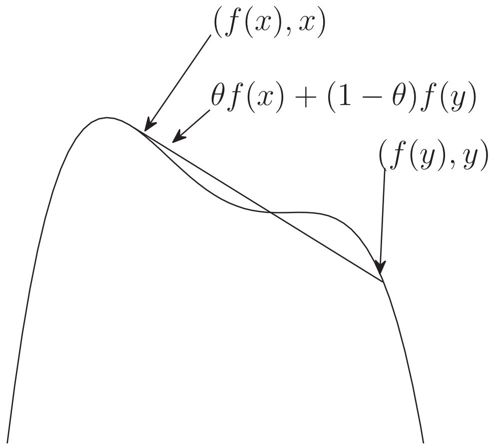

Figure 3.2: Example of a non-concave (quasi-concave) function.

This thesis uses convex optimization with FASs in Section 7.3.1 to find an equivalent quasi-convex form for the non-convex multicast max–min beamforming problem.

3.3 Non-Convex Optimization

In the case of a convex optimization problem efficient algorithms can find the globally optimal value if the objective function is bounded and its domain is compact. However, many technical problems are non-convex. A non-convex minimization problem has a non-convex objective function or non-convex constraints or both. A non-concave maximization problem has a non-concave objective function. This thesis considers non-convex optimization problems with a non-convex objective function and convex constraints. Figure 3.2 depicts a non-concave function; in contrast to Fig. 3.1 the line segment can be also "above" the function.

3.3.1 Quasi-Convex Optimization

A special case of non-convex problems are the quasi-convex optimization problems. A quasi-convex function is defined by its lower level sets:

Definition 17. *[15] A function $f : \mathcal{X} \subset \mathbb{E}^n \to \mathbb{R}$ defined on a convex set $\mathcal{X}$ is quasi-convex if every lower level set*

$$\mathcal{S}_\alpha = \{\boldsymbol{x} \in \mathcal{X} : \ f(\boldsymbol{x}) < \alpha\} \tag{3.14}$$

of $f(\boldsymbol{x})$ is convex for every value of α.

Similarly, a quasi-concave function is defined by its upper level sets:

Definition 18. *[15] A function $f : \mathcal{X} \subset \mathbb{E}^n \to \mathbb{R}$ defined on a convex set $\mathcal{X}$ is quasi-concave if every upper level set*

$$\mathcal{S}_\alpha = \{\boldsymbol{x} \in \mathcal{X} : \ f(\boldsymbol{x}) > \alpha\} \tag{3.15}$$

of $f(\boldsymbol{x})$ is convex for every value of α.

Figure 3.2 shows an example of a quasi-concave function. In contrast to a concave function the line segment can also be “above” the function. Based on these definitions a, e.g., quasi-convex maximization problem is defined by

Definition 19. *Let $f : \mathcal{X} \subset \mathbb{E}^n \to \mathbb{R}$ be a quasi-concave function and all $g_i : \mathcal{X} \subset \mathbb{E}^n \to \mathbb{R}$ are convex, then the problem*

$$\begin{aligned} t_0 = \max_{\boldsymbol{x}\in\mathcal{X}} \quad & f(\boldsymbol{x}) \\ s.t. \quad & g_i(\boldsymbol{x}) \leq 0 \; \forall i = 1, \ldots, m \end{aligned} \tag{3.16}$$

is called quasi-convex.

Analogously, a quasi-convex minimization problem is defined by

Definition 20. *Let $f : \mathcal{X} \subset \mathbb{E}^n \to \mathbb{R}$ be a quasi-convex function and all $g_i : \mathcal{X} \subset \mathbb{E}^n \to \mathbb{R}$ are convex, then the problem*

$$\begin{aligned} t_0 = \min_{\boldsymbol{x}\in\mathcal{X}} \quad & f(\boldsymbol{x}) \\ s.t. \quad & g_i(\boldsymbol{x}) \leq 0 \; \forall i = 1, \ldots, m \end{aligned} \tag{3.17}$$

is called quasi-convex.

A quasi-convex optimization problem has a global and unique optimum. As shown in [15], a quasi-convex optimization problem can be solved by a bisection over a set of convex representations of the quasi-convex objective function. A quasi-convex(concave) function $f : \mathcal{X} \subset \mathbb{E}^n \to \mathbb{R}$ is defined by its lower(upper) level sets as in Definition 17 (Definition 18). The family of convex functions of a quasi-convex function is defined by $\phi_t : \mathcal{X} \subset \mathbb{E}^n \to \mathbb{R}$ with:

$$f(\boldsymbol{x}) \leq t \;\Leftrightarrow\; \phi_t(\boldsymbol{x}) \leq 0. \tag{3.18}$$

With this family of convex functions, the quasi-convex minimization problem (3.17) can be solved by the following feasibility check problem [15]:

$$\begin{aligned} \text{find} \quad & \boldsymbol{x} \\ \text{s.t.} \quad & \phi_t(\boldsymbol{x}) \leq 0 \\ & g_i(\boldsymbol{x}) \leq 0 \; \forall i = 1, \ldots, m. \end{aligned} \tag{3.19}$$

The problem (3.19) is convex. If the problem (3.19) is feasible the quasi-convex objective function satisfies $f(\boldsymbol{x}) \leq t$. If the problem is infeasible, then $t_0 \geq t$. This observation leads to a bisection algorithm [15]. A bisection algorithm for the maximization problem can be derived correspondingly. Algorithm 1 can iterate arbitrary tightly to the global optimum until a precision of ϵ.

Algorithm 1 Bisection algorithm for quasi-convex problems [15]

given $l \leq t_0$, $u \geq t_0$, accuracy $\epsilon > 0$
repeat
  $m := (l + u)/2$
  Solve problem (3.19)
  if problem (3.19) is feasible **then**
    $u := m$
  else
    $l := m$
  end if
until $(u - l) \leq \epsilon$
return x, m

3.3.2 Surrogate Duality

The previous section describes a simple way to solve a quasi-convex problem, e.g., (3.17) by its feasibility check problem (3.19). However, similar to convex optimization, also for quasi-convex problems dual problems, satisfying strong duality, are known.

In the literature, multiple publications for the duality beyond convex duality exist and several dual problems are proposed. The framework of surrogate duality is a generalization. The idea of surrogate duality is the combination of multiple constraints to a single constraint. In this thesis this idea leads to a simple method for the multicell max–min beamforming problem with multiple per-antenna power constraints (see Chapter 4). Strong duality was so far only proved for the case of a single constraint.

For special non-convex problems, e.g., quasi-convex problems, the surrogate dual provides a tight bound. Regard the maximization problem (3.16).

Definition 21. *Let $f : \mathcal{X} \subset \mathbb{E}^n \to \mathbb{R}$ [2] be an arbitrary objective function, let $g_i : \mathcal{X} \subset \mathbb{E}^n \to \mathbb{R}$ be an arbitrary constraint function, let $\boldsymbol{\mu} \in \mathbb{R}_+^m$ be the vector of surrogate variables, and let $\mathbf{g}(\boldsymbol{x}) = [g_1(\boldsymbol{x}), \ldots, g_m(\boldsymbol{x})]^T$ denote the vector of the constraints functions, [107, 117] proposed a solution based on a so-called surrogate dual function*

$$s(\boldsymbol{\mu}) = \max_{x \in \mathcal{X}} \quad f(\boldsymbol{x}) \qquad \text{s.t.} \quad \boldsymbol{\mu}^T \mathbf{g}(\boldsymbol{x}) \leq 0, \;\; \mu_i \geq 0 \;\; i = 1, \ldots, m. \tag{3.20}$$

Let

$$\mathcal{F}(\boldsymbol{\mu}) = \{\boldsymbol{x} \in \mathcal{X} \mid \boldsymbol{\mu}^T \mathbf{g}(\boldsymbol{x}) \leq 0\} \tag{3.21}$$

be the feasible region of $s(\boldsymbol{\mu})$, and let

$$\mathcal{F} = \{\boldsymbol{x} \in \mathcal{X} \mid g_i(\boldsymbol{x}) \leq 0, \; \forall i = 1, \ldots, m\} \tag{3.22}$$

[2] The objective function must not be necessarily quasi-concave.

be the feasible region of (3.16), weak duality,

$$t_0 \leq s(\boldsymbol{\mu}), \tag{3.23}$$

holds, due to $\mathcal{F} \subseteq \mathcal{F}(\boldsymbol{\mu})$. Hence, (3.20) provides an upper bound.

Example 1. *Regard the simple example of an objective function over* $\boldsymbol{x} = [x_1, x_2]^T \in \mathbb{R}^2$

$$f(\boldsymbol{x}) = x_1^3 + x_2^3. \tag{3.24}$$

The function is depicted in Fig. 3.3. Let the optimization problem be

$$\begin{aligned} t_0 = \max_{\boldsymbol{x}} \quad & f(\boldsymbol{x}) \\ \text{s.t.} \quad & x_1 \leq 1, \\ & x_2 \leq 1. \end{aligned} \tag{3.25}$$

The maximal value for the given constraints is $t_0 = 2$ *at* $\boldsymbol{x} = [1, 1]^T$. *Let* $\boldsymbol{\mu} = [\mu_1, \mu_2]^T \in \mathbb{R}_+^2$ *be a non-negative vector, the surrogate function of problem* (3.25) *is:*

$$\begin{aligned} s(\boldsymbol{\mu}) = \max_{\boldsymbol{x}} \quad & f(\boldsymbol{x}) \\ \text{s.t.} \quad & \mu_1(x_1 - 1) + \mu_2(x_2 - 1) \leq 0 \end{aligned} \tag{3.26}$$

Figure 3.4 depicts the lines $\mu_1(x_1 - 1) + \mu_2(x_2 - 1) = 0$ *for different values* $\mu_1, \mu_2 \geq 0$ *Finally, Fig. 3.5 depicts the values of the surrogate function* $s(\boldsymbol{\mu})$. *As it can be observed from Figures 3.3, 3.4, and 3.5, the feasible set* $\mathcal{F}(\boldsymbol{\mu})$ *of* $s(\boldsymbol{\mu})$ *is larger than the feasible set* $\mathcal{F}$ *of* (3.25). *Obviously, weak duality holds*

$$t_0 \leq s(\boldsymbol{\mu}). \tag{3.27}$$

Definition 22. *A function* $f : \mathcal{X} \subset \mathbb{E}^n \to \mathbb{R}$ *is upper semicontinous at* $\boldsymbol{x}_0$ *if there exists the limes superior*

$$\limsup_{\boldsymbol{x} \to \boldsymbol{x}_0} f(\boldsymbol{x}) \leq f(\boldsymbol{x}_0). \tag{3.28}$$

Definition 23. *A function* $f : \mathcal{X} \subset \mathbb{E}^n \to \mathbb{R}$ *is lower semicontinous at* $\boldsymbol{x}_0$ *if there exists the limes inferior*

$$\liminf_{\boldsymbol{x} \to \boldsymbol{x}_0} f(\boldsymbol{x}) \geq f(\boldsymbol{x}_0). \tag{3.29}$$

Luenberger proved the following theorem:

Theorem 2. *[107] Let* $f : \mathcal{X} \subset \mathbb{E}^n \to \mathbb{R}$ *be a quasi-concave lower semi-continuous*[3] *objective function and let all* $g_i : \mathcal{X} \subset \mathbb{E}^n \to \mathbb{R}$ *be convex, assume that* $t_0 = \sup_{\boldsymbol{x} \in \mathcal{X}} \{f(\boldsymbol{x}) : \mathbf{g}(\boldsymbol{x}) \leq \mathbf{0}\}$ *is finite. Then,* $t_0 = \min_{\boldsymbol{\mu}} \{s(\boldsymbol{\mu})\}$, *where the minimum is achieved for some* $\boldsymbol{\mu} \geq \mathbf{0}$.

[3] "Along lines, e.g., every concave function is lower semi-continuous along lines" [107].

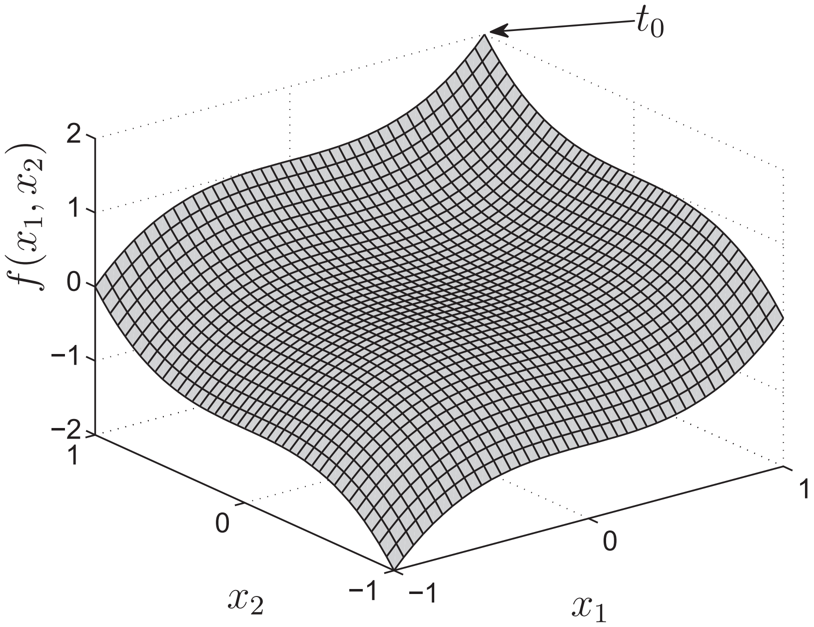

Figure 3.3: Example of a function.

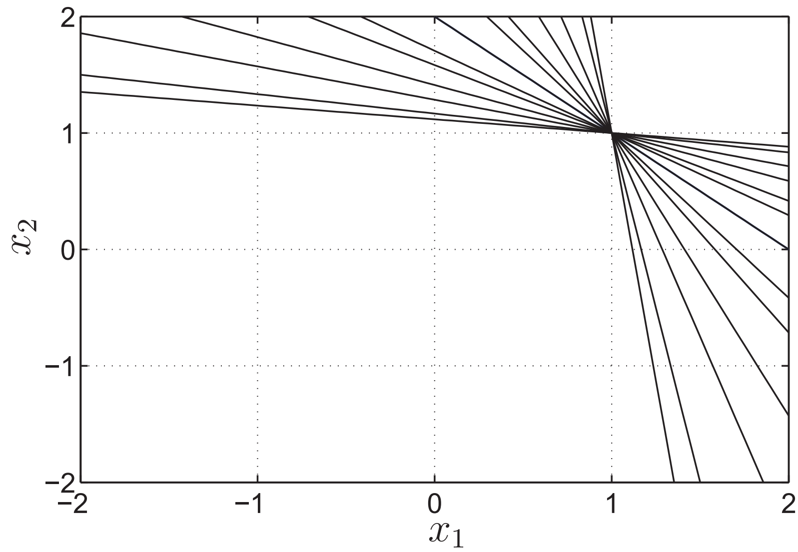

Figure 3.4: The constraint for different values of μ_1 and μ_2.

Definition 24. *In the case of a minimization problem [117]* (3.17) *with an arbitrary objective function $f : \mathcal{X} \subset \mathbb{E}^n \to \mathbb{R}$, convex constraints $g_i : \mathcal{X} \subset \mathbb{E}^n \to \mathbb{R}$, the surrogate dual function of D. Luenberger [107] is given by*

$$s(\boldsymbol{\mu}) = \min_{\boldsymbol{x} \in \mathcal{X}} \quad f(\boldsymbol{x}) \tag{3.30}$$

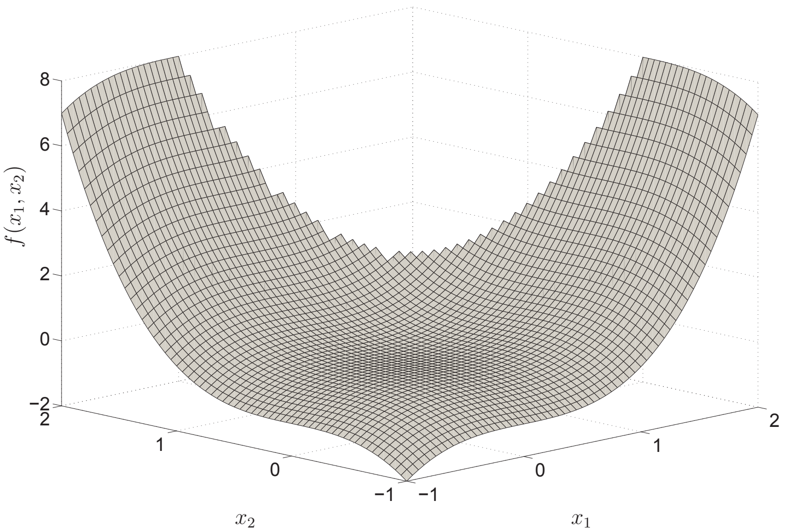

Figure 3.5: The objective function constrained by $\boldsymbol{\mu}^T \mathbf{g}(\boldsymbol{x})$ for a given vector $\boldsymbol{\mu}$.

$$s.t. \quad \boldsymbol{\mu}^T \mathbf{g}(\boldsymbol{x}) \leq 0, \;\; \mu_i \geq 0 \;\; i = 1, \ldots, m.$$

Correspondingly, to the maximization, weak duality

$$t_0 \geq s(\boldsymbol{\mu}), \tag{3.31}$$

always holds. In the case of a minimization the surrogate function provides a lower bound.

Theorem 3. *[107] Let $f : \mathcal{X} \subset \mathbb{E}^n \to \mathbb{R}$ be a quasi-convex upper semi-continuous*[4] *objective function and let all $g_i : \mathcal{X} \subset \mathbb{E}^n \to \mathbb{R}$ be convex, assume that $t_0 = \inf_{\boldsymbol{x} \in \mathcal{X}} \{f(\boldsymbol{x}) : \mathbf{g}(\boldsymbol{x}) \leq \mathbf{0}\}$ is finite. Then, $t_0 = \max_{\boldsymbol{\mu}} \{s(\boldsymbol{\mu})\}$, where the maximum is achieved for some $\boldsymbol{\mu} \geq \mathbf{0}$.*

Note, instead of D. Luenberger's [107] minimization problem, this thesis mainly regards maximization problems, hence the reversals of the minimization and maximization can be used [117]. Here, the surrogate dual aims the tightest of the upper bounds [117] instead of the tightest of the lower bounds like in [107]. The dual problem can have an easier structure and can offer simple methods without the need of a convex solver. In wireless communication this mathematical framework is strongly connected with the so-called uplink–downlink duality which offers simple and optimal low complexity algorithms for transmitter optimization. Theorem 3 requires a quasi-concave objective function. In what follows, the maximization (3.16) is regarded. The theorems for the minimization are analogue. The following theorem generalizes the work of Luenberger:

Theorem 4. *[60, 101] If an $\boldsymbol{x}^*$ solves* (3.20) *for a $\boldsymbol{\mu}^* \in \mathbb{R}^n_+$ and $\boldsymbol{x}^*$ is feasible in* (3.16)*, then $\boldsymbol{x}^*$ solves* (3.16) *and $t_0 = \min_{\boldsymbol{\mu}} \{s(\boldsymbol{\mu})\}$.*

[4] "Along lines, e.g., every convex function is upper semi-continuous along lines" [107].

Proof. The proof is straightforward and outlined briefly for a better understanding. This proof regards a maximization over a function f. Both problems (3.16) and (3.20) have the same objective function f. Note f must not necessarily be quasi-concave. The feasible region $\mathcal{F}$ of the original problem is a subset of the feasible region $\mathcal{F}(\boldsymbol{\mu})$ of the surrogate function, hence, $\mathcal{F} \subseteq \mathcal{F}(\boldsymbol{\mu})$ holds.

The optimal solution of (3.16) with the value t_0^* is denoted by $\boldsymbol{x}^*$.

Assume $\boldsymbol{x}^*$ is feasible in surrogate problem which has the value $s(\boldsymbol{\mu}^*)$. Consequently, because of $\mathcal{F} \subseteq \mathcal{F}(\boldsymbol{\mu}^*)$ and due to the weak duality $t_0^* \leq s(\boldsymbol{\mu}^*)$, $\forall \boldsymbol{\mu}^* \in \mathbb{R}_+^N$, the maximizer $\boldsymbol{x}^*$ must be also an maximizer over (3.16). Consequently, $f(\boldsymbol{x}^*) = t_0^* \leq s(\boldsymbol{\mu}^*) = f(\boldsymbol{x}^*) \;\Rightarrow\; t_0^* = s(\boldsymbol{\mu}^*)$ holds. □

A fundamental result in the surrogate duality theory is proved in [60]:

Theorem 5. *[60] The surrogate dual function $s(\boldsymbol{\mu})$ is quasi-convex in $\boldsymbol{\mu}$.*

Hence, a global minimizer over $\boldsymbol{\mu}$ can always attain the minimum. Furthermore, the surrogate dual problem is connected with the Lagrangian dual problem. Greenberg et. al. have proved the following Theorem [60]:

Theorem 6. *[60,101] The surrogate dual problem $\min_{\boldsymbol{\mu}} s(\boldsymbol{\mu})$ is a tighter bound than the Lagrangian dual problem $\min_{\boldsymbol{\mu}} l(\boldsymbol{\mu})$, hence $\min_{\boldsymbol{\mu}} s(\boldsymbol{\mu}) \leq \min_{\boldsymbol{\mu}} l(\boldsymbol{\mu})$. If $\min_{\boldsymbol{\mu}} s(\boldsymbol{\mu}) = \min_{\boldsymbol{\mu}} l(\boldsymbol{\mu})$ then there exists an $\boldsymbol{x}$ such that $\boldsymbol{\mu}^T \mathbf{g}(\boldsymbol{x}) = 0$. Consequently, the surrogate constraint is satisfied with equality, in this case.*

Proof. The Lagrangian dual function can be upper bounded as follows:

$$l(\boldsymbol{\mu}) = \sup_{\boldsymbol{x}} \Big(f(\boldsymbol{x}) - \boldsymbol{\mu}^T \mathbf{g}(\boldsymbol{x}) \mid \boldsymbol{x} \in \mathcal{X} \Big) \tag{3.32}$$

$$\geq \sup_{\boldsymbol{x}} \Big(f(\boldsymbol{x}) - \boldsymbol{\mu}^T \mathbf{g}(\boldsymbol{x}) \mid \boldsymbol{\mu}^T \mathbf{g}(\boldsymbol{x}) \leq 0,\ \boldsymbol{x} \in \mathcal{X} \Big) \tag{3.33}$$

$$\geq \sup_{\boldsymbol{x}} \Big(f(\boldsymbol{x}) \mid \boldsymbol{\mu}^T \mathbf{g}(\boldsymbol{x}) \leq 0,\ \boldsymbol{x} \in \mathcal{X} \Big) = s(\boldsymbol{\mu}) \tag{3.34}$$

The first row (3.32) is the Lagrangian dual function. It is an unconstrained function; consequently, (3.32) is an upper bound of (3.33). Finally, removing the positive sum $-\boldsymbol{\mu}^T \mathbf{g}(\boldsymbol{x})$, surrogate dual function is the result. Hence, $l(\boldsymbol{\mu}) \geq s(\boldsymbol{\mu})$ holds. If $l(\boldsymbol{\mu}) \geq s(\boldsymbol{\mu})$ also $\min_{\boldsymbol{\mu}} l(\boldsymbol{\mu}) \geq \min_{\boldsymbol{\mu}} s(\boldsymbol{\mu})$ holds.

The constraint $\boldsymbol{\mu}^T \mathbf{g}(\boldsymbol{x}) \leq 0$ is satisfied with equality, if and only if, $\min_{\boldsymbol{\mu}} l(\boldsymbol{\mu}) = \min_{\boldsymbol{\mu}} s(\boldsymbol{\mu})$. Let $\boldsymbol{x}^*$ be a solution of $s(\boldsymbol{\mu}^*)$. If $\boldsymbol{x}^*$ is feasible in $s(\boldsymbol{\mu}^*)$, then the constraint $\boldsymbol{\mu}^T \mathbf{g}(\boldsymbol{x}) \leq 0$ is satisfied. Furthermore, $\boldsymbol{x}^*$ is also feasible in $l(\boldsymbol{\mu}^*)$ and

$$l(\boldsymbol{\mu}^*) \geq f(\boldsymbol{x}^*) - \boldsymbol{\mu}^{*T} \mathbf{g}(\boldsymbol{x}^*) \geq f(\boldsymbol{x}^*) = s(\boldsymbol{\mu}^*) \tag{3.35}$$

holds. If $l(\boldsymbol{\mu}^*) = s(\boldsymbol{\mu}^*)$, the constraint $\boldsymbol{\mu}^{*T} \mathbf{g}(\boldsymbol{x}^*) = 0$. □

3.3.3 Fractional Programming

In various technical applications, a ratio of two functions is optimized. This optimization is called fractional programming. A generalization is the optimization of multiple ratios, called generalized fractional programming. This thesis applies the frame-work of fractional programming in the context of the max–min multicast beamforming problem (see Section 7.5) where the minimal ratio of the received power divided by the interference power of a set of users is maximized over a convex set of power constraints. A generalized fractional program is formally defined by [29]:

Definition 25. *Let $f_i : \mathcal{X} \subset \mathbb{E}^n \to \mathbb{R}$ be a continuous and convex function and let $d_i : \mathcal{X} \subset \mathbb{E}^n \to \mathbb{R}$ be a continuous and concave function on the convex set $\mathcal{X}$, consider the following quasi-convex problem:*

$$\bar{\Theta} = \min_{x \in \mathcal{X}} \max_{i \in \mathcal{I}} \frac{f_i(\boldsymbol{x})}{d_i(\boldsymbol{x})} \tag{3.36}$$

where $\mathcal{I}$ is a finite set of integer numbers.

This quasi-convex program can be solved with the following parametric program [28,29]:

Definition 26. *Let $f_i : \mathcal{X} \subset \mathbb{E}^n \to \mathbb{R}$ be a continuous and convex function and let $d_i : \mathcal{X} \subset \mathbb{E}^n \to \mathbb{R}$ be a continuous and concave function on the convex set $\mathcal{X}$, the parametric program, associated to* (3.36)*, is defined by*

$$F(\Theta) = \min_{x \in \mathcal{X}} \max_{i \in \mathcal{I}} \{f_i(\boldsymbol{x}) - \Theta d_i(\boldsymbol{x})\}. \tag{3.37}$$

The idea of the algorithm presented in this section is based on searching the root $F(\Theta) = 0$. The optimality conditions of the solution $\bar{\Theta}$ based on $F(\Theta)$ are presented in [29] by the following proposition:

Proposition 1. *[29] Among the quasi-convex fractional program* (3.36) *and the parametric program* (3.37) *the following conditions hold:*
(i) F is nonincreasing and upper semicontinuous; (ii) $F(\Theta) < 0$ if and only if $\Theta > \bar{\Theta}$; hence, $F(\bar{\Theta}) \geq 0$; (iii) If (3.36) *has an optimal solution, then, $F(\bar{\Theta}) = 0$; (iv) If $F(\bar{\Theta}) = 0$, then programs* (3.36) *and* (3.37) *have the same set of optimal solutions (which may be empty).*

Proof. A proof is presented in [29, Proposition 2.1]. □

In particular, condition (iii) is useful for an algorithmic solution. If the parametric program (3.37) is very close to zero, the solution is near optimal and the solution of the parametric program is also a solution for the original generalized fractional program.

In general the minimum is replaced by the infimum. However this thesis regards objective functions where the minimum can be attained; hence the infimum equals the minimum. The following example shows general objective functions where only the infimum exists and the minimum can not be attained. In this case $F(\bar{\Theta}) = 0$ does not imply the existence of an optimal solution [29].

Example 2. *[29] Let $\mathcal{I} = \{1\}$, $n = 1$ and $\mathcal{X} = \mathbb{R}$, regard the fractional program*

$$\bar{\Theta} = \inf_{x \in \mathcal{X}} \left(\frac{e^x}{e^{2x}} \right) = \inf_{x \in \mathcal{X}} (e^{-x}). \tag{3.38}$$

The parametric program is then

$$F(\Theta) = \inf_{x \in \mathcal{X}} (e^x - \Theta e^{2x}) = \begin{cases} 0 & \textit{if } \Theta \leq 0 \\ -\infty & \textit{if } \Theta > 0 \end{cases} \tag{3.39}$$

It follows $F(\bar{\Theta} = 0) = 0$ and (3.38) *and* (3.39) *do not have an optimal solution.*

Now regard the following example where the minimum can be attained:

Example 3. *Let $\mathcal{I} = \{1,2\}$, $n = 2$ and $\mathcal{X} = \{\boldsymbol{x} \in \mathbb{R}^2 \mid -1 \leq x_1 \leq 1, -1 \leq x_2 \leq 1\}$, regard the fractional program*

$$\bar{\Theta} = \min_{x \in \mathcal{X}} \max\{\frac{-x_1}{x_2+1}, \frac{-x_2}{x_1+1}\} = -\frac{1}{2} \tag{3.40}$$

Obviously, the value of the solution is $\bar{\Theta} = -1/2$ and the value of the parametric program is

$$F(\bar{\Theta}) = \inf_{x \in \mathcal{X}} \max\{-x_1 - \bar{\Theta}(x_2+1), -x_2 - \bar{\Theta}(x_1+1)\} = 0. \tag{3.41}$$

Hence, in this example the optimal value can be attained. This example can be also seen as a very simple example for SINR balancing, where the negative SINR of two users is minimized. All channel gains are equal to 1 *and the power is given by the variables x_1 and x_2. Due to the noise level of* 1 *and the power constraints $x_1 \leq 1$ and $x_2 \leq 1$, the ratios are always bounded and no definition gaps exist.*

The parametric program is convex if the functions $f_i : \mathcal{X} \subset \mathbb{E}^n \to \mathbb{R}$ are convex, the functions $d_i : \mathcal{X} \subset \mathbb{E}^n \to \mathbb{R}$ are concave, and $\mathcal{X}$ is a closed convex set. The following algorithm can efficiently solve a convex parametric program (3.37). Algo-

Algorithm 2 Root finding algorithm (Dinkelbach type-1 algorithm) [30]:

Let $\boldsymbol{x}^1 \in \mathcal{X}$ and $\Theta^1 = \max_{i \in \mathcal{I}} \frac{f_i(\boldsymbol{x}^1)}{d_i(\boldsymbol{x}^1)}$ and $k = 1$
repeat
  Determine the optimal solution $\boldsymbol{x}^k$ of
  $F(\Theta^k) = \min_{\boldsymbol{x} \in \mathcal{X}} \max_{i \in \mathcal{I}} \{f_i(\boldsymbol{x}) - \Theta^k d_i(\boldsymbol{x})\}$
  Let $\Theta^{k+1} = \max_{i \in \mathcal{I}} \frac{f_i(\boldsymbol{x}^k)}{d_i(\boldsymbol{x}^k)}$ and set $k = k + 1$
until $|F(\Theta^k)| < \epsilon$
return $\boldsymbol{x}^k$

rithm 2 has a linear convergence. If $\mathcal{X}$ is compact and all $d_i : \mathcal{X} \subset \mathbb{E}^n \to \mathbb{R}$ satisfy the Lipschitz condition, Algorithm 3 can reach super-linear convergence [29], which is faster than linear convergence. The theory of generalized fractional programs is used in Chapter 7 to solve the equivalent quasi-convex form of the multicast max–min beamforming problem with long-term CSI in form of Hermitian positive semidefinite Toeplitz matrices.

Algorithm 3 Root finding algorithm (Dinkelbach type-2 algorithm) [30]:

Let $\boldsymbol{x}^1 \in \mathcal{X}$ and $\Theta^1 = \max_{i\in\mathcal{I}} \frac{f_i(\boldsymbol{x}^1)}{d_i(\boldsymbol{x}^1)}$ and $k = 1$
repeat
  Determine the optimal solution $\boldsymbol{x}^k$ of
  $F(\Theta^k) = \min_{\boldsymbol{x}\in\mathcal{X}} \ \max_{i\in\mathcal{I}}\{\frac{f_i(\boldsymbol{x})-\Theta^k d_i(\boldsymbol{x})}{d_i(\boldsymbol{x}^k)}\}$
  Let $\Theta^{k+1} = \max_{i\in\mathcal{I}} \frac{f_i(\boldsymbol{x}^k)}{d_i(\boldsymbol{x}^k)}$ and set $k = k+1$
until $|F(\Theta^k)| < \epsilon$
return $\boldsymbol{x}^k$

3.3.4 Semidefinite Relaxation

Several beamforming problems appear in form of a quadratic program with quadratic constraints which is defined as follows:

Definition 27. ***Quadratically Constrained Quadratic Program:*** *Consider the general minimization problem according to Definition 7. An optimization problem is called a quadratically constrained quadratic program (QCQP) if the objective function* $f(\boldsymbol{x}) = \boldsymbol{x}^H\mathbf{F}\boldsymbol{x}$ *is a quadratic function with a symmetric matrix* $\mathbf{F} \in \mathbb{R}^{n\times n}$ *and the quadratic constraint functions are given by* $g_i(\boldsymbol{x}) = \boldsymbol{x}^H\mathbf{G}_i\boldsymbol{x}$*, with symmetric matrices* $\mathbf{G}_i \in \mathbb{R}^{n\times n}$, $\forall i = 1,\ldots,m$.

If all matrices $\mathbf{F}$ and $\mathbf{G}_i$ $\forall i = 1,\ldots,m$ are positive semidefinite, the problem defined in Definition 27 is convex. The problem defined in Definition 27 is non-convex if at least one of the matrices $\mathbf{F}$ and $\mathbf{G}_i$ $\forall i = 1,\ldots,m$ is not positive semidefinite. Then the problem is called non-convex QCQP.

A non-convex QCQP is $\mathcal{NP}$-hard in general. Using matrices $\mathbf{X} = \boldsymbol{x}\boldsymbol{x}^T$, the problem of Definition 27 can be transformed to the equivalent problem

$$\begin{aligned} \min_{\mathbf{X}} \quad & \mathrm{Tr}\{\mathbf{XF}\} \\ \text{s.t.} \quad & \mathrm{Tr}\{\mathbf{XG}_i\} \le 0,\ \forall i = 1,\ldots,m \\ & \mathrm{rank}(\mathbf{X}) = 1. \end{aligned} \tag{3.42}$$

Removing the non-convex constraint $\mathrm{rank}(\mathbf{X}) = 1$ (rank-1 constraint) and replacing it with the constraint $\mathbf{X} \succeq 0$ [5], the problem (3.42) can be transformed to the following convex problem

$$\begin{aligned} \min_{\mathbf{X}} \quad & \mathrm{Tr}\{\mathbf{XF}\} \\ \text{s.t.} \quad & \mathrm{Tr}\{\mathbf{XG}_i\} \le 0,\ \forall i = 1,\ldots,m \\ & \mathbf{X} \succeq 0. \end{aligned} \tag{3.43}$$

Problem (3.43) is an SDP as defined in Definition 10. This relaxation technique is, therefore, called semidefinite relaxation (SDR). The optimal value of (3.43) is a lower bound for the original non-convex QCQP. The resulting SDP can be efficiently solved with convex solvers as [59, 139]. In this thesis, CVX [59] was used to solve the convex problems.

The technique of SDR offers a straightforward method to solve non-convex beamforming problems. This thesis uses this method in several chapters. The SDR technique is well known and used as a reference method for improved alternative methods to solve beamforming problems. More details concerning SDR are presented in [5, 109].

Chapter 4

Theory of the Unicast Multicell Max–Min Beamforming Problem

The content presented in this Chapter is published in the publications [37, 41]. This chapter only considers unicast beamforming. The term unicast is omitted to shorten the wordings.

4.1 Introduction

Max–min beamforming is a transmitter optimization technique to improve the fairness in wireless networks with a frequency reuse-1 factor.

To achieve a higher spectral efficiency future networks should use the whole bandwidth. However, in such a single frequency network, (intra-cell and inter-cell) interference will occur. Users far away from their serving BS are subject to strong interference of adjacent BSs. An unfair distribution of the SINR among the users in the network will be the result. However, besides a high spectral efficiency, future networks should guarantee fairness among the users as well.

Smart antennas at the BSs allow mitigation of interference and, therefore, the improvement of the SINR of cell edge users. This can be achieved by closed loop beamforming, i.e., by an optimization of the weighting factors of each antenna element based on the available CSI of all links in the considered network. Two different cases of CSI are feasible in general:

1. Instantaneous CSI requires a fast CSI feedback mechanism. Especially in a large network with multiple BSs, a fast backbone network based on fiber is essential to update the information of all users in the network.

2. A more practical approach is the use of long-term CSI. In this case, the spatial correlation matrices are estimated over a longer time interval. Therefore, an update of this form of CSI is required during each local stationary interval which is less frequent compared to the use of instantaneous CSI.

Using the long-term CSI of all links, max–min beamforming (MB) enables to increase the SINR fairness among all jointly scheduled users in a network. However, the MB problem (MBP) is a complex problem if general power constraints and long-term CSI are given. Low complexity solutions are required in pratice. This chapter discusses the complexity and the duality theory of the MBP, which is known to be non-convex in general. However, some equivalent quasi-convex forms are identified. A quasi-convex optimization means in this context that the maximization problem

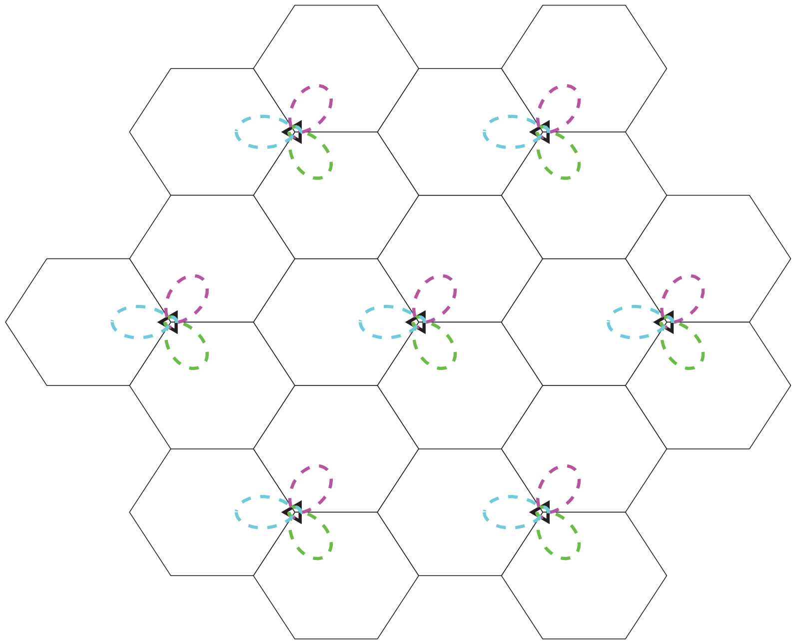

Figure 4.1: Scenario: The lobes show the orientation of the antenna pattern.

has a quasi-concave objective function and convex constraints. Therefore, a global optimum exists and an efficient iterative algorithm can converge arbitrary tight to this optimum [15].

Furthermore, only the unicast MBP is investigated in this chapter. The more general multicast case is discussed later in Chapter 7. In the unicast case, each user in the network gets different contents. Hence there is only one beamforming vector per transmitted information symbol. For the unicast MBP an equivalent quasi-convex form is derived only for instantaneous CSI and per-antenna power constraints [148]. The problem can be solved globally optimal for both instantaneous CSI or arbitrary long-term CSI and a sum power constraint [128]. An open question is whether there exists an efficient solution for the MBP in the case of long-term CSI given by spatial correlation matrices with rank larger than one and more general power constraints.

4.1.1 Scenario

This chapter uses a scenario consisting of a wireless network with multiple BSs denoted by triangles in Fig. 4.1 and multiple users and frequency reuse-1. Each BS array is a ULA and has an antenna spacing of half the wave length. Each antenna element at the BS is equipped with a 120° antenna pattern. Each user in this network has only one antenna. If unicast transmission is considered, only one user will be served inside a cell by the antenna array of the cell serving BS to simplify the signal model.

Table 4.1: Overview of related problems.

Problem	Objective	Power Constraints	CSI	Proved
PMP	sum power	-	long-term or inst. CSI	strong duality
PMP	sum power	per-antenna power	inst. CSI	convex form
MBP	min. SINR	sum power	long-term or inst. CSI	strong duality
MBP	min. SINR	per-antenna	inst. CSI	quasi-convex form

The optimization of the beamforming vectors is based on long-term CSI in the form of spatial correlation matrices.

4.1.2 Related Work

Transmit beamforming has been investigated intensively since 1998. A central aspect of this field is the uplink–downlink duality in unicast beamforming. First works regarding this aspect are [125,161]. Various publications generalize their work or give further proofs and extensions. An overview of these publications is given in Tables 4.2 and 4.3. A deep information theoretic background concerning the duality of the Gaussian broadcast channel is studied in [156].

Unicast beamforming is non-convex with general power constraints and if long-term CSI is used [9]. However, several equivalent quasi-convex or even convex forms are currently identified for some special cases. Table 4.1 gives an overview of all related problems.

Based on long-term CSI, the unicast beamforming problem of minimization of the sum power subject to individual SINR constraints was investigated in [9]. This problem is called power minimization problem (PMP). In [9], the authors showed that the non-convex PMP can be relaxed to a convex semidefinite program which has no relaxation gap. The unicast PMP and the unicast MBP are reciprocal problems [157]. In [10–12,128], the authors presented an optimal solution for the MBP based on long-term CSI and a sum power constraint. The convergence of the iterative low complexity algorithm is later proved in [19]. Later this work was extended with additional soft shaping constraints [64].

The framework of the Lagrangian duality theory was introduced to solve the unicast multiuser beamforming problem in the work of [157] and [163]. In the case of instantaneous CSI, the PMP has an equivalent convex form, as opposed to the MBP which has a merely quasi-convex form. The authors in [163] propose a fast direct solution for the minimization of the maximum power margin over all antennas subject to per-antenna power constraints and individual SINR constraints. The authors of [31] extended the work to the multicell case. The PMP requires a properly chosen SINR. The MBP is more flexible and overcomes this complication. The MBP allows finding the highest SINR constraint such that the problem is feasible. In [143], the authors investigated the max–min weighted SINR problem with individual power constraints. The authors derived a fast algorithm based on the non-linear Perron Frobenius theory. In [148], the authors presented an equivalent quasi-convex form of the unicast MBP

Table 4.2: Overview of some regarded problems of related work in the last 14 years.

Year	Author	Problem	Power constr.	CSI
1998	Rashid-Farrokhi et al, [125]	PMP	-	instant.
1998	Yang, Xu, [161]	MBP	sum power	instant.
2001	Bengtsson, Ottersten, [9]	MBP	sum power	long-term
2002	Boche, Schubert, [10]	MBP	sum power	long-term
2005	Song, Cruz, Rao, [137]	PMP	-	instant.
2006	Wiesel, Eldar, Shamai, [157]	MBP	sum power	instant.
2007	Yu, Lan, [163]	PMP	per-antenna	instant.
2008	Tölli, Codreanu, Juntti [148]	MBP	per-antenna	instant.
2010	Dartmann, Afzal, Gong, Ascheid [32]	MBP	per array	long-term
2011	Tan, Chiang, Srikant [143–145]	MBP	sum power	instant.
2011	Cai, Tan, [19–21]	MBP	per array	instant.
2011	Negro, Cardone, Ghauri, Slock, [116]	MBP	per array	instant.
2012	Dartmann, Gong, Afzal, Ascheid [37]	MBP	per-antenna	long-term.

Table 4.3: Overview of some solutions of related work in the last 14 years.

Year	Author	Theory, Solution
1998	Rashid-Farrokhi et al, [125]	Perron Frobenius Theorem
1998	Yang, Xu, [161]	Perron Frobenius Theorem
2001	Bengtsson, Ottersten, [9]	SDP
2002	Boche, Schubert, [10]	Perron Frobenius Theorem
2005	Song, Cruz, Rao, [137]	Linear programming duality
2006	Wiesel, Eldar, Shamai, [157]	Lagrangian, SOCP
2007	Yu, Lan, [163]	Lagrangian, SOCP
2008	Tölli, Codreanu, Juntti [148]	SOCP
2010	Dartmann, Afzal, Gong, Ascheid [32]	Lagrangian
2011	Tan, Chiang, Srikant [143–145]	Non-linear Perron Frob. Theorem
2011	Cai, Tan, [19–21]	Non-linear Perron Frob. Theorem
2011	Negro, Cardone, Ghauri, Slock, [116]	bisection over convex PMPs
2012	Dartmann, Gong, Afzal, Ascheid [37]	surrogate duality

with per-BS antenna array power constraints for the case of instantaneous CSI. Similar to [157], the authors presented an approach in the form of a feasibility check problem given as SOCP. The work [32] presented a fast direct solution for the MBP with long-term CSI and per-BS antenna array power constraints based on the framework of the Lagrangian duality theory. This scenario is not proved to have an equivalent convex form, hence, strong duality is not given in general. In [40], the MBP based on instantaneous CSI was investigated and the solution is extended to per-antenna power constraints.

4.1.3 Contributions

This chapter presents the following contributions:

- This chapter presents an approach involving a dual uplink problem for the MBP with multiple power constraints based on the surrogate dual problem. If instantaneous CSI is available, an equivalent quasi-convex form of the MBP exists and strong surrogate duality can be directly proved with a duality theorem for quasi-convex programming [107]. The approach presented in [164] also combines the power constraints to a weighted sum power constraint. However, strong duality was not proved in this work.

- If only long-term CSI in the form of higher rank spatial correlation matrices is available no equivalent quasi-convex form is known and the surrogate duality theorem of [107] can not be applied. An additional proof is presented to show strong duality in the case long-term CSI is given and one per BS power constraint is satisfied with equality.

- The surrogate dual problem is proved to be quasi-convex, hence it can be solved efficiently.

- The surrogate dual problem can be proved to be equal to the Lagrangian dual and, at the optimum, the combined power constraint of the surrogate dual problem is satisfied with equality.

- The surrogate dual problem leads to an iterative low complexity algorithm. The convergence of the proposed iterative method is shown.

- In the literature usually scenarios with a balanced SINR are investigated. However, this is not always given. This Chapter presents some conditions where a balanced SINR does not exists for the given set of power constraints.

- In the literature several generalized MB scenarios with a cooperative multipoint (CoMP) transmission exist, e.g, [150]. A beamforming gain can be achieved if the BSs are perfectly synchronized and the instantaneous CSI is available. However, this assumption is very challenging. This thesis extends the MBP with a CoMP transmission based on long-term CSI. Due to the max–min fairness, a gain in the spatial domain can be achieved. Only BSs close to the users are active, the others are switched of to avoid intercell interference. The presented solution is able to out-perform the convex solver based bisection method.

4.1.4 Outline

Section 4.2 gives a detailed description of the system model for the unicast MBP. Each user is served by exactly one BS.

Section 4.3 introduces the MBP and defines the Pareto optimality condition. Note that only interference coupled networks are assumed. Further, this section derives an equivalent quasi-convex form of the MBP for the above mentioned special instances. In the case of higher rank spatial correlation matrices with a Toeplitz structure, the equivalent quasi-convex form is derived for per-BS antenna array power constraints for a unicast and multicast transmission. A convex solver based solution is proposed. Besides the convex solver based solutions a surrogate dual uplink problem of the primal downlink MBP is derived and strong duality is proven.

Section 4.4 presents a fast direct solution for the unicast MBP with per-antenna power constraints based on the surrogate dual problem. The presented algorithms is able to find the same solution as a convex solver based algorithm if a balanced SINR exists. The section underlines the performance of the presented iterative solution with some numerical results and a complexity analysis.

Section 4.6.2 discusses the Pareto optimality of the MBP with general power constraints and generalizes the solution of the MBP, where a balanced SINR is given, to interference decoupled networks without a balanced SINR.

Section 4.6.3 shows a further extension of iterative algorithm which exploits the spatial diversity if multiple BSs transmit jointly to a scheduled user. Hence, multiple BSs are assigned to a scheduled users and this scheme corresponds to non-coherent CoMP transmission based on long-term CSI. This section concludes with some results, which show the performance of the iterative solution compared to classical convex solver based approaches.

4.2 System Model for Unicast Downlink Transmission

As depicted in Figure 4.1, the network consists of $N = M$ cooperating BS arrays, each equipped with N_A antennas. At a time instant, M users of the index set $\mathcal{U} = \{1, \ldots, M\}$, each equipped with a single antenna, are served jointly in this network. A BS array of cell with index c serves a scheduled user inside this cell. In each cell c a set $\mathcal{U}_c$ of N_c users are equally distributed. For simplification there is no intracell interference. Thus, at a given time instant the BS array c serves one user from the set $\mathcal{U}_c$. This scheduled user $i \in \mathcal{U}_{c(i)}$ receives a signal

$$r_i = \mathbf{h}^H_{c(i),i}\boldsymbol{\omega}_{c(i)}s_{c(i)} + \sum_{l \in \mathcal{U}, c(l) \neq c(i)} \mathbf{h}^H_{c(l),i}\boldsymbol{\omega}_{c(l)}s_{c(l)} + n_i. \tag{4.1}$$

from its BS array of the cell $c(i)$. Here, n_i is noise. In the unicast case, there is always one scheduled user per-antenna array. Therefore, the signal model (5.2) can be simplified as follows:

$$r_i = \mathbf{h}^H_{i,i}\boldsymbol{\omega}_i s_i + \sum_{l \in \mathcal{U}, l \neq i} \mathbf{h}^H_{l,i}\boldsymbol{\omega}_l s_l + n_i. \tag{4.2}$$

This section only regards the unicast beamforming problem, hence, only the model (4.2) is used for simplification. The signal transmitted to user i is given by s_i with $E\{|s_i|^2\} = 1$ and $E\{s_l s_i^*\} = 0$ if $l \neq i$. The channel vector between the lth BS array and user i is given by $\mathbf{h}_{l,i}^H \in \mathbb{C}^{1\times N_A}$. The beamforming vector of the lth antenna array with N_A antenna elements is denoted by $\boldsymbol{\omega}_l = [\omega_l(0), \omega_l(1), \ldots, \omega_l(N_A - 1)]^T$.

Definition 28. *With the assumption $E\{|n_i|^2\} = \sigma_i^2$ and $E\{n_i\} = 0$, the instantaneous downlink SINR is:*

$$\hat{\gamma}_i = \frac{|\mathbf{h}_{i,i}^H \boldsymbol{\omega}_i|^2}{\sum_{\substack{l\in\mathcal{U}\\ l\neq i}} |\mathbf{h}_{l,i}^H \boldsymbol{\omega}_l|^2 + \sigma_i^2}. \tag{4.3}$$

A well known performance measure of the wireless channel is the ergodic capacity of the downlink to user i.

$$\hat{R}_i = \mathbb{E}\{\log(1 + \hat{\gamma}_i^D)\}. \tag{4.4}$$

A global optimization based on instantaneous CSI over a large number of slots in a large network with multiple users and BSs is very difficult. However, practically relevant is an optimization based on the long-term CSI. Therefore, as in [93], the ergodic capacity is approximated by

$$\hat{R}_i = \mathbb{E}\{\log(1 + \hat{\gamma}_i)\} \approx \log(1 + \gamma_i^D) = R_i. \tag{4.5}$$

The variable γ_i^D denotes the mean SINR:

$$\gamma_i^D = \frac{\boldsymbol{\omega}_i^H \mathbb{E}\{\mathbf{h}_{i,i}\mathbf{h}_{i,i}^H\}\boldsymbol{\omega}_i}{\sum_{\substack{l\in\mathcal{U}\\ l\neq i}} \boldsymbol{\omega}_l^H \mathbb{E}\{\mathbf{h}_{l,i}\mathbf{h}_{l,i}^H\}\boldsymbol{\omega}_l + \sigma_i^2} \tag{4.6}$$

This section discusses the complexity and solvability of the MBP in general. The quasi-convexity of the MBP depends on the given CSI. Two cases of CSI are considered in this thesis. If **instantaneous CSI** is used, the following matrices normalized to the noise power are given:

$$\mathbf{R}_{l,i} = \frac{1}{\sigma_i^2}\mathbf{h}_{l,i}\mathbf{h}_{l,i}^H. \tag{4.7}$$

Long-term CSI is often used in a multicell optimization due to the reduced CSI feedback rate. The assumption of this long-term CSI results in a mean SINR. Here, an additional expectation over the channel realizations $\mathcal{H}$ is done. The result is the spatial correlation matrix given by

$$\mathbf{R}_{l,i} = \frac{1}{\sigma_i^2}\mathbb{E}\{\mathbf{h}_{l,i}\mathbf{h}_{l,i}^H\}. \tag{4.8}$$

Definition 29. *Downlink SINR: Using the definitions of the spatial correlation matrices* (4.7) *or* (4.8), *the SINR is then defined by*

$$\gamma_i^D(\boldsymbol{\Omega}) = \frac{\boldsymbol{\omega}_i^H \mathbf{R}_{i,i}\boldsymbol{\omega}_i}{\sum_{\substack{l\in\mathcal{U}\\ l\neq i}} \boldsymbol{\omega}_l^H \mathbf{R}_{l,i}\boldsymbol{\omega}_l + 1}. \tag{4.9}$$

Besides the downlink (DL) SINR (4.9), the uplink (UL) SINR (4.9) can be defined as follows:

Definition 30. *[163] Uplink SINR: With the uplink receive beamforming vectors of a BS given by* $\mathbf{v}_i$*, with* $||\mathbf{v}_i|| = 1$, $\forall i \in \mathcal{U}$ *with the UL power* λ_i $\forall i \in \mathcal{U}$*, and with some matrices* $\mathbf{M}_i \succeq 0$*, the dual UL unicast SINR is defined by*

$$\gamma_i^U(\boldsymbol{\mu}, \boldsymbol{\lambda}, \mathbf{v}_i) = \frac{\lambda_i \mathbf{v}_i^H \mathbf{R}_{i,i} \mathbf{v}_i}{\mathbf{v}_i^H (\mathbf{M}_i + \sum_{\substack{l \in \mathcal{U} \\ l \neq i}} \lambda_l \mathbf{R}_{i,l}) \mathbf{v}_i}. \tag{4.10}$$

The diagonal matrix $\mathbf{M}_i \succeq 0$, called UL-scaling matrix in the following, depends on three power constraints and is defined below. Definition 30 is used later in the derivation of the duality in Section 4.3.4 and provides a low complexity solution. In what follows, the matrix $\mathbf{V} \in \mathcal{V}$ with

$$\mathcal{V} = \{\mathbf{V} \in \mathbb{C}^{N_A \times M} : \ ||[\mathbf{V}]_{:,i}|| = 1, \ [\mathbf{V}]_{:,i} \in \mathbb{C}^{N_A \times 1}, \forall i \in \mathcal{U}\} \tag{4.11}$$

is the matrix of all UL receive beamforming vectors of all BS arrays $\mathbf{V} = [\mathbf{v}_1, \ldots, \mathbf{v}_M]$.

Power constraints: In practically relevant networks each transmitting station is subject to a power constraint. These power constraints have a strong impact on the complexity and on the optimality of the solution of the MBP. The power constraints determine the domain where a solution can be found. The domain determined by the power constraints is denoted by $\mathcal{P}$. This set is a convex set. This thesis discusses the following three types of power constraints:

- **Sum power constraint**: The most flexible constraint is the so-called sum power or network power constraint. In this case the total power of all transmitting stations is limited by $P \in \mathbb{R}_+$. This constraint has a more theoretical intention in multicell networks. In a unicast max–min beamforming problem, an optimal balanced SINR can be obtained for higher rank spatial correlation matrices (long-term CSI) [128]. The MBP is convex in this case. The convex cone of beamforming vectors fulfilling the sum power constraint is given by

$$\mathcal{P} = \{\boldsymbol{\omega}_l \in \mathbb{C}^{N_A \times 1} : \sum_{l \in \mathcal{U}} \boldsymbol{\omega}_l^H \boldsymbol{\omega}_l \leq P\}. \tag{4.12}$$

- **Per BS antenna array power constraints**: These constraints are stricter. In this case each antenna array l of a BS will be subject to a total power budget $P_l \in \mathbb{R}_+$ and is, obviously, practically more relevant compared to the sum power constraint. The convex cone of beamforming vectors fulfilling the per-BS antenna array power constraints is given by

$$\mathcal{P} = \{\boldsymbol{\omega}_l \in \mathbb{C}^{N_A \times 1} : \ \boldsymbol{\omega}_l^H \boldsymbol{\omega}_l \leq P_l \ \ \forall l \in \mathcal{U}\}. \tag{4.13}$$

  In the definition of the UL-SINR, the UL-scaling matrix $\mathbf{M}_i = \mu_i \mathbf{I}_{N_A}$ for some $\mu_i \in \mathbb{R}_+$ is used.

- **Per antenna power constraints**: These are strictest constraints. Then the power of each antenna element with index a of the total set of $\mathcal{A}$ is constrained. Therefore, these constraints are closest to the practice, where the power of each antenna amplifier is limited. It is assumed each BS array l has the same number N_A of antenna elements given by the set $\mathcal{A}_l$. The power of each antenna element a of BS array l is constrained by $P_{l,a} \in \mathbb{R}_+$. The convex cone of beamforming vectors fulfilling the per-antenna power constraints is given by

$$\mathcal{P} = \{\boldsymbol{\omega}_l \in \mathbb{C}^{N_A \times 1} : \ |[\boldsymbol{\omega}_l]_a|^2 \leq P_{l,a} \ \ \forall a \in \mathcal{A}_l \ \ \forall l \in \mathcal{U}\}. \tag{4.14}$$

Let diag$(\cdot)$ denote the diagonal matrix, $\mathbf{M}_i = \text{diag}(\mu_{i,1}, \ldots, \mu_{i,N_A})$ denotes the UL scaling matrix in the definition of the UL SINR for some $\mu_{i,a} \in \mathbb{R}_+$.

4.3 Optimization Problem and Uplink–Downlink Duality

In modern wireless networks fairness among the users is desired. A max–min optimization of the DL-SINR achieves SINR fairness among the users and is formally defined by

Definition 31. *MBP: With the definition of downlink SINR according to Definition 29 the max–min optimization of the beamforming matrix $\boldsymbol{\Omega} = [\boldsymbol{\omega}_1, \ldots, \boldsymbol{\omega}_M]$ subject to a set $\mathcal{P}$ of convex cones defining the power constraints, the MBP is defined by*

$$\begin{aligned} \gamma^D = \max_{\boldsymbol{\Omega}} \ \ & \min_{i \in \mathcal{U}} \gamma_i^D(\boldsymbol{\Omega}) \\ & \text{s.t.} \ \ \boldsymbol{\omega}_l \in \mathcal{P} \ \ \forall l \in \mathcal{U}. \end{aligned} \tag{4.15}$$

A balanced SINR can be the result. However, such an approach requires a smart selection of the set $\mathcal{U}$ of active users, otherwise a single bad user can degrade the performance of all jointly active users. Different scheduling techniques discussed, e.g., in [153] can avoid such a such a situation. Chapter 5, investigates this problem in detail.

The introduction of an additional slack variable γ simplifies the problem to:

$$\begin{aligned} \gamma^D = \max_{\boldsymbol{\Omega}, \gamma} \ \ & \gamma \\ \text{s.t.} \ \ & \gamma_i^D(\boldsymbol{\Omega}) \geq \gamma \ \ \forall i \in \mathcal{U} \\ & \boldsymbol{\omega}_l \in \mathcal{P} \ \ \forall l \in \mathcal{U}. \end{aligned} \tag{4.16}$$

The MBP is non-convex because of the non-convex SINR constraints for arbitrary matrices $\mathbf{R}_{l,i}$ and with the constraints (4.13) and (4.14). If a sum power constraint is used, [128] proves the global optimality for arbitrary correlation matrices (4.8) based on the Frobenius Perron theory [70].

4.3.1 Semidefinite Relaxation

The MBP is not convex for arbitrary spatial correlation matrices $\mathbf{R}_{l,i}$ and using stricter power constraints like per-BS antenna array power constraints (4.13). However, for all of these non-convex cases, the MBP can be relaxed to a quasi-convex program. The resulting convex feasibility check problem is an SDP [15]. Definition 10 presents the general form of an SDP. A bisection over γ can iterate arbitrarily tightly to the optimal value if the bisection interval is correctly chosen. This approach is a standard method of solving the MBP and is used as a reference in this chapter.

With $\mathbf{X} = [\mathbf{X}_1, \ldots, \mathbf{X}_N]$ consisting of semidefinite matrices $\mathbf{X}_l = \boldsymbol{\omega}_l \boldsymbol{\omega}_l^H$, dropping the non-convex rank-1 constraint $\text{rank}(\mathbf{X}_l) = 1\ \forall l \in \mathcal{U}$, and fixing γ, the SDP is given by [90]:

$$\text{find} \quad \mathbf{X}, \tag{4.17}$$

$$\text{s.t.} \quad -\frac{1}{\gamma}\operatorname{Tr}\{\mathbf{X}_i \mathbf{R}_{i,i}\} + \sum_{l \in \mathcal{U}, l \neq i} \operatorname{Tr}\{\mathbf{X}_l \mathbf{R}_{l,i}\} + 1 \leq 0,$$

$$\mathbf{X}_i \succeq 0, \ \operatorname{Tr}\{\mathbf{X}_i\} \leq P_i, \ \forall\, i \in \mathcal{U}. \tag{4.18}$$

In the case of a sum power constraint $\sum_{l \in \mathcal{U}} \operatorname{Tr}\{\mathbf{X}_l\} = P$ instead of (4.18), the resulting matrices are proved to all have rank 1 and are, therefore, optimal [9]. With a per-BS antenna array or per-antenna element power constraints and arbitrary spatial correlation matrices, the solution has not been proved to be globally optimal in the literature.

4.3.2 Remark on the Pareto Optimality Condition in Unicast Max–Min Beamforming

Proposition 8 and Proposition 6 of Section 4.3.4, assumes the existence of a balanced SINR among the users.

Definition 32. *A tuple of SINRs* $(\gamma_1^D, \gamma_2^D, \ldots, \gamma_M^D)$ *is balanced if*

$$\gamma_1^D = \gamma_2^D = \ldots = \gamma_M^D. \tag{4.19}$$

In general networks this condition is not always given if, e.g., per-BS antenna array power constraints are used. Figure 4.2 shows an example of a network without the existence of a balanced SINR among users when per-BS antenna power constraints are used. Two users outside the building are served by their adjacent BSs. Each user is subject to interference of the corresponding other BS. The MB will converge to a balanced SINR γ^{opt} among these two coupled users. However, there is a third user inside a building and decoupled from the other two users. This user is served by a small hotspot inside the building. If there is no interference to the outer world and there is no interference from the outer world to the user inside the building, the user is decoupled form the network. The existence of the balanced SINR depends on the power constraints:

Assuming, all BSs are subject to a per-BS antenna array power constraint (4.13), an unbalanced SINR is the result in this scenario. The BS serving the decoupled user can

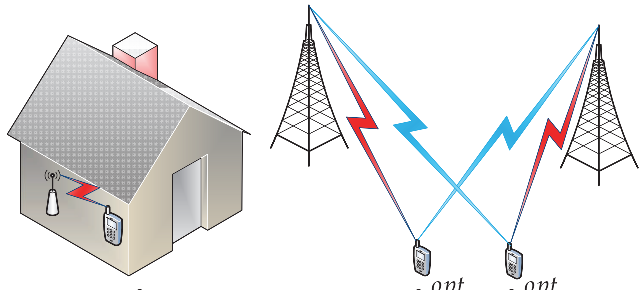

Figure 4.2: Example

increase its power until it reaches its per-BS antenna array power constraint, hence, the SINR of the decoupled user can be larger than the balanced SINR among the two interference coupled users.

The result is different if all BS are subject to a total sum power constraint (4.12) instead of the per-BS antenna array power constraints (4.13). Then, because of the sum power constraint, power of the BS inside the building[1] will be shifted to the two coupled BSs in order to increase the balanced SINR among the coupled users and the SINR of all three users can be balanced.

For the rest of this section only interference coupled networks are considered to achieve a balanced SINR. If the system is not interference coupled, the algorithm presented in Section 4.4 will not provide an optimum solution. Especially the sub-gradient projection based method of (Section 4.4.2) converges slowly if the scenario is not interference coupled. A small violation of the power constraints can be a result in case a balanced SINR can not be achieved. To ensure that a balanced SINR exists, sufficient interference is generated. This assumption is reasonable, because, e.g., cell edge users who are usually considered for cooperative beamforming are subject to strong interference. For the scenario in Fig. 4.1, a weaker antenna pattern (-3dB at 60°) and a broader angular spread (33°) is used. Typical values are between 5° up to 40° [114]. Hence, it is assumed there is a Pareto-optimal solution [165] of the balanced downlink SINR. The following definition is similar to the definition in [84, 165]

Definition 33. *A tuple* $(\gamma_1^D, \gamma_2^D, \ldots, \gamma_M^D)$ *is Pareto optimal if there is no other tuple* $(\hat{\gamma}_1^D, \hat{\gamma}_2^D, \ldots, \hat{\gamma}_M^D)$ *with*

$$(\hat{\gamma}_1^D, \hat{\gamma}_2^D, \ldots, \hat{\gamma}_M^D) \geq (\gamma_1^D, \gamma_2^D, \ldots, \gamma_M^D)$$

(the inequality is component-wise) and

$$(\hat{\gamma}_1^D, \hat{\gamma}_2^D, \ldots, \hat{\gamma}_M^D) \neq (\gamma_1^D, \gamma_2^D, \ldots, \gamma_M^D)$$

Networks where a Pareto optimal balanced DL SINR for the given power constraints exist, are defined as balanced interference coupled networks in this thesis. The more general scenario, with the lack of a balanced SINR, is discussed in Sec-

[1] if the channel conditions of the third user are better the channel conditions of the two coupled users

tion 4.6.2. More details concerning conditions for a balanced SINR are also explained in [129, 130].

4.3.3 Equivalent Quasi-Convex Form

Quasi-convex optimization problems have the advantage of the existence of a unique optimum. Optimization problems are called quasi-convex if the objective function [15] is quasi-convex and the constraints are convex. Such a problem can be solved by the surrogate dual problem [107].

The theory of surrogate duality is used to derive the dual UL problem of the MBP. This dual UL problem offers a low complexity algorithm which solves the MBP. In general, the problem (4.15) is non-convex because of the non-convex objective function over $\mathbf{\Omega}$:

$$f(\mathbf{\Omega}) = \min_{i \in \mathcal{U}} \frac{\boldsymbol{\omega}_i^H \mathbf{R}_{i,i} \boldsymbol{\omega}_i}{\sum_{\substack{l \in \mathcal{U} \\ l \neq i}} \boldsymbol{\omega}_l^H \mathbf{R}_{l,i} \boldsymbol{\omega}_l + 1}. \tag{4.20}$$

The domain $\mathcal{P}$ of the objective function is determined by the power constraints. Due to the power constraints the value of the minimum SINR is bounded: $0 \leq f(\mathbf{\Omega}) < \infty$. If instantaneous CSI is available at the BSs, the MBP has an equivalent quasi-convex form for a sum power constraint, for per-antenna array and for per-antenna power constraints (see Proposition 2). It is desired to maximize (4.20); hence, the objective function must have an equivalent quasi-concave form to prove that the MBP has an equivalent quasi-convex form.

Proposition 2. *Let γ^D denote the solution of the MBP* (4.15)*. Then the MBP* (4.15) *has an equivalent quasi-convex form with an optimal solution γ^{*D} for the given power constraints* (4.12)-(4.14) *and in the case of instantaneous CSI and matrices $\mathbf{R}_{l,i}$ defined in* (4.7)*. Consequently $\gamma^D = \gamma^{*D}$ holds.*

Proof. The point-wise minimum of a quasi-concave function is quasi-concave. Therefore, only the upper level sets (see Definition 18)

$$\mathcal{S}_{\gamma,i} = \{\mathbf{\Omega} \in \mathcal{P} : \frac{\boldsymbol{\omega}_i^H \mathbf{R}_{i,i} \boldsymbol{\omega}_i}{\sum_{\substack{l \in \mathcal{U} \\ l \neq i}} \boldsymbol{\omega}_l^H \mathbf{R}_{l,i} \boldsymbol{\omega}_l + 1} \geq \gamma\} \tag{4.21}$$

must be convex. The same idea as, e.g., in [9, 163] is used to prove the convexity of the SINR constraint

$$\frac{1}{\gamma} \boldsymbol{\omega}_i^H \mathbf{R}_{i,i} \boldsymbol{\omega}_i \geq \sum_{l \in \mathcal{U}, l \neq i} \boldsymbol{\omega}_l^H \mathbf{R}_{l,i} \boldsymbol{\omega}_l + 1. \tag{4.22}$$

An arbitrary phase rotation of the beamforming vectors does not affect the SINR [9], if instantaneous CSI is given. Hence, the constraint (4.22) can be rewritten as in [9]:

$$\frac{1}{\sqrt{\gamma}\sigma_i} \mathbf{h}_{i,i}^H \boldsymbol{\omega}_i \geq \sqrt{\sum_{l \in \mathcal{U}, l \neq i} \boldsymbol{\omega}_l^H \mathbf{R}_{l,i} \boldsymbol{\omega}_l + 1}, \text{ with } \operatorname{Im}\{\mathbf{h}_{i,i}^H \boldsymbol{\omega}_i\} = 0, \; \mathbf{h}_{i,i}^H \boldsymbol{\omega}_i \geq 0, \tag{4.23}$$

if $\mathbf{R}_{l,i}$ is given by (4.7). The constraint (4.23) is a second order cone constraint [15] for a fixed parameter γ. With the SINR constraint (4.23) and per-antenna power constraints, the MBP (4.15) can be rewritten as a SOCP. □

For a fixed (constant) γ, the feasibility check problem of the MBP can be expressed as a SOCP (see Definition 9). The upper level sets of the equivalent form of the objective function are convex. Consequently the objective function has an equivalent quasi-concave form. With the convex form of the SINR constraint (4.23), the MBP can be solved with the following convex feasibility check problem similar to [9]:

$$\begin{aligned} \text{find} \quad & \boldsymbol{\Omega} \\ \text{s.t.} \quad & \frac{1}{\sigma_i\sqrt{\gamma}}\mathbf{h}_{i,i}^H\boldsymbol{\omega}_i \geq \sqrt{\sum_{l\in\mathcal{U},l\neq i}\boldsymbol{\omega}_l\mathbf{R}_{l,i}\boldsymbol{\omega}_l + 1} \\ & |[\mathbf{w}_i]_a|^2 \leq P_{i,a} \ \ \mathrm{Im}\{\mathbf{h}_{i,i}^H\boldsymbol{\omega}_i\} = 0, \ \ \mathbf{h}_{i,i}^H\boldsymbol{\omega}_i \geq 0, \ \forall i,a. \end{aligned} \tag{4.24}$$

A bisection over γ can iterate arbitrarily closely to the global optimum if the bisection interval is correctly chosen. In the case of per-antenna array power constraints, the feasibility check problem can be analogously derived.

Note, the SINR constraints (4.22) are only convex for a fixed parameter γ and if the spatial correlation matrices have rank 1. In the case of instantaneous CSI this is always satisfied. However, arbitrary spatial correlation matrices do not have rank-1 in general. In this case, the spatial correlation matrices (4.8) will usually have a higher rank. Therefore, this technique can not be used to prove the transformation to an equivalent quasi-convex problem if arbitrary long-term CSI is given. Furthermore, the proof only holds for the unicast case, because then an arbitrary phase rotation of the beamforming vector does not affect the SINR. The SINR constraints become real valued and can be written as a second order cone constraint. In the case of more than one user per transmit antenna array vector (multicast case), not all SINR constraints[2] can be made real valued by an arbitrary phase rotation at each BS antenna array. The multicast case[3] with long-term CSI is discussed in Part II of this thesis.

However, this kind of solution still requires a convex solver to solve the convex feasibility check problem. Therefore, the work of [116] proposes a more elegant way of solving the MBP based on the PMP. The PMP corresponds to the feasibility check problem of the MBP. Hence instead of the convex solver, the iterative algorithm developed in [163] can be used for a bisection. However, the iterative solution presented in [163] works with rank-1 spatial correlation matrices or instantaneous CSI and is based on two loops. The solution, presented in the next section, also consists of two loops and solves the MBP directly.

4.3.4 Duality Theory of the Max–Min Beamforming Problem

The dual problem of the MBP formulated in this section delivers an iterative solution based on simpler mathematical operations than in the primal downlink case. Sec-

[2] the SINR constraints for all users belonging to the same multicast group

[3] which also covers the unicast case

tion 4.4 presents the details of the iterative solution which is based on the surrogate dual problem of the MB derived in this section.

The previous Section 4.3.3 presents an equivalent quasi-convex form of the MBP. A quasi-convex problem can be solved directly by using the convex feasibility check problem of the primal problem. A simple bisection over multiple convex feasibility check problems can be made to iterate until a tolerance of ϵ to the optimal solution is reached [15]. This section introduces a duality framework for the MBP with multiple power constraints. The derived dual UL problem can be solved efficiently and finds the same SINR as the original MBP. Furthermore, the dual problem can be solved iteratively based on simpler mathematical operations.

4.3.4.1 Surrogate Duality for the Max–Min Beamforming Problem

This section introduces a new framework for a dual UL problem that is equivalent to the original MBP (4.15) if both, instantaneous CSI, or arbitrary long-term CSI in the form of higher rank spatial correlation matrices is available. Section 4.3.3 illustrates that the MBP has equivalent quasi-convex form if instantaneous CSI is available. A quasi-convex problem can be solved directly by using the convex feasibility check problem of the primal problem.

In [116], the authors propose a similar way to solve the unicast MBP. However, instead of the feasibility check problem of the primal problem, the dual UL problem of the PMP is used which is equivalent to the MBP for a given SINR γ. In [32], a direct solution based on the dual UL problem was proposed. The proposed iterative algorithm is derived based on the Lagrangian dual problem, which provides an upper bound of optimal solution. However, the MBP with more general power constraints, e.g., per-BS antenna array power constraints has merely an equivalent quasi-convex form. Therefore, the strong duality of the Lagrangian dual problem can not be proved so easily in this case. The Lagrangian dual is a tight bound if the original problem is convex and has a non-empty interior [15].

This section proposes an alternative and simpler framework for UL–DL duality based on the work on surrogate duality in quasi-convex programming of D. Luenberger [107]. The surrogate dual provides a tight bound and it can be proved, that the Lagrangian dual problem is equivalent to the surrogate dual, consequently strong duality is also given for the Lagrangian dual.

Several publications on quasi-convex programming exist (e.g., [107]), and several dual problems have been proposed. A detailed overview of the surrogate duality theory is presented in Section 3.3.2.

This duality theory is used in this section to derive a dual UL problem of the unicast MBP. The multiple power constraints are combined to a single power constraint as shown in (3.30). At this point it could be helpful to give a short overview of the propositions for the duality proof in this chapter:

- The combination of multiple power constraints to a single weighted sum power constraint results in a UL MBP with an inner and an outer problem. The inner problem corresponds to a DL MBP with a weighted sum power constraint. Transformation of this problem to the UL domain leads to a problem which can be solved globally optimal. The Lagrangian dual UL problem of this problem is presented in Lemma 4. Strong duality is proved for the sum power constrained case, consequently, the Lagrangian duality is tight.

- In Proposition 3, the surrogate dual function is derived by using the previous result in Lemma 4. The surrogate dual function combines multiple power constraints to a single weighted sum power constraint. This surrogate function is transformed to the UL domain where it can be solved efficiently. The surrogate function in the UL domain leads to the surrogate dual problem of the original MBP with multiple power constraints.

- The question is now whether this surrogate dual problem solves the MBP with multiple power constraints. In the case of instantaneous CSI or rank-1 spatial correlation matrices, an equivalent quasi-convex form exists. Based on the equivalent quasi-convex form, strong (surrogate) duality can be directly proved with the duality theorem of Luenberger (Theorem 2). This is proved for Proposition 5.

- If arbitrary long-term CSI in the form of higher-rank spatial correlation matrices is given no equivalent quasi-convex form is known. Thus Theorem 2 can not be applied. Based on Theorem 4, Proposition 6 represents an alternative proof for strong duality in the case of per BS power constraints and one power constraint is satisfied.

- With the help of Theorem 5, Proposition 7 states that the surrogate dual problem is quasi-convex; hence, a global optimal value exists.

- Proposition 8 shows the equivalence of the surrogate dual problem and the Lagrangian dual problem of the MBP with more general power constraints. According to Theorem 6, it follows that the weighted sum power constraint is satisfied with equality.

The derivation of the surrogate dual problem is based on an inner MBP with a weighted sum power constraint and its Lagrangian dual problem, which is tight if a sum power constraint is given. Consider the following unicast DL MBP where the weighted sum power is limited to P:

$$f^D(\boldsymbol{\mu}) = \max_{\boldsymbol{\Omega}} \min_{i \in \mathcal{U}} \gamma_i^D(\boldsymbol{\Omega}) \tag{4.25}$$

$$\text{s.t.} \sum_{i \in \mathcal{U}} \boldsymbol{\omega}_i^H \mathbf{M}_i \boldsymbol{\omega}_i \leq P. \tag{4.26}$$

where $\mathbf{M}_i = \operatorname{diag}(\mu_{i,1}, \ldots, \mu_{i,N_A}) \succeq 0$ in the case of per-antenna array element power constraints and $\mathbf{M}_i = \mu_i \mathbf{I}_{N_A} \succeq 0$ in the case of per-BS antenna array power constraints. The vector $\boldsymbol{\mu}$ is the vector of all $\mu_{i,a}$s or μ_is. For a fixed $\boldsymbol{\mu}$, this problem is an MBP with a weighted sum power constraint. The Lagrangian dual UL problem is given by the following lemma:

Lemma 4. *With the definition of the UL SINR* (4.10)*, the Lagrangian dual of the unicast DL MBP* (4.25), (4.26) *is given by*

$$f^U(\boldsymbol{\mu}) = \max_{\boldsymbol{\lambda},\mathbf{V}} \min_{i\in\mathcal{U}} \gamma_i^U(\boldsymbol{\mu},\boldsymbol{\lambda},\mathbf{v}_i) \tag{4.27}$$

$$\text{s.t.} \sum_{i\in\mathcal{U}} \lambda_i \leq P \tag{4.28}$$

$$\lambda_i \geq \mathbf{0},\ \forall\, i \in \mathcal{U}. \tag{4.29}$$

At the optimum, the power constraints of problems (4.25) *and* (4.27) *are satisfied with equality and both problems have the same SINR* $f^U(\boldsymbol{\mu}) = f^D(\boldsymbol{\mu})$ *for a* $\boldsymbol{\mu} \geq \mathbf{0}$ *and* $\boldsymbol{\mu} \neq \mathbf{0}$.

Proof. The derivation of the Lagrangian dual problem is a simple extension of [57]. The proof of the strong duality is an extension of [128, Lemma 2]. [19, 20] presents the duality in the case of instantaneous CSI or rank-1 spatial correlation matrices and per-BS power constraints. The proof for the case of per-antenna power constraints is a straightforward extension and presented in Appendix A.1. □

Remark 1. *Note that* $\boldsymbol{\lambda} = \mathbf{0}$ *results in* $\gamma^U = 0$ *which can not be an optimal solution. Consequently, we can also restrict* $\boldsymbol{\lambda}$ *to* $\boldsymbol{\lambda} > \mathbf{0}$.

Proposition 3. *With the diagonal matrices* $\mathbf{P}_i = \mathrm{diag}(P_{i,1}, \ldots, P_{i,N_A})$ *in the case of per-antenna power constraints, or diagonal matrices* $\mathbf{P}_i = \frac{P_i}{N_A}\mathbf{I}_{N_A}$ *in the case of per-BS array power constraints, the surrogate dual function (or surrogate problem) of the unicast DL MBP* (4.15) *with general (per-antenna or per-antenna array) power constraints is given by*

$$s^U(\boldsymbol{\mu}) = \max_{\boldsymbol{\lambda},\mathbf{V}} \min_{i\in\mathcal{U}} \gamma_i^U(\boldsymbol{\mu},\boldsymbol{\lambda},\mathbf{v}_i) \tag{4.30}$$

$$\text{s.t.} \sum_{i\in\mathcal{U}} \lambda_i \leq \sum_{i\in\mathcal{U}} \mathrm{Tr}\{\mathbf{M}_i\mathbf{P}_i\}$$

$$\lambda_i \geq 0,\ \ \mathbf{M}_i \succeq 0,\ \forall\, i \in \mathcal{U}.$$

for a $\boldsymbol{\mu} \geq \mathbf{0}$ *and* $\boldsymbol{\mu} \neq \mathbf{0}$.

Proof. The surrogate dual function of the MBP with per-antenna power constraints is given by

$$s^D(\boldsymbol{\mu}) = \max_{\boldsymbol{\Omega}} \min_{i\in\mathcal{U}} \gamma_i^D(\boldsymbol{\Omega}) \tag{4.31}$$

$$\text{s.t.}\ \ p_\Sigma(\boldsymbol{\mu},\boldsymbol{\Omega}) \leq 0. \tag{4.32}$$

$$\mathbf{M}_i \succeq 0\ \ \forall\, i \in \mathcal{U}.$$

With the diagonal matrices $\mathbf{P}_i = \mathrm{diag}(P_{i,1}, \ldots, P_{i,N_A})$, the per-antenna power constraints are combined to the weighted sum power constraint:

$$p_\Sigma(\boldsymbol{\mu},\boldsymbol{\Omega}) = \sum_{i\in\mathcal{U}} \sum_{a\in\mathcal{A}_i} \mu_{i,a}(|[\boldsymbol{\omega}_i]_a|^2 - P_{i,a}) \leq 0 \Leftrightarrow \sum_{i\in\mathcal{U}} \boldsymbol{\omega}_i^H\mathbf{M}_i\boldsymbol{\omega}_i \leq \sum_{i\in\mathcal{U}} \mathrm{Tr}\{\mathbf{M}_i\mathbf{P}_i\}.$$

With the diagonal matrices $\mathbf{P}_i = \frac{P_i}{N_A}\mathbf{I}_{N_A}$, the per-antenna array power constraints are combined to the weighted sum power constraint:

$$p_\Sigma(\boldsymbol{\mu}, \boldsymbol{\Omega}) = \sum_{i\in\mathcal{U}} \mu_i(\boldsymbol{\omega}_i^H\boldsymbol{\omega}_i - P_i) \leq 0 \Leftrightarrow \sum_{i\in\mathcal{U}} \boldsymbol{\omega}_i^H\mathbf{M}_i\boldsymbol{\omega}_i \leq \sum_{i\in\mathcal{U}} \mathrm{Tr}\{\mathbf{M}_i\mathbf{P}_i\}.$$

Thus, the problem (4.31) can be stated as:

$$s^D(\boldsymbol{\mu}) = \max_{\boldsymbol{\Omega}} \min_{i\in\mathcal{U}} \gamma_i^D(\boldsymbol{\Omega}) \tag{4.33}$$

$$\text{s.t.} \sum_{i\in\mathcal{U}} \boldsymbol{\omega}_i^H\mathbf{M}_i\boldsymbol{\omega}_i \leq \sum_{i\in\mathcal{U}} \mathrm{Tr}\{\mathbf{M}_i\mathbf{P}_i\} \tag{4.34}$$

$$\mathbf{M}_i \succeq 0, \ \ \forall i \in \mathcal{U}.$$

With $P = \sum_{i\in\mathcal{U}} \mathrm{Tr}\{\mathbf{M}_i\mathbf{P}_i\}$ and Lemma 4, the problem (4.33) can be transformed to the UL domain and the problem (4.30) is the result. □

Proposition 4. *If instantaneous CSI according to* (4.7) *is given, let $s^{*D}(\boldsymbol{\mu})$ denote the surrogate dual of the equivalent quasi-convex form of the original MPB* (4.15)*, then $s^{*D}(\boldsymbol{\mu}) = s^D(\boldsymbol{\mu})$ holds.*

Proof. The proof is a straightforward extension of [157]. □

Lemma 5. *The objective function* (4.20) *is a continuous function.*

Proof. The proof is straightforward and presented in Appendix A.3. □

Assuming there exists an equivalent quasi-convex form of the MBP (4.15), the proof of strong duality is straightforward with the help of Theorem 4.

Proposition 5. *If the primal unicast DL MBP* (4.15) *has an equivalent quasi-convex form which has the solution γ^{*D}, the optimal solution γ^D of* (4.15) *is given by*

$$\gamma^D = \gamma_S^U = \min_{\boldsymbol{\mu}} s^U(\boldsymbol{\mu}) \tag{4.35}$$

for a $\boldsymbol{\mu} \geq \mathbf{0}$ and $\boldsymbol{\mu} \neq \mathbf{0}$.

Proof. Problem (4.35) is the surrogate dual problem. Proposition 3 proves the lack of a duality gap for the inner problem hence,

$$s^D(\boldsymbol{\mu}) = s^U(\boldsymbol{\mu})$$

holds. Consequently, also

$$\gamma_S^D = \min_{\boldsymbol{\mu}} s^D(\boldsymbol{\mu}) = \min_{\boldsymbol{\mu}} s^U(\boldsymbol{\mu}) = \gamma_S^U \tag{4.36}$$

holds. Lemma 5 states that the objective function is continuous. According to the duality theorem of Luenberger (Theorem 2), strong duality between the surrogate dual problem and the primal problem holds if the primal problem is quasi-convex, assuming γ^{*D} is the solution of the equivalent quasi-convex form of the MBP (4.15) and $s^{*D}(\boldsymbol{\mu})$ is the equivalent quasi-convex form of the surrogate function. Due to (4.36), also

$$\gamma^{*D} = \min_{\boldsymbol{\mu}} s^{*D}(\boldsymbol{\mu}) = \min_{\boldsymbol{\mu}} s^{*U}(\boldsymbol{\mu}) = \gamma_S^{*U} \tag{4.37}$$

holds. Since $s^{*D}(\boldsymbol{\mu}) = s^D(\boldsymbol{\mu})$, $s^{*U}(\boldsymbol{\mu}) = s^U(\boldsymbol{\mu})$ and since $\gamma_S^{*U} = s^U(\boldsymbol{\mu})$, and $\gamma^{*D} = \gamma^D$ holds,[4] (4.35) holds as well. □

Given arbitrary higher rank spatial correlation matrices as (4.8), the proof of strong duality is not straightforward, because, then, no equivalent quasi-convex form of the MBP is known. The following proposition formulates the general duality result for the case of higher rank spatial correlation matrices.

Proposition 6. *Assuming per BS power constraints and only one power constraint is active in the original problem* (4.15)*. Given arbitrary higher rank spatial correlation matrices as* (4.8)*, the solution of the dual UL problem is equal to the solution of the primal unicast DL MBP* (4.15)*. Hence, with* $\boldsymbol{\mu} \neq \mathbf{0}$ *and* $\gamma_S^U = \gamma^D$*, the solution is given by*

$$\gamma_S^U = \min_{\boldsymbol{\mu}} s^U(\boldsymbol{\mu}). \tag{4.38}$$

Proof. Due to $s^D(\boldsymbol{\mu}) = s^U(\boldsymbol{\mu})$, also

$$\gamma_S^D = \min_{\boldsymbol{\mu}} s^D(\boldsymbol{\mu}) = \min_{\boldsymbol{\mu}} s^U(\boldsymbol{\mu}) = \gamma_S^U \tag{4.39}$$

holds. Assume $\boldsymbol{\Omega}^*$ is optimal for the surrogate dual problem. The question is whether $\gamma_S^D = \gamma^D$. If an $\boldsymbol{\Omega}^*$ is feasible in $s^D(\boldsymbol{\mu}^*)$, there must be a $\boldsymbol{\mu}^* \geq \mathbf{0}$ and $\boldsymbol{\mu}^* \neq \mathbf{0}$ which is also feasible in (4.15) according to Theorem 4. We must show the feasibility of $\boldsymbol{\Omega}^*$ in the original problem so that $\boldsymbol{\omega}_k^{*H}\boldsymbol{\omega}_k^* \leq P_k \ \forall k \in \mathcal{U}$. Let $\boldsymbol{\mu}_k^* \in \mathbb{R}^{M\times 1}$ be a vector with exactly one non-zero element, $\mu_k^* > 0$. Then, the surrogate problem is

$$s^D(\boldsymbol{\mu}_k^*) = \max_{\boldsymbol{\Omega}} \min_{i\in\mathcal{U}} \gamma_i^D(\boldsymbol{\Omega}) \tag{4.40}$$

$$\text{s.t.} \;\; \mu_k^* \boldsymbol{\omega}_k^H \boldsymbol{\omega}_k \leq \mu_k^* P_k \;\; \mu_k > 0. \tag{4.41}$$

where (4.41) is finally $\boldsymbol{\omega}_k^H\boldsymbol{\omega}_k \leq P_k$. The kth constraint of the original problem (4.15) is satisfied if the constraint (4.41) of surrogate problem $s^D(\boldsymbol{\mu}_k^*)$ is satisfied. As in [20, Theorem 4], let $\mathcal{P}$ denotes the feasible set of the original problem (4.15), and

$$\mathcal{P}_k^D = \{\boldsymbol{\Omega}_k^* \in \mathbb{C}^{N_A\times M} \;:\; \boldsymbol{\omega}_k^H\boldsymbol{\omega}_k \leq P_k\}$$

denotes the feasible set of (4.40), (4.41), then $\mathcal{P} = \cap_{k\in\mathcal{U}}\mathcal{P}_k^D$. Furthermore, the SINR is balanced and $s(\boldsymbol{\mu}_k^*)$ is the corresponding SINR. According to Lemma **??**, the index

$$k^* = \text{argmin}_{k\in\mathcal{U}}\{s^D(\boldsymbol{\mu}_k^*)\}$$

[4] In the case of instantaneous CSI and a weighted sum power constraint or per-antenna or per-antenna array power constraints, the MBP has an equivalent quasi-convex form (see Propositions 2 and 4).

can be seen as the limiting link of the fair system where all power constraints are satisfied.

According to Theorem 4, $\mathbf{\Omega}_{k^*}^* \in \mathcal{P}$ solves the surrogate dual problem for a $\boldsymbol{\mu}_{k^*}^* \geq \mathbf{0}$, $\boldsymbol{\mu}_{k^*}^* \neq \mathbf{0}$ and is also feasible in the primal problem (4.15). Consequently, according to Theorem 4, the solution of the surrogate dual problem is a tight upper bound. □

From the proof we can also observe that the worst link k^* determines the SINR of the entire system.

The question is now whether (4.38) attains the optimal value. In [60], the authors prove that the surrogate dual provides a tighter bound than the Lagrangian dual. The following proposition declares the quasi-convexity of the surrogate dual problem.

Proposition 7. *The surrogate dual problem* (4.38) *can be globally optimally solved.*

Proof. Due to Theorem 5, the surrogate dual function is quasi-convex, hence a global minimizer can attain the value of the global minimum. □

If a balanced SINR according to Definition 32 exists, the Lagrangian dual problem and the surrogate dual problem of the MBP (4.15) are equivalent. A balanced SINR may not exist if, e.g., a user does not receive any interference from other BSs in the network; hence the network is not interference coupled. More details concerning conditions for a balanced SINR are explained in [129,130]. The following proposition is used in the next section for the derivation of the iterative algorithm.

Proposition 8. *If a balanced SINR according to Definition 32 exists, the Lagrangian dual problem of the MBP* (4.15) *is given by*

$$\begin{aligned} \gamma_L^U = \min_{\boldsymbol{\mu}} \max_{\boldsymbol{\lambda}, \mathbf{V}} \min_{i \in \mathcal{U}} \; & \gamma_i^U(\boldsymbol{\mu}, \boldsymbol{\lambda}, \mathbf{v}_i) \\ \text{s.t.} \; & \sum_{i \in \mathcal{U}} \lambda_i \leq \sum_{i \in \mathcal{U}} \mathrm{Tr}\{\mathbf{M}_i \mathbf{P}_i\}, \\ & \lambda_i \geq 0, \;\; \mathbf{M}_i \succcurlyeq 0, \; \forall\, i \in \mathcal{U}. \end{aligned} \tag{4.42}$$

and at the optimum the weighted sum power constraint (4.34) *is satisfied with equality.*

Proof. The derivation of the Lagrangian is presented in Appendix A.2. The surrogate dual (4.38) is equivalent to the Lagrangian dual problem (4.42), $\gamma_L^U = \gamma_S^U$. According to Theorem 6, the weighted sum power constraint (4.34) is satisfied with equality. □

4.4 Iterative Algorithm for Interference Coupled Networks

The structure of the dual UL problem (Proposition 6) offers a solution based on simple mathematical operations. The solution consists of an outer minimization over $\boldsymbol{\mu}$ (4.38) and an inner maximization over $\boldsymbol{\lambda}$ and $\mathbf{V}$ (4.30). Thus, two loops (an inner and an outer loop) as in [163] are used in what follows. In [110], the authors proposed a heuristic extension of Schubert's and Boche's method [128] to jointly satisfy the multiple power constraints based on a subgradient method as in [163].

The previous works of this thesis [37, 40] directly derive a solution based on in inner and outer loop for the MBP. The problem (4.25), (4.26) corresponds to an MBP with a weighted sum power constraint. For the problems (4.25), (4.26) and (4.27), (4.28) strong duality is proved in Lemma 4. The corresponding UL problem (4.27), (4.28) is reduced to a computation of the largest eigenvalue and the corresponding eigenvector. This chapter presents an iterative computation of the largest eigenvector instead of an eigenvector decomposition. In [56], the so-called power iteration is shown to be a low complexity solution if only the largest eigenvalue is desired.

Regarding the surrogate dual problem (4.38), the inner problem in the downlink domain for fixed $\boldsymbol{\mu}$ is just an MBP as in [19], [144], with a weighted sum power constraint, where each beamforming vector is scaled by $\mathbf{M}_i$. However, in contrast to [19] and [144], the CSI is given here in the form of higher rank spatial correlation matrices. In the following section (Section 4.4.1), a low complexity method based on an iterative computation of the UL beamforming vectors and the UL power $\boldsymbol{\lambda}$ for a fixed vector $\boldsymbol{\mu}$ is presented. Section 4.4.2 presents a solution, similar to [163], where the optimal vector $\boldsymbol{\mu}$ is found by a subgradient projection algorithm in an outer loop. However, it is known that a subgradient projection method requires a properly chosen step size; otherwise, the convergence is very slow [163]. Therefore, a faster converging low complexity method based on a simple scaling of the μ_is or $\mu_{i,a}$s is presented as well. The iterative algorithm has a lower complexity than to the convex solver based methods, especially for a low accuracy.

4.4.1 Inner Loop

The inner function corresponds to an MBP with a weighted sum power constraint. The inner maximization in the dual UL problem (4.27) of (4.25) is optimized over $\boldsymbol{\lambda}$ and $\mathbf{V}$. This is done iteratively in the inner loop by first computing the optimal receive beamforming vectors $\mathbf{v}_i$s and then updating the optimal UL power allocation $\boldsymbol{\lambda}$ for fixed $\mathbf{V}$ until convergence is achieved. In [157] and [144], where instantaneous CSI is used, a fixed point iteration for the $\boldsymbol{\lambda}$ vector is introduced. The convergence is proved in [19]. The authors of [19] use instantaneous CSI to balance the SINR. Using these resulting rank-1 matrices, an optimal closed form solution is given by the minimum variance distortion-less response (MVDR) beamformers. For a given $\boldsymbol{\lambda}$ vector, a closed form solution for the UL beamformers exists. In contrast to that, the MBP is based here on higher rank spatial correlation matrices. Consequently, no closed form solution exists. A solution based on higher rank spatial correlation matrices for a sum power constraint MBP is already proposed in [128]. In [57], a solution with reduced complexity compared to [128] is proposed. In [57], in each iteration a complete matrix inversion of the interference matrix

$$\mathbf{\Sigma}_i = \mathbf{M}_i + \sum_{l \in \mathcal{U}, l \neq i} \lambda_l \mathbf{R}_{i,l} \tag{4.43}$$

and an eigenvalue decomposition is calculated. The inner problem (4.27) of the surrogate dual problem is the maximization of the balanced UL SINR (4.10) and is equivalent to the eigenproblem

$$\mathbf{R}_{i,i}\mathbf{v}_i = \chi_{i,n}\mathbf{\Sigma}_i\mathbf{v}_i, \tag{4.44}$$

with the largest eigenvalue $\chi_{i,max} = \max_{1 \leq n \leq N_A}(\chi_{i,n}) = (\lambda_i)^{-1}$. The matrix $\mathbf{\Sigma}_i$ is regular if all $\mathbf{R}_{i,l}$ are positive definite, hence, the generalized eigensystem can be transformed to a special eigensystem [56] and the UL power can be directly computed as in [57]:

$$\lambda_i = \frac{1}{\chi_{i,max}(\mathbf{\Sigma}_i^{-1}\mathbf{R}_{i,i})} \tag{4.45}$$

The convergence of the resulting fixed point iteration is proved in [19].

This chapter proposes a further complexity reduction, as a complete eigenvalue decomposition is not necessary. The eigenvalues corresponding to the UL power and the eigenvectors corresponding to the UL beamformers can be computed iteratively and jointly with the uplink power computation. Hence, compared to [57], less complexity per iteration is achieved, because instead of an eigenvalue decomposition, just a matrix vector multiplication $\mathbf{v}_i = \mathbf{\Sigma}_i^{-1}\mathbf{R}_{i,i}\mathbf{v}_i$ is performed. If $(\lambda_i)^{-1}$ is strictly the largest eigenvalue, the eigensystem can be solved iteratively by the power iteration [56]. The inverse of the largest eigenvalue $\chi_{i,max}(\mathbf{\Sigma}_i^{-1}\mathbf{R}_{i,i})$ corresponds to UL power λ_i which is computed for fixed $\mathbf{V}$ directly by

$$\lambda_i = \frac{\mathbf{v}_i^H\mathbf{\Sigma}_i\mathbf{v}_i}{\mathbf{v}_i^H\mathbf{R}_{i,i}\mathbf{v}_i}. \tag{4.46}$$

The power iteration is a low complex algorithm for finding the dominant eigenvector of an eigensystem [56]. It is listed in Algorithm 4. As in [144] and [57], the λ_is are scaled such that the constraint $\sum_{i \in \mathcal{U}} \lambda_i \leq \sum_{i \in \mathcal{U}} \mathrm{Tr}\{\mathbf{M}_i\mathbf{P}_i\}$ of the dual problem in (4.30) is satisfied with equality.

If there exists a unique spectral radius

$$\rho(\mathbf{\Sigma}_i^{-1}\mathbf{R}_{i,i}) = \max_{1 \leq n \leq N_A}(\chi_{i,n}(\mathbf{\Sigma}_i^{-1}\mathbf{R}_{i,i}))$$

of the matrix $\mathbf{\Sigma}_i^{-1}\mathbf{R}_{i,i}$, the power iteration will converge. The convergence is geometric with a ratio of the largest eigenvalue to the second largest eigenvalue [56]. If the largest eigenvalue is significantly larger than the second largest eigenvalue, the convergence of the inner loop is very fast. The numerical results suggest that the case of multiple identical eigenvalues does not occur. The inner loop converges after 29 iterations for a accuracy of 10^{-5}.

Algorithm 4 Inner loop: vector iteration

repeat
  for $i = 1$ to M **do**
    $\mathbf{v}_i \leftarrow \mathbf{\Sigma}_i^{-1}\mathbf{R}_{i,i}\mathbf{v}_i$
    Set $\|\mathbf{v}_i\| = 1 \;\; \forall i \in \mathcal{U}$
    $\lambda_i \leftarrow \frac{\mathbf{v}_i^H \mathbf{\Sigma}_i \mathbf{v}_i}{\mathbf{v}_i^H \mathbf{R}_{i,i}\mathbf{v}_i}$
  end for
  $\lambda_i = \beta\tilde{\lambda}_i, \forall i \in \mathcal{U}$, with $\beta = \frac{\sum_{i\in\mathcal{U}} \mathrm{Tr}\{\mathbf{M}_i\mathbf{P}_i\}}{\sum_{i\in\mathcal{U}} \tilde{\lambda}_i}$
until convergence
$\mathbf{p} = (\frac{1}{\gamma}\mathbf{D}^{-1} - \mathbf{\Psi})^{-1}\mathbf{1}$
return $\mathbf{V}$, $\gamma_{opt}^{U} = \beta$

After obtaining the normalized UL beamformer, the DL beamforming weights can be obtained by $\mathbf{w}_i = \sqrt{p_i}\mathbf{v}_i$. In Appendix A.1, the DL power vector $\mathbf{p}$ is derived and given by

$$\mathbf{p} = (\frac{1}{\gamma}\mathbf{D}^{-1} - \mathbf{\Psi})^{-1}\mathbf{1} \tag{4.47}$$

if $\gamma = \gamma^D = \gamma^U$. Algorithm 4 has similarities to the solution proposed in [19]. However, the proposed solution is also able to solve the MBP if long-term CSI in the form of higher rank spatial correlation matrices is available.

4.4.2 Outer Loop

The outer loop minimizes $f^D(\boldsymbol{\mu})$ (4.25) such that the given transmit power constraints are met. In this chapter, two methods for updating the $\boldsymbol{\mu}$ vector or the $\mathbf{M}_i$ matrices are proposed:

1. **Method 1: Subgradient projection method**: The update of the $\boldsymbol{\mu}$ is based on the subgradient method such that $\sum_{i\in\mathcal{U}} \boldsymbol{\omega}_i^H \mathbf{M}_i \boldsymbol{\omega}_i$ equal to the total power P [32]. This method is based on the subgradient projection method proposed in [163] for the power minimization problem. Later, [21] proposed a subgradient projection method which solves the MBP directly.

2. **Method 2: Low complexity μ-scaling (μ-SC)**: In the constraint (4.34), the two sums are weighted sums over $\boldsymbol{\mu}$. Since, the constraint is satisfied with equality at the optimum (Proposition 8),

$$\sum_{i\in\mathcal{U}} \mathrm{Tr}\{\mathbf{M}_i\mathbf{P}_i\} = \sum_{i\in\mathcal{U}} \boldsymbol{\omega}_i^H \mathbf{M}_i \boldsymbol{\omega}_i \tag{4.48}$$

the $\mathbf{M}_i$s can be updated by comparing the power coupled with each $\mathbf{M}_i$ with $\mathbf{P}_i$ and then scaling the $\mu_{i,a}$s such that the constraint in (4.34) is satisfied with equality [32]. Let $\hat{\mathbf{M}}_i$ be the value of $\mathbf{M}_i$ of the previous iteration, the $\mathbf{M}_i$ s are computed by the following update in the case of per-antenna power constraints:

$$\tilde{\mathbf{M}}_i = \mathrm{diag}(\boldsymbol{\omega}_i \boldsymbol{\omega}_i^H)\mathbf{P}_i^{-1}\hat{\mathbf{M}}_i, \quad \mathbf{M}_i = \frac{\mathbf{1}^T\mathbf{p}}{\sum_{i\in\mathcal{U}} \mathrm{Tr}\{\tilde{\mathbf{M}}_i\mathbf{P}_i\}}\tilde{\mathbf{M}}_i. \tag{4.49}$$

In the case of per-BS antenna array power constraints the update is similar:

$$\tilde{\mathbf{M}}_i = \frac{[\mathbf{p}]_i}{P_i}\hat{\mathbf{M}}_i, \quad \mathbf{M}_i = \frac{\mathbf{1}^T\mathbf{p}}{\sum_{i\in\mathcal{U}} \mathrm{Tr}\{\tilde{\mathbf{M}}_i\mathbf{P}_i\}}\tilde{\mathbf{M}}_i. \tag{4.50}$$

The update of Method 2 is based on the decoupling as in (4.40) and (4.41), where each $\mathbf{M}_i$ is optimized independently. Let $\rho_i = \boldsymbol{\omega}_i\boldsymbol{\omega}_i^H$ in the case of a per-BS antenna array power constraint and $\rho_{i,a} = |[\boldsymbol{\omega}_i]_a|^2$ in the case of a per-antenna power constraint. Furthermore, at the optimum some of the ρ_is or $\rho_{i,a}$s are equal to P_i or $P_{i,a}$, because they can not exceed the power constraint and the μ_is (if a per-BS antenna array constraint is used) or $\mu_{i,a}$s (if a per-antenna constraint is used) corresponding to these ρ_is or $\rho_{i,a}$s have a finite value. Using this observation, the $\mathbf{M}_i$s can be scaled per-BS antenna array with $\alpha_i = \rho_i/P_i$ so that $\tilde{\mu}_i = \alpha_i\hat{\mu}_i$ or per-antenna element with $\alpha_{i,a} = \rho_{i,a}/P_{i,a}$ so that $\tilde{\mu}_{i,a} = \alpha_{i,a}\hat{\mu}_{i,a}$. This factor α_i or $\alpha_{i,a}$ will be larger than one if the ρ_is or $\rho_{i,a}$s do not violate the power constraint P_i or $P_{i,a}$. On the other hand, it will be smaller than one and decrease the μ_i or $\mu_{i,a}$s if the constraint is violated. The ρ_is or $\rho_{i,a}$s are monotonic, therefore, the scaling of the $\mathbf{M}_i$s is monotonic as well. Thus, after sufficient number of iterations the $\mathbf{M}_i$s scale the UL SINR (4.10) so that the power constraint is satisfied for all BS arrays or antenna elements.

For fixed $\boldsymbol{\Omega}$, the update (4.49), (4.50) can be seen as a normalized affine selfmapping satisfing the sum power constraint (4.48). [94, Theorem 1] proves that a normalized selfmapping converges if the mapping is concave or affine. With (4.48), the mappings (4.49), (4.50) are affine in $\boldsymbol{\mu}$ for a fixed $\boldsymbol{\Omega}$. Hence, there can be also a way to prove that the iteration converges to a fixed point based on the theory of [94].

If just a single BS exploits its power constraint (see Proposition 6), the algorithm must only search the worst link. Consequently, a convergence is very fast is this case.

The outer loop is shown in Algorithm 5. With the updates (4.49), (4.50), a convergence is given in the case a balanced DL SINR exists.

Algorithm 5 Outer loop: DL Power and iterations over $\boldsymbol{\mu}$

Initialize $\boldsymbol{\mu} = \mathbf{1}$
repeat
  Inner loop (Algorithm 1)
  Update the $\boldsymbol{\mu}$ vector by method 1 or 2.
until Convergence
return $\boldsymbol{\Omega}$

Table 4.4: Simulation parameters.

Number of user drops	1000
Number of users per user drop	21
Number of BSs drop	21
Transmit antenna arrays	ULA
Number of antenna array elements at BS	4
Number of antenna array elements at MS	1
Intersite distance	2000 m
Antenna spacing	half wavelength
Path loss exponent	3.76
Available CSI	long-term CSI
Power angular density	Laplacian [52, 114]
Power constraint	per-BS antenna array power constraint

4.4.3 Complexity

[57] presents a complexity analysis of the inner loop with an eigenvalue decomposition. In this chapter, the complexity of the inner loop is further reduced by replacing the eigenvalue decomposition with a power iteration method [56]. In Appendix A.4, the computation of the flop count is derived in detail. Assuming K_I is the number of iterations of the inner loop and K_O is the number of iterations of the outer loop, the upper bound of the complexity of the proposed iterative algorithm with update (4.49) and with N users and N_A antenna elements per BS is in the order of

$$\mathcal{O}(K_O K_I N^2 (N_A^3 + N_A^2) + K_O N^2 N_A^2)$$

The complexity of the bisection with an SDP is in the order of

$$\mathcal{O}(K_O \log(1/\epsilon) \sqrt{N N_A} (N^3 N_A^6 + N^2 N_A^2)).$$

4.5 Numerical Results

Table 4.4 summarizes the main simulation parameters for the network. The numerical results are based on long-term CSI in the form of higher rank spatial correlation matrices. The power angular density distribution is assumed to be Laplacian [120] and a similar simulation setup compared to [83] is used here. The pathloss gain is $(r/1000)^{-3.76}$, where r is the distance in meters. For all BSs the same power constraints are given and all users have the same thermal noise level σ^2. The users are randomly distributed in the multicell network, but with a distance larger than 50 meters away form the BSs. Assuming a single antenna at the BS, the largest possible SNR in this

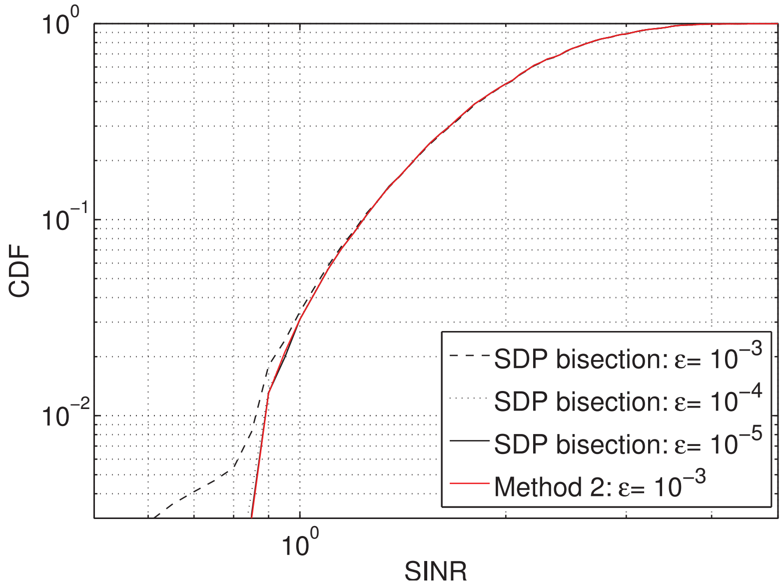

Figure 4.3: Cumulative distribution function (CDF) of the SINR of the new iteration based method of Section 4.4 (red) and the conventional SDP based bisection based method of Section 4.3.1. The scaling of both axes is logarithmic.

model is at a distance of 50 meters in the direction of the antenna broadside. It is given by $SNR = 57.16\text{dB}$.

Three algorithms are compared in this section:

- The bisection algorithm with an SDP as feasibility check problem given in Section 4.3.1. The beamforming vectors are calculated based on the largest eigenvalue of and the correponding eigenvector of solution of the SDP.
- The new iterative algorithm of Section 4.4 with Method 1 (subgradient method).
- The new iterative algorithm of Section 4.4 with Method 2 (4.49), (4.50).

Regarding Figure 4.3, the approach based on the interior point method to solve the SDP [139] requires a higher accuracy for the bisection algorithm to find an optimally balanced solution. As the accuracy increases, the solution for the SDP found by the interior point method improves (see Figure 4.4). The optimality ratio is the ratio of the largest eigenvalue of the solution matrices of the SDP divided by the sum of all eigenvalues of the solution matrix. The solution is nearly optimal at a accuracy smaller than 10^{-5}.

Figure 4.3 shows that the iterative method is already very close to the optimum for a low accuracy around $\epsilon = 10^{-3}$. At a accuracy of $\epsilon = 10^{-5}$, the solution of the interior point method for the SDP is nearly optimal (see Figure 4.4). The new iterative algorithm (Section 4.4) to determine the $\mathbf{M}_i$ matrices iterates over an MBP with a weighted sum power constraint. In each iteration, the matrices $\mathbf{M}_i$ are determined so that, e.g., the per-antenna array power constraints are satisfied. Hence, the balanced SINR decreases per iteration. This convergence behavior can also be observed in Figure 4.5.

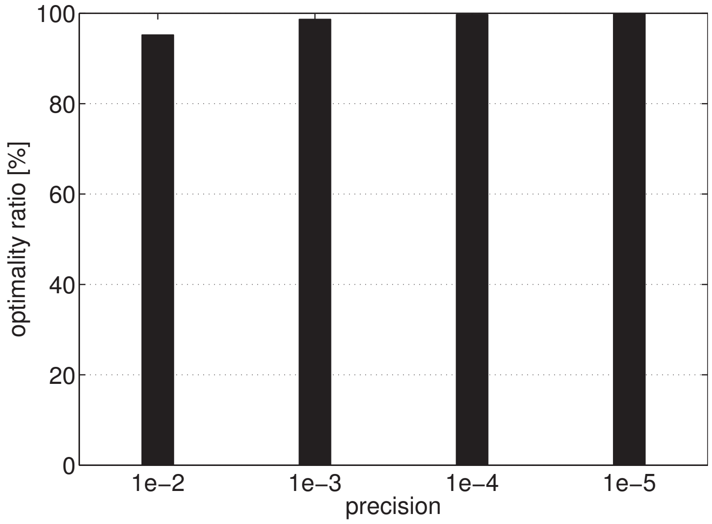

Figure 4.4: Optimality ratio of the SDP based bisection method (Section 4.3.1) for different accuracies.

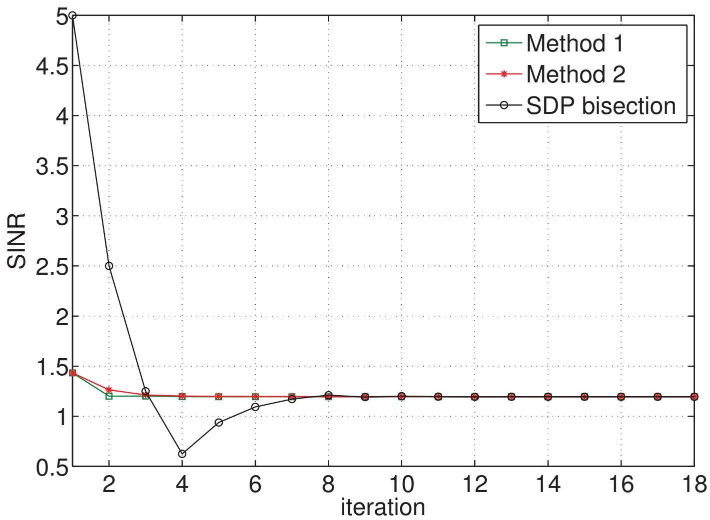

Figure 4.5: Convergence behavior of the different algorithms.

The interior point methods for the SDP perform not sufficiently well for a lower accuracy and, therefore, there are often users with an SINR below the optimal value. An advantage of the presented solution is the convergence behavior. For a low accuracy, after a few iterations, the found SINR is already close to the lower bound or the optimal value. In Figure 4.5 the convergence behavior of the presented algorithm is depicted for an exemplified user drop. After a few iterations the algorithm is very close to the optimal value. The algorithm based on the subgradient based outer update can converge very fast if the step size is correctly chosen. This is not always the case.

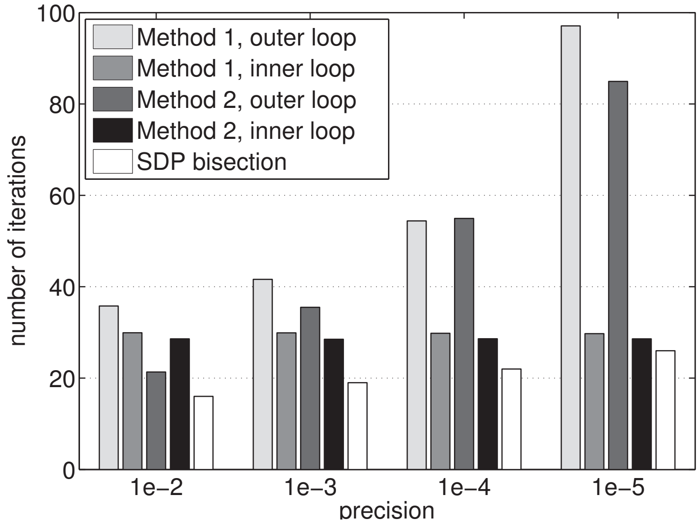

Figure 4.6: Number of iterations for different accuracies.

The outer loop of the presented algorithm is solved by the subgradient projection method or by the μ-SC method (4.49). The subgradient projection method requires a quite low step size to avoid divergence. Here,the step size is adapted as in [163]. Using a sufficiently small step size, the method based on the subgradient method in some cases (user drops) requires a large number of iterations to find the solution.

Figure 4.6 depicts the number of iterations of the presented μ-SC method (4.49), (4.50) (outer loop), the inner loop and the bisection algorithm with the SDP. The number of required iterations increases linearly with the given accuracy. For a high accuracy, the presented algorithm requires more than 50 iterations. However, for a low accuracy, the presented solution with the μ-SC method (4.49) requires only a few iterations. For a low accuracy, the solution of the bisection algorithm with the SDP is not optimal (see Figure 4.4). The bisection algorithm requires a accuracy of $\epsilon = 10^{-5}$ to achieve a balanced SINR and the μ-SC method achieves the same result at a accuracy of 10^{-3} (Figure 4.3). The inner loop has a accuracy of 10^{-5}, then it requires $K_I = 28$ iterations to converge.

Regarding the order of the complexity, the largest term of the $\mathcal{O}$-complexity-function of the conventional convex solver based algorithm grows in $N^{3.5}N_A^{6.5}$ per iteration. The largest term of the new algorithm grows in $N^2N_A^3$ per iteration. Table 4.5 compares the largest terms of the complexity for a precision of $\epsilon = 10^{-3}$. Although the new algorithm needs more iterations, the complexity is smaller compared to the conventional convex solver based approach due to the reduced complexity per iteration.

4.6 More General Scenarios

This sections discusses the MBP in two more general scenarios. The previous sections always assumed a balanced SINR (see Definition 32). This is given in many of scenarios. However, there are cases where a balanced SINR does not exist. Therefore,

Table 4.5: Estimation of the complexity for $\epsilon = 10^{-3}$, $N = 21$ and $N_A = 4$.

Algorithm	largest term	number of iterations
SDP based	$N^{3.5}N_A^{6.5} = 3.47 \cdot 10^8$	$K_O \log(1/\epsilon) = 19 \log(1/\epsilon)$
New iterative	$N^2 N_A^3 = 2.824 \cdot 10^4$	$K_O K_I = 980$

Section 4.6.2 discusses more general scenarios without a balanced SINR for a given set of power constraints.

Additionally, the previous section only considers an assignment of one BS to one user. An extension where users can be served by multiple BSs is presented in Section 4.6.3. Both generalizations can have an influence on the optimality of the proposed solutions.

4.6.1 Weighted Max-Min Beamforming

As illustrated in the previous section, max–min beamforming results in a balanced SINR and, hence, in a fair distribution of the achievable rate among the users. However, the sum rate performance of a system with max–min beamforming can decrease if, e.g., a user with very weak channel conditions is scheduled. Then, due to the balancing of the SINR among the users, the SINR of all jointly scheduled users decreases and a low sum rate can be the result.

A simple solution to avoid this scenario is a weighting of weak users by a factor δ_i. Then the downlink SINR of a user i is given by

Definition 34. *Downlink SINR: Using the definitions of the spatial correlation matrices* (4.7) *or* (4.8) *and a priority vector $\boldsymbol{\delta} = [\delta_1, \ldots, \delta_M]^T$, the weighted downlink SINR is then defined by*

$$\gamma_i^D(\boldsymbol{\Omega}) = \frac{1}{\delta_i} \frac{\boldsymbol{\omega}_i^H \mathbf{R}_{i,i} \boldsymbol{\omega}_i}{\sum_{\substack{l \in \mathcal{U} \\ l \neq i}} \boldsymbol{\omega}_l^H \mathbf{R}_{l,i} \boldsymbol{\omega}_l + 1}. \tag{4.51}$$

Instead of a new definition of the DL SINR, this weighting can be transparently achieved by a weighting of the spatial correlation matrices. Using the matrices

$$\mathbf{R}_{l,i} = \begin{cases} \frac{\mathbb{E}\{\mathbf{h}_{l,i}\mathbf{h}_{l,i}^H\}}{\delta_i \cdot \sigma_i^2} & \text{if } i = l \\ \frac{\mathbb{E}\{\mathbf{h}_{l,i}\mathbf{h}_{l,i}^H\}}{\sigma_i^2} & \text{otherwise,} \end{cases} \tag{4.52}$$

the original definition (Definition 4.9) of the DL SINR can be used. A weighted SINR is used in Chapter 6 for a combination of max–min beamforming with relays. A weighting of weak users results again in an unfair distribution of the SINR. Therefore, Chapters 5 and 6 present better solutions based on an avoidance of weak channel conditions.

4.6.2 Interference Decoupled Scenarios

In this section the theoretical background concerning the optimality of the MBP is investigated. In the previous section, the assumption of an balanced SINR for a given noise level and a given set of power constraints is used. Hence, it is assumed that there exists a balanced Pareto-optimal solution [165] of the DL SINR according to Definition 33.

Definition 35. *Networks, where a Pareto optimal balanced DL SINR for the given power constraints exist, are defined as balanced interference coupled networks.*

This section investigates a more general case, where for a decoupled structure of the network for a given set of per-antenna power constraints or per-station power constraints, a balanced SINR is not feasible. This section considers the same per-BS power constraint P_C for all BS arrays to simplify the discussion. The SINR of a user $i \in \mathcal{U}$ can be expressed by

$$\gamma_i^D(\mathbf{\Omega}) = \frac{p_i}{\sum_{\substack{l \in \mathcal{U} \\ l \neq i}} p_l G_{l,i} + \nu_i}, \tag{4.53}$$

with the resulting interference attenuation and an effective noise level respectively:

$$G_{l,i} = \frac{\mathbf{v}_l^H \mathbf{R}_{l,i} \mathbf{v}_l}{\mathbf{v}_i^H \mathbf{R}_{i,i} \mathbf{v}_i}, \text{ and } \nu_i = \frac{1}{\mathbf{v}_i^H \mathbf{R}_{i,i} \mathbf{v}_i}. \tag{4.54}$$

The optimality conditions for more general power constraints need to be discussed at first. The optimality condition for a per cell constrained max–min optimum is formulated in the following well known proposition. A similar observation is presented in [58].

Proposition 9. *If $\gamma^* = \max_{\mathbf{p}} \min_{i \in \mathcal{U}} \gamma_i^D$ and subject to $p_i \leq P_C$, then at least one $p_i \in \mathbf{p}$ will satisfy $p_i = P_C$.*

Proof. Contrary: Assuming all $p_i < P_C$ and it is further assumed that:

$$\gamma_i^D = \frac{p_i}{\sum_{\substack{l \in \mathcal{U} \\ l \neq i}} p_l G_{l,i} + \nu_i} = \gamma^*, \tag{4.55}$$

then there exists a $\delta > 1$ that at least one $\delta \cdot p_i = P_C$ so that

$$\gamma_i^D = \frac{\delta \cdot p_i}{\sum_{\substack{l \in \mathcal{U} \\ l \neq i}} \delta p_l G_{l,i} + \nu_i} = \frac{p_i}{\sum_{\substack{l \in \mathcal{U} \\ l \neq i}} p_l G_{l,i} + \nu_i / \delta} > \gamma^* \tag{4.56}$$

holds. □

Obviously, users served by BSs transmitting with the full power P_C are the bottleneck.

4.6.2.1 Coupled Network

At first, the case of a network with a balanced SINR is discussed. A coupled network is usually given in outdoor scenarios, where all users are subject to intercell interference. This situation can be formally defined as:

Definition 36. *A user i is coupled with the network if all $G_{l,i} > 0$ and $G_{i,l} > 0\ \forall l \neq i$.*

Proposition 10. *A network with only interference coupled users according to Definition 36, can always balance the SINR among all users.*

Proof. Assuming, there exists one weakest user i with

$$I_i = \sum_{\substack{l \in \mathcal{U} \\ l \neq i}} p_l G_{l,i} + \nu_i \tag{4.57}$$

and $I_i = \max(I_1, \dots I_M)$. Then, the BS serving this user i will transmit with the full power $p_i = P_C$ according to Proposition 9. The resulting SINR of user i is then given by

$$\gamma_i^D = \frac{P_C}{\sum_{\substack{l \in \mathcal{U} \\ l \neq i}} p_l G_{l,i} + \nu_i}.$$

The SINR is balanced if the network is coupled:

$$\gamma^* = \gamma_1^D = \ldots = \gamma_i^D = \ldots = \gamma_M^D$$

By increasing the noise level ν_i an unbalanced SINR could be created. Assuming the noise level ν_i will be scaled by with a $\delta_i > 1$ so that

$$\gamma_i^D = \frac{P_C}{\sum_{\substack{l \in \mathcal{U} \\ l \neq i}} p_l G_{l,i} + \nu_i} > \frac{P_C}{\sum_{\substack{l \in \mathcal{U} \\ l \neq i}} p_l G_{l,i} + \delta_i \cdot \nu_i}. \tag{4.58}$$

The SINR of user i is now decreased without any effect of the SINR of the other users $l \neq i$, their SINR is still balanced. The power of BS i can not be increased to recover a balanced SINR because it already reaches its power constraint. But if the network is coupled, $G_{l,i} > 0\ \forall l \neq i$, each BS $l \neq i$ can reduce its own power to balance the SINR of all users again. □

4.6.2.2 Decoupled Network

A special structure of the network can result in conditions, where a balanced SINR does not exist for a given set of power constraints. In this chapter two cases are identified. The SINR remains unbalanced if a user is physically decoupled from the network, e.g., the user could be strongly protected from intercell interference by buildings, strong antenna patterns. From the first impression this could be a suitable condition for those users, on the other hand the algorithms requiring the existence of a balanced SINR can not converge to a feasible solution in this case. At first, a formal definition for the decoupled user is needed.

Definition 37. *A user i is called decoupled from the network with per cell power constraints,*

1. *if this user does not receive interference from other users $j \neq i$, thus, $G_{j,i} = 0\ \forall j \neq i$,*

2. *if this user does not generate any interference to other users $j \neq i$, thus, $G_{i,j} = 0\ \forall j \neq i$.*

Proposition 11. *For a given set of power constraints P_C it is not always possible to find a balanced SINR γ^* if there exists a user i which is decoupled from the network.*

Proof. In the two cases of Definition 37, a balanced SINR can not be recovered:

1. Assuming user i is the weakest user in the network, which can be achieved by an arbitrary large δ_i as in (4.58) and there is no intercell interference every $G_{l,i} = 0$ $\forall l \neq i$, then the SINR of user i is given by

$$\gamma_i^D = \frac{P_C}{\delta_i \cdot \nu_i} \tag{4.59}$$

   Now, there is no possibility by power control to recover a balanced SINR. The SINR of user i can be made arbitrarily small by increasing δ_i and the BS i can only transmit with the maximal power $p_i = P_C$, because it can not exceed the power constraint P_C. The other BSs can not influence the SINR of user i.

2. Another situation is the opposite case, where the user i is not the weakest user and its BS does not create interference to other users $G_{i,l} = 0\ \forall l \neq i$. Then the transmitted power of BS i to user i can not reduce the SINR of the other users l. The BS i can increase its transmit power until $p_i = P_C$. The resulting SINR γ_i^D can be larger than the SINR γ_l^D of the other users $l \neq i$ because user i does not create any interference to the residual network.

□

In these interference decoupled networks a balanced SINR is not feasible. The solution presented in Section 4.4 requires a balanced SINR to converge to a solution, where all power constraints are met.

4.6.3 Exploiting the Spatial Diversity with a CoMP Transmission

The previous sections only regard the assignment of one previously selected BS to a user. A generalization is the so-called CoMP transmission where multiple BSs can transmit to a user.

A large beamforming gain can be achieved if multiple BSs have a synchronized phase. Then the BS array can be seen as a large virtual array. The received power grows proportionally to the square of the number of antennas [124]. The works [149, 150] investigate the CoMP transmission in the context of a network-wide coordination. Multiple works investigate practical difficulties regarding CoMP in future wireless systems [3,85]. The promising results of a first field trial are proposed in [75].

However, the investigated scenario in this study is small. Furthermore, this study shows, an enormous increase of the backhaul effort to a achieve a coherent transmission and the cell area where CoMP is feasible is limited by the length of the cyclic prefix.

If the phase is not synchronized among the BS arrays, a diversity (spatial, and or temporal) gain can be achieved [17, 102]. Another scenario is proposed in the context with a multicast transmission in [82, 83]. If long-term CSI in the form of spatial correlation information is available, a spatial diversity gain can be achieved. The advantage is a reduced backhaul effort due to the use of long-term CSI. The algorithms presented in the previous section can be simply extended to this CoMP scenario by a simple reformulation of the spatial correlation matrices and beamforming vectors.

4.6.3.1 Extension of the Spatial Correlation Matrices to the CoMP case

In this section, a network with $N > M$ cooperating BSs is investigated. A user inside a cell is served by three stations each equipped with N_A antennas, as depicted in Fig. 4.7. At a time instance in each cell c one user i is jointly served by the three BSs belonging to this cell c. Let $\mathcal{B}_i$ be the set of cooperating BSs for user i, then the signal r_i user i at a time instant is

$$r_i = \sum_{c \in \mathcal{B}_i} \hat{\mathbf{h}}_{i,c}^H \hat{\boldsymbol{\omega}}_c s_i + \sum_{k \in \bar{\mathcal{B}}_i} \hat{\mathbf{h}}_{i,k}^H \hat{\boldsymbol{\omega}}_k s_k + n_i, \tag{4.60}$$

where $\hat{\mathbf{h}}_{i,c} \in \mathbb{C}^{N_A \times 1}$ is the channel vector from the cth BS to the ith user. The set $\bar{\mathcal{B}}_i$ denotes the set of interfering BSs such that $\mathcal{B}_i \cap \bar{\mathcal{B}}_i = \emptyset$ and $\mathcal{B}_i \cup \bar{\mathcal{B}}_i = \mathcal{S}$, $\mathcal{S}$ being the set of the currently active BSs. $\hat{\boldsymbol{\omega}}_k \in \mathbb{C}^{N_A \times 1}$ is the transmit beamforming vector at BS k, s_i is the information signal to user i with $E\{|s_i|^2\} = 1$ and $E\{s_k s_i^*\} = 0$ if $i \neq k$. The noise signal plus the interference of other networks is given by n_i. To simplify the notation, the channel vectors of the cooperating BSs, given by set $\mathcal{B}_l$, can be stacked into a large virtual antenna array $\mathbf{h}_{l,i}$. This corresponds to a channel vector $\mathbf{h}_{l,i}$ between the virtual array serving user l to user i. The same can be done with the beamforming vectors at the BSs of the set $\mathcal{B}_l$, which results in a large virtual beamforming vector $\boldsymbol{\omega}_l$. Using these notations the received signal can be rewritten as:

$$r_i = \mathbf{h}_{i,i}^H \boldsymbol{\omega}_i s_i + \sum_{l \in \mathcal{U}, l \neq i} \mathbf{h}_{l,i}^H \boldsymbol{\omega}_l s_l + n_i. \tag{4.61}$$

Here, $\mathcal{U}$ denotes the set of indices of users or cells with one scheduled user. The perfect knowledge of instantaneous CSI and a perfect synchronization among the cooperative BSs is very challenging in large networks. Instead of the instantaneous CSI, a more practically relevant approach is the usage of the long-term CSI because of its long stationarity compared to the instantaneous CSI [77]. As in the previous section, the assumption of long-term CSI results in the mean SINR where an additional averaging over the channel realizations $\mathcal{H}$ is done. With the assumption $E\{|n_i|^2\} = \sigma_i^2$, the mean SINR is defined by Eq. (4.6). Assuming the channels of the different links are uncorrelated, the spatial correlation matrices in Eq. (4.6) in the case of a CoMP transmission are given by

$$\mathbf{R}_{l,i} = \frac{1}{\sigma_i^2}\mathbb{E}\{\mathbf{h}_{l,i}\mathbf{h}_{l,i}^H\} = \frac{1}{\sigma_i^2} \oplus_{c\in\mathcal{B}_l} \mathbb{E}\{\hat{\mathbf{h}}_{i,c}\hat{\mathbf{h}}_{i,c}^H\} = \frac{1}{\sigma_i^2} \oplus_{c\in\mathcal{B}_l} \hat{\mathbf{R}}_{i,c}. \tag{4.62}$$

Here, $\oplus$ denotes the direct sum of two matrices, e.g, $\oplus_{i\in\{1,2\}}\mathbf{A}_i = \mathrm{diag}(\mathbf{A}_1, \mathbf{A}_2)$. A similar approach is used in [8] for the optimal assignment of a single BSs to users in a network. The extension to the CoMP transmission only results in a new definition of the spatial correlation matrices. Hence, the algorithmic solution in Section 4.4 is unchanged.

The more theoretic case of a coherent transmission of multiple BSs to one user by a virtual large array is presented in [150]. In this case all BS transmit synchronized in phase. Hence, a beamforming gain can be achieved. The spatial correlation matrix for this perfect phase synchronized transmission is

$$\mathbf{R}_{l,i} = \frac{1}{\sigma_i^2}\mathbf{h}_{l,i}\mathbf{h}_{l,i}^H. \tag{4.63}$$

In a similar way the UL SINR can be formulated for the CoMP transmission as follows: The UL (receive) beamforming vectors of a single BS are given by $\hat{\mathbf{v}}_c$. Concatenating the receive beamforming vectors $\hat{\mathbf{v}}_c$ of the set of BSs ($c \in \mathcal{B}_i$) from a user i in a large vector $\mathbf{v}_i$ in the UL, and with $\mu_{a,i} \in \mathbb{R}^+ \ \forall a \in \mathcal{A}_i$, where $\mathcal{A}_i$ is the set of array elements serving user i and $\mathcal{A} = \bigcup_{i\in\mathcal{U}} \mathcal{A}_i$ denotes the total set of antenna elements, and the definition of the matrix $\mathbf{M}_i = \oplus_{a\in\mathcal{A}_i}\mu_a$, the dual UL SINR of the virtual BS array serving user i is given by

$$\gamma_i^U(\boldsymbol{\mu}, \boldsymbol{\lambda}, \mathbf{v}_i) = \frac{\lambda_i \mathbf{v}_i^H \mathbf{R}_{i,i}\mathbf{v}_i}{\mathbf{v}_i^H(\mathbf{M}_i + \sum_{\substack{l\in\mathcal{U}\\ l\neq i}} \lambda_l \mathbf{R}_{i,l})\mathbf{v}_i}. \tag{4.64}$$

Using the DL and UL SINR with spatial correlation matrices according to (4.62), the algorithm presented in Section 4.4 can also exploit the spatial diversity.

4.6.3.2 Numerical Results

This section presents some numerical results for the CoMP assignment scenario presented by Section 4.6.3. The simulation scenario corresponds to the scenario depicted in Fig. 4.7. Three BS arrays form a large virtual array to a user inside a cell. Each array is a ULA. The optimization is based on long-term CSI in the form of Hermitian positive semidefinite Toeplitz matrices among each BS array and user. To a avoid an interference decoupled scenario a weaker antenna pattern is used at each BS. Further simulation parameters are summarized in Tab. 4.6. For all BSs the same per-antenna power constraints are given and all users have the same thermal noise level σ^2. Assuming a single antenna at the BS, the SNR at 50m before the BS is given this scenario by $SNR = 48.9$dB.

Fig. 5.5 depicts the cumulative distribution functions (CDFs) of the following algorithms:

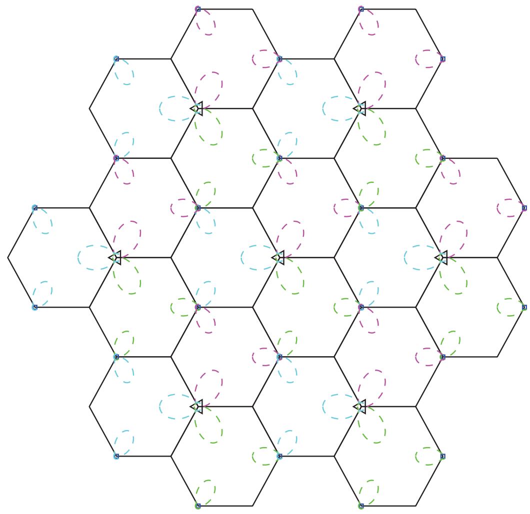

Figure 4.7: Scenario with a CoMP transmission: The lobes show the orientation of the antenna pattern. Users are served by the three BSs of each cell.

Table 4.6: Simulation parameters

Number of user drops	1000
Number of users per user drop	21
Number of BSs	21
Transmit antenna arrays	ULA
Number of antenna array elements at BS	4
Number of antenna array elements at MS	1
Interference of adjacent networks	By ring of omnidir. BSs
Intersite distance	500 m
Antenna spacing	half wavelength
Available CSI	long-term CSI
Path loss exponent	3.76
Power angular density	Laplacian [52, 114]
Power constraint	per-antenna

All algorithms use an accuracy of $\epsilon = 10^{-6}$. The proposed architecture with two additional BSs in the cell edge region results in a higher gain for all users compared

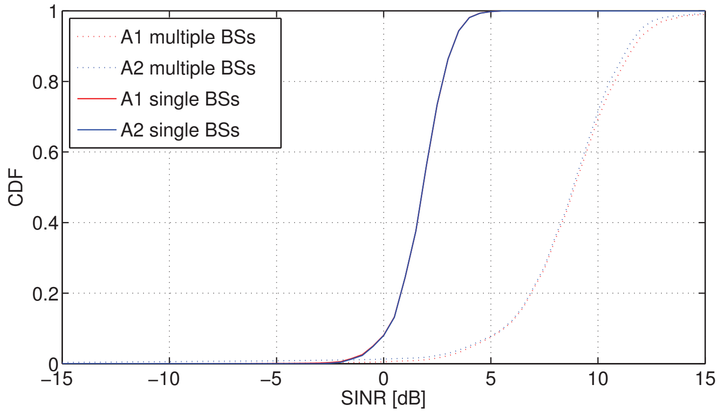

Figure 4.8: Cumulative distribution function (CDF) of the SINR

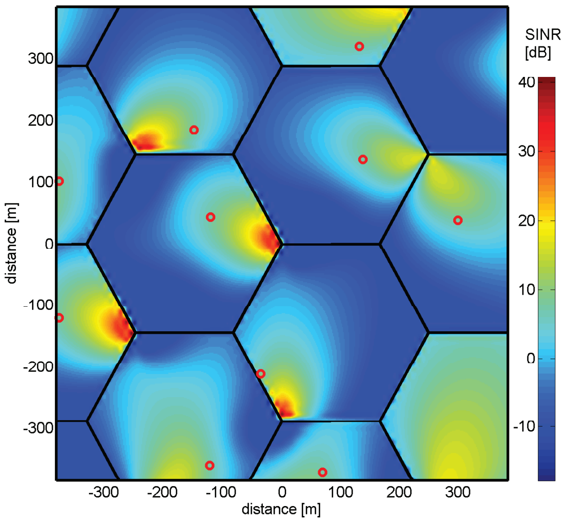

Figure 4.9: The SINR as a function of the location. The red circles denote users.

to the single BS per cell case (see Fig. 4.8). The extended algorithm A1 finds the same SINR as the convex solver based bisection method A2.

Fig. 4.9 depicts the SINR as a function of the location. The color denotes the SINR. High SINR corresponds to red areas, low SINR corresponds to blue areas. Only BSs close to users are active and these BSs focus their power in the direction of the served users, to avoid intercell interference.

4.7 Summary

- This chapter presents a new framework for uplink–downlink duality for the max–min beamforming problem with general power constraints. In the case an equivalent quasi-convex form of the max–min beamforming problem exists, if, e.g, instantaneous CSI is available, strong duality is directly proven by a duality theorem for quasi-convex programming [107].

- If long-term CSI in the form of higher rank spatial correlation matrices is given, no equivalent quasi-convex form is known. However, in this case the max–min beamforming problem can be also solved by derived framework for uplink–downlink duality.
- The presented dual problem can be efficiently solved. Based on this framework a low-complexity iterative solution is presented. This presented algorithm is based on an inner and outer loop and outperforms the known convex solver based solution.
- This chapter further discusses the SINR balancing conditions of the max–min beamforming and gives a discussion of the interference decoupled cases. A finding is, that a balanced SINR can not always be assumed. Decoupled users can get a different SINR than the residual coupled network. However in outdoor scenarios such a situation does not often occur, hence interference coupling is a reasonable assumption.
- Finally, a straightforward extension to cooperative multipoint transmission is presented. An efficient method can be applied is derived in the case each BS array knows the spatial correlation matrices. The applicability of the proposed iterative solution is illustrated.

Chapter 5

Theory of the Multicell Beamscheduling Problem

The content presented in this Chapter is prepublished in the publication [42]. This chapter considers only a unicast downlink transmission.

5.1 Introduction

In multicell networks intercell interference limits the performance if the frequencies are reused in adjacent cells. Section 4 examines a method to achieve a max–min fair SINR among all jointly scheduled users.

However, max–min fairness has the drawback of a low overall sum rate: A user with bad channel conditions can decrease the performance of all jointly scheduled users. This thesis mainly regards a network optimization based on long-term statistics, hence, fast fading does not influence the instantaneous SINR if the beamforming weights are found by using available long-term CSI. Also, shadow fading can decrease the overall performance. Section 6 presents an approach to overcome this shadow fading problem in max–min fair systems.

This section regards another effect, which also results in a low sum rate. In addition to shadow fading, unfavorable scheduling decisions can decrease the sum rate performance.

If two users are closely located and served by different BS arrays and their antenna array vectors are optimized with MBF, a low balanced SINR among the users can be the result. Consequently, different and jointly served links should be spatially separated, otherwise mutual interference can decrease the sum rate. The avoidance of these unfavorable scheduling decisions is called beam-scheduling problem. The combination of MBF and beam scheduling may result in a fair distribution of the SINR and jointly in a larger sum rate of the system.

5.1.1 Scenario

A fully coordinated multicell network, as depicted in Fig. 4.1 on Page 32, is considered. Each of the N BS arrays uses N_A correlated antenna elements to form beam lobes in the direction of scheduled users. The transmit power of each antenna element a of BS array c is limited to a power constraint of $P_{c,a}$. Each user has a single antenna element. The optimization is centralized and based on long-term CSI in form of spatial correlation matrices to reduce the backhaul effort as in the previous sections. For transmit beamforming, this statistical CSI is a practically relevant information to form beam lobes in the direction of users, while considering the interference of adjacent networks [76]. The previous Chapter 4 discusses the unicast MBP. Based on long-term CSI in the form of spatial matrices, a low complexity iterative algorithm exists, hence, the MBP can be solved efficiently.

The previous chapter only assumes properly scheduled users. However, the problem of user selection is another difficult problem and has a strong influence on the system performance, especially, if fairness among the users is desired [153]. This chapter proposes an extension to a joint optimization of the beamforming vectors, the power control, and the beam scheduling along with multiuser scheduling.

5.1.2 Related Work

Intercell interference mitigation based on multicell transmit beamforming with joint power control has been investigated intensively during the last ten years, [9, 31, 150, 157]. Coordinated max–min beamforming (MBF) achieves a fair balanced SINR among all jointly scheduled users in a network while the transmit power per-antenna element or per-antenna array is limited to a power constraint [19, 20]. Iterative low complexity algorithms for the MBF with per-antenna power constraints are proposed in [19,20,40]. Hence, the joint optimization of transmit power and beamforming vectors enables a fair distribution of the SINR among a set of scheduled users. A drawback of MBF is the low sum rate that results in case of unfavorable scheduling decisions. Consequently, a smart scheduling of the users is required.

The work [153] discusses the information theoretical aspects of multiuser scheduling and beamforming. The authors show that in environments with slow fading, the diversity gain can be improved with multiuser scheduling along with opportunistic beamforming.

A problem related to beam scheduling is called channel assignment problem (CAP). In addition to the exploitation of multiuser diversity, interference mitigation is another important issue, especially in multicell networks. The assignment of channels to users or cells also influences the interference in a network. In [112], the authors propose the CAP for cellular networks. The aim was to allocate a number of channels to cells such that certain constraints are satisfied.

Another possibility to improve the SINR is an optimized beam scheduling, since beam lobes cause interference in adjacent sectors [72]. A first simple round-robin beam switching approach to avoid these beam collisions is proposed in [96]. The articles [71, 72] propose optimized approaches which take into account the channel quality information of the users or the geographical data. However, these approaches consider only small, e.g, 2-cell scenarios and do not jointly optimize the beamforming vectors. The work [66] considers a spatial scheduling with the objective to cancel the interference by, e.g. zero-forcing.

In contrast to [66,71,72], this chapter uses long-term CSI in the form of spatial correlation matrices to optimize the beam scheduling, beamforming and user scheduling jointly. The MBF optimization results in a balanced SINR and these SINR values are used to compute a cost function for the beam scheduling problem.

Later, [160] proves the $\mathcal{NP}$-hardness of a similar problem. In contrast to this chapter, where the balanced mean SINR is used for the objective function, the authors in [160] use so-called interference constraints to define groups of beams which are mutually interfering with each other. Hence, instead of the SINR optimization this scheme can be seen as an orthogonal approach of finding non-interfering beams such that the overall performance is maximized.

Instead of an interference avoidance, the authors of [2] propose a max–min fair antenna assignment scheme for a system with geographically dispersed antenna ports. The selection of antenna ports is optimized such that the SINR of the weakest user is maximized. Instead of a simple optimization of the assignment of stations to users [2], this paper proposes optimization techniques to optimize the beamforming vectors along with the temporal scheduling of users such that the sum rate, or the minimum SINR is maximized. This problem is called beam scheduling problem in this paper. This paper shows the close relationship between the multicell beam scheduling problem and the $\mathcal{NP}$-hard multidimensional assignment problem (MAP) [18, 122]. A commonly used approach for the MAP is simulated annealing [23]. In addition to simulated annealing, dimension-wise optimization approaches are recently proved to have a better performance [62].

5.1.3 Contributions

This chapter presents the following extensions:

- Previous works as [66, 71, 72, 160] use predefined beamformers or zero-forcing or avoid interference by a beam selection. This chapter uses the balanced SINR of a max–min beamformer as cost function for a temporal user scheduling. The result is an avoidance of a low balanced SINR which is a known drawback of MBF.

- The schemes in [2, 66, 71, 72, 160] use instantaneous CQI. Furthermore, the optimization is performed only for one time instant. This paper generalizes this approach and optimizes the beam scheduling over the stationary interval of the long-term statistics of channel [76]. Therefore, this chapter considers in addition to SINR fairness also temporal fairness.

- This chapter proves the $\mathcal{NP}$-hardness of the general beamscheduling problem and shows additionally that the general beamscheduling problem in the 2-cell scenario is equivalent to a linear assignment problem which can be optimally solved by a well known polynomial time algorithm. Furthermore, this chapter presents the optimal solution for the 2-cell case. The heuristics for the general N-cell scenario show a similar behavior.

- The N-cell beam scheduling problem has a close relation with the multi-dimensional assignment problem (MAP). A useful approach to solve the MAP is simulated annealing. This chapter proposes a simulated annealing based beam scheduling algorithm and additionally dimension-wise optimization methods based on an extension of the optimal approaches for the 2-cell scenario. The algorithms are compared in terms of complexity, sum rate performance and max–min SINR fairness.

Table 5.1: Overview of the different algorithms

Algorithm	Temp. fairness	Objective	Approach	Complexity
A1: random RRS	RRS	-	random solution	low
A2: dim.-wise sum rate max.	QFS	sum rate	dimension-wise	high
A3: dim.-wise max–min	QFS	max–min	dimension-wise	high
A4: greedy sum rate max.	ORRS	sum rate	greedy algorithm	low
A5: sum rate based SA	QFS	sum rate	local search	high

- Different objective functions are used in this chapter: If the maximized sum rate is the objective, a higher system throughput will be the result in the case of max–min beamforming. If fairness is desired this approach will be not the best choice. Therefore, this chapter additionally presents a novel problem formulation based on a graph theoretical max–min problem which achieves a more fair distribution of the mean SINR in the whole stationary interval of the long-term CSI. Table 5.1 depicts an overview of all proposed algorithms.

- In extension to the sum rate maximization approaches, this paper shows a low complexity algorithm with less than half of the complexity compared to the other algorithms. Additionally, the new approach can guarantee a higher temporal fairness. Instead of a so-called quasi-fair scheduling (QFS), where each user is scheduled equally often, the greedy approach can guarantee so-called opportunistic Round-Robin scheduling (ORRS) fairness which is a temporal fair scheduling scheme (further details are introduced in Section 5.5.1). Table 5.1 depicts an overview of all proposed algorithms.

- This chapter presents an optimization problem for minimizing the delay between two consecutive transmissions to users in the system. This chapter proves the $\mathcal{NP}$-hardness of this problem and shows that multiple heuristics, which are developed for the traveling salesmen problem, are suitable to solve this problem.

- Finally, a detailed analysis of four proposed algorithms concerning complexity, temporal fairness, SINR fairness and sum rate is presented.

Outline: Section 5.2 presents the system setup and the data model of the investigated system depicted in Fig. 4.1. Section 5.3 defines the MB problem and the beamscheduling problem and proves the $\mathcal{NP}$-hardness of the general N-cell beamscheduling problem. For $N = 2$ an optimal solution can be computed in polynomial time. Two optimal approaches, a fair and a sum rate maximizing approach, are presented in Section 5.4. Section 5.5 presents four heuristics for the general N-cell case. Finally, Section 5.6 presents a subsequent optimization which can further enhance the delay between two consecutive transmissions to users in the network. This chapter concludes with a summary and a short discussion in Section 5.7.

5.2 System Setup and Data Model

Consider a network with N cooperative BS arrays as depicted in Fig. 4.1. Each antenna array is equipped with N_A antennas. In this network, M users are equally distributed.

The matrix $\mathbf{S} \in \mathbb{N}^{N \times K}$ defines the assignments of these users to BSs and scheduling slots with index k. Each element in $\mathbf{S}$ with index c, k is given by

$$[\mathbf{S}]_{c,k} = i, \quad \text{user } i \text{ is scheduled by BS } c \text{ in slot } k. \tag{5.1}$$

The variable K denotes the total number of orthogonal slots. Here, orthogonal means orthogonal in the temporal domain or orthogonal scheduling slots. However, an application to channels orthogonal in the frequency domain is also feasible. An extension to a multi-carrier system is straightforward. Let $\mathbf{C}_c \in \mathbb{N}^{K_T \times K_F}$ denote the matrix of all K_T orthogonal time and K_F frequency slots. Then, $\mathbf{s}_c = \text{vec}(\mathbf{C}_c) \in \mathbb{N}^{1 \times [K_T \cdot K_F]}$ denotes the vectorized version of this matrix and corresponds to one row of the matrix $\mathbf{S}$.

This chapter uses a similar signal model as introduced in Chapter 4. However, a few modifications concerning the indexes are required here. At a time instant, each BS array serves one user equipped with one antenna element, hence, N users are scheduled at the same time for a given orthogonal frequency resource. A user $i = [\mathbf{S}]_{c,k}$ in cell c receives from its BS array of the cell c in slot k the signal

$$r_{i,k} = \mathbf{h}_{i,i,k}^H \boldsymbol{\omega}_{i,k} s_i + \sum_{l \in [\mathbf{S}]_{:,k},\, l \neq i} \mathbf{h}_{l,i,k}^H \boldsymbol{\omega}_{l,k} s_l + n_i. \tag{5.2}$$

The vector $\mathbf{h}_{l,i,k} \in \mathbb{C}^{N_A \times 1}$ is the MISO channel between the BS antenna array of cell l serving user l and user i. Each BS antenna array serving a user i uses beamforming vectors $\boldsymbol{\omega}_{i,k} \in \mathbb{C}^{N_A \times 1}$ to form a beam lobe to user i in slot k. The scalar n_i denotes the interference plus noise of adjacent networks with the assumption $\mathbb{E}\{|n_i|^2\} = \sigma_i^2$ and $\mathbb{E}\{n_i\} = 0$. The desired signal transmitted to user i is denoted by s_i with $\mathbb{E}\{|s_i|^2\} = 1$ and $\mathbb{E}\{s_l s_i^*\} = 0$ if $l \neq i$. With the instantaneous downlink SINR

$$\hat{\gamma}_{i,k} = \frac{|\mathbf{h}_{i,i,k}^H \boldsymbol{\omega}_{i,k}|^2}{\sum_{\substack{l \in [\mathbf{S}]_{:,k} \\ l \neq i}} |\mathbf{h}_{l,i,k}^H \boldsymbol{\omega}_{l,k}|^2 + \sigma_i^2}, \tag{5.3}$$

the ergodic capacity a user i achieves is given by

$$\hat{R}_{i,k} = \mathbb{E}\{\log(1 + \hat{\gamma}_{i,k})\}. \tag{5.4}$$

As already mentioned in Section 4.2, the optimization based on the long-term CSI is practically more relevant in a multicell scenario. Therefore, as in Eq. (4.5) the ergodic

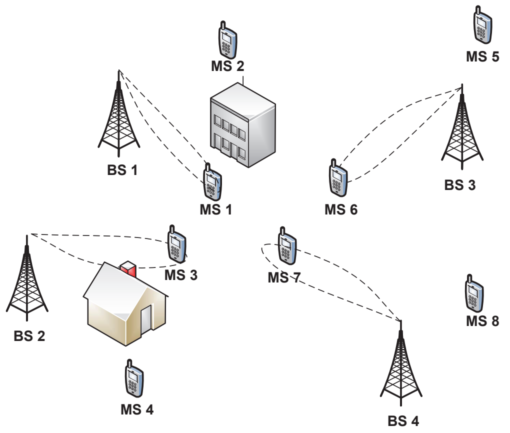

(a) Low balanced SINR

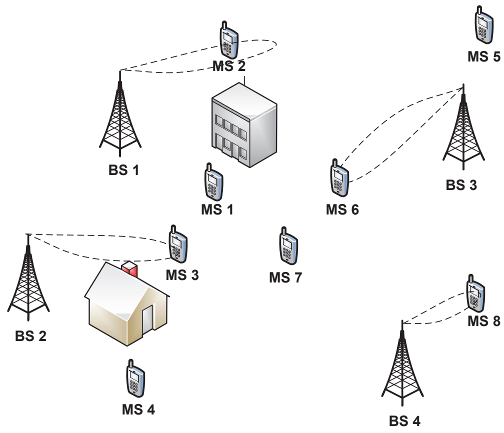

(b) High balanced SINR

Figure 5.1: Example: Beamforming based on scheduling decisions.

capacity is approximated with the mean SINR (by spatial correlation matrices (4.7)) which is denoted as a function of the scheduling matrix $\mathbf{S}$ by

$$\gamma_{i,k} = \frac{\boldsymbol{\omega}_{i,k}^H \mathbf{R}_{i,i} \boldsymbol{\omega}_{i,k}}{\sum_{\substack{l \in [\mathbf{S}]_{:,k} \\ l \neq i}} \boldsymbol{\omega}_{l,k}^H \mathbf{R}_{l,i} \boldsymbol{\omega}_{l,k} + 1}. \tag{5.5}$$

The rate $R_{i,k}$ is an approximation of the ergodic capacity and is the performance measure. All optimizations of the beamforming vectors $\boldsymbol{\omega}_{l,k}$ and the scheduling decisions are made based on the long term CSI given in (2.3). The matrix concatenated by the total set of beamforming vectors in slot k is denoted by $\boldsymbol{\Omega}_k$. For a fixed beamforming strategy (in this chapter MB), the total sum rate over all scheduling slots K

$$R(\mathbf{S}) = \sum_{k=1}^{K} \sum_{i \in [\mathbf{S}]_{:,k}} \log(1 + \frac{\boldsymbol{\omega}_{i,k}^H \mathbf{R}_{i,i} \boldsymbol{\omega}_{i,k}}{\sum_{\substack{l \in [\mathbf{S}]_{:,k} \\ l \neq i}} \boldsymbol{\omega}_{l,k}^H \mathbf{R}_{l,i} \boldsymbol{\omega}_{l,k} + 1}) \tag{5.6}$$

is used as a cost function.

5.3 Problem Formulation

A single frequency network will result in a high spectral efficiency if intercell interference can be mitigated. A promising method to mitigate interference among a set of scheduled users and to achieve fairness is MB. The result is a balanced SINR among all jointly active users using the same channel ressource. However, an unfavorable scheduling decision can result in a low balanced SINR among all jointly scheduled users. Fig. 5.1(a) depicts an example with a low balanced SINR among the scheduled users. Users 1, 3, 6 and 7 are jointly scheduled and located in the same geographical region. Therefore, all beams (denoted by dashed lobes) are directed in the same region. Hence, the number of degrees of freedom to achieve high balanced SINR among the users with MB is limited. Fig 5.1(b) shows a better scheduling decision. The users 2, 3, 4, and 8 are located geographically more separately. Therefore, a higher SINR can be achieved with MB.

5.3.1 Beamforming Problem

It is desired to maximize the lowest SINR $\gamma_{i,k}$ of all jointly scheduled users $i \in [\mathbf{S}]_{:,k}$ in slot k, where the power of each antenna element is subject to a power constraint $P_{c,a}$. This problem can be formally expressed as a MB problem with per-antenna array element power constraints:

$$\gamma_k = \max_{\mathbf{\Omega}_k} \min_{i \in [\mathbf{S}]_{:,k}} \gamma_{i,k} \quad \text{s.t.} \quad |[\boldsymbol{\omega}_l]_a|^2 \leq P_{l,a} \;\; \forall a \in \mathcal{A}_l,\; \forall l \in [\mathbf{S}]_{:,k}. \tag{5.7}$$

The index set of antenna array elements of the BS array serving user i is denoted by $\mathcal{A}_i$. For simplification each BS antenna array uses the same number N_A of array elements. The matrix concatenated by the total set of beamforming vectors in slot k is denoted with $\mathbf{\Omega}_k = [\boldsymbol{\omega}_{1,k}, \ldots, \boldsymbol{\omega}_{N,k}]$. The problem (5.7) is non-convex in general. However, for special instances, Chapter 4 presents efficient solutions of the problem (5.7). Section 4.4 presents a low complex iterative approach for the MBP (5.7) based on the UL-DL duality. Hence, the MBP is solved efficiently.

5.3.2 Beamscheduling Problem

A smart assignment of jointly scheduled users increases the balanced SINR which is the solution of the MBF problem (5.7). The main idea for the optimization presented in this thesis is now the avoidance of unfavorable scheduling decisions such that the beamforming vectors can achieve a higher balanced SINR which results in a higher sum rate.

All optimizations (beamforming and scheduling) presented in this chapter are based on long-term CSI. This approach is based on the idea to compute the assignments of users i to BSs c and scheduling slots k in advance and reuse them as long as the channel is stationary. This assignment is given by the matrix (5.1). Hence, matrix $\mathbf{S}$ is beside the beamforming vectors $\mathbf{\Omega}_k$ another optimization variable. The optimization presented in this section is based on permutations.

Definition 38. *Let $\boldsymbol{\pi}_1 = [i_1, i_2, \ldots i_K] \in \mathbb{N}^K$ be an index vector and let $\mathbf{P}_c \in \{0,1\}^{K \times K}$ be a permutation matrix, with $\sum_{l=1}^{K} [\mathbf{P}_c]_{n,l} = 1$ and $\sum_{l=1}^{K} [\mathbf{P}_c]_{l,n} = 1$, $\forall n = 1, \ldots, K$. A permutation $\boldsymbol{\pi}_c = \boldsymbol{\kappa}(\boldsymbol{\pi}_1)$ of a index-vector $\boldsymbol{\pi}_1 = [i_1, i_2, \ldots, i_K]$ is given by a permutation of the elements of the vector: $\boldsymbol{\pi}_c = \boldsymbol{\kappa}(\boldsymbol{\pi}_1) = \boldsymbol{\pi}_1 \mathbf{P}_c$.*

To simplify the following notations, each cell contains exactly K active users. A straightforward optimization goal is the sum rate maximization of the approximated rate defined in (4.5). With the assumption of an equal number of users per cell and

BS antenna array and with the set $\mathcal{W} = \{\mathbf{\Omega}_1, \ldots, \mathbf{\Omega}_N\}$ of all feasible beamforming matrices, the optimization problem can be stated as:

Definition 39. *Find the optimal permutations $\boldsymbol{\pi}_c$ of row vectors of the scheduling matrix $\mathbf{S}$ such that the sum rate is maximized. The permutation form of the scheduling matrix is $\mathbf{S} = [\boldsymbol{\pi}_1^T, \boldsymbol{\pi}_2^T, \ldots, \boldsymbol{\pi}_N^T]^T$. With the assumption of a fixed first permutation $\boldsymbol{\pi}_1$, the optimization of the scheduling matrix $\mathbf{S}$ is defined by finding optimal permutations of $\boldsymbol{\pi}_2, \ldots, \boldsymbol{\pi}_N$ of the row vectors $\mathbf{S}_{:,2}, \ldots, \mathbf{S}_{:,N}$ such that*

$$R_\Sigma = \max_{\boldsymbol{\pi}_2,\ldots,\boldsymbol{\pi}_N} \sum_{k=1}^{K} \sum_{i \in [[\boldsymbol{\pi}_1^T,\ldots,\boldsymbol{\pi}_N^T]^T]_{:,k}} R_{i,k}(\boldsymbol{\pi}_1, \ldots, \boldsymbol{\pi}_N) \tag{5.8}$$

with

$$R_{i,k}(\boldsymbol{\pi}_1, \ldots, \boldsymbol{\pi}_N) = \log(1 + \frac{\boldsymbol{\omega}_{i,k}^H \mathbf{R}_{i,i} \boldsymbol{\omega}_{i,k}}{\sum_{\substack{l \in [[\boldsymbol{\pi}_1^T,\ldots,\boldsymbol{\pi}_N^T]^T]_{:,k} \\ l \neq i}} \boldsymbol{\omega}_{l,k}^H \mathbf{R}_{l,i} \boldsymbol{\omega}_{l,k} + 1}) \tag{5.9}$$

is maximized.

Using long-term CSI in form of spatial correlation matrices, the solution of problem (5.8) gives the matrix $\mathbf{S}$ for an optimized beamscheduling. The cost function is the sum rate of the approximated rates (4.5). The beamforming vectors stored in matrix $\mathbf{\Omega}_k$ are optimized based on a MB problem given by Eq. (5.7). Both, the set of beamforming matrices $\mathcal{W}$ and the scheduling matrix $\mathbf{S}$, can be computed once at a central unit and reused several times as long as the channels are stationary. Therefore, this technique reduces the overhead in the backhaul network. The problem (5.8) matches to a problem of the graph theory.

Definition 40. *Axial multidimensional assignment problem (MAP) [62]: Having a N-partite graph G with parts $X_1 = X_2 = \ldots = X_N = \{1, 2, \ldots, K\}$, find a set of K disjoint cliques in G of the maximal total weight if every clique e_k in G is assigned a weight $w(e_k)$, with $k = 1, \ldots, K$.*

Proposition 12. *The axial MAP is $\mathcal{NP}$-hard.*

Proof. In [91], the author proves that the 3-dimensional axial assignment problem is $\mathcal{NP}$-hard. This is a special case of the MAP, consequently, the MAP is $\mathcal{NP}$-hard as well. □

Proposition 13. *Finding the optimal scheduling matrix maximizing the sum rate in problem* (5.8) *is $\mathcal{NP}$-hard.*

Proof. The proof of the the $\mathcal{NP}$-hardness is straightforward and is proven by the relation of the beamscheduling problem to the $\mathcal{NP}$-hard axial MAP. This problem given in Definition 40 directly maps to a special case of the beam switching problem (5.8). In the case of exactly K users per cell, the number of scheduling slots assigned to the users is K. Then, each cell c (row index of $\mathbf{S}$) corresponds to a dimension of a N-dimensional axial MAP with K elements per dimension. Note, each user is assigned

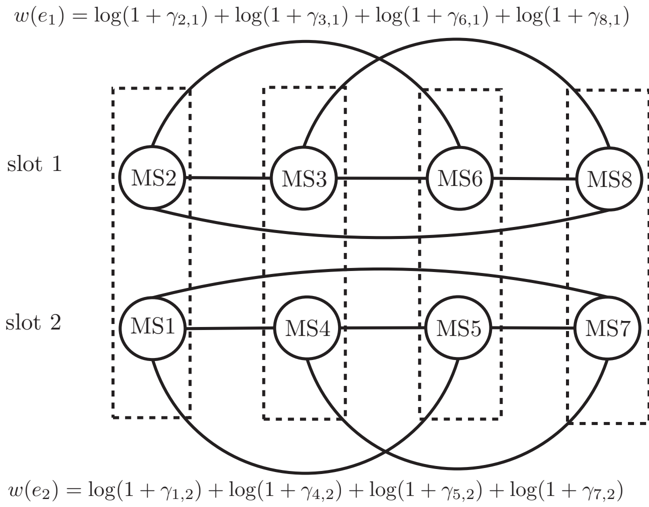

Figure 5.2: Example of a scheduling graph with four cells and two slots. The users (mobile stations (MS)) are denoted by nodes (circles). The selected disjoint cliques are connected with edges. A part corresponds to a cell. Each cell contains two users.
Costs of clique 1: $w(e_1) = \log(1+\gamma_{2,1}) + \log(1+\gamma_{3,1}) + \log(1+\gamma_{6,1}) + \log(1+\gamma_{8,1})$
Costs of clique 2: $w(e_2) = \log(1+\gamma_{1,2}) + \log(1+\gamma_{4,2}) + \log(1+\gamma_{5,2}) + \log(1+\gamma_{7,2})$

exactly once to a scheduling slot. The goal is finding the optimal permutations of row vectors of the matrix $\mathbf{S}$, so that the costs (5.8) are maximized. The costs of scheduling decisions $[\mathbf{S}]_{:,k}$ correspond to the costs $w(e_k)$ of cliques e_k given by

$$w(e_k) := \sum_{i \in [[\boldsymbol{\pi}_1^T, \ldots, \boldsymbol{\pi}_N^T]^T]_{:,k}} R_{i,k}(\boldsymbol{\pi}_1, \ldots, \boldsymbol{\pi}_N).$$

Thus, maximizing the sum rate of all slots k also solves the axial N-dimensional MAP with K elements per dimension. □

Example 4. *Regard the example in Fig. 5.1b) and assume the scheduling decision of a joint scheduling of users* 2, 3, 6, *and* 8 *in the first slot and the scheduling of users* 1, 4, 5, *and* 7 *in the second slot results in a maximized overall sum rate. The optimal scheduling matrix is then given by*

$$\mathbf{S}_{example} = \begin{bmatrix} 2 & 1 \\ 3 & 4 \\ 6 & 5 \\ 8 & 7 \end{bmatrix}. \tag{5.10}$$

Hence there are $K = 2$ *scheduling slots and* $N = 4$ *cells. This corresponds to a N-partite graph with K elements. The problem of finding the maximum sum rate is equivalent to a* 4*-dimensional MAP of finding* 2 *disjoint cliques with* 4 *elements. Fig. 5.2 depicts the equivalent graph representation of the example.*

5.4 Optimal 2-Cell Scenario

To simplify the understanding of the investigations of the general N-cell scenario of Section 5.5, this section investigates the simple 2-cell scenario at first.

The 2-cell scenario is part of the genereal N-cell scenario depicted in Fig. 4.1 where only two adjacent cells are cooperative. As already introduced in Section 5.3, MBF can result in a very low balanced SINR and, therefore, in a low sum rate. The goal is to find optimal scheduling decisions in the adjacent cells such that the balanced SINR is improved. This section discusses two approaches:

1. The first approach targets a maximized sum rate over all scheduling slots (see Section 5.4.1). This approach is useful for applications where a quality-of-service rate is not desired, e.g., internet downloads.

2. The second approach improves the weakest SINR over all scheduling slots. Consequently, the max–min fairness is further improved (see Section 5.4.2). The outcome of this approach is an increased worst SINR. Hence, this approach can be applied in a scenario where each user requires constantly the same rate, e.g, in video conferences.

These two approaches for the 2-cell beam scheduling problem are formulated based on a simple bipartite graph model. Assuming each cell contains K users. The users of each cell correspond to a part of the bipartite graph. The problem of beam scheduling is to find K pairs of users, where one user is selected from both cells, so that the objective (sum rate 1) or minimum SINR 2)) is maximized. Hence, K disjoint cliques in the bipartite graph must be selected. Fig. 5.4 presents an example for the 2-cell scenario. The following sections present two methods to optimize the beam scheduling problem according to the two presented objectives.

5.4.1 Linear Sum Assignment Problem

The first problem is to find the optimal scheduling matrix $\mathbf{S}$ such that the max–min fair beamforming problem (5.7) results in a higher balanced SINR which corresponds to a higher sum rate. One advantage of the 2-cell scenario is the efficient algorithm which exists in this case. As already mentioned in Section 5.3 the N-cell beamscheduling problem maps perfectly to the N dimensional assignment problem. In the 2-cell scenario, this problem corresponds to a linear sum assignment problem.

Definition 41. *Linear sum assignment problem (LSAP): Having a bipartite graph G with parts $X_1 = \{1, 2, \ldots, K\}$ and $X_2 = \{1, 2, \ldots, K\}$, find a set of K disjoint cliques in G of the maximal total weight if every clique e_k in G is assigned a weight $w(e_k)$.*

In Fig. 5.4, a bipartite graph depicts a possible assignment of a 2-cell example with $K = 4$ users per cell. Let $\mathbf{W}$ be a cost matrix with $[\mathbf{W}]_{k_1,k_2} = w_{k_1,k_2} \in \mathbb{R}_+$, and $\mathbf{X}$ be

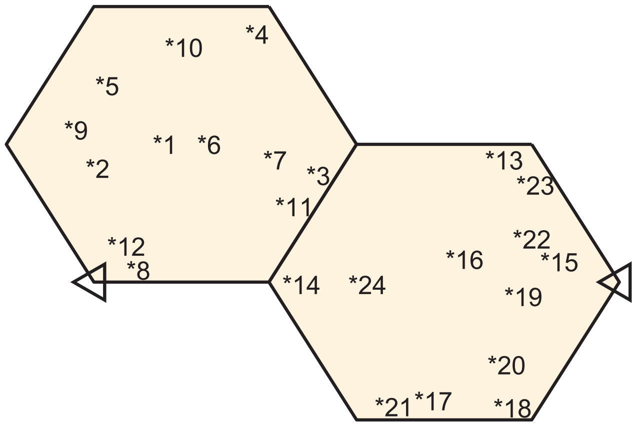

Figure 5.3: 2-cell scenario: The BSs are denoted by triangles and the users are marked users with asterisks $*$ and an index. In each cell $K = 12$ users are randomly distributed.

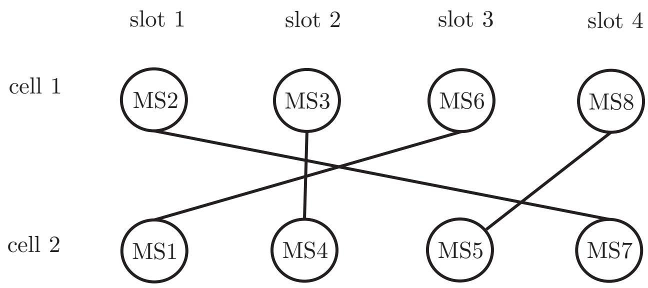

Figure 5.4: Example of a 2-cell scheduling graph. The users are denoted by nodes (circles). The selected disjoint cliques are connected with edges. Each cell contains four users. Each clique corresponds to a scheduling slot. In this example $K = 4$ disjoint cliques are selected.

a matrix of assignments with $[\mathbf{X}]_{k_1,k_2} = x_{k_1,k_2} \in \{0, 1\}$, the LSAP can be also modeled as:

$$\max \overbrace{\sum_{k_1=1}^{K} \sum_{k_2=1}^{K} w_{k_1,k_2} x_{k_1,k_2}}^{=f_0(\mathbf{W},\mathbf{X})} \tag{5.11}$$

$$\text{s.t.} \sum_{k_2=1}^{K} x_{k_1,k_2} = 1 \quad k_1 = 1, \ldots, K,$$

$$\sum_{k_1=1}^{K} x_{k_1,k_2} = 1 \;\; k_2 = 1,\ldots,K,$$
$$x_{k_1,k_2} \in \{0,1\} \;\; k_1,k_2 = 1,\ldots,K.$$

Let $k(i)$ denote the slot in which user i has been scheduled. Regarding the notation of LSAP presented in (5.11), the LSAP corresponds to the bipartite matching problem where the weights $w_{k_1(i_1),k_2(i_2)}$ of the edges among all disjoint node pairs of the two parts X_1 and X_2 are maximized. The variable $x_{k_1(i_1),k_2(i_2)}$ is equal to one if a user i_1 in slot $k_1(i_1)$ of cell 1 is jointly scheduled with a user i_2 in slot $k_2(i_2)$ of cell 2. The objective function $f_0(\mathbf{W},\mathbf{X})$ is then the sum rate of all user pairs i_1, i_2 in the slot pair $k_1(i_1)$, $k_2(i_2)$. Using MB, the cost matrix for a maximized sum rate can be defined as:

$$\begin{aligned}[\mathbf{W}]_{k_1(i_1),k_2(i_2)} = & \log(1+\frac{\boldsymbol{\omega}_{i_1}^H \mathbf{R}_{i_1,i_1}\boldsymbol{\omega}_{i_1}}{\boldsymbol{\omega}_{i_2}^H \mathbf{R}_{i_2,i_1}\boldsymbol{\omega}_{i_2}+1}) \\ + & \log(1+\frac{\boldsymbol{\omega}_{i_2}^H \mathbf{R}_{i_2,i_2}\boldsymbol{\omega}_{i_2}}{\boldsymbol{\omega}_{i_1}^H \mathbf{R}_{i_1,i_2}\boldsymbol{\omega}_{i_1}+1}).\end{aligned} \tag{5.12}$$

To simplify the notation the index k is removed at the beamforming matrix and vectors. In this chapter, the SINR fairness is desired and the solution of a MB problem is used for the beamforming matrices $\mathbf{\Omega}$. The LSAP can be solved optimally in polynomial time. In [95] and [115] the authors present the first polynomial time algorithm that computes the optimal solution of the LSAP based on a cost matrix $\mathbf{W}$. The so-called Hungarian method solves the LSAP in $O(K^4)$. Later, the work [100] presents an $O(K^3)$ implementation of the Hungarian method. In this thesis, the Munkres assignment algorithm [22] was used.

5.4.2 Linear Bottleneck Assignment Problem

Another objective function for the optimization of the scheduling matrix $\mathbf{S}$ is a further improvement of the fairness. The idea is to find scheduling decisions in the two cells such that the SINR of the weakest slot is maximized. This corresponds to an additional SINR balancing over all slots by an optimal assignment of jointly scheduled users.

The linear bottleneck assignment problem (LBAP) of the graph theory matches perfectly to this approach. It has a similar linear programming formulation as the LSAP:

$$\max \min_{1\leq k_1,k_2\leq K} w_{k_1,k_2} x_{k_1,k_2} \tag{5.13}$$
$$\text{s.t.} \sum_{k_2=1}^{K} x_{k_1,k_2} = 1 \;\; k_1 = 1,\ldots,K,$$
$$\sum_{k_1=1}^{K} x_{k_1,k_2} = 1 \;\; k_2 = 1,\ldots,K,$$
$$x_{k_1,k_2} \in \{0,1\} \;\; k_1,k_2 = 1,\ldots,K.$$

Table 5.2: Simulation parameters

Number of user drops	1000
Number of users per user drop and cell	12
Transmit antenna arrays	ULA
Number of antenna array elements at BS	4
Number of antenna array elements at MS	1
Intersite distance	2000 m
Antenna spacing	half wavelength
Path loss exponent	3.76
Power angular density	Laplacian, 10° [52, 114]
Power constraint	per-BS antenna array power constraint

The only difference to the LSAP is the objective function. The optimal value of the objective function is one of the coefficients w_{k_1,k_2} of the cost matrix. The result is an assignment such that the lowest costs are maximized. The MB (5.7) directly delivers the coefficients of the cost matrix:

$$[\mathbf{W}]_{k_1(i_1),k_2(i_2)} = \max_{\boldsymbol{\Omega}} \ \min\left\{\frac{\boldsymbol{\omega}_{i_1}^H \mathbf{R}_{i_1,i_1}\boldsymbol{\omega}_{i_1}}{\boldsymbol{\omega}_{i_2}^H \mathbf{R}_{i_2,i_1}\boldsymbol{\omega}_{i_2}+1}, \frac{\boldsymbol{\omega}_{i_2}^H \mathbf{R}_{i_2,i_2}\boldsymbol{\omega}_{i_2}}{\boldsymbol{\omega}_{i_1}^H \mathbf{R}_{i_1,i_2}\boldsymbol{\omega}_{i_1}+1}\right\} \tag{5.14}$$
$$\text{s.t.} \ |[\boldsymbol{\omega}_{i_1}]_a|^2 \le P_{i_1,a} \ \ \forall a \in \mathcal{A}_{i_1}, \quad |[\boldsymbol{\omega}_{i_2}]_a|^2 \le P_{i_2,a} \ \ \forall a \in \mathcal{A}_{i_2}.$$

As in the previous section the index k is removed at the beamforming matrix and vectors. The LBAP can be solved with less complexity compared to the LSAP.

Theorem 7. *[18, page,174] An LBAP with an $K \times K$ cost matrix $\mathbf{W}$ can be solved in $O(K^{2.5}\sqrt{\log(K)})$.*

To find the optimal solution of the LBAP, this chapter uses the threshold algorithm presented in [18].

5.4.3 Numerical Results

The results presented in this section are based on the scenario depicted in Fig. 5.3. Tab. 5.2 summarizes the main simulation parameters. As in Section 4.5, the pathloss gain is $(r/1000)^{-3.76}$, where r is the distance in meters. For all BSs the same power constraints are given and all users have the same thermal noise level σ^2. The users are randomly distributed in the multicell network, but with a distance larger than 50 meters away form the BSs. In this two cell example no antenna patter is needed, because no interference of adjacent cells is considered in the optimization. Fig. 5.5 depicts the cumulative distribution functions (CDFs) of the following algorithms:

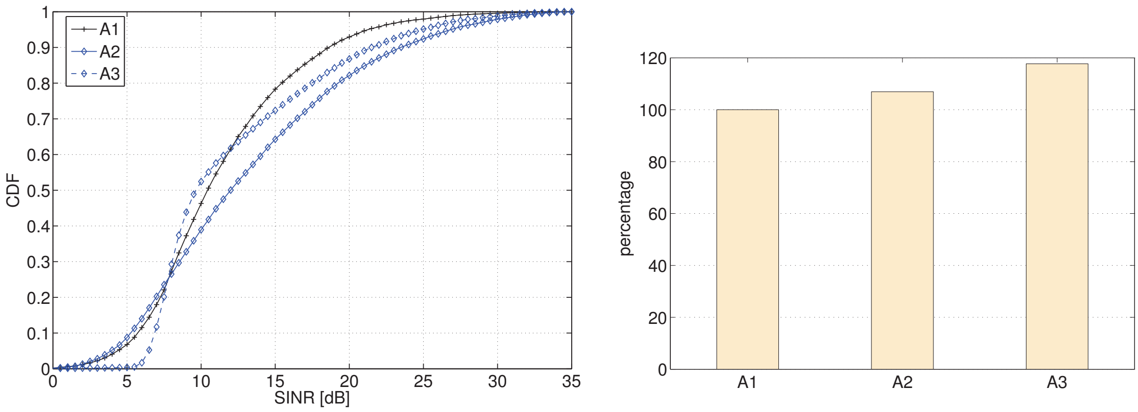

(a) CDF of the mean SINR. (b) Sum rates (5.6) relative to A1 in percentage.

Figure 5.5: Performance (SINR and sum-rate) of the 2-cell scenario.

- A1: MB and random scheduling
- A2: MB and optimized scheduling based on a LSAP presented in Section 5.4.1
- A3: MB and optimized scheduling based on a LBAP presented in Section 5.4.2

As expected, algorithm A2, where a maximized sum rate is desired, maximizes the overall sum rate with a marginal impairment of the fairness. The fair LBAP improves the fairness and is able to outperform the random approach also for higher SINRs.

Figure 5.5.b depicts the sum rate (5.6) gains of the algorithms A2 and A3 relative to A1. As expected, A2 has the best sum rate performance with nearly 20% performance gain. However, even the max–min fair approach A3 can achieve an improvement of the sum rate.

These gains are relatively small. The reason for these small gains is the limited scenario. Only two cells are regarded. Consequently, the degrees of freedom for a scheduling optimization are limited compared to a scenario with a large number of cells. Therefore, the following section presents an optimization scenario with $N = 21$ cells. In this case, the beam scheduling problem is $\mathcal{NP}$-hard, however due to the large number of cell, more degrees of freedom for an optimized beamscheduling are available.

5.5 N-Cell Scenario

The optimization of the beamscheduling problem in a N-cell scenario is $\mathcal{NP}$-hard. No optimal polynomial time solution exists. The beam scheduling problem is a graph theoretical problem. As explained in Section 5.3.2, the optimization of the scheduling matrix $\mathbf{S}$ corresponds to a MAP. An $N = 4$-cell scenario is presented in Example 4. Each cell contains $K = 2$ users. The optimization of the beam scheduling is to find $K = 2$ disjoint groups of users where exactly one user out of each cell is selected, such that a performance metric (e.g., sum rate) is maximized. This group of users is served together in a slot. The graph theoretic interpretation as an MAP is as follows: a slot corresponds to a clique in the N-partite graph. Each user i is a node in this graph. The set of users in a cell c corresponds to a part of nodes X_c. Hence, the problem is the search for K disjoint cliques in a N-partite graph, such that the costs of the each clique are maximized. The costs are given by the total sum rate (5.6).

Definition 42. *Using permutations $\pi_1, \ldots, \pi_N$ of the parts $X_1, \ldots, X_N$ of an N-partite graph, the permutation form of the MAP is given by [62]:*

$$\max_{\pi_2,\ldots,\pi_N} \sum_{i=1}^{K} w(i, \pi_2(i), \ldots, \pi_N(i)). \tag{5.15}$$

Comparing (5.15) with (5.8) underlines the perfect matching of the beamscheduling problem with the MAP. The MAP or the beamscheduling problem can also be seen as a generalized (multidimensional) LSAP [62]:

$$\begin{aligned}
\max \quad & \sum_{\substack{k_j=1 \\ j=1,\ldots,N}}^{K} w_{k_1,\ldots,k_N} x_{k_1,\ldots,k_N} && (5.16)\\
\text{s.t.} \quad & \sum_{\substack{k_j=1 \\ j=1,\ldots,N\ j\neq 1}}^{K} x_{k_1,\ldots,k_N} = 1, \ \ k_1 = 1, \ldots, K, \\
& \cdots \\
& \sum_{\substack{k_j=1 \\ j=1,\ldots,N\ j\neq N}}^{K} x_{k_1,\ldots,k_N} = 1, \ \ k_N = 1, \ldots, K, \\
& x_{k_1,\ldots,k_N} \in \{0, 1\} \ \ k_1, \ldots, k_N = 1, \ldots, K
\end{aligned}$$

with a multidimensional cost matrix $\mathbf{W} \in \mathbb{R}_+^{\overbrace{K \times K \times \cdots \times K}^{N \text{ times}}}$. The axial MAP is $\mathcal{NP}$-hard, therefore, only suboptimal solutions are feasible. In the next sections four different heuristics are investigated.

5.5.1 Scheduling Fairness

The previous sections always assume an equal number of active users per cell. This is an ideal scenario because usually the number of users is different among adjacent cells. In addition to a fair distribution of the mean SINR per user and slot, a fair allocation of the scheduling slots to users is desired. Let $\mathcal{U}_{c,0}$ be the set of $N_c = |\mathcal{U}_{c,0}|$ active users in cell c. To achieve an equal number of users per cell, in cells with less than K users, a user index can be inserted several times. However, all users must be scheduled equally often. To guarantee a fair allocation of the scheduling slots to users in each cell at least

$$K = \text{LCM}\{N_1, N_2, \ldots, N_N\} \tag{5.17}$$

scheduling slots are needed. After K slots the scheduling matrix $\mathbf{S}$ and the set of beamforming vectors $\mathcal{W}$ can be reused as long as the long-term CSI is stationary.

Example 5. *Consider a small network with a cell c_1 with users $\mathcal{U}_{c_1} = \{1,2,3\}$ and a cell c_2 with users $\mathcal{U}_{c_2} = \{4,5\}$. The number of scheduling slots to achieve a fair allocation of scheduling slots per user in a cell is $K =$LCM$\{2,3\} = 6$. Hence, a valid scheduling matrix could be*

$$\mathbf{S}_1 = \begin{bmatrix} 3 & 3 & 2 & 2 & 1 & 1 \\ 4 & 4 & 5 & 4 & 5 & 5 \end{bmatrix}. \tag{5.18}$$

According to the scheduling matrix $\mathbf{S}_1$ in cell c_1, each user is scheduled twice and in cell c_2 each user is scheduled three times.

In some applications, besides the overall fair allocation of all scheduling slots to users, temporal fairness is also important. The delay between two consecutive transmissions should not be too large. This chapter uses two definitions of temporal fairness:

Definition 43. *In opportunistic Round Robin scheduling (ORRS), the transmission time of each BS is divided to $r_c = K/N_c$ rounds, whereby each user in the cell must be served once in every round without a fixed order. With this scheme, the maximum time interval between two consecutive slots allocated to a user equals to $2(N_c - 1)$ scheduling slots.*

Definition 44. *In quasi fair scheduling (QFS), the users can be arbitrarily assigned to the K time slots. With this scheme, the maximum delay between two consecutive transmissions to a user equals to $(N_c - 1)K/N_c$ time slots. This constraint is temporally unfair.*

Example 6. *The scheduling matrix* (5.18) *of example 5 satisfies the QFS criterion but violates the ORRS criterion, because, e.g, in the first round of cell c_1 the user 1 is not scheduled. The following permutation of row vectors of matrix $\mathbf{S}$ given by*

$$\mathbf{S}_2 = \begin{bmatrix} 2 & 1 & 3 & 2 & 3 & 1 \\ 4 & 5 & 5 & 4 & 5 & 4 \end{bmatrix} \tag{5.19}$$

satisfies the ORRS fairness constraint.

5.5.2 Heuristics

Many heuristics for the axial MAP rely on a so-called local neighborhood search. The heuristics in this chapter use two different types of local neighborhoods:

1. Local neighborhood with a permutation in s dimensions (see Definition 45) and
2. local p-exchange neighborhood (see Definition 46).

The next two sections define these two types of local neighborhoods.

Definition 45. *Dimension-wise permutation neighborhood: Using the permutation form* (5.15) *of the MAP, a local neighborhood can be defined by a permutation over a subset of dimensions $\mathcal{D}$ [62]. Let $\boldsymbol{\pi}_1, \ldots, \boldsymbol{\pi}_N$ be arbitrary permutations of the parts $X_1, \ldots, X_N$ of* *an N-partite graph and let* $\mathbf{\Psi} = \{\boldsymbol{\rho}_1, \ldots, \boldsymbol{\rho}_N\}$ *be permutations of* $\mathbf{\Pi} = \{\boldsymbol{\pi}_1, \ldots, \boldsymbol{\pi}_N\}$*. Then* $a(\mathbf{\Pi}, \mathbf{\Psi})$ *is the assignment obtained by permutations* $\boldsymbol{\rho}_1, \ldots, \boldsymbol{\rho}_N$*. A dimension-wise permutation over a subset of dimensions* $\mathcal{D}$ *can then be formally defined by [62]*

$$\hat{d}(\mathbf{\Pi}, \mathbf{\Psi}, \mathcal{D}) = a\left(\mathbf{\Pi}, \left[\begin{cases} \boldsymbol{\rho}_1 & \text{if } 1 \in \mathcal{D} \\ \boldsymbol{\pi}_1 & \text{otherwise} \end{cases}, \ldots, \begin{cases} \boldsymbol{\rho}_N & \text{if } N \in \mathcal{D} \\ \boldsymbol{\pi}_N & \text{otherwise} \end{cases}\right]\right). \tag{5.20}$$

With (5.20), a local neighborhood of size $s = |\mathcal{D}|$ of a dimension-wise heuristic is denoted by

$$\mathcal{N}_{\hat{d}}(\mathbf{\Pi}, s) = \{\hat{d}(\mathbf{\Pi}, \mathbf{\Psi}, \mathcal{D}) : \mathcal{D} \subset \{1, \ldots, N\}, |\mathcal{D}| = s\}. \tag{5.21}$$

The work [62] computes the size of the neighborhood $\mathcal{N}_{\hat{d}}(\mathbf{\Pi}, s)$ with a permutation of one dimension to

$$|\mathcal{N}_{\hat{d}}(\mathbf{\Pi}, s)| = s \cdot (K! - 1) + 1. \tag{5.22}$$

Example 7. *In the regarded multicell network with* $N = 21$ *and, e.g,* $K = 12$ *users per cell the size of the neighborhood* $\mathcal{N}_{\hat{d}}([\boldsymbol{\pi}_1, \ldots, \boldsymbol{\pi}_{21}], 2) \approx 1.0059e{+}10$.

Definition 46. *p-exchange neighborhood: The p-exchange neighborhood is a special case of the dimension-wise permutation neighborhood, where in one of the N dimensions p elements are exchanged. Let* $\boldsymbol{\xi}(p, \boldsymbol{\pi}_n)$ *be the permutation of p elements of* $\boldsymbol{\pi}_n$ *then the p-exchange permutation is formally given by*

$$\hat{p}(\mathbf{\Pi}, p, n) = a\left(\mathbf{\Pi}, \left[\begin{cases} \boldsymbol{\xi}(p, \boldsymbol{\pi}_n) & \text{if } 1 = n \\ \boldsymbol{\pi}_1 & \text{otherwise} \end{cases}, \ldots, \begin{cases} \boldsymbol{\xi}(p, \boldsymbol{\pi}_n) & \text{if } N = n \\ \boldsymbol{\pi}_N & \text{otherwise} \end{cases}\right]\right). \tag{5.23}$$

With (5.23), a local neighborhood of a p-exchange heuristic is denoted by

$$\mathcal{N}_{\hat{p}}(\mathbf{\Pi}, p) = \{\hat{p}(\mathbf{\Pi}, p, n) : \forall n = 1, \ldots, N\}. \tag{5.24}$$

Proposition 14. *[61] For any* $p = 2, \ldots, K$*, the size* $\mathcal{N}_{\hat{p}}(\mathbf{\Pi}, p)$ *of the p-exchange local neighborhood of a feasible solution of a MAP is equal to*

$$|\mathcal{N}_{\hat{p}}(\mathbf{\Pi}, p)| = N \sum_{k=2}^{p} D(k) \binom{K}{k} \tag{5.25}$$

with

$$D(k) = \sum_{j=0}^{k} (-1)^{k-j} \binom{k}{j} j!. \tag{5.26}$$

In practice 2-exchange local neighborhoods are often used [61].

Example 8. *Using the same* $K = 12$ *and* $N = 21$ *setting as in Example 7, the size of 2-exchange local neighborhood is given by* $|\mathcal{N}_{\hat{p}}([\boldsymbol{\pi}_1, \ldots, \boldsymbol{\pi}_{21}], p = 2)| = 1386$.

Comparing the size of the 2-exchange neighborhood with the total number of possible solutions given by $(K!)^{N-1} = 4.0433e{+}173$ it is clear that a 2-exchange heuristic is not the best solution.

Comparing the size of the 2-exchange neighborhood with the size of the dimension-wise permutation neighborhood according to Definition 45, it is obvious that the solution space of the dimension-wise permutation is larger. Therefore, a dimension-wise algorithm can possibly find better solutions than an algorithm based on a 2-exchange neighborhood. In what follows different heuristic are proposed. At first, Section 5.5.2.1 introduces a method based on simulated annealing with a 2-exchange neighborhood. This section is followed by dimension-wise approaches (Section 5.5.2.2 and 5.5.2.3) which outperform the simulated annealing technique. The simulated annealing and the dimension-wise algorithms satisfy the QFS constraint. Therefore, Section 5.5.2.4 additionally presents a low complexity greedy approach that satisfies the ORRS constraint.

5.5.2.1 Simulated Annealing based Sum Rate Maximization

In [23], the authors propose a 2-exchange local search to solve a MAP. A similar approach is applied in this chapter for the N-cell beamscheduling problem. The number of beamforming problems increases strongly with the number of scheduling matrices. Simulated annealing is a local search algorithm and has less computational complexity compared to, e.g., genetic algorithms where multiple solutions (scheduling matrices) are required. The algorithm presented in [23] is based on four simple steps and can be directly applied to the scheduling matrix $\mathbf{S}$:

1. Random selection of a cell c (dimension) of the initial matrix $\mathbf{S}_a$.

2. Random selection of two user indexes i and j of this cell c.

3. Compute $\mathbf{S}_b$ by exchanging the two indexes i and j in c.

4. If the new solution $\mathbf{S}_b$ has a higher sum rate (5.6) than $\mathbf{S}_\alpha$, then accept the new solution. The search is continued until some maximum number of iterations is reached.

Local search algorithms can stay in local optima. To escape from these suboptimal solutions, an extension of the local search to a randomization algorithm as simulated annealing is useful. At the first iterations, the simulated annealing algorithm takes with some probability $Prob(T, R(\mathbf{S}_a), R(\mathbf{S}_b))$ a weaker solution $\mathbf{S}_b$ with $R(\mathbf{S}_b) \leq R(\mathbf{S}_a)$. With an increased number of iterations this probability decreases, so that at the end only the strong solutions are taken. To avoid the multiple computation of one solution, the investigated simulated annealing heuristic never computes the same 2-exchange solution again. Algorithm 6 depicts the used simulated annealing heuristic. The algorithm starts with an initial solution $\mathbf{S}_0$ and returns the best solution $\mathbf{S}_{best}$ that is computed during the whole search. In each iteration, two columns are changed due to the 2-exchange approach, Consequently, two beamforming problems of a network with N users are solved to calculate the cost matrix.

5.5.2.2 Dimension-Wise Sum Rate Maximization

Compared to a p-exchange neighborhood, a dimension-wise permutation neighborhood is much larger and a heuristic using such a large neighborhood can achieve

Algorithm 6 Sum rate based simulated annealing

Initialize: T_0, $T := T_0$
Create random solution $\mathbf{S}_0$
$\mathbf{S}_{best} := \mathbf{S}_0$, $\mathbf{S}_a := \mathbf{S}_0$
while $T > 0$ **do**
  Take randomly a cell c
  Compute random neighboring solution : $\mathbf{S}_b := \hat{p}(\mathbf{S}_a^T, 2, c)$
  Solve the kth MB problem (5.7) with $\mathbf{S} = \mathbf{S}_b \rightarrow \mathcal{W}$
  With $\mathcal{W}$ compute (5.6) $\rightarrow R(\mathbf{S}_b)$
  if $R(\mathbf{S}_b) \geq R(\mathbf{S}_{best})$ **then**
    $\mathbf{S}_{best} := \mathbf{S}_b$
  end if
  if $R(\mathbf{S}_b) \geq R(\mathbf{S}_a)$ **then**
    $\mathbf{S}_a := \mathbf{S}_b$
  else
    Generate random number r uniformly in the range $(0, 1)$
    if $r \leq Prob(T, R(\mathbf{S}_a), R(\mathbf{S}_b))$ **then**
      $\mathbf{S}_a := \mathbf{S}_b$
    end if
  end if
  $T := T - 1$
end while
return $\mathbf{S}_{best}$, $\mathcal{W}$

better solutions at the expense of an increased number of solutions which must be investigated. This section presents a heuristic based on a dimension-wise permutation heuristic for the N-cell beamscheduling problem based on the following observations:

- A user i in a cell c mainly receives interference from its two adjacent cells if a sector pattern as in Fig. 4.1 is used.
- In the case of $N = 2$, the MAP is a LSAP. In this case the MAP can be solved optimally in $O(K^3)$ as presented in Section 5.4.1.

Due to the pattern and the property that most of the interference is received from the two adjacent cells, a LSAP finds near optimal solutions. Consequently, the algorithm must investigate a lower number of solutions. The dimension-wise heuristic combines the two observations to reduce the number of beamforming optimizations. The idea of the algorithm can be summarized in the following steps:

- The algorithm starts in cell $c = 1$ and selects an adjacent cell $c = 2$. For all users with index i_1 of cell $c = 1$ and all users with index i_2 of cell $c = 2$ a cost matrix $\mathbf{W}$ of a LSAP according to (5.14) is computed by solving the beamforming problem (5.7) for all user combinations. The first row of the final scheduling matrix is $\mathbf{S} = [\boldsymbol{\pi}_1^T]^T$. The result of the LSAP is an optimal permutation $\boldsymbol{\pi}_2$. The solution is then fixed and stored in the scheduling matrix $\mathbf{S} = [\boldsymbol{\pi}_1^T, \boldsymbol{\pi}_2^T]^T$.

- With the fixed assignments stored in $\mathbf{S}$, the algorithm selects the next adjacent cell c and finds the optimal permutation $\boldsymbol{\pi}_c$ of users with index i_c in slot k_c in this cell to the previously fixed assignments based on the 2-dimensional cost matrix, as in (5.14)

$$[\mathbf{W}]_{k,k_c(i_c)} = \sum_{i \in \{[\mathbf{S}]_{:,k} \cup i_c\}} \log\Big(1 + \frac{\boldsymbol{\omega}_i^H \mathbf{R}_{i,i} \boldsymbol{\omega}_i}{\sum_{\substack{l \in \{[\mathbf{S}]_{:,k} \cup i_c\} \\ l \neq i}} \boldsymbol{\omega}_l^H \mathbf{R}_{l,i} \boldsymbol{\omega}_l + 1}\Big). \tag{5.27}$$

  The result is the optimal 2-dimensional assignment of users of a new cell c to all previous selected and fixed assignments stored in $\mathbf{S}$. Note, the overall assignment is still suboptimal. However, the result of this dimension-wise optimization is already near optimal due to the fact that the majority of the interference is caused by the adjacent cells. To simplify the notation, the index k is removed from the beamforming vectors $\boldsymbol{\omega}_l$. The MB algorithm optimizes in each step k the beamforming vectors of all selected cells and stores them in a matrix $\boldsymbol{\Omega}_k$.

- If all N cells are visited, the algorithm terminates and returns the optimal scheduling matrix $\mathbf{S}$ and the set of all optimized beamforming matrices $\mathcal{W}$.

The dimension-wise heuristic optimizes the beamforming vectors only for the already selected cells. In each iteration the beamforming problem grows by one cell. Especially, at the beginning, the beamforming problems are small. Alg. 7 depicts the details of the implementation.

Algorithm 7 Dimension-wise sum rate maximization

Initialize: $\mathbf{S} = [\boldsymbol{\pi}_1^T]^T$
for $c = 2$ to N **do**
  Select an adjacent cell c with the users with index i_c stored in $\mathcal{U}_c$.
  for all slots $k_c(i_c) = 1, \ldots K$ of users with index i_c in cell c **do**
    for all slots $k = 1$ to K **do**
      Compute the beamforming matrices $\boldsymbol{\Omega}_k$:

$$\boldsymbol{\Omega}_k = \operatorname{argmax}_{\boldsymbol{\Omega}} \min_{i \in \{[\mathbf{S}]_{:,k} \cup k_c\}} \frac{\boldsymbol{\omega}_i^H \mathbf{R}_{i,i} \boldsymbol{\omega}_i}{\sum_{\substack{l \in \{[\mathbf{S}]_{:,k} \cup i_c\} \\ l \neq i}} \boldsymbol{\omega}_l^H \mathbf{R}_{l,i} \boldsymbol{\omega}_l + 1}$$
$$\text{s.t. } |[\boldsymbol{\omega}_i]_a|^2 \leq P_{i,a}$$
$$\forall a \in \mathcal{A}_i, \ \ \forall i \in \{[\mathbf{S}]_{:,k} \cup i_c\}.$$

      With $\boldsymbol{\Omega}_k$ determine the cost matrix
      $[\mathbf{W}]_{k,k_c(i_c)} = \sum_{i \in \{[\mathbf{S}]_{:,k} \cup i_c\}} \log(1 + \frac{\boldsymbol{\omega}_i^H \mathbf{R}_{i,i} \boldsymbol{\omega}_i}{\sum_{\substack{l \in \{[\mathbf{S}]_{:,k} \cup i_c\} \\ l \neq i}} \boldsymbol{\omega}_l^H \mathbf{R}_{l,i} \boldsymbol{\omega}_l + 1})$
    end for
  end for
  Compute the optimal assignment for $\mathbf{W}$ with a LSAP $\rightarrow \boldsymbol{\pi}_c$.
  $\mathbf{S} = [\mathbf{S}^T, \boldsymbol{\pi}_c^T]^T$
end for
return $\mathbf{S}, \mathcal{W}$

5.5.2.3 Dimension-wise Max–Min Optimization

In addition to the optimization of the sum rate, fairness is often desired. MB achieves a balanced mean SINR for a given scheduling slot k. However, the mean SINR can vary among different scheduling slots. Therefore, an optimization of the sum rate is not the best strategy if fairness among the users is desired. An optimal solution for a fair assignment is presented in Section 5.4.2 for the 2-dimensional case. This approach can be extended to the N-dimensional generalized (multidimensional) LBAP

Definition 47. *Using permutations $\boldsymbol{\pi}_1, \ldots, \boldsymbol{\pi}_N$ of the parts $X_1, \ldots, X_N$ of a N-partite graph, the permutation form of the MAP is given by [92]:*

$$\max_{\pi_2, \ldots, \pi_N} \min_{i=1,\ldots,K} w(i, \boldsymbol{\pi}_2(i), \ldots, \boldsymbol{\pi}_N(i)). \tag{5.28}$$

The equivalent linear programming form is defined by [92]:

$$\max \min_{1 \leq k_1, \ldots, k_N \leq K} w_{k_1,\ldots,k_N} x_{k_1,\ldots,k_N} \tag{5.29}$$

$$\text{s.t.} \quad \sum_{\substack{k_j=1 \\ j=1,\ldots,N\ j\neq 1}}^{K} x_{k_1,\ldots,k_N} = 1, \;\; k_1 = 1,\ldots,K,$$
$$\cdots$$
$$\sum_{\substack{k_j=1 \\ j=1,\ldots,N\ j\neq N}}^{K} x_{k_1,\ldots,k_N} = 1 \;\; k_N = 1,\ldots,K,$$
$$x_{k_1,\ldots,k_N} \in \{0,1\} \;\; k_1,\ldots,k_N = 1,\ldots,K$$

Theorem 8. *The multidimensional bottleneck assignment problem (MBAP) is $\mathcal{NP}$-hard.*

Proof. In [91], the author proved the $\mathcal{NP}$-hardness of the 3-index bottleneck assignment problem which follows form the $\mathcal{NP}$-completeness of the 3-dimensional matching problems with cost in $\{0,1\}$. □

The dimension-wise heuristic Alg. 7 can be simply modified to solve a MABP by using the following cost matrix

$$[\mathbf{W}]_{k,k_c(i_c)} = \max_{\mathbf{\Omega}} \min_{i\in\{[\mathbf{S}]_{:,k}\cup i_c\}} \frac{\boldsymbol{\omega}_i^H \mathbf{R}_{i,i}\boldsymbol{\omega}_i}{\sum_{\substack{l\in\{[\mathbf{S}]_{:,k}\cup i_c\} \\ l\neq i}} \boldsymbol{\omega}_l^H \mathbf{R}_{l,i}\boldsymbol{\omega}_l + 1} \tag{5.30}$$
$$\text{s.t.} \;\; |[\boldsymbol{\omega}_i]_a|^2 \leq P_{i,a} \;\; \forall a \in \mathcal{A}_i, \;\; \forall i \in \{[\mathbf{S}]_{:,k} \cup i_c\}.$$

To achieve a max–min fairness over all slots, the dimension-wise heuristic based on a LBAP uses the MB optimization (5.30) to balance the mean SINR among users as in Section 5.4.2 (for the 2-dimensional case). The dimension-wise max–min optimization is similar to the algorithm presented in Section 5.5.2.2. The heuristic stores fixed assignments in $\mathbf{S}$ and keeps them unchanged. Then heuristic computes the costs of combinations of the users i_c of a new cell c to the previous assignments based on the resulting mean SINR after MB. The MB optimization results in max–min-fair mean SINR for a given slot k among all active users in this slot k. The MBAP, on the other hand, searches for an optimal assignment so that the mean SINR over all scheduling slots k is balanced. Hence, fairness in both directions, among the users and among the slots, can be achieved. Alg. 8 depicts the detail of the implementations.

5.5.2.4 Greedy Algorithm

Straightforward heuristics for $\mathcal{NP}$-hard graph problems are based on a greedy strategy. A greedy algorithm always takes the best decision for the moment. It never reconsiders previous decisions [73], therefore, it is only able to find suboptimal solutions. On the other hand, due to the simple decisions, a greedy algorithm has a low complexity. These decisions should be as good as possible which is the idea of the developed greedy algorithm.

In a given slot k, the algorithm starts in a randomly selected cell and randomly selects a user. The idea is similar to a puzzle: Rotate the beampattern in an adjacent

Algorithm 8 Dimension-wise max–min optimization

Initialize: $\mathbf{S} = [\boldsymbol{\pi}_1^T]^T$
for $c = 2$ to N **do**
  Select an adjacent cell c with the users with index i_c stored in $\mathcal{U}_c$.
  for all slots $k_c(i_c) = 1, \ldots K$ of users with index i_c in cell c **do**
    for all slots $k = 1$ to K **do**

$$[\mathbf{W}]_{k,k_c(i_c)} = \max_{\Omega} \min_{i \in \{[\mathbf{S}]_{:,k} \cup i_c\}} \frac{\boldsymbol{\omega}_i^H \mathbf{R}_{i,i} \boldsymbol{\omega}_i}{\sum_{\substack{l \in \{[\mathbf{S}]_{:,k} \cup i_c\} \\ l \neq i}} \boldsymbol{\omega}_l^H \mathbf{R}_{l,i} \boldsymbol{\omega}_l + 1}$$
$$\text{s.t. } |[\boldsymbol{\omega}_i]_a|^2 \leq P_{i,a}$$
$$\forall a \in \mathcal{A}_i, \ \forall i \in \{[\mathbf{S}]_{:,k} \cup i_c\}.$$

    end for
  end for
  Compute the optimal assignment for $\mathbf{W}$ with a LBAP $\rightarrow \boldsymbol{\pi}_c$.
  $\mathbf{S} = [\mathbf{S}^T, \boldsymbol{\pi}_c^T]^T$
end for
return $\mathbf{S}, \mathcal{W}$

cell by a proper user selection such that the mutual interference among the selected users is minimized. Hence, the newly found user perfectly fits to the already selected users. The algorithm uses the following steps.

- For a given slot k, the algorithm starts randomly in a cell of the network and schedules randomly a user i_0.
- The interference, a user receives, is caused almost exclusively from its adjacent BSs. The algorithm continues the search in an adjacent cell c (adjacent to the cells of previous selected users). In the chosen adjacent cell, the greedy algorithm selects the strongest user i_{best} form set of available unscheduled users.
- The strongest user is the user that maximizes the sum rate achieved in slot k (greedy step).
- After the selection of the strongest user i_{best} in cell c, the algorithm continues the search in the next adjacent cell until all cells are visited. Then the next slot $k+1$ is optimized.
- The algorithm terminates until all slots are optimized.

The algorithm requires a set of free users $\mathcal{U}_c$ given for each cell c. According to the QFS criterion, a user with index i can appear several times in the set $\mathcal{U}_c$. Therefore, this set is formally defined as a multiset [141].

Definition 48. *Assume the multiset $\mathcal{A}$ contains n_a times the element a:*

$$\mathcal{A} = \{\underbrace{a, a, \ldots a}_{n_a \text{ times}}, b, c, \ldots\}, \tag{5.31}$$

The set minus operation $\mathcal{A} \setminus a$ applied to a multiset $\mathcal{A}$ results in the set

$$\tilde{\mathcal{A}} = \{\underbrace{a, a, \ldots a}_{n_a - 1 \text{ times}}, b, c, \ldots\}. \tag{5.32}$$

Definition 49. *With Definition 48 the following update function*

$$F(\mathcal{A}, \mathcal{B}, a) = \begin{cases} \mathcal{A} \setminus a & \text{if} \quad \mathcal{A} \setminus a \neq \emptyset \\ \mathcal{B} & \text{if} \quad \mathcal{A} \setminus a = \emptyset \end{cases} \tag{5.33}$$

for the greedy algorithm can be defined.

Function (5.33) will remove a selected element (user index) a from multiset (or set of free users) $\mathcal{A}$ if $\mathcal{A}$ without a unequals the empty set. Otherwise the set is initialized with a new set $\mathcal{B}$. With the definition of function (5.33), the greedy algorithm achieves either QFS fairness or ORRS fairness with different initializations of the matrices $\mathcal{U}_c$.

- QFS: The set of free users is a multiset $\mathcal{U}_c$. With $K = \text{LCM}\{N_1, N_2, \ldots, N_N\}$, the multiset $\mathcal{U}_c$ contains each user i exactly K/N_c times. Therefore, the BS antenna array of cell c serves each user equally often during the K slots.

- ORRS: The set of free users is a simple set $\mathcal{U}_c$ and contains each user only once. After N_c slots, each user is scheduled again. Therefore, this initialization results in a ORRS fair scheduling.

The greedy algorithm is depicted in Alg. 9. The index $c(i)$ denotes the cell of user i. At the initialization the sets (ORRS) or multisets (QFS) $\mathcal{U}_{c,0}$ are initialized for each cell. If ORRS is desired, the set $\mathcal{U}_{c,0}$ contains each user exactly once. If QFS is desired, the set $\mathcal{U}_{c,0}$ contains each user K/N_c times. The algorithm uses a working set or multisets $\mathcal{U}_c = \mathcal{U}_{c,0}$. If a user is scheduled by the greedy approach, the user will be removed from this set with the update function (5.33). If, e.g., ORRS is desired, the user can not be scheduled until all other users of the set are scheduled. One advantage of the greedy algorithm is, therefore, the possibility of a ORRS fair scheduling. Low delays between two consecutive transmissions are guaranteed. Another advantage is the low complexity.

5.5.3 Complexity Analysis

Regarding all beamscheduling algorithms presented in Sections 5.5.2.1-5.5.2.4, the computation of the beamforming weights for the cost computation has the largest complexity. The complexity of, e.g., the LSAP to compute the assignments is low compared to the complexity of the beamforming optimization to compute the cost matrix. Therefore, the overall complexity is expressed in terms of required beamforming optimizations. The beamforming optimizations can have different sizes and their complexity depends on the number of participating BS arrays. In the following section, the complexity of a beamforming problem with a size of N cells or BS arrays is denoted by $\mathcal{O}_B(N)$.

Algorithm 9 Sum-rate based greedy user selection

Initialize: Compute all $\mathcal{U}_{c,0}$ $\forall c = 1...N$
Set $\mathcal{U}_c = \mathcal{U}_{c,0}$ $\forall c = 1...N$
for $k = 1$ to K **do**
 $\mathcal{S} := \emptyset$
 Randomly take a user i_0
 $[\mathbf{S}]_{c(i_0),k} := i_0$
 Update: $\mathcal{U}_{c(i_0)} := F(\mathcal{U}_{c(i_0)}, \mathcal{U}_{c,0}, i_0)$
 for $c = 1$ to N **do**
  Find next cell c adjacent to the visited cells $\mathcal{C}$
  $\mathcal{C} := \mathcal{C} \cup c$
  for all $i_c \in \mathcal{U}_c$ **do**

$$\mathbf{\Omega}_k = \operatorname{argmax}_{\mathbf{\Omega}} \min_{i \in \{[\mathbf{S}]_{:,k} \cup i_c\}} \frac{\boldsymbol{\omega}_i^H \mathbf{R}_{i,i} \boldsymbol{\omega}_i}{\sum_{\substack{l \in \{[\mathbf{S}]_{:,k} \cup i_c\} \\ l \neq i}} \boldsymbol{\omega}_l^H \mathbf{R}_{l,i} \boldsymbol{\omega}_l + 1}$$
$$\text{s.t.} \quad |[\boldsymbol{\omega}_i]_a|^2 \leq P_{i,a}$$
$$\forall a \in \mathcal{A}_i, \quad \forall i \in \{[\mathbf{S}]_{:,k} \cup i_c\}.$$

   Compute $R^{\Sigma}_{i_c} = \sum_{i \in \{[\mathbf{S}]_{:,k} \cup i_c\}} \log(1 + \frac{\boldsymbol{\omega}_i^H \mathbf{R}_{i,i} \boldsymbol{\omega}_i}{\sum_{\substack{l \in \{[\mathbf{S}]_{:,k} \cup i_c\} \\ l \neq i}} \boldsymbol{\omega}_l^H \mathbf{R}_{l,i} \boldsymbol{\omega}_l + 1})$
  end for
  $i_{\text{best}} = \underset{i_c \in \mathcal{U}_c}{\operatorname{argmax}} (R^{\Sigma}_{i_c})$
  $[\mathbf{S}]_{c,k} := i_{\text{best}}$
  Update: $\mathcal{U}_{c(i_{\text{best}}} := F(\mathcal{U}_{c(i_{\text{best}})}, \mathcal{U}_{c,0}, i_{\text{best}})$
 end for
end for
return $\mathbf{S}$, $\mathcal{W}$

5.5.3.1 Sum Rate based Simulated Annealing

To compute the costs $R(\mathbf{S}_b)$ for the solution based on simulated annealing presented in Alg. 6, the beamforming weights for the exchanged columns of the scheduling matrix must be computed. Hence, problem (5.7) is solved with $\mathbf{S}_b$ as a given scheduling matrix. In total 2 beamforming problems of size N are solved. Let $\mathcal{O}_B(N)$ be the complexity of a MB problem with N BS arrays the total complexity of the cost computation is given by $2 \cdot \mathcal{O}_B(N)$. Assuming the annealing process needs T_0 iterations the total complexity is

$$C = T_0 \cdot 2 \cdot \mathcal{O}_B(N). \tag{5.34}$$

5.5.3.2 Dimension-wise Optimization

The dimension-wise optimizations presented in Sections 5.5.2.2 and 5.5.2.3 are based on the computation of a cost matrix. The algorithm iterates over all cells with index

c. In each iteration a new cell c is added to the set of the visited cells. Therefore, the beamforming problem grows in each iteration by one BS. Assuming the current cell index is c, then c cells are added to the set of visited cells $\mathcal{S}$. With this assumption the beamforming algorithm in iteration c has a complexity of $\mathcal{O}_B(c)$, the computation of the cost matrix requires K^2 beamforming optimizations with a complexity of $\mathcal{O}_B(c)$ to compute the cost matrix in iteration c. In total, the algorithm visits N cells, therefore, the total complexity is

$$C = K^2 \cdot \mathcal{O}_B(2) + \ldots + K^2 \cdot \mathcal{O}_B(N) = K^2 \cdot \sum_{c=2}^{N} \mathcal{O}_B(c). \tag{5.35}$$

5.5.3.3 Sum Rate Based Greedy Algorithm

the greedy algorithm iterates over all slots K and in each slot with index k, the algorithm iterates over all cells. For a given selected cell c, the greedy algorithm searches the strongest user in this cell. Assume each cell has K users, to determine the strongest user, K beamforming optimizations are computed. Hence, the total complexity of slot $k = 1$ is given by

$$C_1 = K \cdot \mathcal{O}_B(2) + \ldots + K \cdot \mathcal{O}_B(N) \tag{5.36}$$

Then, the algorithm removes the strongest user from the set $\mathcal{U}_c$. In the next step $k = 2$ in cell c the algorithm searches the strongest user out of the set $K - 1$ users and the complexity in step $k = 2$ is

$$C_2 = (K-1) \cdot \mathcal{O}_B(2) + \ldots + (K-1) \cdot \mathcal{O}_B(N)). \tag{5.37}$$

In the last step just one user is left in each cell and the complexity is simply

$$C_K = \mathcal{O}_B(2) + \ldots + \mathcal{O}_B(N) \tag{5.38}$$

to compute the last beamforming vectors. The total complexity is then $C = C_1 + \ldots C_K$. Rearranging the sum, the overall complexity is given by

$$C = \mathcal{O}_B(2) \cdot (K + (K-1) + \ldots + 1) + \ldots + \mathcal{O}_B(N) \cdot (K + (K-1) + \ldots + 1). \tag{5.39}$$

Using the formula of the arithmetic serie the final complexity can be simplified to

$$C = \frac{(K-1) \cdot K}{2} \cdot \sum_{n=2}^{N} \mathcal{O}_B(n). \tag{5.40}$$

5.5.3.4 Comparison

For a large K, the greedy algorithm has approximately half of complexity of the dimension-wise optimization approaches in the sense of required beamforming optimizations. The complexity of the simulated annealing approach depends on the start temperature T_0. This chapter selects a start temperature such that the complexity of the simulated annealing approach is as large as the complexity of the two dimension-wise approaches. Consequently the equality

$$C = K^2 \cdot \sum_{c=2}^{N} \mathcal{O}_B(c) = T_0 \cdot 2 \cdot \mathcal{O}_B(N). \tag{5.41}$$

must hold. With

$$T_0 = \frac{K^2 \cdot \sum_{c=2}^{N} \mathcal{O}_B(c)}{2 \cdot \mathcal{O}_B(N)}. \tag{5.42}$$

the complexity (5.34) of the simulated annealing approach is equal to the complexity of the dimension-wise approaches.

5.5.4 Results and Discussion

The simulation parameters are the different from Section 5.4.3. In this section $N = 21$ cells and 100 user drops are optimized. In each drop 12 users are placed in each cell. In this scenario, interference is dominating the noise. The antenna pattern is set to -3dB at 45°. The largest possible SNR in this model is at a distance of 50 meters in the direction of the BS antenna. It is given by $SNR = 64.94$dB. Fig. 5.5 depicts the cumulative distribution functions (CDFs) of the following algorithms:

For a fair comparison of the SINR performance, all cells have the same number of active users, therefore, all algorithms satisfy the QFS constraint according to Definition 44. The CDFs of the following algorithms are compared:

- A1: Random ORRS and MB
- A2: Dimension-wise sum rate maximization according to Section 5.5.2.2
- A3: Dimension-wise max–min SINR optimization according to Section 5.5.2.3
- A4: Greedy user selection according to Section 5.5.2.4
- A5: Simulated annealing according to Section 5.5.2.1

As expected all algorithms outperform the random ORRS (A1) concerning the sum rate performance. The greedy algorithm (A4) is a bit weaker for the low SINR region but achieves the best results for a high SINR. Regarding the high SINR, the dimension-wise sum rate maximization (A2) achieves the best result. The fair version of a dimension-wise optimization (A3) is the best approach regarding the SINR fairness. However, as expected, the strongest users do not gain as much from this approach. The simple simulated annealing based approach (A5) is outperformed by all approaches for the strongest 35% of the users. Only for the weakest users, the simulated annealing approach achieves better results than A4. Regarding the complexity, the simulated annealing based approach (A5) has the same complexity as the dimension-wise approaches (A2 and A4).

The new method A3 has the advantage of an improved SINR fairness compared to the sum rate based approach A4. The weakest 45% of the users gain in SINR compared to A5 and compared to the random solution A1 all users gain in SINR.

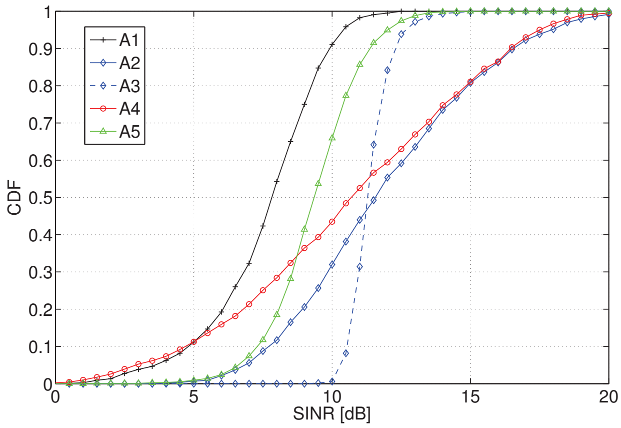

(a) CDF of the mean SINR.

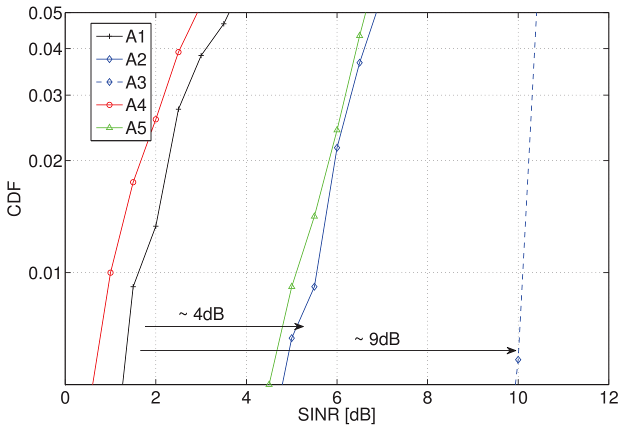

(b) CDF of the mean SINR of the lowest 5%.

Figure 5.6: Comparison of the SINR CDF of the different algorithms A1-A5.

An often used indicator in multicell optimization is the performance of the weakest 5% of the users. Figure 5.6(b) shows the mean SINR of the weakest 5% of the users in all slots and simulation runs. Regarding fairness, the max–min fair dimension-wise approache A3 achieve a significant performance gain. Hence, this approach can be useful in applications where fairness among the users is desired.

As it can be observed from Fig. 5.7(a), all proposed algorithms outperform the random and simulated annealing approach regarding the sum-rate performance. The new max–min fair scheduling algorithm A3 achieves the best SINR fairness and a system with the sum-rate based dimension-wise approach will have the best sum-rate performance. Figure 5.7(b) depicts the relative complexity of all algorithms compared to the reference simulated annealing approach. According to [90], the complexity of the max–min fair beamforming approach grows cubically in the number of users N. Hence, the complexity is of each beamforming problem of size N is in the order of $\mathcal{O}_B(N) = \mathcal{O}(N^3 \cdot K_C)$. Here, K_C denotes a constant factor. Regarding the trade-off between complexity and sum-rate performance the greedy approach A4 is the best approach. For a large number of users per cell K, the greedy algorithm A4 requires the half number of beamforming optimizations compared to A2, A3, and A5. Additionally, A4 can guarantee the ORRS fairness constraint. Therefore, this approach

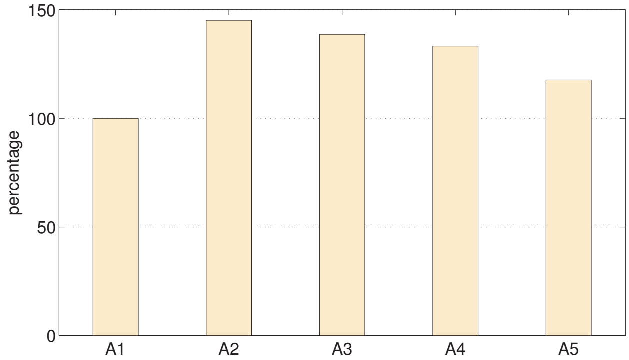

(a) Sum rates (5.6) relative to A1 in percentage.

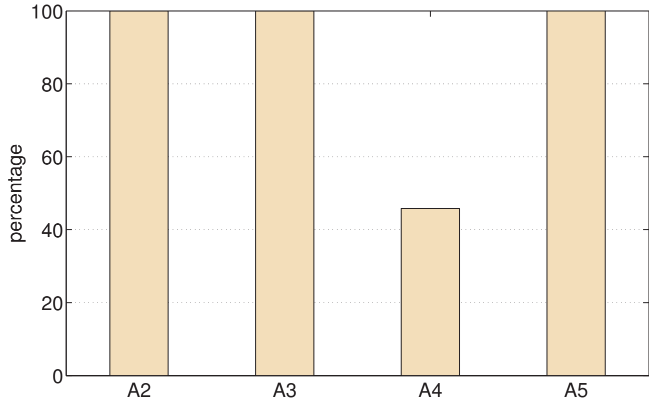

(b) Complexity relative to A3 in percentage.

Figure 5.7: Comparison of the sum rate performance and complexity of the new algorithms.

may be useful in systems where the delay among two consecutive transmissions to a users can not be too large. The other approaches satisfy the QFS constraint. To achieve a lower delay, a post-processing (Appendix) for the scheduling matrix can reduce the delays.

The other approaches satisfy the QFS constraint. To achieve a lower delay, a post-processing (Section 5.6) for the scheduling matrix can be applied. However, a low delay can not be guaranteed as in the greedy based approach A4. Table 5.3 summarizes the results of the algorithms A1-A5.

5.6 Latency Optimization to Improve the Temporal Fairness

Depending on the application, besides the SINR fairness or the sum rate performance, the delay among consecutive transmissions is another design criterion. Assuming an arbitrary number N_c of users per cell c, large delays between two consecutive transmissions to a user are possible. In Definition 44 and 43 two temporal fairness constraints are defined. The ORRS constraint guarantees a small delay because a user

Table 5.3: Summary of the advantages of the different algorithms regarding different properties ((++): very good, (+): good, (0): fair, (-): weak).

Algorithm	Temp. fairness	Sum rate	SINR fairness	Complexity
A1: random RRS	(++)	(-)	(-)	(+)
A2: dim.-wise sum rate max.	(0)	(++)	(+)	(-)
A3: dim.-wise max–min opt.	(0)	(+)	(++)	(-)
A4: greedy sum rate max.	(+)	(+)	(-)	(0)
A5: SA based sum rate max.	(0)	(0)	(0)	(-)

must be scheduled exactly once per scheduling round. The greedy approach presented in Section 5.5.2.4 maximizes the sum rate while the ORRS constraint is satisfied. However, the other approaches, e.g., the dimension-wise optimizations presented in Sections 5.5.2.2 and 5.5.2.3 only satisfy the QFS constraint. Therefore, our earlier work [39] presents a further improvement to reduce the delay when the scheduling matrix only satisfies the QFS constraint. Our earlier work [39] presents a low complexity greedy algorithm for the delay optimization. However, it does not discuss the complexity of the resulting optimization problem. Therefore, this section gives a detailed complexity theory for the latency optimization to conclude the work.

The total costs defined by the sum rate $R(\mathbf{S})$ in (5.6) of a scheduling matrix $\mathbf{S}$ are given by a summation of the rates per scheduling slot k of each column of the scheduling matrix.

$$R_k = \sum_{i \in [\mathbf{S}]_{:,k}} \log(1 + \frac{\boldsymbol{\omega}_{i,k}^H \mathbf{R}_{i,i} \boldsymbol{\omega}_{i,k}}{\sum_{\substack{l \in [\mathbf{S}]_{:,k} \\ l \neq i}} \boldsymbol{\omega}_{l,k}^H \mathbf{R}_{l,i} \boldsymbol{\omega}_{l,k} + 1}). \tag{5.43}$$

If the columns are fixed, the mean SINR does not change if the column-vectors are rearranged. Hence, rearranged columns $[\mathbf{S}]_{:,k}$ do not change the total rate $R(\mathbf{S})$ as well. However, the delay between two consecutive transmissions to a user can be reduced. Note, the scheduling matrices can be reused as long as the channel is stationary and as long as the number of active users does not change. Hence, the scheduling matrix can be concatenated several times and a big matrix $\mathbf{S}_\sigma = [\mathbf{S}, \ldots, \mathbf{S}]$ is the result. The overall sum rate is still unchanged, as long as the statistics are unchanged.

First of all the question arises whether all matrices satisfying the QFS constraint can be rearranged in a way so that they satisfy the ORRS constraint. This can be simply proven by contradiction.

Proposition 15. *Not every matrix $\mathbf{S}_{QFS}$ satisfying the QFS constraint can be column-wise rearranged to a matrix $\mathbf{S}_{ORRS}$ satisfying the ORRS constraint.*

Proof. The proof is straight-foreward and can be proven by contradiction. The following matrix

$$\mathbf{S}_{QFS} = \begin{bmatrix} a & b & c & a & b & c \\ g & f & g & f & e & e \\ h & i & j & j & h & i \\ k & l & l & k & l & k \end{bmatrix} \tag{5.44}$$

satisfies the QFS constraint. However, it can not be column-wise rearranged to a matrix $\mathbf{S}_{ORRS}$ satisfying the ORRS constraint. □

A solution satisfying the QFS constraint can not be guaranteed. However, an algorithm can rearrange the columns of a matrix $\mathbf{S}$:

1. Rearrange the columns so that the maximum delay among all consecutive transmissions to all users i is minimized. This is the maximal fairness constraint.

2. Another criterion could be a minimized total delay among all users.

Definition 50. *The maximum delay $d_{i,c}$ of all consecutive transmissions to a user i in cell c is the maximum number (circular) of slots of all consecutive transmissions to user i.*

Example 9. *Regard the matrix* (5.44)*, the maximum delay of user e in cell* 2 *is $d_{e,2} = 5$. User e is served in the* 5*th slot and in the* 6*th slot. The delay from the* 5*th to the* 6*th slot is* 1 *but the circular delay to the next* 5*th slot is* 5*. The curricular delay is the result of the concatenation of the optimized scheduling matrices, which are reused (possibly) several times to reduce the backhaul overhead.*

The maximum delay of all users in a cell is then $\delta_c = \max_{i \in [\mathbf{S}]_{c,:}} d_{i,c}$.

Definition 51. *Column-wise delay optimization problem (CDP) of a scheduling matrix:*

1. *The minimization of the maximum delay is the search of the optimal permutation of columns $[\mathbf{S}]_{:,k}$ of the scheduling matrix such that*

$$\delta(\mathbf{S}) = \max_{c=\{1,\ldots,N\}} \max_{i \in [\mathbf{S}]_{c,:}} d_{i,c} \tag{5.45}$$

   is minimized.

2. *The optimization of the total delay is the search of the optimal permutation of columns $[\mathbf{S}]_{:,k}$ of the scheduling matrix such that*

$$\delta(\mathbf{S}) = \sum_{c=1}^{N} \sum_{i \in [\mathbf{S}]_{c,:}} d_{i,c} \tag{5.46}$$

   is minimized.

The question is now, whether a polynomial time algorithm exists which finds the optimal solution for the CDP. The answer is no. The following $\mathcal{NP}$-hard problems are helpful to prove the $\mathcal{NP}$-hardness of the CDP.

Definition 52. *The bottleneck traveling salesman problem (BTSP): Search for a Hamiltonian cycle C in a weighted graph $G = (V, E)$ which minimizes the weight of the maximal weighty edge of the C.*

Definition 53. *The traveling salesman problem (TSP): Search for a Hamiltonian cycle C in a weighted graph $G = (V, E)$ which minimizes the total weight of the C.*

It is well known that both problems, the TSP and the BTSP, are $\mathcal{NP}$-hard [63].

Proposition 16. *The CDP of finding the optimal permutation of rearranged columns $[\mathbf{S}]_{:,k}$ of a scheduling matrix $\mathbf{S}$, so that the maximum or the total delay $\delta(\mathbf{S})$ of all consecutive transmissions to all users is minimized, is $\mathcal{NP}$-hard.*

Proof. To prove the $\mathcal{NP}$-hardness, the following proof shows that the CDP contains the BTSP, if fairness is desired, as a special case or it contains the TSP if minimized total delay is desired. The search for the optimum permutation of column vectors to achieve for all users a, e.g., perfectly balanced delay of consecutive transmissions to users can be expressed by a search for a weighted Hamiltonian cycle (HC) in a graph. This graph is constructed as follows: The nodes of the graph correspond to the columns of the scheduling matrix $\mathbf{S}$. Hence, a node $v_k \in V$ is given by $[\mathbf{S}]_{:,k}$. All nodes K are connected by an edge $e \in E$ so that a complete graph $G = (V, E)$ is the result. The search of a minimized largest delay of all users in all cells corresponds to a search of an HC with the following costs: Assuming there is an already determined part of an HC H which starts at a node v_1 and ends at a node v_k and the next node v_{k+1} will be added to the HC and let $\mathbf{q}(H, v_1, v_k, v_{k+1}) \in \mathbb{N}^{N\times 1}$ be a vectorial function, then $q_c(H, v_1, v_k, v_{k+1})$ determines the minimum feasible delay the user with the largest delay in cell c will have if all previously selected nodes v_1 to v_k are considered. If fairness among all users in all cells is desired, the goal is now to find HC H such that

$$\max_{k=\{1,\ldots,K-1\}} \max_{c=\{1\ldots,N\}} q_c(H, v_1, v_k, v_{k+1}) \tag{5.47}$$

is minimized. This problem is equivalent to case 1 of the CDP. A special case of the fair CDP is a BTSP if

$$\max_{c=\{1\ldots,N\}} q_c(H, v_1, v_k, v_{k+1}) = w(v_k, v_{k+1}) \tag{5.48}$$

and if $w(v_k, v_{k+1}) \in \mathbb{N}$ are some arbitrary cost values which do not depend on the previously selected part of an HC H. Hence, the result is now the search for a HC H that minimizes the weight of the maximal weighty edge on H. If a minimized total delay is desired, the goal is now to find HC H such that

$$\sum_{k=1}^{K-1} \sum_{c=1}^{N} q_c(H, v_1, v_k, v_{k+1}) \tag{5.49}$$

is minimized. This problem is equivalent to the second case of the CDP and it contains the TSP as special case if

$$\sum_{c=1}^{N} q_c(H, v_1, v_k, v_{k+1}) = w(v_k, v_{k+1}). \tag{5.50}$$

Hence, the result is now the search for an HC H that minimizes the total weight of an HC H. □

Example 10. *The following matrix is optimized so that the overall sum rate is maximized:*

$$\mathbf{S} = \begin{bmatrix} a & b & c & c & a & b \\ e & e & e & f & f & f \\ g & h & h & h & g & g \\ j & k & k & i & i & j \end{bmatrix} \tag{5.51}$$

The maximum delay in cell 1 *is* $d_1 = \max\{4,4,5\}$*, in cell* 2 *it is* $d_2 = \max\{4,4\}$*, in cell* 3 *it is* $d_3 = \max\{4,4\}$ *and in cell* 4 *is* $d_4 = \max\{5,5,5\}$*. Fig. 5.8 depicts the graph representation of CDP. The four numbers in each box correspond to the four cells. Assume the starting node is* (a,e,g,j)*, the costs of selecting the next node* (b,e,h,k) *are then* $(3,3,2,3)$*. For example, the minimum feasible worst delay in the second cell is then* 3 *if e is the first and in the second node. Selecting the next node* (c,e,h,k) *increases the minimum feasible worst user delay from* 3 *to* 4*, because user e is now* 3 *times scheduled and now user f must be scheduled* 3 *times and the next transmission for user e will be in* 4 *slots. If fairness is desired, the green and the blue HC are equivalent. If a minimized total delay is desired, the blue is selected. The green HC shows the initial solution given by* (5.51)*. The red HC has the best temporal fairness.*

Due to the similarity of the CDP to the TSP multiple approaches in the literature developed for the TSP can also find local optimal solutions for the CDP. The approach presented here has similarities to the nearest neighbor algorithm [63]. However, multiple different algorithms for the TSP or the BTSP are possible and exist in the literature.

The total costs of a scheduling matrix are given by a summation of the costs of each column of the scheduling matrix. Thus, rearranging the columns $[\mathbf{S}]_{:,k}$ does not change the total costs but the delay between two consecutive transmissions to a user can be reduced. The following final post-processing of the scheduling matrix can reduce the delay by rearranging the column vectors of the scheduling matrix. Algorithm 10 creates a new scheduling matrix $\mathbf{S}_{LD}$ with a lower delay between two consecutive transmissions to the scheduled users. The algorithm searches in the initial matrix $\mathbf{S}_{QFS}$ for column vectors $\mathbf{s}$, which together with the already found column vectors in $\mathbf{S}_{LD}$, do not violate the ORRS constraint. If no column exists in $\mathbf{S}_{QFS}$, the algorithm takes the best fitting vector $\tilde{\mathbf{s}}$, which violates the ORRS constraint in the lowest number of cells. In several cases, the algorithm rearranges $\mathbf{S}_{QFS}$ to $\mathbf{S}_{LD}$ satisfying the ORRS temporal fairness constraint in all cells. Fig. 5.9 compares the histogram of the delay between two consecutive transmissions to a user of a random ORRS scheduling matrix, a non optimized scheduling matrix as a result of e.g. Algorithm 7 and the optimized scheduling matrix after applying Algorithm 10. The number of delay values larger than 10 is significantly reduced after applying Algorithm 10.

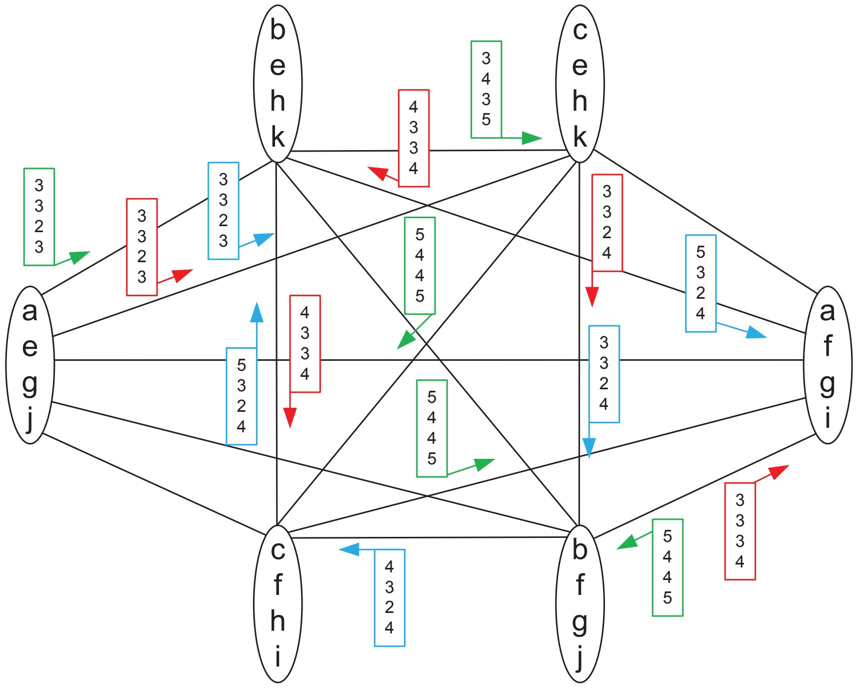

Figure 5.8: Graph representation of (5.44). Three Hamiltonian cycles (a green, a blue and a red one) are depicted. The numbers at the edges denote the minimum feasible delay the user with the largest delay will have in this cell if the next node (in the direction of the arrow) is selected.

Algorithm 10 Delay optimization

Require: Scheduling matrix $\mathbf{S}_{QFS} = \mathbf{S}$
  $[\mathbf{S}_{LD}]_{:,1} = [\mathbf{S}]_{:,1}$
  for $k = 2$ to K **do**
    Find a column vector $\mathbf{s} = [\mathbf{S}_{QFS}]_{:,\kappa}$, so that
    $\mathbf{S}_{LD} = [\mathbf{S}_{LD}, \mathbf{s}]$ does not violate ORRS in any cell
    if $\exists \ \mathbf{s} \in \mathbf{S}_{QFS}$ **then**
      $\mathbf{S}_{LD} = [\mathbf{S}_{LD}, \mathbf{s}]$
    else if $\nexists \ \mathbf{s} \in \mathbf{S}_{QFS}$ **then**
      Take a column vector $\tilde{\mathbf{s}} = [\mathbf{S}_{QFS}]_{:,\kappa}$, so that
      $\mathbf{S}_{LD} = [\mathbf{S}_{LD}, \tilde{\mathbf{s}}]$ violates ORRS in the lowest number of row vectors $[\mathbf{S}_{LD}, \tilde{\mathbf{s}}]_{c,:}$
    end if
  end for
  return $\mathbf{S}_{LD}$

5.7 Summary

This chapter presents the general graph theoretic background of the multicell beamscheduling problem. The following most significant insights into the beamscheduling problem can be stated:

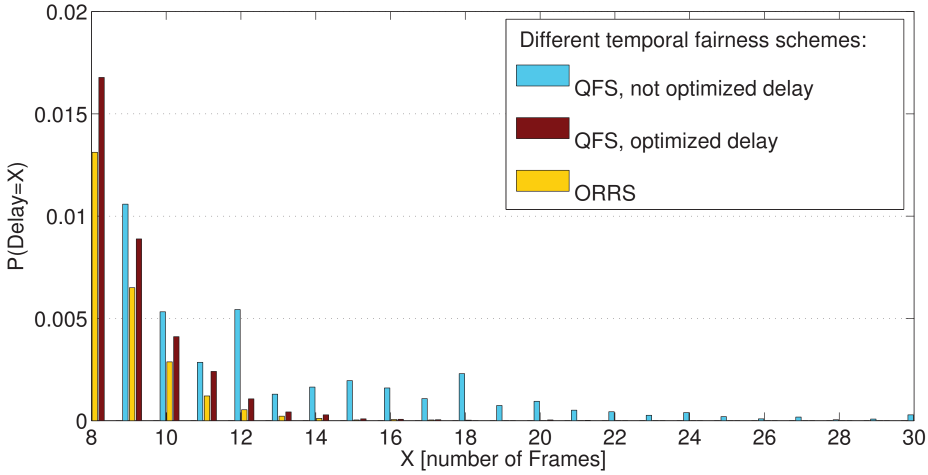

Figure 5.9: Histogram of the delays for different temporal fairness schemes [39].

- Max–min beamforming can result in a low balanced SINR and, therefore, in a low sum rate if there is a beam collision. A beam collision is given if two different links are in the same region. A high mutual interference can be the consequence. In particular, cell edge users are often affected. The avoidance of these beam collisions based on the long-term channel statistics is called beam-scheduling. Different objective functions are investigated.
- The general N-cell beamscheduling problem is $\mathcal{NP}$-hard in general. However, in the 2-cell scenario optimal solutions are feasible.
- The result of a 2-cell optimization is optimal because it is equivalent to the linear sum assignment problem. Based on a fixed 2-cell approach the assignments of users in a new cell can be obtained by considering the assignment of the fixed 2-cell approach. By a cell by cell optimization, a near optimal solution maximizing the sum rate can be found. This optimization technique is called dimension-wise optimization.
- In addition to the sum rate maximizing approach, a max–min fair approach can achieve large gains for the weakest users.
- A simple greedy-based approach can find temporal fair solutions maximizing the sum rate with half the complexity compared to the dimension-wise optimization methods at the expense of a reduced SINR performance for the weakest users.
- A final post-processing optimization to reduce the delay among two consecutive transmissions to the users is proven to be $\mathcal{NP}$-hard as well. However, a close relation to the traveling salesmen problem enables a variety of useful approaches.

Chapter 6

Application: Multicell Unicast Beamforming with One-Way Relays

The content presented in this Chapter is published in the publications [46, 47].

6.1 Introduction

This chapter shows a practically relevant application of unicast beamforming in multicell networks. BSs are usually expensive; hence, cheaper alternatives are desired. Relays can be an alternative because they can be applied without a direct connection to the backhaul network, especially in scenarios where low-cost small BSs are desired to increase the coverage. The low cost BSs can be placed in regions where users are strongly shadowed. These small BSs usually have a lower transmit power and a smaller coverage; hence, these networks consist of different types of stations and are called heterogeneous.

This chapter investigates beamforming in a heterogeneous multicell network with BSs and relay stations. As in the previous chapters, a frequency reuse-1 is desired to increase the spectral efficiency of the network. However, then intercell interference will occur and an unfair distribution of the SINR of all jointly served users can be a consequence.

In Chapter 4, max–min beamforming was introduced, its duality was established and a low complexity iterative algorithm was employed form the previous research. With max–min beamforming, the SINR among the users can be balanced. Hence, a fair distribution of achievable rate among the users is possible. However, in networks where fairness is desired, some bad links can decrease the performance of the entire system. Chapter 5 presents beam scheduling techniques to avoid unfavorable scheduling decisions which result in beam collisions. All jointly active links can gain from the avoidance of these bad beam scheduling decisions.

In addition to beam collisions, shadowed[1] users can deteriorate the performance of all jointly active users as well. Smart beam scheduling can not help in this case. A solution would be a weighted SINR to avoid the sum rate degradation if these users are scheduled. However, an unfair system will be the consequence.

Another approach is the usage of low-cost relays which can be placed in regions with bad coverage. Relays are located closer to the users, therefore, a link without strong shadowing is more likely. The SINR of all other jointly served users increases.

[1] This thesis considers shadowing in a urban cell model. Shadow fading can be caused by multiple reasons, e.g., high buildings.

In addition to the intercell interference, this chapter considers shadow fading as another performance limiting factor. These two technologies are combined to jointly overcome the interference and shadow fading problems:

- Coordinated max–min beamforming is a well known technique to deal with the interference in a multiple input single output (MISO) channel. It results in a fair distribution of the SINR among the users. In some cases even a balanced SINR can be achieved.

- Relays are a well known approach to overcome the shadowing problem. Shadowed users can gain a larger spatial diversity or an improved received power of the desired signal due to a reduced distance or by a line-of-sight connection to a relay.

Figure 6.1 illustrates the motivation of beamforming with relays. Figure 6.1a shows a conventional network with BSs and max–min beamforming. Several users are shadowed; hence, the balanced SINR will be possibly low. An improvement of the balanced SINR can be achieved if relays serve shadowed users as depicted in Fig. 6.1b. If the relays have a line-of-sight (LOS) connection to their BSs, the SINR in the first hop (green) will be high. Due to avoidance of shadow fading, also the SINR of the second hop (blue) will be higher compared to the scenario in Fig. 6.1a. The question is whether the capacity loss due to the half duplex transmission over the relays can be compensated by this SINR gain.

6.1.1 Scenario

Figure 4.7 shows the considered multicell network with $N = 21$ cells, each equipped with one BS and two relay station (RSs) arrays. Each BS has a height of 32 meters and the decode-and-forward half duplex RSs have a height of 20 meters. Each station (BS or RS) consists of three sectors with a 120° antenna pattern. The sector pattern is illustrated with lobes in Figure 4.7 on Page 64. Each BS antenna array or RS antenna array directed to the cell center can serve users inside this cell. The relays are so-called in-band relays. Hence, each relay will cause interference to all jointly active BS-mobile station (MS) and RS-BS links. Three types of DL-transmissions are considered in this chapter:

- Only the RS serves the user. The BS transmits in the first hop to the RS (backhaul link) and the RS decodes and forwards the signal to the user.

- The user is served jointly by a RS and the BS. The BS transmits the signal in the first hop to the RS and in the second hop the RS helps the BS in the transmission to the user. In the case of a coherent transmission based on instantaneous CSI, a beamforming gain can be achieved. Without a tight synchronization, e.g., if long-term CSI is used, only a spatial diversity gain is feasible, e.g., [82, 83].

- Direct transmission: The BS transmits the signal directly to the user without a RS.

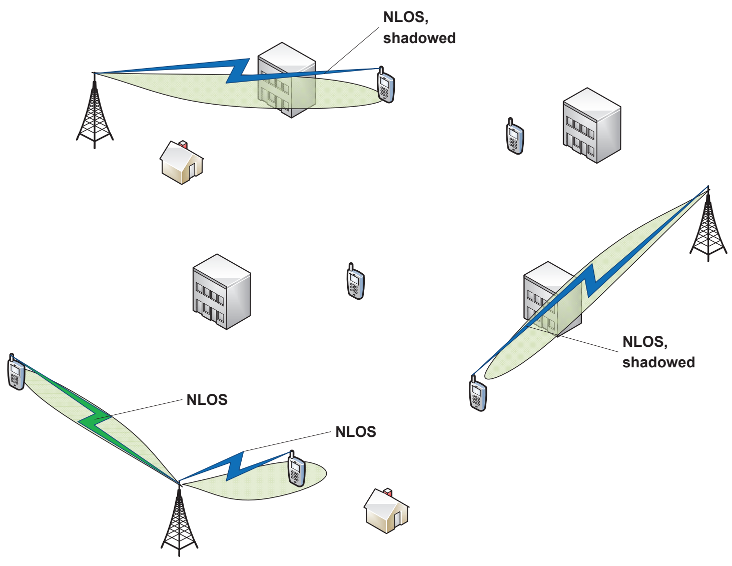

(a) Low balanced SINR

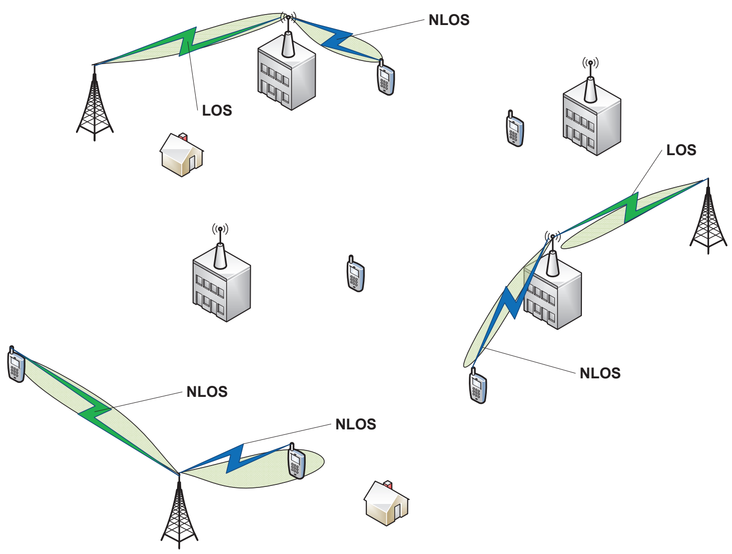

(b) High balanced SINR

Figure 6.1: Example: Beamforming with and without relays.

To guarantee a strong backbone (BS-RS) link this chapter considers a static line of sight (LOS) connection in a rooftop-to-rooftop scenario. All other links (BS-MS and RS-MS) have a non-LOS (NLOS) connection.

Furthermore, all stations in the network are assumed to be synchronized. [86] presents a simple synchronization scheme based on global positioning system (GPS) signals.

6.1.2 One-Way Relays

Multiple types of relays are proposed in the last years. The two most famous types are called one-way amplify-and-forward and one-way decode-and-forward relays.

- Amplify-and-forward relays amplify the signal received from the source in the first hop and forward the amplified signal to the destination in the second hop. Due to this amplification, the noise also is amplified.

- Decode-and-forward relays decode the signal received from the source in the first hop, encode it again and forward the signal to the destination in the second hop. Decode and forward relays are considered in current standards due to the minimal standardization effort. These relays can be simply integrated in systems appearing in the next future, as LTE. Furthermore, several studies show advantages of decode-and-forward relays compared to amplify-and-forward relays in multicell applications regarding the cell edge region [13].

6.1.3 Related Work

The information theoretical fundamentals of the relay channel were investigated in [27]. In the later work [99], space-time-diversity-achieving half duplex relay protocols called selective relaying or selection decode-and-forward were investigated. In [99], the BS transmits to the RS and the user in the first hop. In the second hop the relay forwards the correctly decoded signal to the user. A diversity gain is achieved due to the relayed transmission. Another transmission scheme is presented in, e.g. [167]. In this article the BS transmits in a first hop to the RSs. After decoding only the relays forward the signal to the user. The BS stays silent. In both hops precoding vectors are optimized. Zero-forcing beamforming was used to avoid mutual interference among the jointly transmitting RSs. However, this scenario was limited to a single cell. An extension to a multicell scenario is presented in [121]. The authors propose different relay techniques (one-way and two-way relaying) to mitigate intercell interference in a multicell network.

Coordinated beamforming is useful for interference mitigation. Chapter 4 presents the theoretical background of the downlink beamforming and SINR balancing. Beamforming as a promising technique to mitigate interference and can be combined with RSs which is a useful solution to achieve spatial diversity and to overcome shadow fading. Combinations of beamforming and relaying are presented in [68] and [46].

6.1.4 Contributions

- Using decode-and-forward relays, the total (achievable) rate over the two hops is the minimum rate achieved in each hop. This chapter extends the MBP by an additional SINR constraint to constrain the SINR of the second hop to the SINR of the first hop. Power is wasted if, e.g., the SINR of the second hop is larger than the SINR of the first hop. This idea results in an additional constraint. A reduction of the transmit power is possible. Therefore, a new formulation of the optimization problem is introduced which results in a low complexity solution. If instantaneous CSI is available a reduced transmit power without any performance loss is feasible. If only long-term CSI in the form of spatial correlation matrices is available for the optimization, a performance loss is possible because of the lack of the fading information. However, due to the assumed static LOS link in the first hop, the SINR in the first hop has a very low and slow fading. Therefore, only the fading of the second hop can cause a performance loss. Simulation results have shown that this performance loss is relatively small compared to the achieved reduction of the transmit power.

- Finally, this chapter proposes joint optimization of beamforming and beamscheduling in a multicell network with RSs at the cell edge region. Techniques for joint optimization of beamforming and beamscheduling, presented in Chapter 5, are extended by an additional optimization of the assignment of RSs or BSs to users. This approach searches for the optimal selection of users and serving stations so that the mutual interference among all links is minimized and, therefore, the sum rate of the network is maximized.

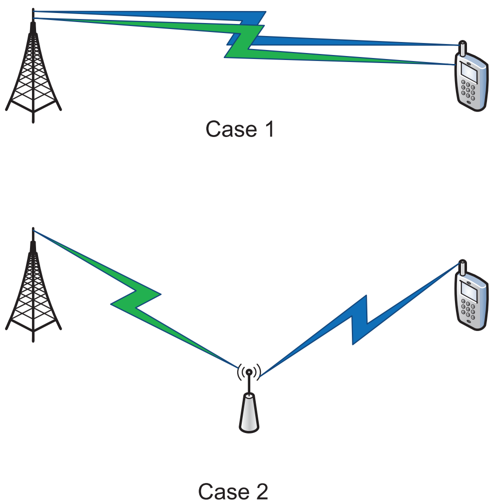

Figure 6.2: Possible assignments of BSs and RSs to users (MSs).

6.2 System Setup

Figure 4.7 on Page 64 depicts the investigated network layout consisting of $N_S = 63$ cooperative antenna arrays, $N_B = 21$ at BSs and $N_R = 42$ at the RSs. Each cell has one BS and two RS antenna arrays with $N_A = 4$ antenna elements. Figure 6.2 illustrates the possible assignments of stations to users. The blue connection denotes the

Table 6.1: Assignment of stations to MSs and time division channel allocation

	1st hop	2nd hop
BS1 cell 1	MS1	MS1
RS1 cell 1		
RS2 cell 1		
BS2 cell 2	RS3	
RS3 cell 2		MS2
RS4 cell 2		

transmission of the first hop, the green connection is the transmission of the second hop.

1. Case 1 shows the conventional transmission scheme. Mobile station (MS) 1 is served by a BS in two hops.

2. Case 2 is a transmission of a BS via a RS to MS 2.

All a priori assignments of users to BSs or RSs are based on local long-term CSI. Figure 6.3 and Table 6.1 illustrate possible transmissions by a small two cell example. The situation in the first cell correspond to case 1. The BS 1 serves user MS 1 over the two hops. In cell 2, BS 2 transmits to RS 3 in the first hop and then RS 3 forwards the decoded signal to MS 2. In the first hop, there is intercell interference among BS 1 and BS 2. In the second hop, there is interference among BS 1 and RS 3.

In the first hop the channel matrix $\mathbf{H}_{b,r(i)}^H \in \mathbb{C}^{N_A \times N_A}$ denotes the MIMO channel between the RS $r(i)$ assigned to user i and the BS b. The transmit beamforming vectors at the BSs are denoted with $\boldsymbol{\omega}_{b(r(i))}$. The index $b(r(i))$ denotes the BS $b(r(i))$ serving RS $r(i)$ serving user i. With the assumption of maximum ratio combing (MRC) $\mathbf{V}_{r(i)} = \boldsymbol{\omega}_{b(r(i))}^H \mathbf{H}_{b(r(i)),r(i)}$ at the RSs, a RS serving user i receives the signal

$$g_{r(i),k}^1 = \mathbf{V}_{r(i)} \left(\mathbf{H}_{b(r(i)),r(i)}^H \boldsymbol{\omega}_{b(r(i))} x_{r(i)} + \mathbf{f}_{r(i),k} + \mathbf{n}_{r(i)} \right) \tag{6.1}$$

where the interference signal of different BS-RS or BS-MS links is given by

$$\mathbf{f}_{i,k} = \sum_{\substack{b(l) \in \mathcal{B}_k^1, \\ b(l) \neq b(r(i))}} \mathbf{H}_{b(l),r(i)}^H \boldsymbol{\omega}_{b(l)} x_l. \tag{6.2}$$

The set of active BSs is given by $\mathcal{B}_k^t$, where $t \in \{1,2\}$ is the index of the hop. The vector $\mathbf{n}_{r(i)}$ is the noise signal plus the interference of adjacent networks and the transmitted symbols are denoted with $x_{r(i)}$ with the assumptions $E\{|x_r|^2\} = 1$ and $E\{x_l x_k^*\} = 0$ if $k \neq l$.

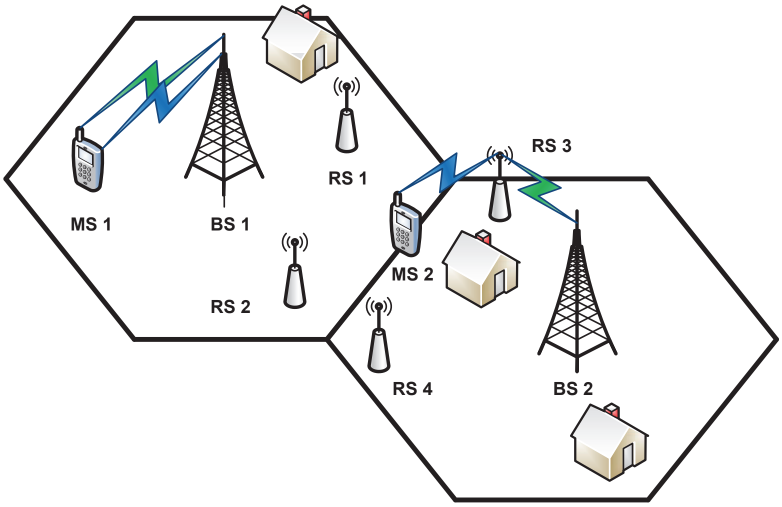

Figure 6.3: Two cell scenario with 2 BSs, 4 RSs and 2 MSs.

User i has a single antenna element and receives at a time instant k in hop $t \in \{1, 2\}$ the signal

$$g_{i,k}^{t} = \mathbf{h}_{s(i),i}^{H} \boldsymbol{\omega}_{s(i)} x_i + \sum_{\substack{s(j) \in \mathcal{S}_k^t, \\ j \neq i, s(j) \neq s(i)}} \mathbf{h}_{s(j),i}^{H} \boldsymbol{\omega}_{s(j)} x_j + n_i \tag{6.3}$$

where $\mathbf{h}_{i,s}$ is the channel vector from the station s serving the user i and $\boldsymbol{\omega}_s$ is the beamforming vector of station s. The set $\mathcal{S}_k^t$ denotes the set of active transmitting stations (BSs or RSs) in hop t of slot k. In hop $t = 1$ only BSs $s \in \mathcal{B}_k^1$ serve users and in hop $t = 2$ BSs and RSs $s \in \mathcal{S}_k^1$ can serve a user. The noise signal plus interference of adjacent networks is given by n_i.

Using a decode-and-forward relay, the total rate R_i user i has over two hops is given by [121, 167]:

$$R_i = \min\{R_{r(i)}^1, R_i^2\}. \tag{6.4}$$

Here $R_{r(i)}^1$ is the rate, the RS $r(i)$ serving user i achieves in the first hop with an SINR $\gamma_{r(i)}^1$:

$$R_{r(i)}^1 = \log_2(1 + \gamma_{r(i)}^1) \tag{6.5}$$

and

$$R_i^2 = \log_2(1 + \gamma_i^2) \tag{6.6}$$

is the rate user i achieves in the second hop by a transmission of RS $r(i)$ to user i. If user i is served by a BS directly, the user receives two different symbols and the rate is given by

$$R_i = R_i^1 + R_i^2. \tag{6.7}$$

Therefore, a link over a RS causes a capacity loss. A network-wide optimization based on instantaneous CSI over both hops in all cells is difficult due to the fast fading. Two practically relevant assumptions are made here:

- The optimization is made based on the long-term CSI in the form of spatial correlation matrices $\mathbf{R}_{m,s}$ [162] between a transmitting station s and a receiving station m. The result is the approximation of the SINRs $\gamma_{r(i)}^1$ or γ_i^2 by the mean SINR and given by

$$\gamma_m^t \approx \bar{\gamma}_m^t(\mathbf{\Omega}_k^t) = \frac{(\boldsymbol{\omega}_{s(m)}^t)^H \mathbf{R}_{s(m),m} \boldsymbol{\omega}_{s(m)}^t}{\sum_{\substack{l \in \mathcal{S}_k \\ l \neq s(l)}} (\boldsymbol{\omega}_{s(l)}^t)^H \mathbf{R}_{s(l),m} \boldsymbol{\omega}_{s(l)}^t + \sigma_m^2}, \tag{6.8}$$

  where $\mathbf{\Omega}_k^t$ denotes the matrix consisting of all beamforming vectors $\boldsymbol{\omega}_s^t$ of hop t in slot k. The beamformer for different scheduling decisions are computed by a central unit in advance and they can be reused as long as the channels are stationary.

  Due to the fixed roof-top to roof-top LOS connection between the BSs and the RSs, the instantaneous SINR does not vary very much. In this case, the mean SINR is a good measure for the optimization.

  The basic idea for the following approach is the optimization of the spatial dimension to find links (BS-MS or BS-RS-MS) with minimized mutual interference. Additional RSs in a network offer more degrees of freedom for the optimization. On the other hand, the capacity loss due to the half duplex transmission results in a seldom selection of RSs. However, in some cases RSs are useful for shadowed users, for users at the cell edge region, or if a beam collision among two BSs can not be avoided.

- A low complexity receiver technology is feasible at the RSs due to the static BS-RS and the assumed rooftop-to-rooftop link. Therefore, this chapter assumes a simple maximum ratio combining (MRC) based receiver at the RSs based on the local CSI, which has low complexity. Due to this static behavior, the first hop long-term CSI is a good performance measure.

Hence, the rate a receiving station achieves can be approximated like in [93] by

$$R_m^t = \mathrm{E}\{\log(1 + \gamma_m^t)\} \approx \log(1 + \bar{\gamma}_m^t(\mathbf{\Omega}_k^t)) \tag{6.9}$$

Note the achievable rate (6.9) is only used for an optimization of, e.g., the beamforming vectors or the beam scheduling. The final results are determined by the instantaneous rates, e.g., (6.4).

6.3 Unicast Beamforming Optimization Problem with Relays

This section presents the beamforming optimization for the relay network. Similar to the previous section max–min fairness is targeted. This section shows, that a max–min fair system can profit from relays. An a priori assignment of either a BS (Case 1) or a RS (Case 2) to a user i, based on the best local long-term CSI, is made. To achieve fairness in a multicell network it is desired to maximize the SINR of the weakest link. This problem is called MBP [40, 128]. The two SINRs in the first and the second hop are decoupled if all transmitting stations are subject to a per-antenna array power constraint. The transmission in the first hop does not create interference to a transmission in the second hop, therefore, the beamforming problem is separated in two sub-problems: The MBP in the first hop is:

$$\begin{aligned}\bar{\gamma}^1 = \max_{\mathbf{\Omega}_k^1, \gamma} \quad & \gamma \\ \text{s.t.} \quad & \bar{\gamma}_i^1 \geq \gamma \;\; \forall i \in \mathcal{U}_k \cup \mathcal{R}_k \\ & (\boldsymbol{\omega}_b^1)^H \boldsymbol{\omega}_b^1 \leq P_b \quad \forall b \in \mathcal{B}_k^1,\end{aligned} \tag{6.10}$$

where $\mathcal{U}_k$ denotes the set of active users and $\mathcal{R}_k$ denotes the set of active RSs in slot k. As in [46], the second hop is optimized by

$$\begin{aligned}\bar{\gamma}^2 = \max_{\mathbf{\Omega}_k^2, \gamma} \quad & \gamma \\ \text{s.t.} \quad & \bar{\gamma}_i^2 \geq \gamma \;\; \forall i \in \mathcal{U}_k \\ & (\boldsymbol{\omega}_s^2)^H \boldsymbol{\omega}_s^2 \leq P_s \quad \forall s \in \mathcal{B}_k^2 \cup \mathcal{R}_k.\end{aligned} \tag{6.11}$$

One further aspect in the network design is a reduced power consumption of the network. In a relay transmission with decode-and-forward relays, power is wasted if there is a rate missmatch in the two hops. Consequently, no power is wasted if $\bar{\gamma}_{r(i)}^1 = \bar{\gamma}_i^2$. Note that here only long-term SINR is regarded for the optimization of the beamforming vectors. The final results in Section 6.3.1 are based on the instantaneous channels. For the optimization of the beamforming vectors long-term CSI is a good assumption, especially in a scenario where the channel of the first hop has a very low fading, as in a roof-top-to-roof-top connection. The mean SINR is very close to the actual SINR. In this case only the fading of the second hop can cause a performance loss if the optimization is based on the mean SINR. If global instantaneous CSI is available, no performance loss will result.

This idea results in, e.g., additional constraints for the MBP of the second hop:

$$\begin{aligned}\max_{\mathbf{\Omega}_k^2, \gamma} \quad & \gamma \\ \text{s.t.} \quad & \bar{\gamma}_{r(i)}^1 \geq \bar{\gamma}_i^2 \geq \gamma \;\; \forall i \in \mathcal{U}_k \\ & (\boldsymbol{\omega}_s^2)^H \boldsymbol{\omega}_s^2 \leq P_s \quad \forall s \in \mathcal{B}_k^2 \cup \mathcal{R}_k.\end{aligned} \tag{6.12}$$

Here $\bar{\gamma}^1_{r(i)}$ is a parameter and represents the mean SINR the RS achieves in the first hop. Hence, the optimized SINR $\bar{\gamma}^2_i$ is constrained by $\bar{\gamma}^1_{r(i)} \geq \bar{\gamma}^2_i \geq \gamma$. If a user is served only by a BS, then $\bar{\gamma}^1_{r(i)} = \infty$ and there will be no constraint like in (6.11). The constraint $\bar{\gamma}^1_{r(i)} \geq \bar{\gamma}^2_i \geq \gamma$ for RSs in the second hop results in:

- A reduced transmit power at the RSs.
- Due to the reduced transmit power a reduced interference to other links is possible.

However, the problem (6.12) is non-convex and difficult to solve. Therefore, this chapter regards a different approach which can be solved via the uplink downlink duality introduced in Section 4.3.4.1:

$$\begin{aligned} \gamma^D(\boldsymbol{\delta}) = \max_{\boldsymbol{\Omega}^2_k, \gamma} \quad & \gamma \\ \text{s.t.} \quad & \frac{\bar{\gamma}^2_i}{\delta_i} \geq \gamma \ \ \forall i \in \mathcal{U}_k \\ & (\boldsymbol{\omega}^2_s)^H \boldsymbol{\omega}^2_s \leq P_s \quad \forall s \in \mathcal{B}^2_k \cup \mathcal{R}_k. \end{aligned} \tag{6.13}$$

Here $\boldsymbol{\delta} = [\delta_1, \ldots, \delta_M]$ is a parameter vector which scales the SINRs of the problem (6.13). The objective function is now the balancing of ratios $\bar{\gamma}^2_i / \delta_i$. To constrain the SINR of the second hop to the SINR of the first hop the parameter δ_i is given by

$$\frac{\bar{\gamma}^2_i}{\delta_i} = \bar{\gamma}^1_{r(i)} \ \Leftrightarrow \ \delta_i = \frac{\bar{\gamma}^2_i}{\bar{\gamma}^1_{r(i)}}. \tag{6.14}$$

A low complexity solution for the MBP with general power constraints is proposed in Section 4.3.4.1. It is based on the duality of an inner problem, which corresponds to a MBP with a weighted sum power constraint:

$$f^D(\boldsymbol{\delta}, \boldsymbol{\mu}) = \max_{\boldsymbol{\Omega}} \min_{i \in \mathcal{U}_k} \frac{\bar{\gamma}^2_i}{\delta_i} \tag{6.15}$$

$$\text{s.t.} \sum_{s \in \mathcal{B}^2_k \cup \mathcal{R}_k} (\boldsymbol{\omega}^2_s)^H \mathbf{M}_s \boldsymbol{\omega}^2_s \leq P. \tag{6.16}$$

The weighting factor $\mathbf{M}_s = \mu_s \mathbf{I}$ concatenated in vector $\boldsymbol{\mu} = [\mu_1, \ldots, \mu_M]$ has to be determined to fulfill the per-antenna array power constraints. In Section 4.3.4.1, an update of the matrices $\mathbf{M}_s$ is presented so that the per-station power constraints are met. The total power of the inner problem is given by $P = \boldsymbol{\mu}^T \hat{\mathbf{p}}$, with $\hat{\mathbf{p}} = [P_1, \ldots, P_M]^T$. With the UL (receive) beamforming vectors of a station serving user i given by $\mathbf{v}_i$ and the UL powers $\boldsymbol{\lambda} = [\lambda_1, \ldots, \lambda_M]$, the dual UL SINR of the antenna array serving user i is given by

$$\bar{\gamma}^{2,U}_i = \frac{\lambda_i \mathbf{v}_i^H \mathbf{R}_{s(i),i} \mathbf{v}_i}{\mathbf{v}_s^H (\mathbf{M}_i + \sum_{\substack{l \in \mathcal{U}_k \\ l \neq s}} \lambda_l \mathbf{R}_{s(i),l}) \mathbf{v}_i}. \tag{6.17}$$

Note: The beamforming problem is formulated for a unicast transmission. Hence, there is one beamforming vector per-station and user pair. Therefore, the sets $\mathcal{U}_k$ and $\mathcal{S}_k$ denote the same set of indexes.

As in Section 4.3.4.1, the inner problem (6.15), (6.16), can be solved with the dual UL problem

$$f^U(\boldsymbol{\delta}, \boldsymbol{\mu}) = \max_{\boldsymbol{\lambda},\mathbf{V}} \min_{i \in \mathcal{S}} \frac{\bar{\gamma}_i^{2,U}}{\delta_i} \tag{6.18}$$

$$\text{s.t. } \boldsymbol{\lambda}^T \cdot \mathbf{1} \leq P \ \ \lambda_i \geq 0, \ ||\mathbf{v}_i|| = 0, \ \forall\, i \in \mathcal{S}_k, \tag{6.19}$$

which achieves the same SINR as the DL problem with less complexity. As presented in Section 4.3.4.1, considering an outer minimization over $\boldsymbol{\mu}$, the per-antenna array power constraints are met if a balanced SINR exists or if the network is interference coupled. The results are the optimized transmit beamforming vectors which achieve a balanced SINR with per-antenna array power constraints. The problems (6.10) and (6.11) are solved by the algorithm presented in Section 4.4. Strong duality for the UL and DL problem is proven by Proposition 6.

To determine the vector $\boldsymbol{\delta}$, the SINRs $\bar{\gamma}_{r(i)}^1$ and $\bar{\gamma}_i^2$ are required. The SINRs are computed by solving the problems (6.10) and (6.11). With $\bar{\gamma}_{r(i)}^1$ and $\bar{\gamma}_i^2$, the vector $\boldsymbol{\delta}$ can be computed according to

$$\delta_i = \begin{cases} \frac{\bar{\gamma}_i^2}{\bar{\gamma}_{r(i)}^1} & \text{if } \bar{\gamma}_{r(i)}^1 \leq \bar{\gamma}_i^2 \text{ and } i \text{ is served by a RS} \\ 1 & \text{otherwise.} \end{cases} \tag{6.20}$$

With $\boldsymbol{\delta}$ the problem (6.13) is solved and the result is an SINR $\bar{\gamma}_i^2$ which is limited to the SINR $\bar{\gamma}_{r(i)}^1$ of the first hop in the corresponding link. Algorithm 11 presents the data flow.

Algorithm 11 Max–min beamforming

Solve (6.10) $\rightarrow \bar{\gamma}_{r(i)}^1$ and $\boldsymbol{\Omega}_k^1$
Solve (6.11) $\rightarrow \bar{\gamma}_i^2$
With $\bar{\gamma}_{r(i)}^1$ and $\bar{\gamma}_i^2$ compute $\boldsymbol{\delta}$ according to (6.20)
With $\boldsymbol{\delta}$ solve (6.13) $\rightarrow \boldsymbol{\Omega}_k^2$
return $\boldsymbol{\Omega}_k^1$ and $\boldsymbol{\Omega}_k^2$

6.3.1 Numerical Results

Table 6.2 depicts the main simulation parameters. The Winner II channel model [97, 98] creates the required channels. The rooftop-to-rooftop connection between a BS and a RS corresponds to the stationary B5a scenario of the Winner II model. These channels are line-of-sight and have a very flat fading. Consequently, a high and constant SNR can be achieved in the first hop. All scenarios have the same power

Table 6.2: Simulation parameters

Number of users per user drop	60
Number of user drops	40
Number of antenna array elements at BS	4
Number of antenna array elements at RS	4
Number of antenna array elements at MS	1
BS height	32 m
RS height	20 m
MS height	1.5 m
Antenna spacing	half wavelength
BS-RS channel	B5a (Winner II)
BS-MS channel	C1 (Winner II)
RS-MS channel	C1 (Winner II)

constaints $P_i = 4$ at all BSs and RSs and the same thermal noise of $\sigma^2 = 10^{-17}$ at each user or relay. For the antenna arrays the simplified 2D model is generated. Hence, only a pattern over the azimuth angle is generated. Single polarized linear arrays with a 120° sectorization are used at the BSs and RSs. The users are equipped with the default single polarized, istopic antenna arrays of the Winner model. The users are randomly distributed in the multicell network, but with a distance larger than 50 meters away form the BSs. The long-term statistics are generated based on averaging over 50 channel frames per link. Each channel is assumed to be frequency flat. The geometry factor of the generated model is depicted in Figure 8.2. This section compares three approaches:

- A1: No RSs (Case 1), only max–min beamforming at the BSs.
- A2: BSs and RSs with consideration of the backhaul. The problem (6.13) is solved with a priory computation of the δ according to (6.20).
- A3: BSs and RSs without consideration of the SINR of the first hop (backhaul).

Figure 6.4 depicts the CDF of the individual achievable rates based on instantaneous CSI per second hop of the different algorithms A1-A3. All algorithms using RSs (A2-A4) outperform the conventional network (A1) without RSs. A2 reduces the transmit power of the second hop so that the mean SINR in both hops is equal. Therefore, a reduced instantaneous achievable rate in the second hop is the result. On the other hand, A3 still achieves a higher rate than in the conventional case without RSs while it requires 20% less transmit power (see Figure 6.6). Figure 6.11 depicts the CDF of the transmitted power of all RSs and BSs in every slot. As it can be observed the power constraints are mostly satisfied. The small violation is caused due to the low accuracy of the applied algorithm and due to the seldomly occurred decoupled scenarios.

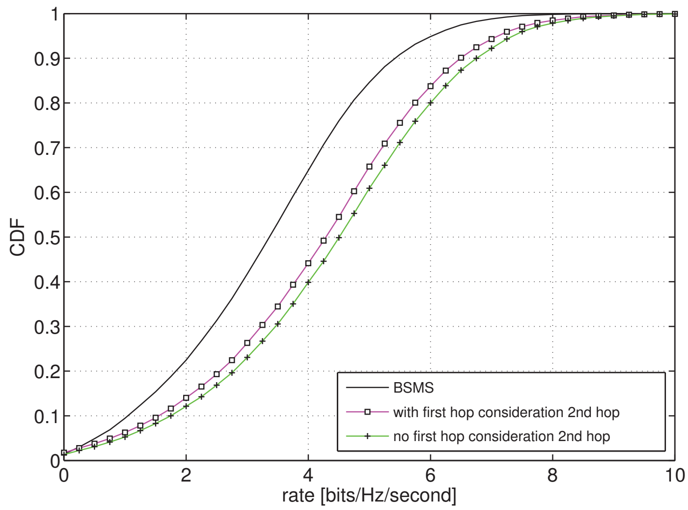

Figure 6.4: CDF of the individual per user achievable rate per 2nd hop.

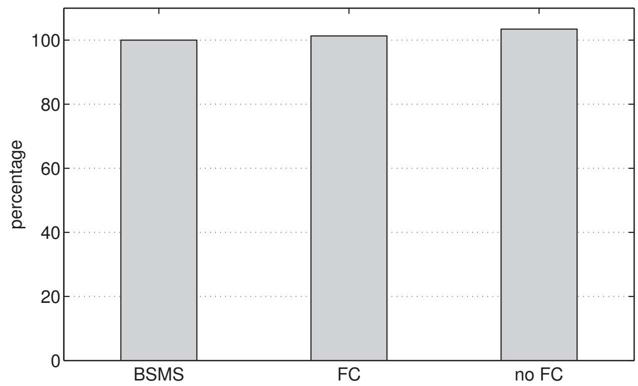

Figure 6.5: Sum rates of all algorithms.

The individual achievable rate is not an adequate measure to compare the performance in a network. Therefore, Figure 6.5 depicts the sum rates of all algorithms in percentage compared to the conventional network A1 (in percentage). Algorithms A2 and A3 outperform A1. Algorithm A2 has a slightly lower achievable sum rate compared to A3 since long-term CSI is used for the computation of the beamformer. Due to the usage of long-term CSI there is still a rate missmatch in some cases. If instantaneous CSI would be available, this rate mismatch could be completely eliminated.

Figure 6.6 shows the sum powers of all algorithms in percentage compared to A1. As expected, A2 with the consideration of the first hop, has the lowest sum power and saves approximately 20% of the total power compared to A1, while it has a higher sum rate.

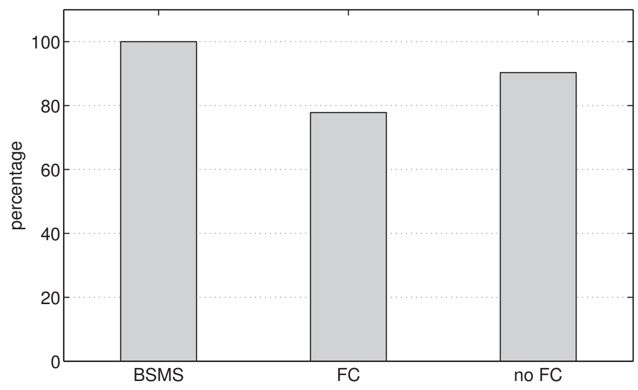

Figure 6.6: Sum power of all algorithms.

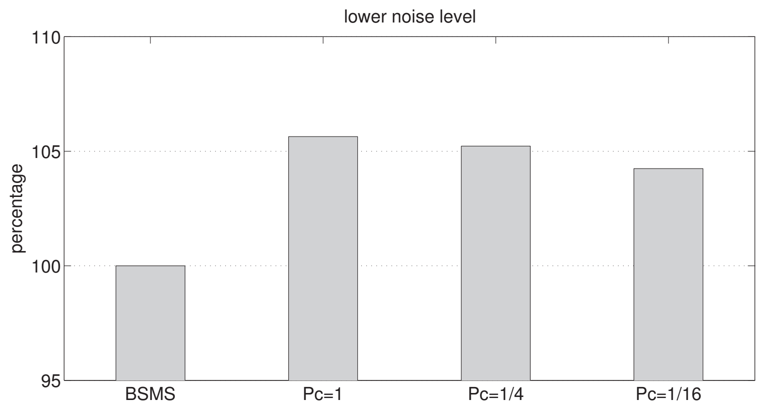

Figure 6.7: Sum rates of all algorithms, $\sigma^2 = 10^{-17}$.

Finally, Figures 6.7 and 6.8 depict the sum rates for different power constraints at the RSs. Figure 6.7 shows the sum rate of scheme A2 (no consideration of the backhaul) in a predominantly interference limited scenario. The performance degradation due to stricter power constraints at the RSs is smaller compared to the predominantly noise limited scenario in Figure 6.8. Hence, a noise limited scenario is more sensitive concerning very strict power constraints. Also here, it is possible that the power constraints are slightly violated in case a balanced SINR is not given.

6.4 Scheduling and Assignment Problem

The results presented in this section are based on the published paper [46]. In the previous section the beamforming problem is presented. The RSs and BSs are assigned to users based on local long-term CSI. Besides the beamforming, a smart assignment of stations (RSs or BSs) to MSs is promising to improve the performance of the network. Unnecessary assignments of RSs to MSs should be avoided to increase the system achievable rate.

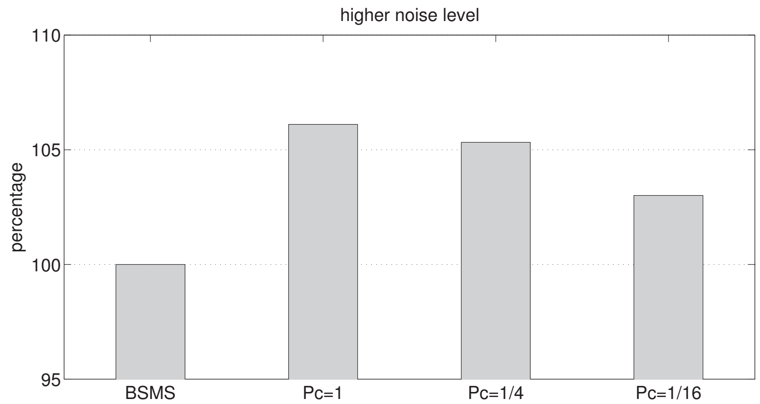

Figure 6.8: Sum rates of all algorithms, $\sigma^2 = 10^{-16}$.

Another concept is the avoidance of active links that are very close together. For example, it should be avoided that a BS-MS link disturbs a different BS-RS link if a MS is very close to the BS-RS link. The main idea of this algorithm can be simplified as a search of the necessary links to maximize the sum rate of the proposed SINR-fair network. This section optimizes the beam scheduling, user scheduling, and assignment based on the long-term CSI. The concept is based on the previously proposed ideas of Chapter 5 without RSs. The user scheduling and the assignment of stations is defined by the matrix $\mathbf{S} \in \mathbb{N}^{N \times K}$. Each element in $\mathbf{S}$ with index c, k is given by the tuple (i, s)

$$[\mathbf{S}]_{c,k} = \begin{cases} (i, s) & \text{if user } i \text{ in cell } c \text{ is served} \\ & \text{by station } s \text{ in hop 2 of slot } k \\ 0 & \text{if cell } c \text{ contains no user.} \end{cases} \tag{6.21}$$

Here, K denotes the number of optimized scheduling slots. It is desired to maximize the overall rate of the network by a smart assignment of stations to MSs and a smart user scheduling. A useful optimization criterion is the mean sum rate (see Section 5.3.2):

$$R(\mathbf{S}) = \sum_{k=1}^{K} \sum_{i \in [\mathbf{S}]_{:,k}} R_i([\mathbf{S}]_{:,k}) \tag{6.22}$$

where

$$R_i([\mathbf{S}]_{:,k}) = \begin{cases} \log(1 + \bar{\gamma}_i^1([\mathbf{S}]_{:,k}) + \log(1 + \bar{\gamma}_i^2([\mathbf{S}]_{:,k}) & \text{user } i \text{ is served by a BS} \\ \min\{\log(1 + \bar{\gamma}_{r_i}^1([\mathbf{S}]_{:,k}), \log(1 + \bar{\gamma}_i^2([\mathbf{S}]_{:,k})\} & \text{user } i \text{ is served by a RS} \end{cases} \tag{6.23}$$

is the mean rate of a user i which is served in slot k. Two cases have to be distinguished here: A MS can either receive two information symbols in the two hops by a BS or it can receive one information symbol through two hops over a RS. The resulting mean rate for the computation of the cost function is given in (6.23). The second case of Eq. (6.23) is motivated by the instantaneous rate in the case of a two hop transmission [167]. Note that the considered rates here are rate functions based on the mean SINR. Consequently, they are only approximations of the actual rates [93] but this approximation gives a good measure of the overall mean link quality in the two hops. Due to max–min beamforming, the mean SINR of the two hops can be different. In each hop different links are active, e.g., in the first hop users and RSs are served by BSs and in the second hop users are served by RSs and BSs. Consequently, the mean interference power varies over two hops and influences the instantaneous rates. The final rate is determined by the rate achieved in each hop. Therefore, this thesis takes into account the overall end-to-end mean rate. The set $\mathcal{W}$ denotes the set of all beamforming matrices $\mathbf{\Omega}_k$ with $k = 1, \ldots, K$. Using (6.22) as a cost function the optimization problem can be stated as:

$$\max_{\mathbf{S}} R(\mathbf{S}) \tag{6.24}$$

For the computation of the rate of each slot, the two beamforming problems have to be optimized to maximize the weakest SINRs. Thus, for each scheduling assignment $[\mathbf{S}]_{:,k}$ the beamforming weights $\mathbf{\Omega}_k$ are determined by the problems (6.10) and (6.11). Finding this optimal scheduling matrix maximizing the sum rate, and fulfilling the temporal fairness constraint is $\mathcal{NP}$-hard. More details are given in Chapter 5. Section 5.5.2 proposes several heuristic to optimize the beam scheduling problem. A promising algorithm presented in Section 5.5.2, useful for the application in the case of RSs, is the Greedy algorithm due to its low complexity. Furthermore, this algorithm shows a good sum rate performance and achieves ORRS fairness according to Definition 43.

In this chapter, the greedy approach of Section 5.5.2.4 is slightly modified. The greedy approach is based on a slot-by-slot iteration. In each slot k, the sum rate is maximized individually. For each slot k in the first step the greedy approach starts with a (strongest) user in a given cell c. For this user the best station considering the balanced mean SINR is selected. Then the algorithm continues in the next cell and selects the user which enables the largest overall sum rate

$$R_k([\mathbf{S}]_{:,k}) = \sum_{i \in [\mathbf{S}]_{:,k}} R_i([\mathbf{S}]_{:,k}) \tag{6.25}$$

for the slot k. Additionally, a search over all possible stations in this cell c has to be performed for this user. The user in combination with the best station will be selected. The algorithm continues with the next adjacent cell ($c := c + 1$) and repeats the last step until all N cells are visited. Then the same procedure is performed in the next slot until all K slots are optimized. To guarantee a temporal fairness among the users, each user is scheduled equally often. Therefore, a set $\mathcal{U}_{c,0}$ containing all active users of cell c is used.

6.4.1 Numerical Results

In Table 6.2, the main simulation parameters are summarized. The channels are created based the same setting as in Section 6.3.1. The results are based on the instantaneous rates, e.g., (6.4). Three cases are compared in this section:

- No RSs, only max–min beamforming with random Round-Robin scheduling (RRS).

Algorithm 12 Greedy user selection and station assignment

Initialization: Compute $\mathcal{U}_{c,0}\ \forall\ c = 1, \ldots, N$
for $k = 1$ to K **do**
  $\mathcal{U}_c = \mathcal{U}_{c,0}\ \forall\ c$
  start in $c = 1$, find the strongest user $i_{\max}$ and the station $s_{\max}$ serving this user based on the long-term link quality
  $[\mathbf{S}]_{1,k} = (i_{\max}, s_{\max})$.
  Update: $\mathcal{U}_1 := F(\mathcal{U}_1, \mathcal{U}_{1,0}, i_{\max})$
  for $c = 2$ to N **do**
    search a user $i_{\text{best}} \in \mathcal{U}_c$ of cell c with a station s_{best} which serves this user maximizing the sum rate (6.25). For the computation of the sum rate the beamforming vectors are optimized based on max–min beamforming.
    $[\mathbf{S}]_{c,k} = (i_{\text{best}}, s_{\text{best}})$
    Update: $\mathcal{U}_c := F(\mathcal{U}_c, \mathcal{U}_{c,0}, i_{\text{best}})$
  end for
end for
return $\mathbf{S}, \mathcal{W}$

- Max–min beamforming with RSs and random RRS. A station (RS or BS) is assigned to the user based on the best mean local link quality.

- Max–min beamforming with the proposed greedy scheduling (GS).

In Fig. 6.9, the cumulative distribution function (CDF) of the individual achievable rate per hop is depicted. The additional usage of RSs results in an improved per link achievable rate. But in this figure, the multiplexing loss is not visible. In case of a RS serving a user, the transmission of a symbol requires two hops, therefore, in Fig. 6.10 the sum rate of all scheduled users per hop is depicted. Regarding the sum rate, the usage of RSs improves the rate only marginally in the case of random RRS. On the other hand, the presented low complexity GS is able to outperform the conventional case without RS by more than 25%. The question arises, whether these RSs are useful at all to improve the sum rate of a multicell network. This question is answered in Fig. 6.13 which shows the amount of used RS links. In the case of RRS with a local (per-cell) assignment based on the mean link quality, the RSs are selected in 28% of the cases. Using the GS this amount is reduced to 12%. That means only in a few cases (e.g. cell edge users, or strongly shadowed users), the usage of RSs can increase the system performance in the sense of a maximized achievable sum rate. Only in cases where a RS is useful, the RS is used for the improvement of the achievable rate of the scheduled user.

6.5 Summary

This chapter proposes a multicell network with half duplex decode-and-forward RSs. The results can be summarized as follows:

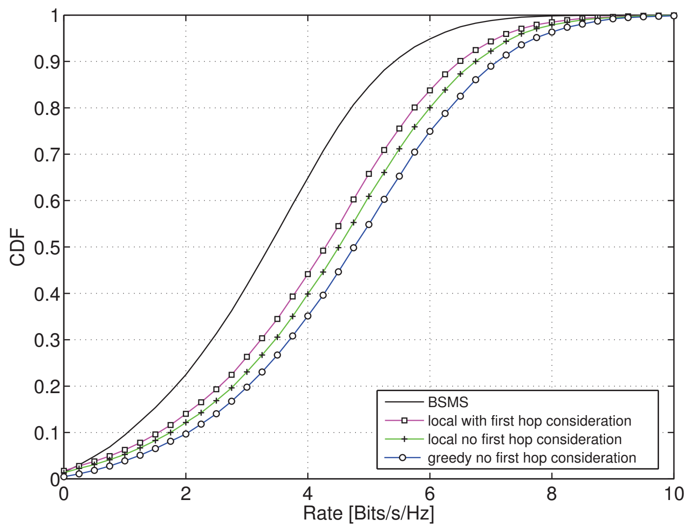

Figure 6.9: CDF of the individual per user achievable rate per 2nd hop.

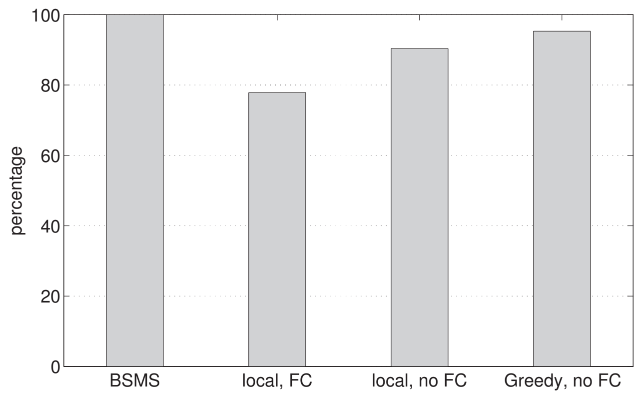

Figure 6.10: Sum power of all algorithms.

- This chapter shows an improvement of max–min beamforming with relays. The beamforming problem is then separated in two hops which can be solved independently. The presented max–min fair algorithms with one-way relays are based on long-term CSI and they are able to achieve a higher sum rate compared to a max–min fair system without relays.

- A consideration of the backhaul for the optimization of the beamforming vectors in the second hop reduces the transmitted power of the relays in the second hop. In the case of instantaneous CSI no performance loss will occur. In the case of long-term CSI a small performance loss is visible due to the fading of the channels and the resulting rate mismatch.

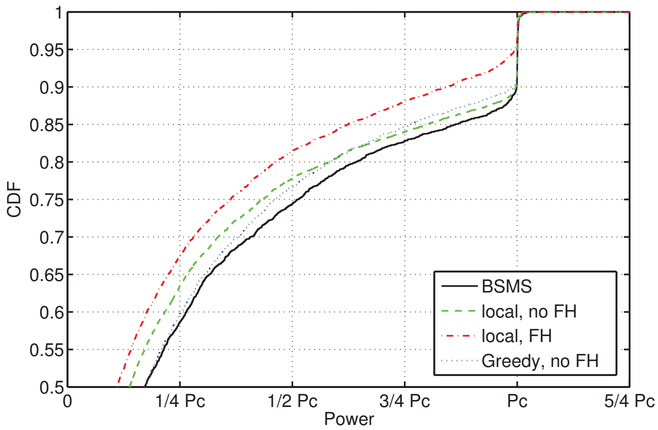

Figure 6.11: CDF of the transmit power per station and BF vector of all algorithms.

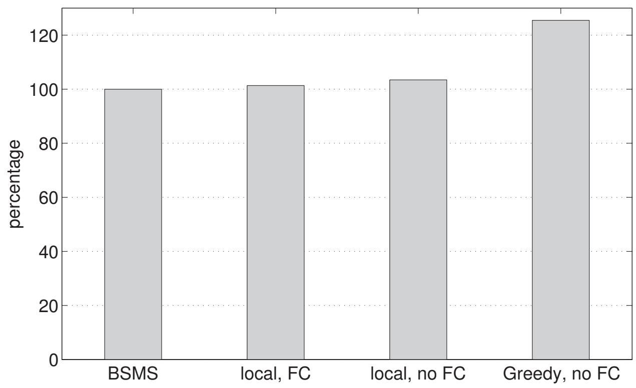

Figure 6.12: Sum rates of all algorithms.

- In an SINR fair system, relays are useful in some cases to improve the overall achievable sum rate. An optimized beam scheduling and an optimized assignment of relay stations or base stations to users results in an amount of 12% of relay links in the regarded scenario. Those users can be shadowed and located in the cell edge region where the transmission via a relay is helpful to increase the achievable sum rate of a fair system. In a max–min fair system strongly shadowed user decrease the SINR of all jointly active users. Consequently, a very low sum rate for all users in the system is the result in this case. An avoidance of these shadowed links (channels) can result in a gain for all users in the system and, therefore, also in an increased sum rate.

Several future extensions are possible:

- In addition to the local assignment based on local long-term CSI, a global assignment and joint optimization of the beamforming weights can be achieved with the CoMP optimization presented in Section 4.6.3. The best transmitting

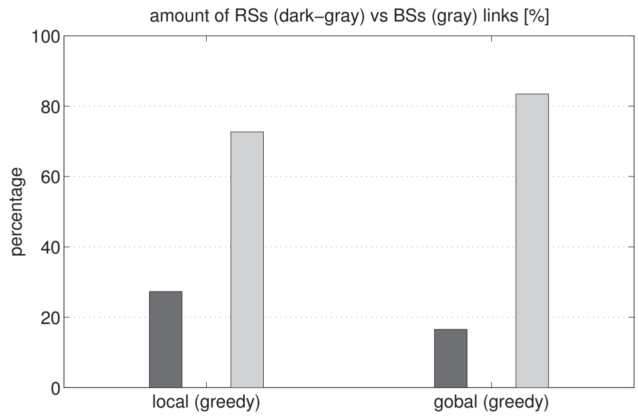

Figure 6.13: Amount of RSs used to serve users in the network.

station of a cell can derived with a consideration of the second hop interference. The max–min beamforming algorithm optimizing the beamforming weights and assignment can be solved efficiently. However, an open issue is here the consideration of the end-to-end rates. The end-to-end sum rate could be a better objective function instead of the max–min fairness. However, this problem is again $\mathcal{NP}$-hard.

- In the presented system, the users are assumed to be strongly shadowed from the BSs. Hence, in the first hop, the BS only transmits to the relay and the relay decodes and forwards the signal to the user in the second hop. In scenarios where the users are not strongly shadowed from the BSs, a multicast transmission from the BS to the RS and the user can result in an additional temporal diversity gain. The beamforming problem in the first hop must then be replaced by a multicast beamforming problem. Further details concerning multicast beamforming are presented in Chapter 7.

- The one-way half duplex relay system has a capacity loss due to the transmission over two hops where the relay is not able to jointly transmit and receive. A promising extension is the usage of two-way relays where the source and the destination transmit jointly to the relay in the first hop. The relay combines the two signals and broadcasts them in the second hop. Hence uplink and downlink are combined. A reduced capacity loss can be the result. Recently, attracts a novel approach the interest of many scientists. The articles [14,25,67,78,127,131,146,152,154,155] present optimization methods for the bi-directional relay channel precoding problem. In this scenario two sets of users exchange information via a two-way relay and the precoding vectors at the relay are optimized such that the worst SINR among all user pairs is maximized. A replacement of one user set by a base station or multiple base stations leads to a scenario similar to the scenario as presented in this chapter. In a future work, a joint optimization of base station beamforming vectors and two-way relay station beamforming vectors can improve the fairness among the users with less degradation of the sum rate performance.

Chapter 7

Theory of the Multicell Multicast Beamforming Problem

The content presented in this Chapter is published in the publications [35, 43]. This chapter considers only a multicast downlink transmission.

7.1 Introduction

Regard a multicell network with multiple BSs with the capability of multicast beamforming. Figure 7.1 depicts the network. Each BS serves multiple users, each equipped with one antenna. In one time slot, a BS transmits the same content to all users inside the cell which corresponds to the multicast scenario. If only one user per cell is scheduled, a unicast transmission is possible as well. The optimization of the beamforming vectors is based on available long-term CSI in the form of Hermitian positive semidefinite Toeplitz matrices.

If a frequency reuse-1 is used to increase the spectral efficiency, interference among the different BSs or cells reduces the fairness of the network. The optimization of the beamforming weights to cover all users inside a cell based on long-term CSI results in an adaptation of the sector pattern[1] based on the available spatial correlation information. An improved fairness among the users can be the result. This long-term sector pattern adaptation results in low fluctuations of the beamforming weights and, therefore, low fluctuations of the instantaneous SINR are the consequence. A low variation of the beamforming weights will result in a measured instantaneous SINR at the MS that is close to the actual instantaneous SINR. Techniques like channel-aware scheduling or adaptive modulation and coding can profit from an accurate knowledge of the instantaneous SINR.

A global adaptation of the sector pattern can be achieved by closed loop multicast max–min beamforming based on the available CSI of all links in the considered network. A practically relevant approach is the use of long-term CSI in the form of estimated spatial correlation matrices due to their longer stationarity intervals. More details concerning the sector pattern adaptation approach are presented in Chapter 8.

7.1.1 Related Work

The multicast MBP and multicast beamforming in general have been investigated in the last 15 years. As cited in [89], the first work regarding multicast beamforming

[1] Sector pattern is ideally hexagonal if the users are uniformly distributed.

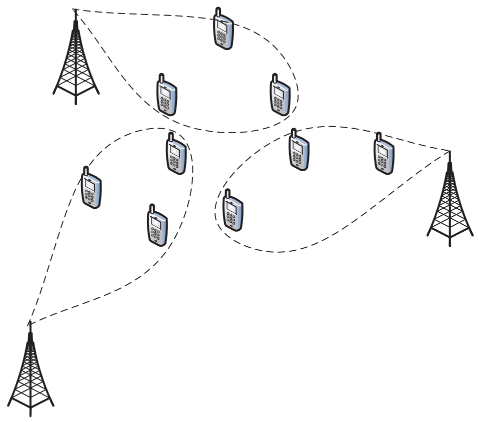

Figure 7.1: Scenario: The lobes show the multicast groups.

is [106]. The author proposed a maximization of the average received signal power. This approach is unfair and does not satisfy a quality-of-service constraint.

In 2004 Sidropoulos et al. [133] proposed the multicast power minimization problem (PMP) defined by a minimization of the total transmit power given a minimal signal-to-noise ratio (SNR). The authors further introduce the generalization of PMP called multicast MBP defined by the maximization of the minimum SNR given a total power budget. These so-called single group mulitcast beamforming problems are proven to be $\mathcal{NP}$-hard in general by the same authors in [134]. The work [89] extends the work [134] to the case of multiple multicast groups with interference among different groups in a single cell. The authors propose a semidefinite relaxation technique to find sub-optimal solutions.

Although these problems are non-convex in general, quasi-convex or convex equivalent forms for special instances may exist. In 2007, Karipidis et al. [89] derived an equivalent convex form for the PMP and an equivalent quasi-convex form of the MBP if the BS uses ULAs and far-field LOS propagation conditions are given. The channel vector is then given by a Vandermonde vector. In this case, the PMP can be expressed by an equivalent convex problem with optimization variables given by finite autocorrelation sequences (FASs). A spectral factorization of these FASs can recover the equivalent beamforming vectors. Furthermore, the authors prove in their article the tightness of the semidefinite relaxation in this case.

Similar to the equivalent convex form of the PMP, an equivalent quasi-convex form of the MBP can be derived [89]. The equivalent quasi-convex form of the multicast MBP is only derived for the special instance of LOS channels with instantaneous CSI and using ULAs with a sum power constraint [89]. An open question is whether there are some cases where the multicast MBP becomes quasi-convex for long-term CSI and more general power constraints. Table 7.1 gives an overview of all related problems. The last line is the contribution of this chapter. A broader overview of the related work of the last 10 years is presented in Tables 7.2 and 7.3.

Table 7.1: Overview of some related multicast MBPs.

Power constr.	CSI	Convexity
sum power	long-term	non-convex
per-antenna	long-term	non-convex
sum power	LOS inst. CSI, ULA	quasi-convex
per array	long-term, ULA	quasi-convex

Table 7.2: Overview of the regarded scenarios in the related work since 2002.

Year	Author	Problem	Power constr.	CSI	Scenario
2002	Lopez [106]	Max SNR	-	inst.	single group
2004	Sun et al. [140]	MBP	sum power	inst.	single group
2004	Sidropoulos et al. [133]	PMP/MBP	sum power	inst.	single group
2005	Karipidis et al. [87]	PMP	-	inst.	mult. groups
2006	Sidropoulos et al. [134]	PMP/MBP	sum power	inst.	single group
2006	Karipidis et al. [88]	PMP	-	far field	mult. groups
2007	Karipidis et al. [89]	MBP	sum power	far field	mult. groups
2008	Karipidis et al. [90]	MBP	sum power	inst.	mult. groups
2008	Chang et al. [24]	MBP	sum power	inst.	mult. groups
2008	Jordan et al. [82,83]	MBP	sum power	long-term	mult. cells
2009	Silva et al. [136]	MBP	sum power	inst	mult. groups
2010	Dartmann et al. [38]	MBP	per-BS	long-term.	mult. cells

7.1.2 Contributions

In multicell networks, instead of instantaneous CSI, the use of long-term CSI in the form of higher rank (larger than one) spatial correlation matrices is more realistic. Therefore, this chapter regards the multicast MBP based on long-term CSI with per-antenna array power constraints.

- This chapter proves the existence of a rank-1 solution of the relaxed semidefinite feasibility check problem of the MBP with per-antenna array power constraints in the case of long-term CSI in the form of Hermitian positive semidefinite Toeplitz matrices.

- Furthermore, this chapter presents the equivalent quasi-convex form for the multicast MBP for long-term CSI in the form of Hermitian positive semidefinite Toeplitz matrices and per-antenna array power constraints. This quasi-convex form uses FASs as optimization variables and the optimal beamforming vectors are recovered by spectral factorization.

Table 7.3: Overview of the presented solutions of related work since 2002.

Year	Author	Problem	Power constr.	CSI	Theory, Solution
2002	Lopez [106]	Max SNR	-	inst.	convex opt.
2004	Sun et al. [140]	MBP	sum power	inst.	seq. quadr. progr.
2004	Sidropoulos et al. [133]	PMP/MBP	sum power	inst.	SDP relaxation
2005	Karipidis et al. [87]	PMP	-	inst.	SDP relaxation
2006	Sidropoulos et al. [134]	PMP/MBP	sum power	inst.	$\mathcal{NP}$-hardness proof
2006	Karipidis et al. [88]	PMP	-	far field	equiv. convex form
2007	Karipidis et al. [89]	MBP	sum power	far field	equiv. convex form
2008	Karipidis et al. [90]	MBP	sum power	inst.	SDP relaxation
2008	Chang et al. [24]	MBP	sum power	inst.	approx. bounds
2008	Jordan et al. [82, 83]	MBP	sum power	inst.	SDP relaxation
2009	Silva et al. [136]	MBP	sum power	inst	duality (with gap)
2011	Dartmann et al. [34]	MBP	sum power	long-term	duality (with gap)
2012	Dartmann et al. [35]	MBP	per-BS	Toeplitz	equiv. quasi-convex
2012	Dartmann et al. [43]	MBP	per-BS	long-term	duality (with gap)

- The equivalent quasi-convex form can be solved with a simple bisection based algorithm with linear convergence. Besides this standard solution, this chapter proposes an algorithm with super-linear convergence based on a so-called parametric program of the equivalent quasi-convex fractional program of the MBP.

- In addition to methods based on convex solvers, this chapter proposes a new approach based on uplink–downlink duality. The result is an iterative solution based on a linear fractional program and simple mathematical operations.

7.2 System Model for the Multicast Downlink Transmission

A multiuser multicell network is considered with a set $\mathcal{S} = \{1, \ldots, N\}$ of N cooperating BSs equipped with N_A antennas each, serving a set $\mathcal{U}$ of M users, each equipped with a single antenna. A group of users is served by one BS $c(i)$, i.e., $N \leq M$. The signal r_i received by a user i is given by

$$r_i = \mathbf{h}_{c(i),i}^H \boldsymbol{\omega}_{c(i)} s_{c(i)} + \sum_{c \in \mathcal{S},\, c \neq c(i)} \mathbf{h}_{c,i}^H \boldsymbol{\omega}_c s_c + n_i, \tag{7.1}$$

where $\mathbf{h}_{c,i} \in \mathbb{C}^{N_A \times 1}$ is the channel vector from BS c to the ith user. The transmit beamforming vector at BS c is $\boldsymbol{\omega}_c = [\omega_c(0), \ldots, \omega_c(N_A - 1)]^T \in \mathbb{C}^{N_A \times 1}$, s_c is the information signal transmitted by cth BS with $\mathcal{E}\{|s_c|^2\} = 1$ and $n_i \sim \mathcal{CN}(0, \sigma_i^2)$ is the complex additive Gaussian noise with $E\{n_i\} = 0$ and variance $E\{|n_i|^2\} = \sigma_i^2$. With the assumption $E\{|s_c|^2\} = 1$ and $E\{s_c s_k^*\} = 0$ if $c \neq k$, the instantaneous DL SINR of user i is:

$$\gamma_i^D = \frac{|\mathbf{h}_{c(i),i}^H \boldsymbol{\omega}_{c(i)}|^2}{\sum_{\substack{c \in \mathcal{S} \\ c \neq c(i)}} |\mathbf{h}_{c,i}^H \boldsymbol{\omega}_c|^2 + \sigma_i^2}. \tag{7.2}$$

Long-term CSI is often used in a multicell optimization due to its longer stationary interval and, therefore, reduced required CSI feedback rate. The assumption of this long-term CSI results in the mean SINR:

$$\gamma_i^D(\boldsymbol{\Omega}) = \frac{\boldsymbol{\omega}_{c(i)}^H \mathbf{R}_{c(i),i} \boldsymbol{\omega}_{c(i)}}{\sum_{\substack{c \in \mathcal{S} \\ c \neq c(i)}} \boldsymbol{\omega}_c^H \mathbf{R}_{c,i} \boldsymbol{\omega}_c + 1}. \tag{7.3}$$

Here, an additional expectation over the channel realizations $\mathcal{H}$ is made. The result is the spatial correlation matrix normalized to the noise power given by

$$\mathbf{R}_{c,i} = \frac{1}{\sigma_i^2} \mathbb{E}_{\mathcal{H}}\{\mathbf{h}_{c,i} \mathbf{h}_{c,i}^H\}. \tag{7.4}$$

Note that the spatial correlation matrices (7.4) are normalized by the noise power. Considering a ULA with N_A antenna elements and an antenna spacing d of half the wave length at the BS, the spatial correlation matrix is given by a Toeplitz matrix and can be decomposed as in Chapter 2 [1]:

$$\mathbf{R}_{c,i} = \frac{1}{\sigma_i^2} \mathbf{A}(\boldsymbol{\theta}_{c,i}) \mathbf{P}_{c,i} \mathbf{A}(\boldsymbol{\theta}_{c,i})^H. \tag{7.5}$$

Chapter 2 presents more details concerning long-term CSI in the case of ULAs.

Power constraints: This chapter investigates two different power constraints that are given by convex cones.

- In the case of a **sum power constraint**, the total power of the entire network is limited by P and can be expressed by the following convex cone:

$$\mathcal{P} = \{\boldsymbol{\omega}_c \in \mathbb{C}^{N_A \times 1} : \sum_{c \in \mathcal{S}} \boldsymbol{\omega}_c^H \boldsymbol{\omega}_c \leq P\}. \tag{7.6}$$

  This constraint is reasonable if only one BS and multiple multicasting groups are regarded. However, in a multicell scenario a sum power constraint is not a practically relevant assumption.

- The **per-BS antenna array power constraints** are practically more relevant. In this case, each antenna array c of a BS will be subject to a total power budget P_c. The convex cone of beamforming vectors satisfying the per-BS antenna array power constraints is given by

$$\mathcal{P} = \{\boldsymbol{\omega}_c \in \mathbb{C}^{N_A \times 1} : \boldsymbol{\omega}_c^H \boldsymbol{\omega}_c \leq P_c, \ \forall c \in \mathcal{S}\}. \tag{7.7}$$

7.3 Optimization Problem

To achieve fairness, it is desired to improve the worst SINR of the currently scheduled users. Therefore, the MBP can be stated as

Definition 54. *Let* $\mathbf{\Omega} = [\boldsymbol{\omega}_1, \dots, \boldsymbol{\omega}_N]$ *be the beamforming matrix and let* $M > N$, *the multicast MBP is defined by*

$$\gamma_M^D = \max_{\mathbf{\Omega}} \min_{i \in \mathcal{U}} \gamma_i^D \quad \text{s.t.} \quad \boldsymbol{\omega}_c \in \mathcal{P} \ \forall c \in \mathcal{S}. \tag{7.8}$$

A balanced SINR can be the result. The problem can be simplified by using an additional slack variable γ:

$$\begin{aligned} \gamma_M^D = \max_{\mathbf{\Omega},\gamma} \quad & \gamma \\ \text{s.t.} \quad & \gamma_i^D \geq \gamma \ \forall i \in \mathcal{U}, \\ & \boldsymbol{\omega}_c \in \mathcal{P} \ \forall c \in \mathcal{S}. \end{aligned} \tag{7.9}$$

7.3.1 Equivalent Quasi-Convex Forms

The problem (7.8) is non-convex in general because of the non-convex objective function:

$$f(\mathbf{\Omega}) = \min_{i \in \mathcal{U}} \frac{\boldsymbol{\omega}_{c(i)}^H \mathbf{R}_{c(i),i} \boldsymbol{\omega}_{c(i)}}{\sum_{\substack{c \in \mathcal{S} \\ c \neq c(i)}} \boldsymbol{\omega}_c^H \mathbf{R}_{c,i} \boldsymbol{\omega}_c + 1}. \tag{7.10}$$

However, this problem can be relaxed to a quasi-convex problem. It is desired to maximize (7.10); hence, the objective function must have an equivalent quasi-concave form to prove that the MBP has an equivalent quasi-convex form.

The non-convex optimization problem (7.8) can always be relaxed to a quasi-convex problem with a semidefinite problem as a feasibility check problem. With semidefinite matrices $\mathbf{X}_c = \boldsymbol{\omega}_c \boldsymbol{\omega}_c^H$ and $\mathbf{X} = [\mathbf{X}_1, \dots, \mathbf{X}_N]$, the DL SINR is given by

$$\gamma_i^{\tilde{D}}(\mathbf{X}) = \frac{\text{Tr}\{\mathbf{X}_{c(i)} \mathbf{R}_{c(i),i}\}}{\sum_{c \in \mathcal{S}, c \neq c(i)} \text{Tr}\{\mathbf{X}_c \mathbf{R}_{c,i}\} + 1}. \tag{7.11}$$

Removing the non-convex rank-1 constraint $\text{rank}(\mathbf{X}_c) = 1 \ \forall c \in \mathcal{S}$, the MBP (7.8) with per-antenna array power constraints can be relaxed to

$$\gamma^{\tilde{D}} = \max_{\mathbf{X}} \min_{i \in \mathcal{U}} \gamma_i^{\tilde{D}}(\mathbf{X}) \quad \text{s.t.} \quad \text{Tr}\{\mathbf{X}_c\} \leq P_c, \ \mathbf{X}_c \succeq 0 \ \forall c \in \mathcal{S}. \tag{7.12}$$

This problem is quasi-convex due to its quasi-concave objective function and can be solved by convex feasibility check problems in the form of semidefinite programs (SDPs) [15]. A bisection algorithm can iterate arbitrarily tightly to the value of the global optimum. This solution is a standard method of solving the MBP and is used as a reference in this thesis. For a fixed γ, the upper level sets of the objective function are given by

$$\mathcal{S}_\gamma = \{\mathbf{X} \in \mathcal{P} : \ \tilde{f}(\mathbf{X}) = \min_{i \in \mathcal{U}} \gamma_i^{\tilde{D}}(\mathbf{X}) > \gamma\}. \tag{7.13}$$

Proposition 17. *The upper level set* (7.13) *is convex.*

Proof. The point-wise minimum of a quasi-concave function is quasi-concave. Furthermore, the constraint

$$-\frac{1}{\gamma}\operatorname{Tr}\{\mathbf{X}_{c(i)}\mathbf{R}_{c(i),i}\} + \sum_{c \in \mathcal{S}, c \neq c(i)} \operatorname{Tr}\{\mathbf{X}_c \mathbf{R}_{c,i}\} + 1 \leq 0 \tag{7.14}$$

is convex for a fixed γ and $\mathbf{X}_c \succeq 0 \ \forall c \in \mathcal{S}$. □

The unicast MBP with a sum power constraint $\sum_{c \in \mathcal{S}} \operatorname{Tr}\{\mathbf{X}_c\} = P$ has solution matrices which are proven to have all rank-1 and, therefore, the solution is optimal [9]. This proof does not hold in the multicast case.

If long-term CSI in the form of Hermitian positive semidefinite Toeplitz matrices is available, simulation results show that for such a scenario, the solutions of the semidefinite relaxation often yields matrices $\mathbf{X}_c \ \forall c \in \mathcal{S}$ having rank-1. Thus, the solution may be optimal in some cases and a rank-1 solution may exist. Using the Riesz-Fejer theorem [142], this observation can be formally proven.

Theorem 9. *A non-negative real valued trigonometric polynomial*

$$X(e^{j\phi}) = \sum_{k=-n+1}^{n-1} x(k) e^{-jk\phi} \tag{7.15}$$

with the FAS $x(-n+1), \ldots, x(0), \ldots, x(n-1)$ *can be expressed in the form*

$$X(e^{j\phi}) = |W(e^{j\phi})|^2 \tag{7.16}$$

for some polynomial $W(e^{j\phi}) = \sum_{k=0}^{n-1} w(k) e^{-jk\phi}$.

Proof. A short outline of the proof is presented in Appendix A.6. □

Proposition 18. *In the case of long-term CSI in the form of matrices* $\mathbf{R}_{c,i}$ *given by* (7.5) *and with* (2.6)*, there exists a solution for the MBP* (7.12) *with all matrices* $\mathbf{X}_c \ \forall c \in \mathcal{S}$ *having rank-1.*

Proof. As in [89], an optimal solution $\mathbf{X}_c$ of the SDP is assumed. In general, this solution has rank $\rho_c = \operatorname{rank}(\mathbf{X}_c)$ larger than one. Thus $\mathbf{X}_c$ can be decomposed to $\mathbf{X}_c = \sum_{r=1}^{\rho_c} \hat{\boldsymbol{\omega}}_{c,r} \hat{\boldsymbol{\omega}}_{c,r}^H$. Next it is shown that a rank-1 solution $\boldsymbol{\Psi}_c = \boldsymbol{\omega}_c \boldsymbol{\omega}_c^H$ can achieve the optimum. The signal power received at user i from BS array c is given by

$$\operatorname{Tr}(\mathbf{X}_c \mathbf{R}_{c,i}) = \operatorname{Tr}(\sum_{r=1}^{\rho_c} \hat{\boldsymbol{\omega}}_{c,r} \hat{\boldsymbol{\omega}}_{c,r}^H \mathbf{R}_{c,i}) \tag{7.17}$$

$$= \sum_{r=1}^{\rho_c} \mathrm{Tr}(\hat{\boldsymbol{\omega}}_{c,r} \hat{\boldsymbol{\omega}}_{c,r}^H \mathbf{R}_{c,i}).$$

Using the decomposition of positive semidefinite Toeplitz matrices according to (7.5) and with (2.6), the received signal can be simplified to

$$\begin{aligned}
\mathrm{Tr}(\mathbf{X}_c \mathbf{R}_{c,i}) &= \sum_{r=1}^{\rho_c} \mathrm{Tr}(\hat{\boldsymbol{\omega}}_{c,r} \hat{\boldsymbol{\omega}}_{c,r}^H \sum_{p=1}^{N_P} q_{c,i,p} \mathbf{a}(\theta_{c,i,p}) \mathbf{a}(\theta_{c,i,p})^H) \\
&= \sum_{p=1}^{N_P} \sum_{r=1}^{\rho_c} \mathrm{Tr}(\hat{\boldsymbol{\omega}}_{c,r} \hat{\boldsymbol{\omega}}_{c,r}^H q_{c,i,p} \mathbf{a}(\theta_{c,i,p}) \mathbf{a}(\theta_{c,i,p})^H) \\
&= \sum_{p=1}^{N_P} q_{c,i,p} \sum_{r=1}^{\rho_c} \mathrm{Tr}(\mathbf{a}(\theta_{c,i,p})^H \hat{\boldsymbol{\omega}}_{c,r} \hat{\boldsymbol{\omega}}_{c,r}^H \mathbf{a}(\theta_{c,i,p})) \\
&= \sum_{p=1}^{N_P} q_{c,i,p} \sum_{r=1}^{\rho_c} |\mathbf{a}(\theta_{c,i,p})^H \hat{\boldsymbol{\omega}}_{c,r}|^2. \qquad (7.18)
\end{aligned}$$

As in [89], the nonnegative complex trigonometric polynomial

$$\sum_{r=1}^{\rho_c} |\mathbf{a}(\theta_{c,i,p})^H \hat{\boldsymbol{\omega}}_{c,r}|^2 \geq 0 \qquad (7.19)$$

is positive for any value of $\theta_{c,i,p} \in [0, 2\pi)$. With the help of the Riesz-Féjer theorem (Theorem 9), we can find a vector $\boldsymbol{\omega}_c$ which does not depend on $\theta_{c,i,p}$ such that for all $\theta_{c,i,p}$ [89]

$$\sum_{r=1}^{\rho_c} |\mathbf{a}(\theta_{c,i,p})^H \hat{\boldsymbol{\omega}}_{c,r}|^2 = |\mathbf{a}(\theta_{c,i,p})^H \boldsymbol{\omega}_c|^2 \qquad (7.20)$$

holds. Inserting this in (7.18) results in

$$\begin{aligned}
\mathrm{Tr}(\mathbf{X}_c \mathbf{R}_{c,i}) &= \sum_{p=1}^{N_P} q_{c,i,p} |\mathbf{a}(\theta_{c,i,p})^H \boldsymbol{\omega}_c|^2 \\
&= \sum_{p=1}^{N_P} q_{c,i,p} \, \mathrm{Tr}(\boldsymbol{\omega}_c \boldsymbol{\omega}_c^H \mathbf{a}(\theta_{c,i,p}) \mathbf{a}(\theta_{c,i,p})^H) \\
&= \mathrm{Tr}(\boldsymbol{\omega}_c \boldsymbol{\omega}_c^H \sum_{p=1}^{N_P} q_{c,i,p} \mathbf{a}(\theta_{c,i,p}) \mathbf{a}(\theta_{c,i,p})^H) \\
&= \mathrm{Tr}(\boldsymbol{\omega}_c \boldsymbol{\omega}_c^H \mathbf{R}_{c,i}).
\end{aligned}$$

The last part of the proof follows [89, Eq. (5)], where it is shown that the same feasible set is obtained by matrices having rank-1. Thus, an equivalent rank 1 positive semidefinite matrix $\mathbf{X}_c = \boldsymbol{\omega}_c \boldsymbol{\omega}_c^H$ exists, which results in the same receive power at the user i, consequently, the convex feasibility check problem of the MBP (7.12) has a solution $\mathbf{X}$ with all matrices $\mathbf{X}_c$ $\forall c \in \mathcal{S}$ having rank-1. □

The multicast beamforming problem (7.12) has a solution where all matrices $\mathbf{X}_c$ $\forall c \in \mathcal{S}$ have rank-1. However, problem (7.12) is not guaranteed to always yield solutions with rank-1. There are cases where the feasibility check problem of (7.12) has higher rank solutions. The work of [89] describes the same observation for Vandermonde channels where also a rank-1 solution exists but the proposed semidefinite relaxation does not consistently yield rank-1 solutions.

The next part of this section proposes an equivalent quasi-convex form of the MBP (7.8). The derived solution yields quasi-optimal beamforming vectors based on an equivalent quasi-convex formulation of the original problem with FASs. The technique of convex optimization with FASs [4] to derive an equivalent quasi-convex form of the MBP as in [89] is extended in this paper to higher rank correlation matrices according to (7.5). These matrices are Toeplitz matrices:

$$\begin{aligned}
[\mathbf{R}_{c,i}]_{k,l} &= [\sum_{p=1}^{N_P} q_{c,i,p} \mathbf{a}(\theta_{c,i,p}) \mathbf{a}(\theta_{c,i,p})^H]_{k,l} \\
&= \sum_{p=1}^{N_P} q_{c,i,p} [\mathbf{a}(\theta_{c,i,p}) \mathbf{a}(\theta_{c,i,p})^H]_{k,l} \\
&= \sum_{p=1}^{N_P} q_{c,i,p} e^{j2\pi d(k-l)\sin(\theta_{c,i,p})}.
\end{aligned} \tag{7.21}$$

With (7.21) and $m = k - l$, the coefficients of the Hermitian positive semidefinite Toeplitz matrix are given by

$$r_{c,i}(m) = \sum_{p=1}^{N_P} q_{c,i,p} e^{j\, 2\pi d m \sin(\theta_{c,i,p})} \quad \forall m = 0, \ldots, N_A - 1. \tag{7.22}$$

With this definition, the spatial correlation matrix can be equivalently expressed by

$$\mathbf{R}_{c,i} = \begin{bmatrix} r_{c,i}(0) & r_{c,i}(1) & \ldots & r_{c,i}(N_A - 1) \\ r_{c,i}(-1) & r_{c,i}(0) & \ddots & \vdots \\ \vdots & \ddots & \ddots & r_{c,i}(1) \\ r_{c,i}(-N_A + 1) & & r_{c,i}(-1) & r_{c,i}(0) \end{bmatrix} \tag{7.23}$$

The idea of convex optimization with FASs is based on the following definition:

Definition 55. $\tilde{\mathbf{E}}_k \in \{0,1\}^{n \times n}$ *denotes the matrix which has zero entries except on the kth subdiagonal where it has only ones,* $k \in \{-n+1, \ldots, 1, 0, 1, \ldots, n-1\}$.

Definition 56. $\mathbf{E}^k$ *denotes the kth power of the matrix* $\mathbf{E}$ *which has zero entries except on the 1st lower subdiagonal where it has only ones.*

Using this technique of convex optimization with FASs presented in Section 3.2.2, the non-convex original problem (7.8) can be expressed as a quasi-convex problem, where the optimization variables (beamforming vectors) are converted to FASs. The reformulation leads to additional convex constraints. The optimal beamforming vectors can be obtained by spectral factorization techniques, e.g. [158]. The following proposition claims the original problem has an equivalent quasi-convex form.

Proposition 19. *In the case of long-term CSI in the form of matrices* $\mathbf{R}_{c,i}$ *given by* (7.23), *and variables in the form of* $\mathbf{x}_c = [x_c(0), \ldots, x_c(N_A-1)]^T$, $x_c(k) \in \mathbb{C}$, *and semidefinite matrices* $\mathbf{U}_c \in \mathbb{C}^{N_A \times N_A}$, $\mathbf{U}_c \succeq 0$ *stored in* $\boldsymbol{U} = [\mathbf{U}_1, \ldots, \mathbf{U}_N]$, *and the vectors* $\mathbf{r}_{c,i} = [r_{c,i}(0), \ldots, r_{c,i}(N_A-1)]$ $\forall c \in \mathcal{S}$, $\forall i \in \mathcal{U}$, *the equivalent quasi-convex form of the original problem* (7.8) *is given by*

$$\max_{\gamma, \mathbf{x}, \boldsymbol{U}} \quad \gamma \tag{7.24}$$

$$\text{s.t.} \quad \frac{\mathrm{Re}\{\mathbf{r}_{c(i),i}\tilde{\mathbf{I}}_{N_A}\mathbf{x}_{c(i)}\}}{\sum_{\substack{c\in\mathcal{S}\\ c\neq c(i)}} \mathrm{Re}\{\mathbf{r}_{c,i}\tilde{\mathbf{I}}_{N_A}\mathbf{x}_c\} + 1} \geq \gamma \quad \forall i \in \mathcal{U}$$

$$x_c(0) \leq P_c \quad \forall c \in \mathcal{S} \tag{7.25}$$

$$x_c(k) = \mathrm{Tr}\{\mathbf{E}^k\mathbf{U}_c\}, \quad \mathbf{U}_c \succeq 0 \quad \forall c \in \mathcal{S} \quad \forall k = 0, \ldots, N_A-1. \tag{7.26}$$

Proof. The objective function (7.10) can be proven to have an equivalent quasi-concave form if the upper level sets of the objective function are convex. Observe that (7.23) can be rewritten as [103]

$$\mathbf{R}_{c,i} = \sum_{k=-N_A+1}^{N_A-1} r_{c,i}(k)\tilde{\mathbf{E}}_k. \tag{7.27}$$

With Definition 55 and $n = N_A$, the signal power received at a user i by the ULA c is given by

$$\begin{aligned}
\boldsymbol{\omega}_c^H\mathbf{R}_{c,i}\boldsymbol{\omega}_c &= \boldsymbol{\omega}_c^H\Big(\sum_{k=-N_A+1}^{N_A-1} r_{c,i}(k)\tilde{\mathbf{E}}_k\Big)\boldsymbol{\omega}_c \\
&= \sum_{k=-N_A+1}^{N_A-1} r_{c,i}(k)\boldsymbol{\omega}_c^H\tilde{\mathbf{E}}_k\boldsymbol{\omega}_c \\
&= \sum_{k=-N_A+1}^{N_A-1} r_{c,i}(k)x_c(k).
\end{aligned} \tag{7.28}$$

With Definition 55 we have

$$x_c(k) = \boldsymbol{\omega}_c^H\tilde{\mathbf{E}}_k\boldsymbol{\omega}_c = \mathrm{Tr}\{\tilde{\mathbf{E}}_k\boldsymbol{\omega}_c\boldsymbol{\omega}_c^H\} \tag{7.29}$$

which is an FAS [4], (7.28) is a linear function over $x_c(k)$ with the coefficients $r_{c,i}(k)$. It is evident that the coefficients of (7.27) and $x_c(k)$ are conjugate symmetric

$$\begin{aligned} r_{c,i}(-k) &= r_{c,i}(k)^* \\ x_c(-k) &= x_c(k)^*. \end{aligned}$$

Therefore, (7.28) can be rewritten as in [89] as

$$\begin{aligned} \boldsymbol{\omega}_c^H \mathbf{R}_{c,i} \boldsymbol{\omega}_c &= x_c(0) r_{c,i}(0) + \sum_{k=1}^{N_A-1} x_c(k) r_{c,i}(k) + x_c(-k) r_{c,i}(-k) \\ &= x_c(0) r_{c,i}(0) + \sum_{k=1}^{N_A-1} x_c(k) r_{c,i}(k) + x_c(k)^* r_{c,i}(k)^* \\ &= x_c(0) r_{c,i}(0) + 2 \sum_{k=1}^{N_A-1} \mathrm{Re}\{x_c(k) r_{c,i}(k)\}. \end{aligned} \tag{7.30}$$

Using the following matrix as in [89]

$$\tilde{\mathbf{I}}_{N_A} = \begin{bmatrix} 1 & \mathbf{0}_{1\times N_A-1} \\ \mathbf{0}_{N_A-1\times 1} & 2\mathbf{I}_{N_A-1} \end{bmatrix} \in \mathbb{N}^{N_A \times N_A} \tag{7.31}$$

and the finite autocorrelation vector $\mathbf{x}_c = [x_c(0), \ldots, x_c(N_A-1)]^T$ and the vector $\mathbf{r}_{c,i} = [r_{c,i}(0), \ldots, r_{c,i}(N_A-1)]$, the received power (7.30) can be simplified to

$$\boldsymbol{\omega}_c^H \mathbf{R}_{c,i} \boldsymbol{\omega}_c = \mathrm{Re}\{\mathbf{r}_{c,i} \tilde{\mathbf{I}}_{N_A} \mathbf{x}_c\}. \tag{7.32}$$

In addition to the received power, also the per-BS antenna array power constraints can be rewritten with the use of FASs $\{x_c(k)\}$:

$$\boldsymbol{\omega}_c^H \boldsymbol{\omega}_c = \boldsymbol{\omega}_c^H \mathbf{E}^0 \boldsymbol{\omega}_c = x_c(0). \tag{7.33}$$

With $\mathbf{x} = [\mathbf{x}_1, \mathbf{x}_2, \ldots, \mathbf{x}_N]$ and the set of positive semidefinite auxiliary matrices $\{\mathbf{U}_c, \ \forall l \in \mathcal{S}\}$, with $\mathbf{U}_c \in \mathbb{C}^{N_A \times N_A}$, the set

$$\mathcal{P} = \{\mathbf{x} : x_c(k) = \mathrm{Tr}\{\mathbf{E}^k \mathbf{U}_c\}, \ x_c(0) \le P_c, \ \ \mathbf{U}_c \succeq 0 \ \ \forall c \in \mathcal{S} \ \ \forall k = 0, \ldots, N_A - 1\} \tag{7.34}$$

is convex. Due to Lemma 3 the constraint $x_c(k) = \mathrm{Tr}\{\mathbf{E}^k \mathbf{U}_c\}$ describes the same set as (7.29). Due to convexity of $\mathcal{P}$, the upper level sets

$$\mathcal{S}_{\gamma,i} = \{\mathbf{x} \in \mathcal{P} : \ \frac{\mathrm{Re}\{\mathbf{r}_{c(i),i} \tilde{\mathbf{I}}_{N_A} \mathbf{x}_c\}}{\sum_{\substack{c \in \mathcal{S} \\ c \neq c(i)}} \mathrm{Re}\{\mathbf{r}_{c,i} \tilde{\mathbf{I}}_{N_A} \mathbf{x}_c\} + 1} \ge \gamma\} \tag{7.35}$$

are also convex. The constraints (7.26) are convex constraints [4]. For a fixed γ, the final problem (7.24)-(7.26) is equivalent to (7.8) and is an SDP [89], which is known to be convex. Hence, the original problem (7.8) has an equivalent quasi-convex form in the case of long-term CSI in the form of Hermitian positive semidefinite Toeplitz matrices. □

The Toeplitz property of long-term CSI in the case of a ULA offers, therefore, low complexity and near-optimal solutions for the multicast beamforming problem.

7.4 Spectral Factorization

Problem (7.24)-(7.26) is a quasi-convex problem. Consequently, the optimal autocorrelation sequence can be computed efficiently. The question remains: How to obtain the beamforming weights $\boldsymbol{\omega}_c$ from the FASs $\mathbf{x}_c$ $\forall c \in \mathcal{S}$? Let n be $n = N_A$, the polynomial of the FAS $\mathbf{x}_c$ for a $c \in \mathcal{S}$ is given by $X_c(z) = \sum_{k=-N_A+1}^{N_A-1} x_c(k) z^{-k}$. As in the proof of Theorem 9 presented in Appendix A.6, the polynomial $X_c(z)$ can be factorized by its roots:

$$X_c(z) = W_c(z) \cdot \tilde{W}_c(z)$$

Let A be a constant factor, as presented in Appendix A.6, the spectral factor of $X(z)$ is the polynomial

$$W_c(z) = \sqrt{A} \prod_{k=1}^{N_A-1} (1 - z^{-1} z_k) = \sum_{n=0}^{N_A-1} \omega_c(k) z^{-k}.$$

This polynomial yields the desired coefficients (beamforming weights) $\omega_c(k)$ of the spectral factor. In [158], more efficient methods based on the fast Fourier transform (FFT) are presented which are also used in [89] and in this thesis.

7.5 Solution Based on Fractional Programming

In the previous section, a quasi-convex form of the multicast MBP is derived. This quasi-convex form can be solved with a simple bisection based algorithm. These algorithms have a linear convergence behavior. The quasi-convex form of the MBP can be also seen as a so-called generalized fractional program (see Section 3.3.3). For these quasi-convex optimization problems a super-linear converging algorithm is feasible. Such an algorithm is introduced in Section 3.3.3.

If long-term CSI in the form of Hermitian positive semidefinite Toeplitz matrices is available, the equivalent quasi-convex form of the multicast MBP is given in Proposition 19. This quasi-convex form can be expressed as a quasi-convex fractional program (3.36) as defined in Definition 25.

Proposition 20. *The parametric program of the equivalent quasi-convex form* (7.24)-(7.26) *of the multicast MBP* (7.9) *is given by*

$$F(\gamma) = \min_{\mathbf{x} \in \mathcal{X}} \max_{i \in \mathcal{I}} \{ -\operatorname{Re}\{ \mathbf{r}_{c(i),i} \tilde{\mathbf{I}}_{N_A} \mathbf{x}_{c(i)} \} - \gamma (\sum_{\substack{c \in \mathcal{S} \\ c \neq c(i)}} \operatorname{Re}\{ \mathbf{r}_{c,i} \tilde{\mathbf{I}}_{N_A} \mathbf{x}_c \} + 1) \} \tag{7.36}$$

Proof. The objective function of (7.9) can be equivalently rewritten to:

$$f(\mathbf{x}) = \min_{i \in \mathcal{U}} \frac{\mathrm{Re}\{\mathbf{r}_{c(i),i}\tilde{\mathbf{I}}_{N_A}\mathbf{x}_{c(i)}\}}{\sum_{\substack{c\in\mathcal{S}\\ c\neq c(i)}} \mathrm{Re}\{\mathbf{r}_{c,i}\tilde{\mathbf{I}}_{N_A}\mathbf{x}_c\}+1} = -\max_{i \in \mathcal{U}} \frac{-\mathrm{Re}\{\mathbf{r}_{c(i),i}\tilde{\mathbf{I}}_{N_A}\mathbf{x}_{c(i)}\}}{\sum_{\substack{c\in\mathcal{S}\\ c\neq c(i)}} \mathrm{Re}\{\mathbf{r}_{c,i}\tilde{\mathbf{I}}_{N_A}\mathbf{x}_c\}+1}. \tag{7.37}$$

Hence, with the convex set

$$\mathcal{X} = \{\mathbf{x} : x_c(k) = \mathrm{Tr}\{\mathbf{E}^k\mathbf{U}_c\},\ x_c(0) \leq P_c,\ \ \mathbf{U}_c \succeq 0\ \ \forall c \in \mathcal{S}\ \ \forall k = 0,\dots,N_A-1\}, \tag{7.38}$$

the optimization problem (7.24)-(7.26) can be expressed as a quasi-convex generalized fractional program

$$\bar{\gamma} = -\min_{\mathbf{x}\in\mathcal{X}} \max_{i\in\mathcal{U}} \frac{-\mathrm{Re}\{\mathbf{r}_{c(i),i}\tilde{\mathbf{I}}_{N_A}\mathbf{x}_{c(i)}\}}{\sum_{\substack{c\in\mathcal{S}\\ c\neq c(i)}} \mathrm{Re}\{\mathbf{r}_{c,i}\tilde{\mathbf{I}}_{N_A}\mathbf{x}_c\}+1} \tag{7.39}$$

with the negative affine functions $f_i(\mathbf{x}) = -\mathrm{Re}\{\mathbf{r}_{c(i),i}\tilde{\mathbf{I}}_{N_A}\mathbf{x}_{c(i)}\}$ and the positive affine functions $d_i(\mathbf{x}) = \sum_{\substack{c\in\mathcal{S}\\ c\neq c(i)}} \mathrm{Re}\{\mathbf{r}_{c,i}\tilde{\mathbf{I}}_{N_A}\mathbf{x}_c\}+1$. With Definitions 25 and 26 the parametric program (7.36) results. □

In [28, 29], the authors propose a root finding algorithm for the parametric program (3.37) with a faster convergence than the conventional bisection method.

7.5.1 Algorithm

The optimal FAS for the quasi-convex fractional program (7.39) can be found by a bisection method. A bisection method has a linear convergence and requires an interval containing the optimal value. In [30], the authors propose a faster algorithm with super-linear convergence to solve a quasi-convex fractional program. The algorithm exploits results of Proposition 1 which gives connections among the quasi-convex fractional program and its parametric program (7.36). According to Proposition 1, if the parametric program (7.36) results in $F(\gamma) = 0$, the optimal SINR is found. The conditions (ii) and (iv) of Proposition 1 imply the following theorem proving the convergence of Algorithm 13:

Theorem 10. *[30] Assume $\mathcal{X}$ is compact. If $F(\gamma^k) = 0$, then $\gamma^k = -\bar{\gamma}$ and $\mathbf{x}^k$ is the optimal solution.*

As it can be observed from the numerical results, the root finding algorithm (Alg. 13) always iterates to $F(\gamma) \approx 0$. If the domain is compact we can formally prove the optimality.

Proposition 21. *The set $\mathcal{P}$ is compact.*

Proof. We have to show that $\mathcal{X}$ is closed and bounded. The set has a lower bound because of $\mathbf{U}_c \succeq 0 \ \forall c \in \mathcal{S}$. Furthermore, it has an upper bound:

$$\begin{aligned} |x_c(k)| &= |\operatorname{Tr}\{\mathbf{E}^k \mathbf{U}_c\}| \\ &\leq |\operatorname{Tr}\{\mathbf{U}_c\}| = |\operatorname{Tr}\{\mathbf{E}^0 \mathbf{U}_c\}| = x_c(0) \leq P_c. \end{aligned}$$

For a given $n \in \{-N_A+1, \dots, N_A-1\}$. the first inequality holds due to

$$\sum_{\substack{i,j \in \{0,\dots,N_A-1\} \\ j-i=n}} |[\mathbf{U}_c]_{i,j}| \leq \sum_{i \in \{0,\dots,N_A-1\}} |[\mathbf{U}_c]_{i,i}| \tag{7.40}$$

if $\mathbf{U}_c$ is a Hermitian positive semidefinite matrix. The sum of absolute value of each sub-diagonal is always smaller or equal than the sum of the main diagonal. This can be proved by $|[\mathbf{U}_c]_{i,j}|^2 \leq [\mathbf{U}_c]_{i,i}[\mathbf{U}_c]_{j,j}$ [70, Page 398]. Consequently, $|[\mathbf{U}_c]_{i,j}| \leq \sqrt{[\mathbf{U}_c]_{i,i}[\mathbf{U}_c]_{j,j}} \leq \frac{1}{2}([\mathbf{U}_c]_{i,i} + [\mathbf{U}_c]_{j,j})$. For a given $n \in \{-N_A+1, \dots, N_A-1\}$, the left side of (7.40) can be bounded by

$$\sum_{\substack{i,j \in \{0,\dots,N_A-1\} \\ j-i=n}} |[\mathbf{U}_c]_{i,j}| \leq \frac{1}{2} \sum_{\substack{i,j \in \{0,\dots,N_A-1\} \\ j-i=n}} [\mathbf{U}_c]_{i,i} + [\mathbf{U}_c]_{j,j}. \tag{7.41}$$

The right side of (7.41) is obviously smaller than the right side of (7.40). Consequently $\mathcal{X}$ is bounded. Furthermore, $\mathcal{X}$ is closed because all bounds can be satisfied with equality. □

Under the special condition that the functions $d_i(\mathbf{x}) \ \forall i \in \mathcal{U}$ fulfill the Lipschitz condition, the convergence is even super-linear instead of only linear [29]. The numerical results, presented in the next section, show this fast convergence as well. The outline of the algorithm is presented in Alg. 13.

Algorithm 13 Root finding algorithm (Dinkelbach algorithm):

Let $\mathbf{x}^1 \in \mathcal{X}$ and $\gamma^1 = \max_{i \in \mathcal{U}} \frac{f_i(\mathbf{x}^1)}{d_i(\mathbf{x}^1)}$ and $k = 1$
repeat
  Determine the optimal solution $\mathbf{x}^k$ of $F(\gamma^k) = \min_{\mathbf{x} \in \mathcal{X}} \ \max_{i \in \mathcal{U}} \{\frac{f_i(\mathbf{x}) - \gamma^k d_i(\mathbf{x})}{d_i(\mathbf{x}^k)}\}$
  Let $\gamma^{k+1} = \max_{i \in \mathcal{U}} \frac{f_i(\mathbf{x}^k)}{d_i(\mathbf{x}^k)}$ and set $k = k+1$
until $|F(\gamma^k)| > \epsilon$
return $\mathbf{x}^k$

7.5.2 Numerical Results

Table 7.4 presents the main simulation parameters of the simulated multicell network presented in Fig. 7.1. Two algorithms are compared in this section:

Table 7.4: Simulation parameters.

Number of user drops	4000
Number of users per user drop	15
Number of BSs drop	3
Number of users per group drop	5
Transmit antenna arrays	ULA
Number of antenna array elements at BS	4
Number of antenna array elements at MS	1
Intersite distance	500 m
Antenna spacing	half wavelength
Path loss exponent	3.76
Available CSI	long-term CSI
Power angular density	Laplacian 15° [83]
Power constraint	per-BS antenna array power constraint

- A1: Conventional bisection method to solve problem (7.12). The beamforming vectors are calculated based on the largest eigenvalue of and the corresponding eigenvector of solution of the SDP.
- A2: Root finding algorithm Alg. 13 with parametric program (7.36).

As in Section 4.5, the pathloss gain is $(r/1000)^{-3.76}$, where r is the distance in meters. For all BSs the same normalized power constraints are given and all users have the same thermal noise level σ^2. The users are randomly distributed in the multicell network, but with a distance larger than 50 meters away form the BSs. The largest possible SNR in this model is at a distance of 50 meters in the direction of the antenna broadside. It is given by $SNR = 38.92$dB assuming a single antenna element at the BS.

For the generation of the statistics, in total 4000 user drops are randomly generated. In each user drop, the long-term CSI in the form of Hermitian positive semidefinite Toeplitz matrices is generated based on the location of the users and BSs. Each BS belongs to a cell and each cell is a multicast group consisting of five users. For each user drop, programs A1 and A2 are optimized for a setting of $M = 15$ users and $N = 3$ BSs. Each user group contains 5 users.

Figure 7.7 shows the CDF of the SINR for a precision[2] of $\epsilon = 10^{-5}$. Comparing both CDFs, the new algorithm A2 outperforms the conventional SDP based bisection A1 especially for the weakest users. The new algorithm A2 achieves a higher minimum SINR. Figure 7.8 shows the CDF of the transmit power. Both algorithms fulfill the per-antenna array power constraints.

[2] The term precision means the accuracy of the algorithm, hence the absolute difference to the optimal solution.

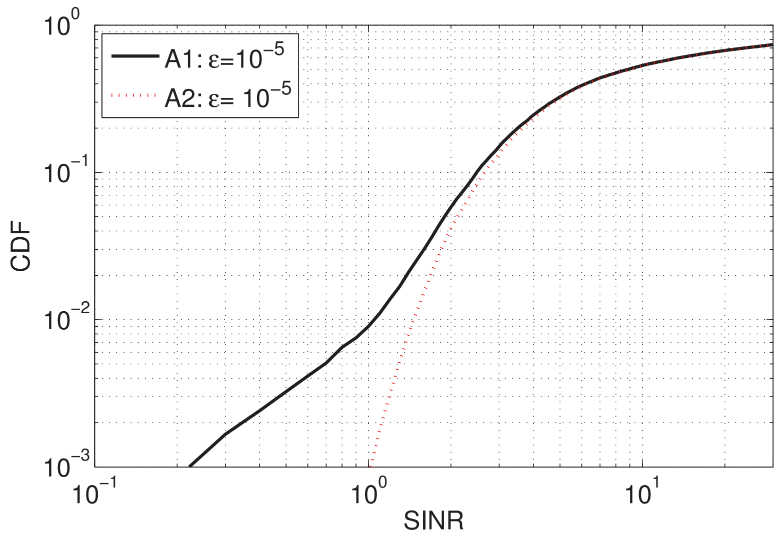

Figure 7.2: CDF of the SINR of the new algorithm based on the Dinkelbach iteration presented in Section 7.5 (red, dotted) and the conventional SDP based bisection based method for the problem (7.12) (black, solid).

Figure 7.9 presents the CDF of the number of iterations algorithms A1 and A2 required for the given precision $\epsilon = 10^{-5}$. As it can be observed from this figure, A2 requires less iterations than A1 due to its super-linear convergence in multiple cases (95%). However, in a few cases (5%), the new algorithm converges slowly. In these cases the algorithm aborts after 45 iterations and takes the solution of the last iteration.

Finally, Figure 7.5 shows the value of $F(\gamma^k)$ of the parametric program. As it can be observed from this figure, the solution of the parametric program is nearly optimal and in more than 95% percent of the simulation runs smaller than the precision interval of $\epsilon = 10^{-5}$.

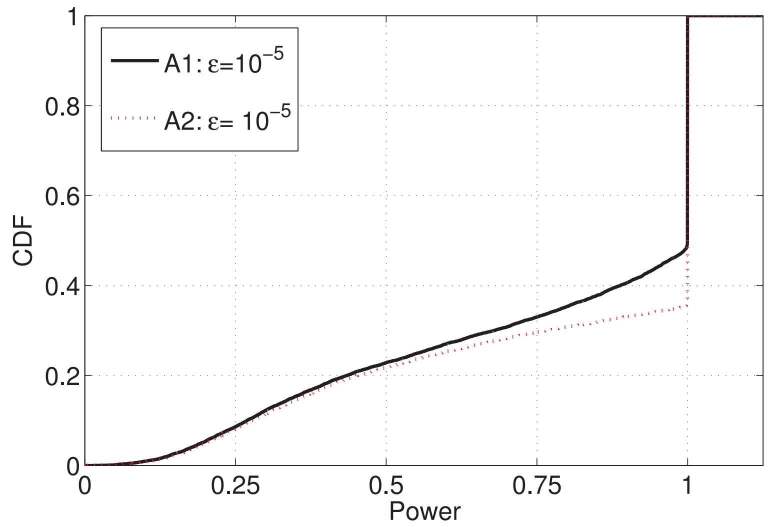

Figure 7.3: CDF of the transmit power of the new algorithm based on the Dinkelbach iteration presented in Section 7.5 (red, dotted) and the conventional SDP based bisection based method for the problem (7.12) (black, solid).

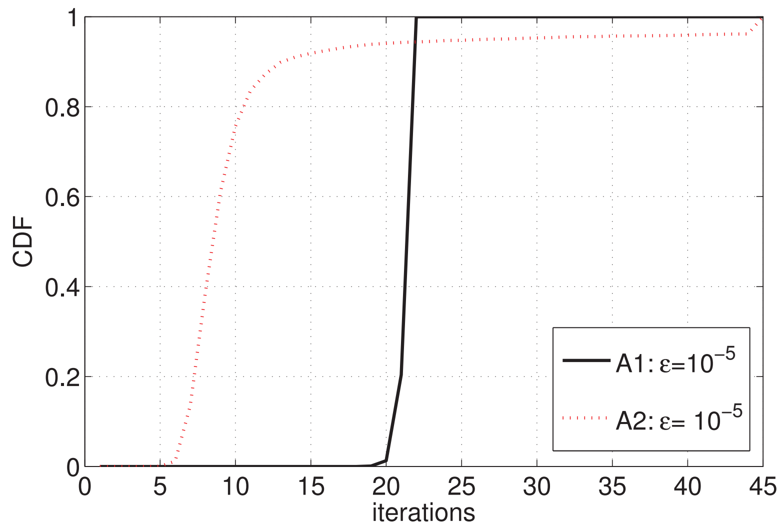

Figure 7.4: CDF of the number of iterations for a precision ϵ.

7.6 Uplink–Downlink Duality

Instead of the SDP based on a semidefinite relaxation of the previous section, this section presents a low complexity approach based on Lagrangian duality theory. The concept, presented in this section, can be applied to arbitrary long-term CSI. Remember, the optimal method presented in the previous section require long-term CSI in the form of Hermitian positive semidefinite Toeplitz matrices. The approach based on the uplink-downlink duality delivers also suboptimal solutions if the matrices do not

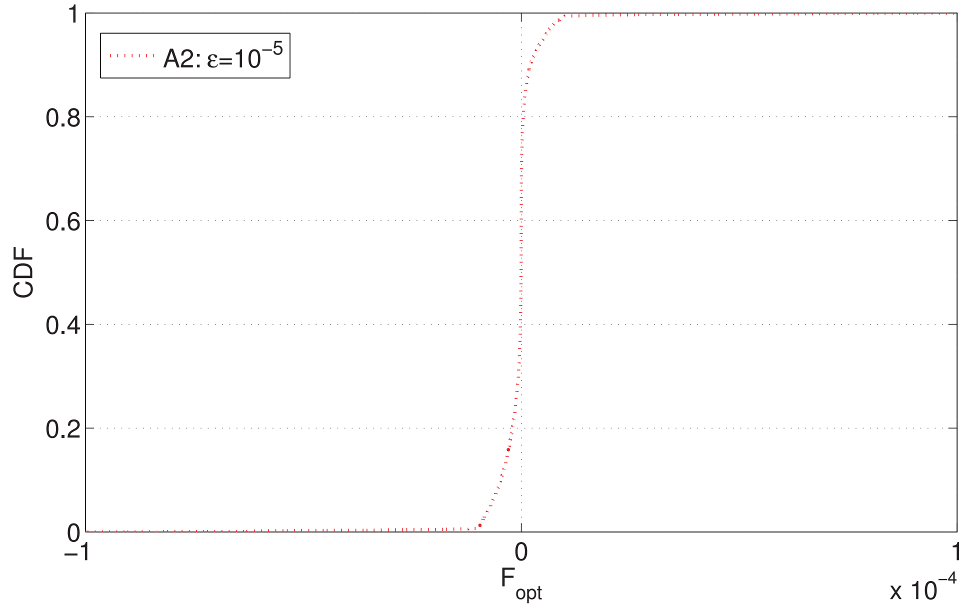

Figure 7.5: CDF of the solution of the parametric program.

have a Toeplitz structure, which is given if, e.g., the arrays are not ULAs. The idea for this framework is similar to the unicast scenario presented in Chapter 4.

The original multicast MBP is non-convex, therefore, the dual problem delivers only an upper bound of the MBP. The PMP is equivalent to the MBP if the SINR constraint of the PMP is equal to the balanced SINR of the MBP [134]. In [134] it was proven that the duality gap of the dual problem of the PMP is as tight as the gap of the SDP to the optimal problem. The optimization of the dual variables of the dual problem results in a further SDP [134].

In this section, the uplink–downlink relation is derived based on the Lagrangian dual problem of the original problem. The procedure is similar to the procedure presented in Section 4.3.4. Instead of an SDP, the uplink–downlink based approach of this section is based on a inner loop with an eigenvalue decomposition and an outer loop with a linear fractional program which has less complexity compared to an SDP. At this point it is helpful to give a short overview of the procedure:

- Proposition 22 gives the Lagrangian dual problem of the multicast MBP with a sum power constraint. This dual problem is only an upper bound. Strong duality does not hold in general due to the non-convexity of the original multicast MBP.

- Similar to Section 4.3.4, Proposition 23 presents the surrogate dual function of the MBP with per-antenna array power constraints (7.9). The result is a combination of the multiple power constraints to a single weighted sum power constraint.

- Finally, Proposition 24 presents the surrogate dual problem of the original multicast MBP 7.9 with general power constraints. This dual problem is only an upper bound, strong duality is not proven in this thesis.

Similar to Section 4.3.4, the UL–DL based solution requires a virtual UL SINR.

Definition 57. *Uplink SINR (multicast): With the uplink receive beamforming vectors of a BS given by* $\mathbf{v}_c$*, with* $||\mathbf{v}_c|| = 1$*,* $\forall c \in \mathcal{S}$*, with the UL power* $\lambda_i \ \forall i \in \mathcal{U}$*, with some matrices* $\mathbf{M}_c \succeq 0 \ \forall c \in \mathcal{S}$*, and with the sets* $\mathcal{U}_c$ *of users served by BS arrays with index c, the dual UL unicast SINR is defined by*

$$\gamma_c^U(\boldsymbol{\mu}, \boldsymbol{\lambda}, \mathbf{v}_c) = \frac{\mathbf{v}_c^H(\sum_{i\in\mathcal{U}_c} \lambda_i \mathbf{R}_{c,i})\mathbf{v}_c}{\mathbf{v}_c^H(\mathbf{M}_c + \sum_{j\notin\mathcal{U}_c} \lambda_j \mathbf{R}_{c,j})\mathbf{v}_c}. \tag{7.42}$$

In what follows, the matrix $\mathbf{V} \in \mathcal{V}$ with

$$\mathcal{V} = \{\mathbf{V} \in \mathbb{C}^{N_A\times M} : \ ||[\mathbf{V}]_{:,c}|| = 1, \ [\mathbf{V}]_{:,c} \in \mathbb{C}^{N_A\times 1}, \forall c \in \mathcal{S}\}$$

is the matrix of all UL receive beamforming vectors of all BS arrays $\mathbf{V} = [\mathbf{v}_1, \ldots, \mathbf{v}_N]$. Similar to the unicast MBP, the multicast MBP can be defined by a weighted sum power constraint:

Definition 58. *With the vector* $\boldsymbol{\lambda} = [\lambda_1, \ldots, \lambda_M]$*, the multicast MBP with a weighted sum power constraint is defined by*

$$f_M^D(\boldsymbol{\mu}) = \max_{\boldsymbol{\Omega}} \min_{i\in\mathcal{U}} \gamma_i^D(\boldsymbol{\Omega}) \tag{7.43}$$

$$\text{s.t.} \ \sum_{i\in\mathcal{S}} \boldsymbol{\omega}_c^H \mathbf{M}_c \boldsymbol{\omega}_c \le P. \tag{7.44}$$

The Lagrangian dual problem leads to the upper bound of the original multicast MBP (7.43), (7.44):

Proposition 22. *With the new dual variables* $\boldsymbol{\lambda} = [\lambda_1, \ldots, \lambda_M]$ *and* $\mathbf{V} = [\mathbf{v}_1, \ldots, \mathbf{v}_N]$*, the upper bound of the non-convex MBP* (7.43), (7.44) *is given by*

$$f_M^U(\boldsymbol{\mu}) = \min_{\boldsymbol{\lambda}} \max_{\gamma,\mathbf{V}} \ \gamma \tag{7.45}$$

$$\begin{aligned} \text{s.t.} \ & \gamma \ge \gamma_c^U(\boldsymbol{\mu}, \boldsymbol{\lambda}, \mathbf{v}_c), \\ & \sum_{i\in\mathcal{U}} \lambda_i \le P \ \ \lambda_i \ge 0, \ \forall i \in \mathcal{U} \\ & \forall c \in \mathcal{S} \end{aligned} \tag{7.46}$$

Proof. The proof is presented in Appendix A.5. □

The constraint (7.46) is an upper bound of the optimal balanced SINR γ. In the case of $N_c = |\mathcal{U}_c| = 1 \ \forall c \in \mathcal{S}$, strong duality is satisfied (see Proposition 4). In this case, the reversal of the SINR constraints and the reversal of the minimization as a maximization over λ_is do not affect the optimal solution. However, this is not given in general, in the case of $|\mathcal{U}_c| > 1 \ \forall c \in \mathcal{S}$, a balanced SINR cannot be achieved. Then (7.45), (7.46) will be an upper bound and strong duality is not satisfied. Only weak duality is given in this case:

$$f_M^U(\boldsymbol{\mu}) > f_D(\boldsymbol{\mu}) \tag{7.47}$$

The dual UL problem of the multicast MBP with general power constraints can be derived based on the surrogate duality theory similar to Proposition 3.

Proposition 23. *With the diagonal matrices* $\mathbf{P}_c = \frac{P_c}{N_A}\mathbf{I}_{N_A}$ *in the case of per-BS array power constraints, the upper bound of the surrogate dual function of the multicast DL MBP* (7.9) *with general (per-antenna or per-antenna array) power constraints is given by*

$$\begin{aligned} s_M^U(\boldsymbol{\mu}) = \min_{\boldsymbol{\lambda}} \max_{\gamma,\mathbf{V}} \ & \gamma \\ \text{s.t. } & \gamma \geq \gamma_c^U(\boldsymbol{\mu},\boldsymbol{\lambda},\mathbf{v}_c), \\ & \sum_{i\in\mathcal{U}} \lambda_i \leq \sum_{c\in\mathcal{S}} \mathrm{Tr}\{\mathbf{M}_c\mathbf{P}_c\} \\ & \lambda_i \geq 0, \ \forall i \in \mathcal{U}, \ \mathbf{M}_c \succeq 0, \forall c \in \mathcal{S}. \end{aligned} \tag{7.48}$$

for a $\boldsymbol{\mu} \geq 0$ *and* $\boldsymbol{\mu} \neq \mathbf{0}$.

Proof. The proof is a straightforward extension of the proof of Proposition 3. The surrogate dual function

$$s_M^D(\boldsymbol{\mu}) = \max_{\boldsymbol{\Omega}} \min_{i\in\mathcal{U}} \gamma_i^D(\boldsymbol{\Omega}) \tag{7.49}$$

$$\text{s.t. } p_\Sigma(\boldsymbol{\mu},\boldsymbol{\Omega}) \leq 0. \tag{7.50}$$

$$\mathbf{M}_c \succeq 0 \ \forall c \in \mathcal{S}.$$

is an upper bound of the original multicast MBP (7.9), The multiple power constraints of (7.9) in the case of per-BS antenna array power constraints can be combined to a single power constraint as follows:

$$p_\Sigma(\boldsymbol{\mu},\boldsymbol{\Omega}) = \sum_{c\in\mathcal{S}} \mu_c(\boldsymbol{\omega}_c^H\boldsymbol{\omega}_c - P_c) \leq 0 \Leftrightarrow \sum_{c\in\mathcal{S}} \boldsymbol{\omega}_c^H\mathbf{M}_c\boldsymbol{\omega}_c \leq \sum_{c\in\mathcal{S}} \mathrm{Tr}\{\mathbf{M}_c\mathbf{P}_c\}.$$

and using the upper bound of Proposition (22), the upper bound (7.48) is the result. □

The upper bound (7.48) is tight if $|\mathcal{U}_c| = 1 \ \forall c \in \mathcal{S}$. Finally, with the surrogate function (7.48), the surrogate dual problem is given by the following proposition:

Proposition 24. *The upper bound of the multicast MBP* (7.9) *with per-antenna array power constraints is:*

$$\begin{aligned} \gamma_M^U = \min_{\boldsymbol{\mu},\boldsymbol{\lambda}} \max_{\gamma,\mathbf{V}} \ & \gamma \\ \text{s.t. } & \gamma \geq \gamma_c^U(\boldsymbol{\mu},\boldsymbol{\lambda},\mathbf{v}_c), \\ & \sum_{i\in\mathcal{U}} \lambda_i \leq \sum_{c\in\mathcal{S}} \mathrm{Tr}\{\mathbf{M}_c\mathbf{P}_c\} \\ & \lambda_i \geq 0, \ \forall i \in \mathcal{U}, \ \mathbf{M}_c \succeq 0, \forall c \in \mathcal{S}. \end{aligned} \tag{7.51}$$

Proof. Due to $s_M^D(\boldsymbol{\mu}) \leq s_M^U(\boldsymbol{\mu})$ also $\min_{\boldsymbol{\mu}} s_M^D(\boldsymbol{\mu}) \leq \min_{\boldsymbol{\mu}} s_M^U(\boldsymbol{\mu})$ holds and due to $\gamma^D \leq \min_{\boldsymbol{\mu}} s_M^D(\boldsymbol{\mu})$ also $\gamma^D \leq \min_{\boldsymbol{\mu}} s_M^U(\boldsymbol{\mu}) = \gamma_M^U$ holds. □

7.6.1 Iterative Algorithm

Section 7.6 derives a new framework for UL–DL duality. In the unicast case, presented in Chapter 4, this framework offers a simple iterative algorithm which has a lower complexity compared to conventional convex solver based solutions. This section presents a similar approach for the multicast case. The works [135, 136] present a similar concept, however the authors only regard the sum power constraint multicast MBP and they do not propose a dual problem. The authors heuristically extend the well known solution of Schubert and Boche [128] for the unicast case.

This section presents an extended algorithm, which finds sub-optimal solutions for the multicast MBP with practically relevant per-base station power constraints based on the virtual dual uplink problem (7.51). The solution consists of three parts:

1. The problem (7.51) consists of an inner problem which corresponds to a weighted sum power constrained MBP. The solution of the inner problem depends on vector $\boldsymbol{\mu}$. For a given vector $\boldsymbol{\mu}$, Algorithm 14 determines the normalized beamforming vectors $||\mathbf{v}_c|| = 1\ \forall c \in \mathcal{S}$.

2. Based on the normalized beamforming vectors given by the matrix $\mathbf{V}$ and for a given vector $\boldsymbol{\mu}$, a subsequent algorithm (Algorithm 15) calculates the DL beamforming vectors $\boldsymbol{\Omega}$. The inner problem of (7.51) delivers an upper bound of the SINR but not the actual SINR γ. Therefore, the actual SINR for a given matrix $\mathbf{V}$ and a vector $\boldsymbol{\mu}$ must be determined to calculate the DL power $\mathbf{p}$ which is required for the DL beamforming matrix $\boldsymbol{\Omega}$.

3. Finally, an outer algorithm (Algorithm 16), updates $\boldsymbol{\mu}$.

This concept shows, that the multicast MBP with general power constrains can be decomposed to simpler subproblems. E.g., for a given set of normalized receive beamforming vectors $||\mathbf{v}_c|| = 1\ \forall c \in \mathcal{S}$, the optimization of the of the DL power is quasi-convex $\mathbf{p}$.

7.6.1.1 Inner Loop

Firstly, this section regards the multicast MBP (7.43) with a sum power constraint. The optimal solution of the dual problem (7.45) delivers an upper bound of the primal problem (7.43). Figure 7.6 illustrates the UL–DL relation based on the previous derivation of the Lagrangian duality. In the UL case (a), a BS c using the UL beam pattern $\mathbf{v}_c$, receives UL signals from its users with the UL power λ_i, with $i \in \mathcal{U}_c$. however, the BS c also receives interference from users of other cells, e.g., cell k. In the DL case (b), a user receives the useful signal transmitted from the BS c over the beam pattern $\boldsymbol{\omega}_c = \sqrt{p_c}\mathbf{v}_c$, where p_c denotes the DL power transmitted by BS c. On the other hand, the user receives interference from adjacent BSs, e.g., BS k. Based on this investigation the following computation of the beam pattern is made. Regarding the upper bound (7.46) of the UL SINR

$$\gamma_c^U(\boldsymbol{\mu}, \boldsymbol{\lambda}, \mathbf{v}_c) = \sum_{i \in \mathcal{U}_c} \frac{\mathbf{v}_c^H \lambda_i \mathbf{R}_{c,i} \mathbf{v}_c}{\mathbf{v}_c^H (\mathbf{M}_c + \sum_{j \notin \mathcal{U}_c} \lambda_j \mathbf{R}_{c,j}) \mathbf{v}_c}, \tag{7.52}$$

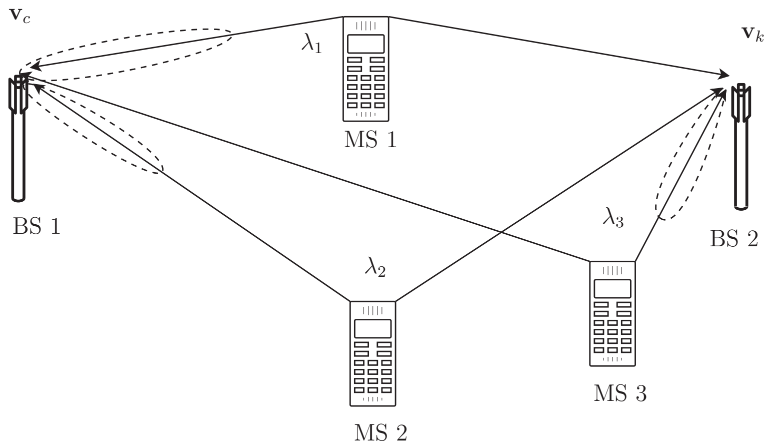

(a) Uplink

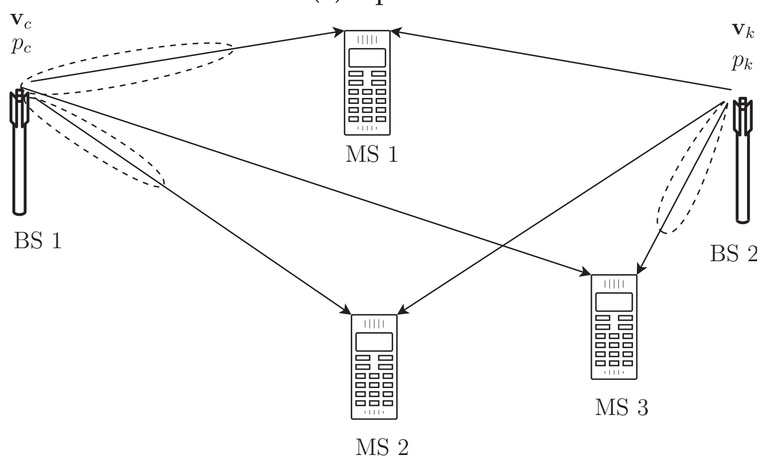

(b) Downlink

Figure 7.6: UL–DL relation for the derived upper bound given in Proposition 22 and the Definition of the multicast MBP given in Definition 58. In the UL presentation (a), each user i transmits with a UL power λ_i while the BS c receives via a receive beamforming vector $\mathbf{v}_c$. In the DL presentation (b), a BS c transmits a DL signal weighted by a beamforming vector $\mathbf{v}_c$ with power p_c.

the UL signal received at a BS consists of $\mathcal{U}_c$ links of different MSs served by this BS c. Strong duality between UL and DL is not given in general for multicast beamforming. However, a simple heuristic offers good results. The maximization of UL SINR has to be done by an independent optimization of the beamformer for each user, otherwise only the strongest users will get high DL SINR. Thus, a smarter computation of the UL beamforming vectors $\mathbf{v}_c$ is needed. The heuristic for the beamforming vector is given by the linear hull

$$\operatorname{span}(\mathbf{v}_{c,1}, \ldots, \mathbf{v}_{c,N_c}) = \{\lambda_1 \mathbf{v}_{c,1} + \ldots + \lambda_{N_c} \mathbf{v}_{c,N_c} \mid \lambda_1, \ldots, \lambda_{N_c} \in \mathbf{K}\}, \tag{7.53}$$

spanned by the $\mathcal{U}_c$ UL beamforming vectors of the $\mathcal{U}_c$ users over the field $\mathbf{K}$ of the UL powers. A vector of this vector space is then given by

$$\mathbf{v}_c = \sum_{i \in \mathcal{U}_c} \lambda_i \mathbf{v}_{c,i}, \tag{7.54}$$

where in each link the optimal beamforming vector $\mathbf{v}_{c,i}$ is computed by

$$\mathbf{v}_{c,i} = \arg\max_{\mathbf{v}_{c,i}} \frac{\mathbf{v}_{c,i}^H \lambda_i \mathbf{R}_{c,i} \mathbf{v}_{c,i}}{\mathbf{v}_{c,i}^H (\mathbf{M}_c + \sum_{j \notin \mathcal{U}_c} \lambda_j \mathbf{R}_{c,j}) \mathbf{v}_{c,i}}. \tag{7.55}$$

For fixed beamforming vectors $\mathbf{v}_c$, the UL powers λ_i are then given by

$$\lambda_i = \frac{\mathbf{v}_c^H (\mathbf{M}_c + \sum_{j \notin \mathcal{U}_c} \lambda_j \mathbf{R}_{c,j}) \mathbf{v}_c}{\mathbf{v}_c^H \mathbf{R}_{c,i} \mathbf{v}_c}. \tag{7.56}$$

Consequently, weak links are weighted stronger than strong links in Eq. (7.54). As in [19, 57, 157], if the total transmit power $P_\Sigma = \sum_{i \in \mathcal{U}} \lambda_i$ has not reached the power budget $P = \sum_{c \in \mathcal{S}} \mathrm{Tr}\{\mathbf{M}_c \mathbf{P}_c\}$, every UL power can be scaled by P/P_Σ. In Algorithm 14, the complete outline for the UL beam pattern optimization is listed. The UL powers are initialized with $\lambda_i = 1 \; \forall i$ and the initial beamforming vectors are given by $\mathbf{v}_c = [1, 0, 0, 0]^T$, $\forall c$.

Algorithm 14 UL vector iteration for the multicast MBP

repeat
  for $c = 1$ to N_c **do**
    for $i = 1$ to M **do**
      $\tilde{\lambda}_i = \frac{\mathbf{v}_c^H (\mathbf{I} + \sum_{j \notin \mathcal{U}_c} \lambda_j \mathbf{R}_{c,j}) \mathbf{v}_c}{\mathbf{v}_c^H \mathbf{R}_{c,i} \mathbf{v}_c}$
      $\mathbf{v}_{c,i} = \arg\max_{\mathbf{v}_{c,i}} \frac{\mathbf{v}_{c,i}^H \lambda_i \mathbf{R}_{c,i} \mathbf{v}_{c,i}}{\mathbf{v}_{c,i}^H (\mathbf{I} + \sum_{j \notin \mathcal{U}_c} \lambda_j \mathbf{R}_{c,j}) \mathbf{v}_{c,i}}$
    end for
    $\mathbf{v}_c = \sum_{i \in \mathcal{U}_c} \tilde{\lambda}_i \mathbf{v}_{c,i}$
    $\lambda_i = \beta \tilde{\lambda}_i, \forall i \in \mathcal{U}, \text{with } \beta = \frac{\sum_{c \in \mathcal{S}} \mathrm{Tr}\{\mathbf{M}_c \mathbf{P}_c\}}{\sum_{i \in \mathcal{U}} \tilde{\lambda}_i}$
  end for
until convergence
return $\mathbf{V}$

7.6.1.2 Downlink Power Computation

After Algorithm 14 has converged, the computation of the uplink power and the beam pattern is finished. However, the DL power is not determined. In contrast to the unicast case, the DL power can not be computed by solving a linear system of equations [57] by using the uplink SINR because it is an upper bound. The actual uplink SINR $\gamma_c^U(\boldsymbol{\mu}, \boldsymbol{\lambda}, \mathbf{v}_c)$ is unknown. Furthermore, in the multicast case, the uplink SINR is not balanced.

The correct uplink SINR has to be correctly determined afterwards based on the given uplink power vector $\boldsymbol{\lambda}$ and the determined uplink beamformers stored in $\mathbf{V}$. The DL beamforming weights are given by $\boldsymbol{\omega}_c = \sqrt{p_c}\mathbf{v}_c$. The authors of [135, 136] present a solution based on a generalized eigenvalue decomposition where the upper bound of the uplink SINR is required. This solution can be improved by a better estimation of the actual DL SINR.

It is desired to improve the worst DL SINR of all users with the per-antenna array power constraint given by P_c. With the domain of the feasible DL power $\mathcal{P} = \{\mathbf{p} \in \mathbb{R}_+^N | p_c \leq P_c \ \forall c \in \mathcal{S}\}$, this can be defined as:

$$\bar{\gamma} = \max_{\mathbf{p} \in \mathcal{P}} \min_{i \in \mathcal{U}} \frac{p_{c(i)} g_{c(i),i}}{\sum_{c \neq c(i)} p_c g_{c,i} + 1} \tag{7.57}$$

with $g_{c,i} = \mathbf{v}_c^H \mathbf{R}_{c,i} \mathbf{v}_c$. The problem (7.57) can be equivalently rewritten as

$$\bar{\gamma} = -\min_{\mathbf{p} \in \mathcal{P}} \max_{i \in \mathcal{U}} \frac{-p_{c(i)} g_{c(i),i}}{\sum_{c \neq c(i)} p_c g_{c,i} + 1} \tag{7.58}$$

The problem (7.58) is a linear fractional program [28, 29]. Let $f_i(\mathbf{p}) = -p_{c(i)} g_{c(i),i}$ and $d_i(\mathbf{p}) = \sum_{c \neq c(i)} p_c g_{c,i} + 1$, $\forall i \in \mathcal{U}$ be linear functions over $\mathbf{p}$, it can be solved with the help of the parametric program [28, 29]

$$F(\gamma) = \min_{\mathbf{p} \in \mathcal{P}} \max_{i \in \mathcal{U}} \{f_i(\mathbf{p}) - \gamma \, d_i(\mathbf{p})\} \tag{7.59}$$

In [28, 29], the authors propose a root finding algorithm for the parametric program (7.59) with a faster convergence than the conventional bisection method. Algorithm 15 shows the root finding algorithm to solve (7.58).

Algorithm 15 Root finding algorithm:

Let $\mathbf{p}^1 \in \mathcal{U}$ and $\gamma^1 = \max_{i \in \mathcal{U}} \frac{f_i(\mathbf{p}^1)}{d_i(\mathbf{p}^1)}$ and $k = 1$
repeat
  Determine the optimal solution $\mathbf{p}^k$ of
  $F(\gamma^k) = \min_{\mathbf{p} \in \mathcal{X}} \ \max_{i \in \mathcal{I}} \{\frac{f_i(\mathbf{p}) - \gamma^k d_i(\mathbf{p})}{d_i(\mathbf{p}^k)}\}$
  Let $\gamma^{k+1} = \max_{i \in \mathcal{U}} \frac{f_i(\mathbf{p}^k)}{d_i(\mathbf{p}^k)}$ and set $k = k + 1$
until $|F(\gamma^k)| > \epsilon$
return $\mathbf{p}^k$

Theorem 11. *If $F(\gamma^k) = 0$, then $\gamma^k = -\bar{\gamma}$ and $\mathbf{p}^k$ is the optimal solution.*

Proof. In [30, Theorem 2.1], the authors present the proof for a quasi-convex fractional program with non-negative functions d_i over a compact domain. The functions $f_i(\mathbf{p}) = -p_{c(i)} g_{c(i),i}$ and $d_i(\mathbf{p}) = \sum_{c \neq c(i)} p_c g_{c,i} + 1 \ \forall i \in \mathcal{U}$ are linear function, hence the fractional program (7.58) is quasi-linear and, therefore, also quasi-convex. Furthermore, the functions $g_i(\mathbf{p})$ are non-negative. Finally, $\mathcal{P}$ is closed and bounded, consequently it is compact. Therefore, all conditions for [30, Theorem 2.1] are satisfied. □

7.6.1.3 Outer Loop

With the knowledge of the optimal DL beamforming vectors $\boldsymbol{\omega}_c = \sqrt{p_c}\mathbf{v}_c$, the matrices $\mathbf{M}_c$ can be determined similar to the unicast case presented in Section 4.4.2 The final algorithm is listed in Alg. 16.

Algorithm 16 Outer loop: DL power and iterations over $\boldsymbol{\mu}$

```
Initialize μ = 1
repeat
   Inner loop (Algorithm 14) → V
   Solve the fractional program (7.58) → Ω
   Update the μ vector according to (4.49)
until Convergence
return Ω
```

7.6.2 Numerical Results

The numerical results are made for the scenario presented in Fig. 7.1 and are based on the same setting as presented in Section 7.5.2.

Three algorithms are compared in this section for a precision of $\epsilon = 10^{-5}$:

- A1: Conventional bisection method to solve problem (7.12). The beamforming vectors are calculated based on the largest eigenvalue of and the correponding eigenvector of solution of the SDP.
- A2: Root finding algorithm Algorithm 13 with parametric program (7.36).
- A3: The iterative solution given by Algorithms 14-16.

Figure 7.7 depicts the CDF of the SINR. The new algorithm Alg. 16 outperforms the conventional solution for low and very high SINR. Hence, the weakest and strongest users profit from the new solution.

Figure 7.8 shows the CDF of the transmit power. Both algorithms fulfill the per-antenna array power constraints. The new Algorithm A2 uses higher transmit power in several user drops.

Figure 7.9 presents the CDF of the iterations for both algorithms. In 15% of the drops the new algorithm A2 requires less iterations than the conventional bisection based SDP A1. In several drops the number of iterations of the new algorithm is larger than 45. Hence, in some scenarios the new algorithm has a very slow convergence. The algorithm aborts after 45 iterations and takes the solution of the last iteration.

Although the new algorithm (Alg. 16) needs more iterations, than the convex solver based approaches, it has less complexity. As already shown in Section 4.4.3, the

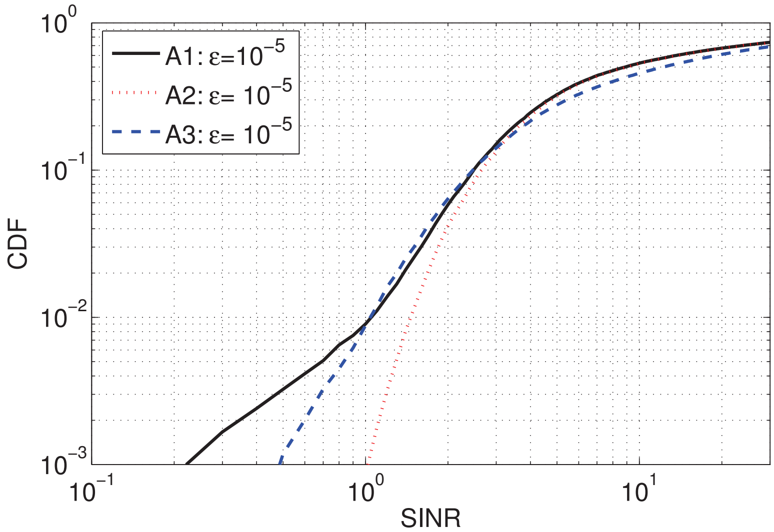

Figure 7.7: CDF of the SINR of the new algorithm based on Algorithm 16 (blue, dashed), the new root finding Algorithm 13, the conventional SDP based bisection based method for the problem (7.12) (black, solid). The red dotted curve denotes the CDF of Algorithm 13.

iterative solution requires much less computational effort to find a solution with similar or even better performance than convex solver based approaches. In the multicast case, the iterative approach must determine the correct DL SINR by a linear fractional program. Such a program requires an iteration over linear programs. Hence, in the outer loop multiple linear programs must be solved instead of a single linear system of equations (4.47). However, this approach has less complexity than an SDP which is solved in the outer loop of conventional bisection based methods.

7.7 Summary

- This chapter investigates the multicast max–min beamforming problem with per-antenna array power constraints. The max–min beamforming problem can be solved with a convex feasibility check problem in the form of a semidefinite program. This chapter proves the existence of a rank-1 solution if long-term CSI in the form of positive semidefinite Hermitian Toeplitz matrices is available.

- Besides the semidefinite program, this chapter proposes an equivalent problem based on convex programming with finite autocorrelation sequences. The resulting equivalent problem is a quasi-convex fractional program which can be solved by a root finding algorithm. The convergence of the root finding algorithm is super-linear, consequently, it is faster than a bisection algorithm. The new solution achieves a higher and better balanced SINR than the conventional bisection based solution.

- Besides approaches based on convex solvers, this section proposes a new uplink–downlink duality based method. The new framework has similarities with the

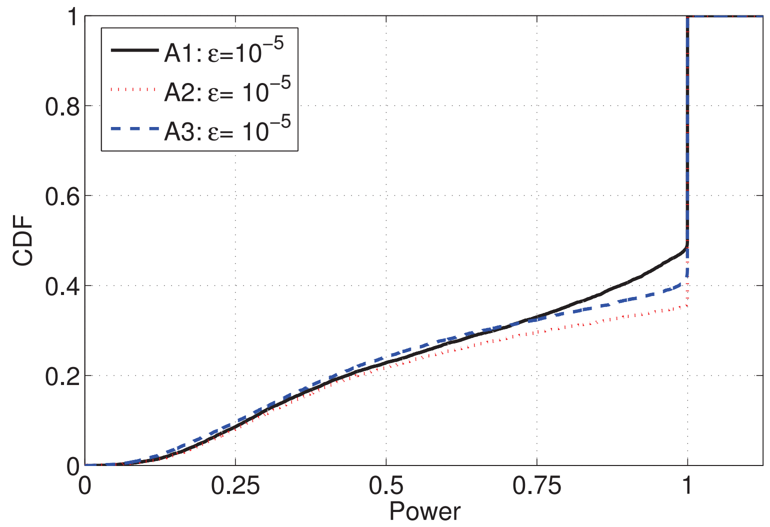

Figure 7.8: CDF of the transmit power of the new algorithm based on Algorithm 16 (blue, dashed), the new root finding Algorithm 13, the conventional SDP based bisection based method for the problem (7.12) (black, solid). The red dotted curve denotes the CDF of Algorithm 13.

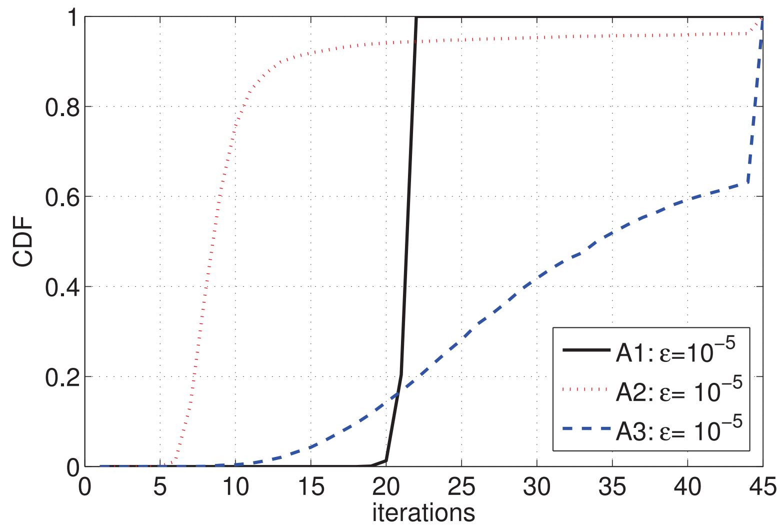

Figure 7.9: CDF of the number of iterations for a precision ϵ of the transmit power of the new algorithm based on Algorithm 16 (blue, dashed), the new root finding Algorithm 13, the conventional SDP based bisection based method for the problem (7.12) (black, solid). The red dotted curve denotes the CDF of Algorithm 13.

unicast case. It is also based on simple mathematical operations and requires only a linear program instead of a semidefinite program. The uplink–downlink based solution achieves a higher SINR than the conventional bisection based solution. However, in some cases the convergence is slow, but a break after 45 iterations results in an improved minimal SINR compared to the conventional bisection based method. Future research regarding the convergence is required to improve on this result.

Chapter 8

Application: Interference Mitigation with Sector Pattern Adaptation (SPA)

The content presented in this chapter is in part published in the publications [38, 44, 45]. This chapter considers both, a multicast and a unicast downlink transmission.

The previous chapter presents the theoretical background of multicast beamforming as a technique to optimize the SINR of multicast groups. Chapter 7 derives an equivalent quasi-convex form of the multicast MBP and presents different algorithms to solve the MBP. In a multicast transmission multiple users jointly receive the same content. Hence, a BS transmits the same symbol by using one beamforming vector to all users inside the multicast group.

A famous example for a multicast transmission is digital audio broadcasting (DAB) [49] and digital video broadcasting (DVB) [50]. In addition to these well known examples, multiple wireless physical layer technologies require a multicast transmission. An upcoming technology is two-way relaying [65, 118, 166], where in the so-called broadcast hop a relay transmits a signal jointly to the users and the BS array.

8.1 Adaption of the Sector Pattern Based on Long-Term Multicast Beamforming

Multicast beamforming also has a useful application in networks with a unicast transmission. The following section proposes a simple scheme for interference mitigation in multicell networks based on max–min multicast beamforming. In wireless networks, a fast variation of the beamforming weights will result in a measured SINR at the user that is not very close to the actual SINR.

Techniques such as channel aware scheduling (CAS) or adaptive modulation and coding (AMC) require an accurate knowledge of the SINR. Consequently, a higher feedback rate is required if the SINR fluctuates rapidly. A lower variance of the SINR can be achieved by slower adaptation of the beamforming weights.

However, beamforming can be used to mitigate interference in multicell networks. A practically relevant solution which can be combined with CAS would be a slow adaptation of the sector pattern. In multicell networks with a frequency reuse-1, cell edge users suffer from the largest interference and their distance to the serving BS is maximal. Consequently the SINR is often much lower compared to users in the cell center. With multicast beamforming, a beamforming vector can cover all users inside a cell jointly. If the optimization of this beamforming vector is based on long-term

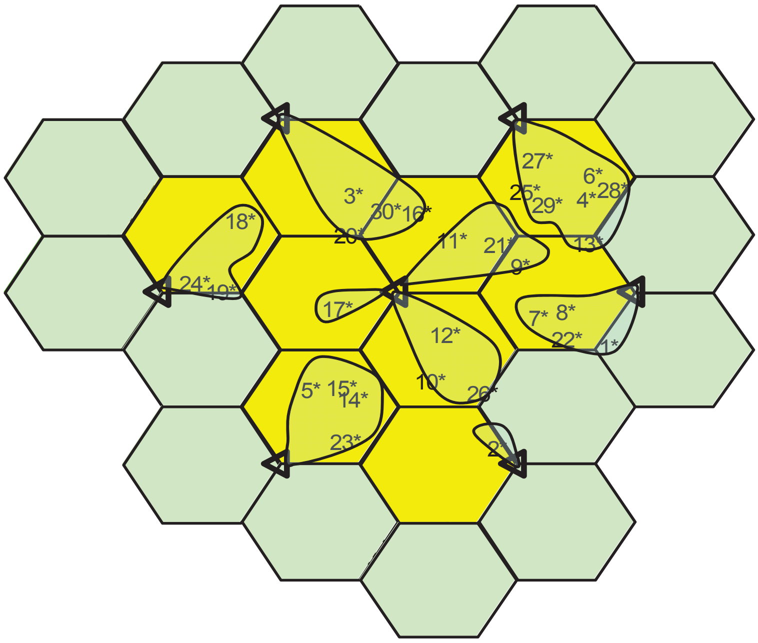

Figure 8.1: Scenario: Triangles denote BSs, asterisks with the numbers denote users with their index. Yellow cells are cooperative. Lobes denote the multicast groups.

CSI in form of spatial correlation matrices, this adaptation of the beams can also be seen as an adaptation of the sector pattern according to user positions.

Figure 8.1 depicts an example of SPA. The yellow cells form a cooperative network of 9 cooperative BS arrays. Without cooperation, the sector pattern is formed according to this hexagonal grid. Applying long-term multicast max–min beamforming, the adapted sector pattern denoted by the lobes will be the result. Hence, the BSs arrays form, based on the spatial correlation knowledge of all users, beam lobes in the direction of the user cluster. Areas without users are not covered which results in a reduced intercell interference. Max–min beamforming results in a fair distribution of the SINR among the users in the cooperative network because it maximizes the minimum SINR, hence, it maximizes the SINR of the weakest users.

The sector pattern, optimized based on the available spatial correlation knowledge, is constant during the stationarity interval of the available long-term CSI [76]. Each user inside a user group can be scheduled based on the instantaneous local channel quality information (CQI).

8.2 Combination of SPA and Multiuser Scheduling

Various multiuser scheduling schemes have been proposed in the last 10 years. A famous work regarding multiuser scheduling is [153]. The best known multiuser scheduling schemes are

1. Round-Robin Scheduling (RRS)
2. Opportunistic Round-Robin Scheduling (ORRS)
3. Proportional Fair Scheduling (PFS)
4. Maximum SINR Scheduling

Among all of these scheduling schemes, a trade-off between fairness and performance exists. These schemes (1-4) are sorted by fairness and performance with the Round-Robin scheme being the fairest scheme with the lowest sum rate and maximum SINR scheduling being the most unfair scheme with the best sum rate performance.

This section presents a straightforward combination of the sector pattern adaptation based on multicast beamforming and these CAS schemes. Each cell forms a multicast group where the sector pattern is adapted based on max–min multicast beamforming according to Definition 54. Each BS antenna array, forming the sector pattern, is subject to a per antenna array power constraint. Therefore, each sector can have different power constraints. Such a network configuration is called heterogeneous.

Inside each cell all users belong to the same multicast group and are jointly covered by the adapted sector pattern. A user belonging to this multicast group can be scheduled by the four scheduling schemes. The procedure can be summarized as follows:

- The sector pattern is optimized based on the available spatial correlation knowledge by multicast max–min beamforming.
- During each local stationarity interval [76], the sector pattern of all cells belonging to the cooperative network is constant, hence, a low fluctuation of the SINR is the result.
- During each local stationary interval [76], the users inside a cell are scheduled based on local instantaneous CQI information and no intercell synchronization is required.

8.2.1 Opportunistic Round-Robin Scheduling (ORRS)

Let $i^*(k)$ denote the user scheduled in time slot k and let $\hat{\gamma}_i(k)$ be the instantaneous SINR of user i in time slot k. Furthermore, let $\mathcal{U}(k)$ be the set of indices of users who have not been scheduled for $\Delta \in \mathbb{N}_+$ time slots. The opportunistic Round-Robin scheduling scheme, introduced in [6], schedules a user according to the following rule:

$$i^*(k) = \operatorname{argmax}_{i \in \mathcal{U}(k)} \hat{\gamma}_i(k). \tag{8.1}$$

Let N_c be the number of users in cell c, the maximum inter-access time is $2\Delta(N_c - 1)$ [6]. For $\Delta = 1$ the standard ORR algorithm is the result. This scheme can be simply extended to CAS combined with SPA. Remember, the number of non-scheduled users belonging to the multicast group of a given cell c is $\mathcal{U}_c$.

$$i^*(k) = \text{argmax}_{i \in \mathcal{U}_c} \hat{\gamma}_i(k) \tag{8.2}$$

Let $\mathcal{U}_{c,0}$ denote the number of active users belonging to the multicast group cell c. After a user i^* is scheduled, the set $\mathcal{U}_c$ is updated according to Definition 49:

$$\mathcal{U}_c := F(\mathcal{U}_c, \mathcal{U}_{c,0}, i^*) \tag{8.3}$$

Let $\Delta = 1$, the maximum inter-access time is $2(N_c - 1)$. The ORR scheduling scheme is the fairest scheme after Round-Robin scheduling.

8.2.2 Proportional Fair Scheduling

Another well known fair scheme with a higher sum rate performance is called PFS [153]. This scheme gives higher scheduling priorities to users with a currently high achievable rate. However, this current achievable rate is considered relative to their past rates. This relative weighting results in a fair distribution of the resources. A user $i^*(k)$ is scheduled in cell c in time slot k according to the following rule:

$$i^*(k) = \text{argmax}_{i \in \mathcal{U}_c} \frac{R_i(k)}{\bar{R}_i(k)} \tag{8.4}$$

where $R_i(k) = \log(1 + \gamma_i(k))$ is the instantaneous achievable rate a user can achieve under the current channel conditions[1]. The rate $\bar{R}_i(k)$ is the rate a user had in the past:

$$\bar{R}_i(k) = (1 - \alpha)\bar{R}_i(k) + \alpha R_i(k) \tag{8.5}$$

where $\alpha = 1/T$ is the parameter for PFS and determines the delay among to consecutive transmissions to a user.

8.2.3 Maximum SINR Scheduling

Maximum SINR scheduling has the highest sum rate performance of all presented schemes. This scheme always schedules the user with the best current channel conditions. Hence, an unfair distribution of the resources can be the consequence. A user $i^*(k)$ is scheduled in slot k according to the rule

$$i^*(k) = \text{argmax}_{i \in \mathcal{U}_{c,0}} \hat{\gamma}_i(k). \tag{8.6}$$

Note, this scheme has similarities to the ORRS scheme, the only difference is the set $\mathcal{U}_{c,0}$ which is not updated as in the ORRS scheme. Consequently, the same user can be always scheduled if he has the best channel conditions.

[1] In practice one would use the requested throughput of user i instead of the achievable rate.

8.3 Evaluation of SPA and Fast Beam Scheduling in a Joint Scenario

This section evaluates the different applications of the beamforming technologies of Chapter 4 and 7 along with scheduling (beam-scheduling/CAS) techniques presented in Chapters 5 and 8.

The numerical results are based on a scenario created by the Winner II model [97]. Table 6.2 presents the setting of the scenario. The setting is the same as in Section 6.3.1. However, this section does not use relays, therefore, the scenario corresponds to Fig. 4.1. The results are not intended to present the realistic system performance, however, these results illustrate the performance differences among the proposed algorithms presented in this chapter. The scenario is interference dominated. User are scheduled to a base station if they are located inside the associated cell. One third of the cells contains 2, 3 and 4 users respectively. Consequently, a reduced multiuser diversity compared to Chapter 5 is given.

All beamforming optimizations are based on global long-term CSI in the form of spatial correlation matrices. The Statistics are generated based on averaging over the channel vectors. The CAS schemes require local instantaneous CQI. A frequency reuse one factor is used. Furthermore, the scenario is interference limited. This section evaluates the SINR performance of the following algorithms:

- Multicast beamforming based sector pattern adaptation with Round-Robin scheduling (SPA RRS)
- Multicast beamforming based sector pattern adaptation with opportunistic Round-Robin scheduling (SPA ORRS) according to Section 8.2.1
- Multicast beamforming based sector pattern adaptation with proportional fair scheduling (SPA PFS) according to Section 8.2.2
- Unicast beamforming based fast beam-scheduling with Round-Robin scheduling (FBS RRS)
- Unicast beamforming based fast beam-scheduling with dimension-wise sum rate maximization (FBS DWS sum-rate) according to Section 5.5.2.2
- Without any coordination (beamforming, scheduling) and reuse-1, which can be seen as the geometry factor [147] of the 40 user drops.

Figure 8.2 depicts the CDF of the mean SINR of the 40 user drops. The blue dotted curve shows the CDF of the geographical factor due to the considered scenario which is this case frequency reuse one and no beamforming, power control and scheduling. Therefore, the intercell interference is high. Figure 8.3 compares the instantaneous SINR of the SPA and FBS algorithms. SPA with ORRS offers a gain of 1dB. Relaxing a bit the fairness, with PFS, a gain of 4-5 dB is possible. The FBS approach slightly out-performs SPA with PFS. FBS with DWS achieves an approximately 2-3 dB higher SINR for the majority of the users. However, SPA with PFS achieves a higher SINR for the weakest 5% of the users compared to the FBS with DWS.

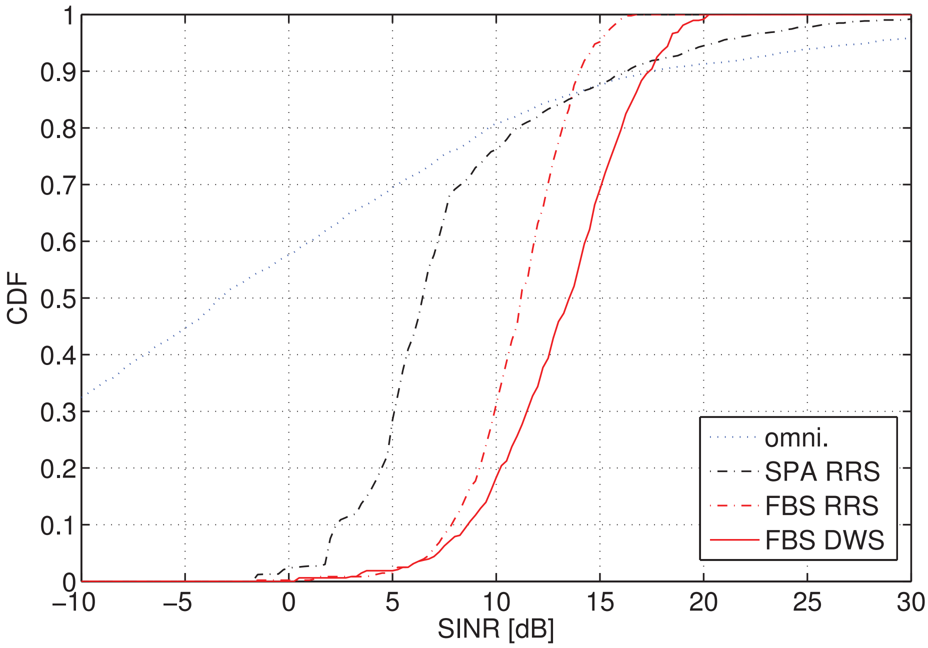

Figure 8.2: CDF of the individual per user mean SINR of the algorithms.

Finally, Figure 8.4 compares the relative sum rate (relative to SPA RRS) of the different CAS with FBS algorithms. As expected FBS with optimized scheduling offers the largest gain of more than 50%. With SPA and PFS a gain of more than 25% is feasible.

8.3.1 Discussion

Comparing SPA with CAS and FBS there is a trade-off between SINR performance, synchronization effort, temporal fairness, complexity, and backhaul effort.

8.3.1.1 SINR performance

FBS shows the best overall SINR performance. The better SINR performance is due to unicast beamforming. The whole transmit power of a BS is transmitted only to the scheduled user. The optimization is based on global available long-term CSI.

If SPA is used, the beam lobe of a BS covers all users inside a cell. Hence, transmit power is wasted in the direction of the not scheduled users. As a result SPA shows a lower SINR performance. An additional application of CAS techniques increases the sum rate of the system. A combination of SPA with PFS requires local knowledge of the instantaneous CQI. If this knowledge is perfectly known, the weakest users can achieve a higher SINR than the best FBS scheme.

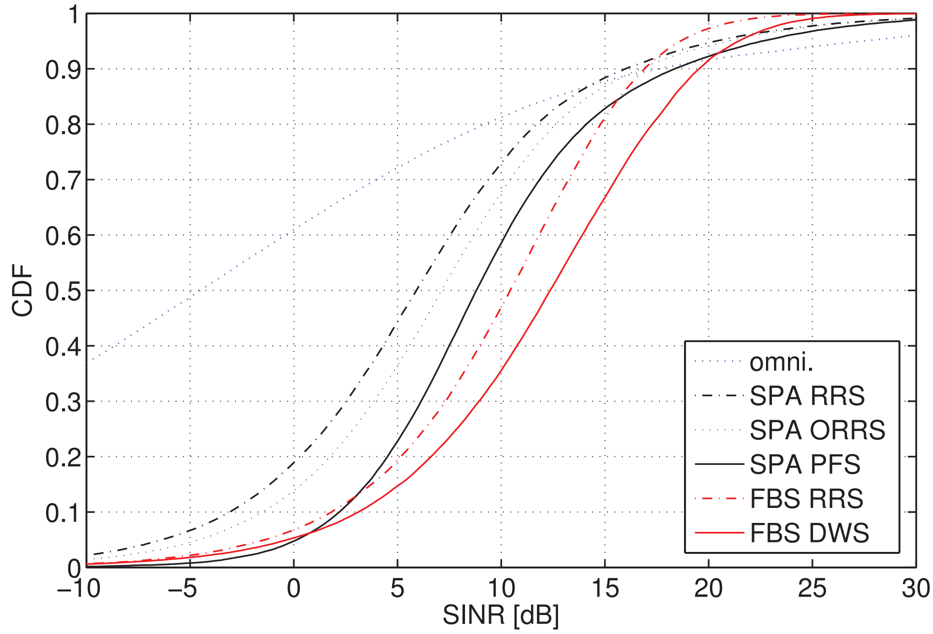

Figure 8.3: CDF of the individual per user instantaneous SINR of the different SPA (and CAS) and FBS algorithms.

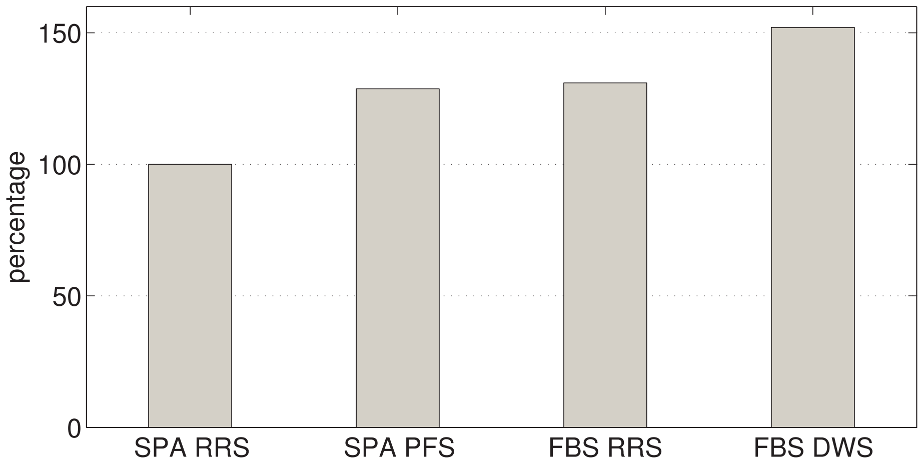

Figure 8.4: Sumrate relative to SPA RRS of the different FBS and SPA algorithms.

8.3.1.2 Synchronization Effort

FBS requires a fast beam switching and a synchronization of the beams and beam scheduling decisions. SPA requires only one beamforming optimization which is valid as long as the statistics of the channel are unchanged. Due to the low fluctuations of the beams, the estimated instantaneous CSI is close to the actual SINR and

CAS techniques can be combined with SPA. However, then each BSs requires local instantaneous CQI.

8.3.1.3 Temporal Fairness

In addition to synchronization effort and SINR performance, temporal fairness is another important design criterion:

- The maximum inter-access time or maximum delay of SPA with ORRS is given by $2(N_c - 1)$.
- Let K be the length of the scheduling matrix (5.1), the maximum inter-access time of FBS with DWS is given by $(N_c - 1)K/N_c$. The parameter K is defined in (5.17) as the lowest common multiple of all numbers of users in all cells.

If all cells have the same number of users and $K = 2N_c$, both approaches have the same maximum delay. The exact determination of the maximum inter-access times for PFS is not so straightforward. In [79], the interscheduling time is numerically evaluated. PFS usually shows significantly higher maximum inter-access times than ORRS.

8.3.1.4 Complexity

A further issue is complexity. FBS with DWS requires multiple beamforming optimizations to calculate the cost matrix for the scheduling optimization. Hence, a fast processor is required at a central unit if a centralized coordination is used or at each BS if a distributed coordination is realized. SPA requires only one beamforming optimization where a local optimum can be achieved by a low complexity algorithm (see Section 7.6.1). CAS on the other hand requires an accurate knowledge of the instantaneous CQI, while FBS only requires long-term CSI.

8.3.1.5 Backhaul

The backhaul effort is identical for both algorithms. CAS and FBS require long-term CSI of all coordinated links of the considered network which can be estimated during the local stationary interval [76]. A future work can be an evaluation in a scenario where stationarity is not given. Therefore, also new system level simulations and channel models are required. Based on this evaluations, a realistic estimation of the backhaul overhead can be performed and further extension of the algorithms to non-stationary scenarios can be developed.

Chapter 9

Conclusions

The scope of this thesis was a development of a theoretical and algorithmic framework for intercell interference mitigation in multicell networks with unicast and multicast beamforming.

One key issue in multicell scenarios is the development of low complexity algorithms. In multicell networks, channel state information changes rapidly; therefore, a fast update of the beamforming weights is required. The theory of the unicast max–min beamforming problem in a single base station broadcast scenario with a single sum power constraint is well understood. The unicast max–min beamforming problem is non-convex in general. However, given a sum power constraint, a dual problem, which can be solved efficiently, exists. This dual problem can be solved by a low complexity algorithm based on fixed point iterations. Regarding the questions stated in Section 1.1. One question was: Can the duality for the unicast max–min beamforming problem in the single base station broadcast scenario be extended to a multicell scenario with multiple power constraints?

This thesis gives the answer to this question in Chapter 4. Based on the surrogate duality framework, the multiple power constraints are combined to a single weighted sum power constraint. The result is a virtual dual uplink max–min beamforming problem with an inner problem given by a weighted sum power constraint. This inner problem can be solved based on the given theory already developed for the broadcast scenario. The variables weighting the multiple power constraints in the weighted sum power constraints are optimized in an outer optimization. It should be highlighted that a formal proof for strong duality is presented. Consequently, the original non-convex max–min beamforming problem can be efficiently solved by its dual problem.

Based on this finding, Chapter 4 presents a fast converging low complexity algorithm which finds near optimal solutions for the weighting variables. In addition to the extension to multicell scenarios, this thesis presents also an improved solution for the inner loop. The literature mostly investigates the broadcast channel. The usage of instantaneous CSI is reasonable in this scenario. An advantage of this scenario is the closed form solution for the beamforming vectors if the dual uplink power is known. In multicell scenarios long-term CSI in the form of higher rank spatial correlation matrices is practically more relevant. The beamforming vectors are then given by an eigenvalue problem. Chapter 4 derives a simple low complexity algorithm to compute the beamformers iteratively. The algorithm has a significantly lower complexity than the conventional semidefinite relaxation based approach while it finds better solutions in several cases.

In addition to the duality theory another question of Chapter 4 regards the solution of the unicast max–min beamforming problem with general power constraints.

In the sum power constrained case, a balanced SINR can always be achieved. This is not given in multicell scenarios if users are decoupled from the network. Two cases are identified in Section 4.6.2 and an analytical proof is presented as well.

Another question regards the assignment of distributed antenna arrays to users along with beamforming. The question was: Does there exists a solution which jointly finds the optimal beamformers and the optimal assignment of antenna arrays to users? Remarkably, both problems can be solved jointly by a simple concatenation of the beamforming vectors of all jointly serving arrays.

As already illustrated in the introduction, a problem of max–min fairness is a decreased sum rate performance in some cases. One reason is interference due to beam collisions. The question arises whether such a situation can be avoided and if there exists a low complexity method maximizing the sum rate in a max–min fair system by a smart beam scheduling. Chapter 5 gives a simple mathematical formulation of the problem and proves its $\mathcal{NP}$-hardness by proving a close relationship to the multidimensional assignment problem. An optimal solution can only be obtained in the 2-cell case. However, multiple low complex methods achieving good solutions are proposed. The presented algorithms find local optimal solutions with a fair scheduling which means that each users inside a cell is scheduled equally often. In addition to the maximized sum rate, the beam scheduling algorithms should also consider the delays between two consecutive transmission to a user.[1] Although this problem is also proved to be $\mathcal{NP}$-hart, "good" local optimal solution can be found by a simple greedy approach.

Another reason for an impairment of the sum rate in max–min fair systems are strongly shadowed users. If a shadowed user is served with multiple other users and their SINR is balanced by max–min beamforming, a low SINR for all users can be the result. An avoidance of scheduling shadowed users could be an approach. Another option would be a weighting of these users to avoid a negative effect on the SINR for all other jointly scheduled users. However, then again an unfair system is the result. Chapter 6 proposes another approach: Relays can be used as cheap base stations to increase the coverage, especially, in not covered regions. Users which are originally shadowed by, e.g., high buildings can have a much better link to a closely located relay. These relays must be mounted on the roof-top of buildings to achieve a high SINR in the backhaul link. These shadowed users could have much better channel conditions to their serving relay. Consequently, SINR balancing among the active links will result in higher SINR compared to the situation without relays. However, practically relevant half duplex relays have a capacity loss because this type of relay cannot jointly receive and transmit. Consequently, two time slots are required. This so-called half-duplex loss is considered in the presented simple greedy algorithm. Users are only served by relays if the total (end-to-end) sum rate gains from this transmission. A finding was that the sum rate of the system can gain from half duplex relays if fairness among the users is desired. A system using relays can achieve a 20% higher sum rate than a system without relays if fairness is desired.

In a addition to this simple sum rate maximizing algorithm for max–min fair systems, a power saving approach for half duplex decode and forward relays was

[1] This delay is also-called inter-scheduling time

presented. If half duplex relays are used, the SINR of the two hops is decoupled.[2] Consequently, the SINR in the two hops can be balanced independently. If the SINR of relayed links of the second hop is larger than the SINR in the first hop, power (and therefore also energy) will be wasted. Due to the decode and forward transmission, the final rate is determined by the minimum SINR of both hops. Consequently, the SINR of the second hop can be limited to the SINR achieved in the first hop. The result is a reduced transmit power in the second hop. This idea is realized by a simple iterative algorithm which achieves in the presented scenario a 20% reduction of the transmit power at the expense of a small reduction of the sum rate.

The second part of the thesis considers multicast beamforming. Multicast beamforming has several applications in future wireless networks. The general form of the max–min multicast beamforming problem is $\mathcal{NP}$-hard. The question arises: Are there sub-problems which can be solved efficiently? Chapter 7 presents an equivalent quasi-convex form if long-term CSI in the form of Hermitian positive semidefinite Toeplitz matrices is used, which is a reasonable assumption if uniform linear arrays are used at the base stations. Furthermore, Chapter 7 presents an algorithm with superlinear convergence solving the equivalent convex form. The solution found by this new algorithm even finds higher balanced SINRs than the conventional semidefinite relaxation based solution. Consequently uniform linear arrays offer allow to implement efficient an near-optimal algorithms for the multicast problem.

Another question arises in this context: Does there exists a dual problem which can be solved efficiently? In the unicast case, duality offers an efficient solution which finds near optimal solutions. Chapter 7 shows that, similar to the unicast scenario, also in the multicast scenario a dual solution exists. However, strong duality is not given then. Based on the derived duality, Chapter 7 presents a new iterative solution for the multicast max–min beamforming problem with per-antenna array power constraints that finds better solutions than the conventional semidefinite relaxation based method. The derived duality has a broader scope because it holds for general CSI and is not limited to long-term CSI in the form of Hermitian positive semidefinite Toeplitz matrices.

In addition to broadcast applications, multicast beamforming is also useful in a unicast scenario. Max–min multicast beamforming offers a simple method to adapt the sector pattern based on long-term spatial correlation information. Chapter 8 presents this scheme. Due to the slow fluctuations of the beams, a low fluctuation of the SINR is possible. Hence, this scheme can be combined with channel aware scheduling schemes which offers an additional gain.

In Chapter 6, one-way relays are used for an improvement of the worst SINR among multiple users. This type of relays has the disadvantage of a capacity loss due to the one-way transmission. Our recent work [48] presents, therefore, a max–min fair precoding optimization for the bi-directional relay channel which overcomes this capacity loss. This optimization problem is closely related to the multicast beamforming problem and non-convex. A novel closed form of the upper bound of the max–min fair SINR was presented and based on this upper bound a novel low complexity algorithm is derived. Due to the combination of uplink and downlink, the capacity loss is avoided. Consequently, the presented optimization for the max–min

[2] The transmission of the first hop does not cause interference in the second hop.

fair bi-directional relay channel is a promising approach for future heterogeneous multicell systems, where, small base station can be implemented as bi-directional relay stations. An addition to the optimization of the relay station (small base station) precoding matrices, also the base station (serving base station) precoding matrices can be optimized to achieve a max–min fair SINR among the served users. The development of an alternating optimization for optimization of both precoding matrices is, therefore, promising for a future research.

This thesis investigates several technologies for a network-wide interference mitigation. The proposed algorithms can be applied centralized, at a central unit, or distributed at each base station. However, all algorithms require global knowledge of the long-term statistics of all links. An extension to isolated optimizations with instantaneous CSI of only a few links is a promising extension for future research. This thesis presents globally optimal approaches for an optimization based on global CSI knowledge. Future isolated or competitive approaches can be compared with the theory of a centralized optimization presented in this thesis.

Algorithms proposed in this thesis are derived with the assumption of base stations with small antenna arrays consisting of 4 to 8 antennas which is a reasonable assumption with present technology. However, progress in antenna technologies, in particular if higher carrier frequencies are used, can result in antenna arrays with a very large number of antennas. New effects are feasible in these so-called massive MISO systems [111]. Several studies investigate massive MISO only in a broadcast scenario or without cooperation [111]. In future networks, the cell size will shrink. Consequently, multiple small base stations transmit to a large number of users. In these scenarios, effects of massive MISO in combination with cooperative interference mitigation techniques, presented in this thesis, can offer new algorithms with very high spectral efficiency and less synchronization effort.

Appendix A

Appendix

A.1 Proof of Proposition 4

Proof. Let $\boldsymbol{\omega}_i = \sqrt{p_i}\mathbf{v}_i$ with $\|\mathbf{v}_i\| = 1$ $\forall i \in \mathcal{U}$ and introducing additional implicit constraints $p_i \geq 0$ $\forall i \in \mathcal{U}$ with dual variables $\xi_i \geq 0$ $\forall i \in \mathcal{U}$ composed to the vector $\boldsymbol{\xi}$. It is shown that the Lagrangian dual problem of (4.25) is (4.27). For fixed matrices $\mathbf{M}_i$ and the Lagrange multipliers α and $\boldsymbol{\lambda} = [\lambda_1, \ldots, \lambda_M]$, the Lagrangian of the problem (4.25) is given by:

$$L(\gamma, \mathbf{p}, \mathbf{V}, \boldsymbol{\lambda}, \alpha, \boldsymbol{\xi}) = \gamma - \alpha \left(\sum_{i \in \mathcal{U}} p_i \mathbf{v}_i^H \mathbf{M}_i \mathbf{v}_i - P \right) + \sum_{i \in \mathcal{U}} \xi_i p_i \tag{A.1}$$
$$- \sum_{i \in \mathcal{U}} \lambda_i \left[p_i \mathbf{v}_i^H (\frac{-\mathbf{R}_{i,i}}{\gamma}) \mathbf{v}_i + \sum_{l \in \mathcal{U}, l \neq i} p_l \mathbf{v}_l^H \mathbf{R}_{l,i} \mathbf{v}_l + 1 \right].$$

This Lagrangian can be rephrased as:

$$L(\gamma, \mathbf{p}, \mathbf{V}, \boldsymbol{\lambda}, \alpha, \boldsymbol{\xi}) = \gamma + \alpha P - \sum_{i \in \mathcal{U}} \lambda_i \tag{A.2}$$
$$+ \sum_{i \in \mathcal{U}} p_i \mathbf{v}_i^H \left[\frac{\lambda_i}{\gamma} \mathbf{R}_{i,i} - \alpha \mathbf{M}_i - \sum_{l \in \mathcal{U}, l \neq i} \lambda_l \mathbf{R}_{i,l} + \xi_i \right] \mathbf{v}_i.$$

With this Lagrangian, the dual function of this problem is:

$$l(\alpha, \boldsymbol{\lambda}, \boldsymbol{\xi}) = \sup_{\gamma, \mathbf{V} \in \mathcal{V}, \mathbf{p}} L(\gamma, \mathbf{p}, \mathbf{V}, \alpha, \boldsymbol{\lambda}, \boldsymbol{\xi}).$$

As in [159], since $\partial L(\gamma, \mathbf{p}, \mathbf{V}, \boldsymbol{\lambda}, \boldsymbol{\mu}, \boldsymbol{\xi}) / \partial p_i = 0$ at the optimum implies that

$$\mathbf{v}_i^H [\frac{\lambda_i}{\gamma} \mathbf{R}_{i,i} - \alpha \mathbf{M}_i - \sum_{l \in \mathcal{U}, l \neq i} \lambda_l \mathbf{R}_{i,l}] \mathbf{v}_i \leq 0,$$

which implies the constraint of the dual function. Hence, the Lagrangian dual problem can be stated as:

$$\gamma_I^L = \min_{\alpha, \boldsymbol{\lambda}} \max_{\gamma, \mathbf{V} \in \mathcal{V}} \gamma + \alpha P - \sum_{i \in \mathcal{U}} \lambda_i \tag{A.3}$$

$$\text{s.t.}\quad \mathbf{v}_i^H[\frac{\lambda_i}{\gamma}\mathbf{R}_{i,i} - \alpha\mathbf{M}_i - \sum_{l\in\mathcal{U},l\neq i}\lambda_l\mathbf{R}_{i,l}]\mathbf{v}_i \leq 0,$$
$$\alpha \geq 0,\ \lambda_i \geq 0,\ \forall\, i \in \mathcal{U}.$$

With the assumption that the SINR is balanced and if strong duality holds, and with $\mu_{i,a} \geq 0\ \forall i \in \mathcal{U}$, for a fixed $\boldsymbol{\mu}$, the same equivalent reformulations as in [57] can be made and the problem is finally given by:

$$\gamma_I^L = \min_{\alpha}\ \max_{\lambda,\gamma,\mathbf{V}\in\mathcal{V}}\ \gamma \tag{A.4}$$
$$\text{s.t.}\quad \gamma \leq \frac{\lambda_i\mathbf{v}_i^H\mathbf{R}_{i,i}\mathbf{v}_i}{\mathbf{v}_i^H(\alpha\mathbf{M}_i + \sum_{\substack{l\in\mathcal{U}\\ l\neq i}}\lambda_l\mathbf{R}_{i,l})\mathbf{v}_i},$$
$$\sum_{i\in\mathcal{U}}\lambda_i \leq P,\ 0 \leq \alpha \leq 1$$
$$\lambda_i \geq 0,\ \forall\, i \in \mathcal{U}.$$

Regarding the objective function of (A.4), the optimal value of the dual variable α is $\alpha^* = 1$ (upper bound) because it is aimed to maximize γ. Thus, the dual UL problem (4.27) is the result. We can restrict $\boldsymbol{\lambda}$ to $\boldsymbol{\lambda} > \mathbf{0}$ otherwise $\boldsymbol{\lambda} = \mathbf{0}$ results in $\gamma_I^L = 0$ which can not be an optimal solution. Furthermore, we can also restrict $\boldsymbol{\mu}$ to $\boldsymbol{\mu} \geq \mathbf{0}$ and $\boldsymbol{\mu} \neq \mathbf{0}$.

The proof of strong duality is an extension of [128, Lemma 2]. With $\boldsymbol{\omega}_i = \sqrt{p_i}\mathbf{v}_i$ the definition of the DL SINR in this thesis can be adapted to the definition in [128]:

$$\gamma_i^D = \frac{p_i\mathbf{v}_i^H\mathbf{R}_{i,i}\mathbf{v}_i}{\sum_{\substack{l\in\mathcal{U}\\ l\neq i}} p_l\mathbf{v}_l^H\mathbf{R}_{l,i}\mathbf{v}_l + 1}. \tag{A.5}$$

With

$$\begin{aligned}\sum_{i\in\mathcal{U}}\boldsymbol{\omega}_i^H\mathbf{M}_i\boldsymbol{\omega}_i &= \sum_{i\in\mathcal{U}} p_i\mathbf{v}_i^H\mathbf{M}_i\mathbf{v}_i\\ &= \sum_{i\in\mathcal{U}} p_i\,\mathrm{Tr}\{\mathbf{v}_i^H\mathbf{M}_i\mathbf{v}_i\}\\ &= \sum_{i\in\mathcal{U}} p_i\,\mathrm{Tr}\{\mathbf{M}_i\mathbf{v}_i\mathbf{v}_i^H\},\end{aligned}$$

the MBP with a weighted sum power is then equivalently given by:

$$\gamma^D = \gamma_I^L = \max_{\mathbf{V}\in\mathcal{V},\mathbf{p}}\ \min_{i\in\mathcal{U}}\gamma_i^D \tag{A.6}$$
$$\text{s.t.}\quad \sum_{i\in\mathcal{U}} p_i\,\mathrm{Tr}\{\mathbf{M}_i\mathbf{v}_i\mathbf{v}_i^H\} = P. \tag{A.7}$$

It has to be shown that for the same sum power the same SINR feasible region is the result. As in [128] with $\boldsymbol{D} = \operatorname{diag}(\frac{1}{\mathbf{v}_1^H \mathbf{R}_{1,1}\mathbf{v}_1}, \ldots, \frac{1}{\mathbf{v}_M^H \mathbf{R}_{M,M}\mathbf{v}_M})$ and $\mathbf{p} = [p_1, \ldots, p_M]$ and $\boldsymbol{\lambda} = [\lambda_1, \ldots, \lambda_M]$

$$[\boldsymbol{\Psi}]_{i,k} = \begin{cases} \mathbf{v}_k^H \mathbf{R}_{k,i} \mathbf{v}_k & k \neq i \\ 0 & k = i, \end{cases} \tag{A.8}$$

and $\mathbf{d}(\mathbf{V}, \boldsymbol{\mu}) = [\mathrm{Tr}\{\mathbf{M}_1 \mathbf{v}_1 \mathbf{v}_1^H\}, \ldots, \mathrm{Tr}\{\mathbf{M}_M \mathbf{v}_M \mathbf{v}_M^H\}]^T$ and for a balanced DL SINR $\gamma^D = \gamma$ the following set of equations for fixed $\mathbf{V}$ and $\mathbf{M}_i$ is the result:

$$\begin{aligned} &\frac{1}{\gamma}\mathbf{p} = \mathbf{D}\boldsymbol{\Psi}\mathbf{p} + \mathbf{D} \cdot \mathbf{1} \\ \Leftrightarrow &(\frac{1}{\gamma}\mathbf{D}^{-1} - \boldsymbol{\Psi})\mathbf{p} = \mathbf{1} \\ \Leftrightarrow &\mathbf{p} = (\frac{1}{\gamma}\mathbf{D}^{-1} - \boldsymbol{\Psi})^{-1}\mathbf{1}. \end{aligned} \tag{A.9}$$

We assume all $\mathbf{R}_{k,i}$ are positive definite. Hence, all links are interference coupled (see Section 4.6.2). The same holds for the balanced UL SINR $\gamma_I^L = \gamma$

$$\begin{aligned} &\frac{1}{\gamma}\boldsymbol{\lambda} = \mathbf{D}\boldsymbol{\Psi}^T\boldsymbol{\lambda} + \mathbf{D} \cdot \mathbf{d}(\mathbf{V}, \boldsymbol{\mu}) \\ \Leftrightarrow &(\frac{1}{\gamma}\mathbf{D}^{-1} - \boldsymbol{\Psi}^T)\boldsymbol{\lambda} = \mathbf{d}(\mathbf{V}, \boldsymbol{\mu}) \\ \Leftrightarrow &\boldsymbol{\lambda} = (\frac{1}{\gamma}\mathbf{D}^{-1} - \boldsymbol{\Psi}^T)^{-1}\mathbf{d}(\mathbf{V}, \boldsymbol{\mu}). \end{aligned} \tag{A.10}$$

In [12] and [10], the authors show that the spectral radius indicates the feasibility of the SINR constraints. Note, $\rho(\gamma\mathbf{D}\boldsymbol{\Psi}) < 1$, because the MBP is always feasible (4.25). The question is now whether for both problems (4.25) and (4.27), in the weighted sum power case the same sum power for the feasible SINR γ will be the result. With (A.10), the UL power of the UL MBP is given by:

$$\begin{aligned} \boldsymbol{\lambda}^T \cdot \mathbf{1} &= [(\frac{1}{\gamma}\mathbf{D}^{-1} - \boldsymbol{\Psi}^T)^{-1}\mathbf{d}(\mathbf{V}, \boldsymbol{\mu})]^T\mathbf{1} \qquad \text{(A.11)} \\ &= \mathbf{d}^T(\mathbf{V}, \boldsymbol{\mu})[(\frac{1}{\gamma}\mathbf{D}^{-1} - \boldsymbol{\Psi}^T)^{-1}]^T\mathbf{1} \\ &= \mathbf{d}^T(\mathbf{V}, \boldsymbol{\mu})[(\frac{1}{\gamma}\mathbf{D}^{-1} - \boldsymbol{\Psi}^T)^T]^{-1}\mathbf{1} \\ &= \mathbf{d}^T(\mathbf{V}, \boldsymbol{\mu}) \underbrace{(\frac{1}{\gamma}\mathbf{D}^{-1} - \boldsymbol{\Psi})^{-1}\mathbf{1}}_{=\mathbf{p}} \\ &= \mathbf{d}^T(\mathbf{V}, \boldsymbol{\mu})\mathbf{p}. \end{aligned}$$

Note in case of per BS power constraints we have $\mathbf{d}(\mathbf{V}, \boldsymbol{\mu}) = \boldsymbol{\mu}$. The last line is the weighted sum power constraint (A.7) of the DL MBP. Thus, the UL and DL MBP achieve the same SINR with the same total transmit power. Therefore, both problems have the same balanced SINR. □

A.2 Derivation of the Lagrangian Dual Problem in Proposition 8

Proof. Let $\boldsymbol{\omega}_i = \sqrt{p_i}\mathbf{v}_i$ with $\|\mathbf{v}_i\| = 1\ \forall i \in \mathcal{U}$ and introducing additional implicit constraints $p_i \geq 0\ \forall i \in \mathcal{U}$ with dual variables $\xi_i \geq 0\ \forall i \in \mathcal{U}$ composed to the vector $\boldsymbol{\xi}$. The Lagrangian of the primal problem (4.15) is given by

$$L(\gamma, \mathbf{p}, \mathbf{V}, \boldsymbol{\lambda}, \boldsymbol{\mu}, \boldsymbol{\xi}) = \gamma + \sum_{i\in\mathcal{U}} \mathrm{Tr}\{\mathbf{M}_i\mathbf{P}_i\} - \sum_{i\in\mathcal{U}} \lambda_i$$
$$+ \sum_{i\in\mathcal{U}} p_i \mathbf{v}_i^H [\frac{\lambda_i}{\gamma}\mathbf{R}_{i,i} - \mathbf{M}_i - \sum_{l\in\mathcal{U}, l\neq i} \lambda_l \mathbf{R}_{i,l} + \xi_i]\mathbf{v}_i.$$

The dual function of this problem is:

$$l(\boldsymbol{\lambda}, \boldsymbol{\mu}, \boldsymbol{\xi}) = \sup_{\gamma, \mathbf{p}, \mathbf{V}\in\mathcal{V}} L(\gamma, \mathbf{p}, \mathbf{V}, \boldsymbol{\lambda}, \boldsymbol{\mu}, \boldsymbol{\xi}).$$

As in [159], since $\partial L(\gamma, \mathbf{p}, \mathbf{V}, \boldsymbol{\lambda}, \boldsymbol{\mu}, \boldsymbol{\xi})/\partial p_i = 0$ at the optimum implies that

$$\mathbf{v}_i^H [\frac{\lambda_i}{\gamma}\mathbf{R}_{i,i} - \mathbf{M}_i - \sum_{l\in\mathcal{U}, l\neq i} \lambda_l \mathbf{R}_{i,l}]\mathbf{v}_i \leq 0,$$

from which the constraint of the dual function follows. Hence, the Lagrangian dual problem can be stated as:

$$\begin{aligned} \gamma^L = \min_{\boldsymbol{\lambda},\boldsymbol{\mu}} \max_{\gamma,\mathbf{V}\in\mathcal{V}} \ & \gamma + \sum_{i\in\mathcal{U}} \mathrm{Tr}\{\mathbf{M}_i\mathbf{P}_i\} - \sum_{i\in\mathcal{U}} \lambda_i \\ \text{s.t.} \ & \mathbf{v}_i^H[\mathbf{M}_i + \sum_{\substack{l\in\mathcal{U}\\ l\neq i}} \lambda_l \mathbf{R}_{i,l}]\mathbf{v}_i \geq \frac{\lambda_i}{\gamma}\mathbf{v}_i^H\mathbf{R}_{i,i}\mathbf{v}_i, \\ & \mathbf{M}_i \succcurlyeq 0,\ \lambda_i \geq 0,\ \forall\, i \in \mathcal{U}. \end{aligned}$$

With the definition of the new optimization variable χ and the additional constraint $\chi \geq \sum_{i\in\mathcal{U}} \lambda_i$, the problem can be rephrased to

$$\begin{aligned} \gamma^L = \max_{\chi} \min_{\boldsymbol{\lambda},\boldsymbol{\mu}} \max_{\gamma,\mathbf{V}\in\mathcal{V}} \ & \gamma + \sum_{i\in\mathcal{U}} \mathrm{Tr}\{\mathbf{M}_i\mathbf{P}_i\} - \chi \\ \text{s.t.} \ & \mathbf{v}_i^H[\mathbf{M}_i + \sum_{\substack{l\in\mathcal{U}\\ l\neq i}} \lambda_l \mathbf{R}_{i,l}]\mathbf{v}_i \geq \frac{\lambda_i}{\gamma}\mathbf{v}_i^H\mathbf{R}_{i,i}\mathbf{v}_i, \\ & \chi \geq \sum_{i\in\mathcal{U}} \lambda_i, \end{aligned} \tag{A.12}$$

$$\mathbf{M}_i \succcurlyeq 0,\ \lambda_i \geq 0,\ \forall\, i \in \mathcal{U}.$$

As in [159], using the additional variable substitutions $\chi = \chi' P$, $\mathbf{M}_i = \mathbf{M}_i'\chi'$, where $P = \sum_{i\in\mathcal{U}} \mathrm{Tr}\{\mathbf{M}_i'\mathbf{P}_i\}$ and $\lambda_i = \lambda_i'\chi'$ and considering χ' as the dual variable for the minimization over $\boldsymbol{\mu}'$, the following simplification of the problem (A.12) is given by:

$$\begin{aligned}\gamma^L = \min_{\boldsymbol{\lambda}',\boldsymbol{\mu}'} \max_{\gamma,\mathbf{V}\in\mathcal{V}} \ & \gamma \\ \text{s.t.}\ & \mathbf{v}_i^H[\mathbf{M}_i' + \sum_{\substack{l\in\mathcal{U}\\ l\neq i}} \lambda_l'\mathbf{R}_{i,l}]\mathbf{v}_i \geq \frac{\lambda_i'}{\gamma}\mathbf{v}_i^H\mathbf{R}_{i,i}\mathbf{v}_i, \\ & \sum_{i\in\mathcal{U}} \lambda_i' \leq \sum_{i\in\mathcal{U}} \mathrm{Tr}\{\mathbf{M}_i'\mathbf{P}_i\}, \\ & \mathbf{M}_i' \succcurlyeq 0\ , \lambda_i' \geq 0,\ \forall\, i \in \mathcal{U}.\end{aligned} \tag{A.13}$$

With the substitutions $\lambda_i = \lambda_i'$ and $\mathbf{M}_i = \mathbf{M}_i'$ and rearranging the first constraint in (A.13) [159], it can be rewritten as

$$\gamma \geq \frac{\lambda_i\mathbf{v}_i^H\mathbf{R}_{i,i}\mathbf{v}_i}{\mathbf{v}_i^H(\mathbf{M}_i + \sum_{\substack{l\in\mathcal{U}\\ l\neq i}} \lambda_l\mathbf{R}_{i,l})\mathbf{v}_i}. \tag{A.14}$$

With the assumption of a balanced SINR among all users, the first constraint is met with equality if the $\mathbf{M}_i$s and $\mathbf{V}$ are fixed [163]. Therefore, the reversal of the SINR constraints and the reversal of the minimization as a maximization over λ_i do not affect the optimal solution [163].

$$\begin{aligned}\gamma^L = \min_{\boldsymbol{\mu}} \max_{\boldsymbol{\lambda},\gamma,\mathbf{V}\in\mathcal{V}} \ & \gamma \\ \text{s.t.}\ & \gamma \leq \gamma_i^U(\boldsymbol{\mu},\boldsymbol{\lambda},\mathbf{v}_i) \\ & \mathbf{M}_i \succcurlyeq 0,\ \ \lambda_i \geq 0,\ \ \forall\, i \in \mathcal{U}, \\ & \sum_{i\in\mathcal{U}} \lambda_i \leq \sum_{i\in\mathcal{U}} \mathrm{Tr}\{\mathbf{M}_i\mathbf{P}_i\}.\end{aligned} \tag{A.15}$$

Replacing γ with the right hand side of the first constraints in (A.15), the optimization problem is formulated as in (4.42). □

A.3 Proof of Lemma 5

Proof. The proof is straightforward. First of all the minimum of two continuous functions $f_1(\boldsymbol{x})$, $f_2(\boldsymbol{x})$ is continuous,

$$\min(f_1(\boldsymbol{x}), f_2(\boldsymbol{x})) = \frac{1}{2}(f_1(\boldsymbol{x}) + f_2(\boldsymbol{x}) - \mid f_1(\boldsymbol{x}) - f_2(\boldsymbol{x}) \mid), \tag{A.16}$$

because the sum, difference, and absolute value of continuous functions are continuous. Hence, (4.20) can be proven to be continuous by a recursive definition

$$f(\mathbf{\Omega}) = \min\{\gamma_1(\mathbf{\Omega}), \min\{\gamma_2(\mathbf{\Omega}), \dots \min\{\gamma_{N-1}(\mathbf{\Omega}), \gamma_N(\mathbf{\Omega})\}\}. \quad \text{(A.17)}$$

The second part is to prove that each $\gamma_i(\mathbf{\Omega})$ is continuous. The $\gamma_i(\mathbf{\Omega})$ are obviously continuous. Because $\sum_{\substack{l\in\mathcal{U}\\ l\neq i}} \boldsymbol{\omega}_l^H \mathbf{R}_{l,i} \boldsymbol{\omega}_l + 1 > 0$, therefore, $\gamma_i(\mathbf{\Omega})$ has no definition gaps. Furthermore, the nominator and the denominator are polynomial functions and continuous. The fraction of two continuous functions is also continuous. □

A.4 Complexity Analysis

As in [57], the complexity of the inner loop can be summarized as follows:

- The complexity of the matrix $\mathbf{\Sigma}_i$ (4.43) is in the order of $\mathcal{O}(NN_A^2)$ [57].
- The computation of the inverse matrix $\mathbf{\Sigma}_i^{-1}$ is in the order of $\mathcal{O}(N_A^3)$.
- The matrix-matrix multiplication of the symmetric matrix $\mathbf{\Sigma}_i^{-1}\mathbf{R}_{i,i}$ has a complexity in the order of $\mathcal{O}(N_A^3)$.
- The matrix-vector multiplication $\mathbf{\Sigma}_i^{-1}\mathbf{R}_{i,i}\mathbf{v}_i$ has a complexity in the order of $\mathcal{O}(N_A^2)$.
- The normalization step $\|\mathbf{v}_i\| = 1$ has a low complexity compared to the other steps, therefore, it is ignored.
- The eigenvalue computation (4.46) consists of two vector-matrix-vector products. The complexity is in the order of $\mathcal{O}(N_A^2)$.

Consequently, the order total complexity of all these operations can be upper bounded by $\mathcal{O}(NN_A^3 + NN_A^2)$. These steps are made for each of the N users, hence, the order total complexity is $\mathcal{O}(N^2N_A^3 + N^2N_A^2)$. The downlink power computation has the following complexity:

- The computation of the matrix $\mathbf{D}^{-1}$ has a complexity in the order of $\mathcal{O}(NN_A^2)$ and the computation of $\mathbf{G}$ has a complexity in the order of $\mathcal{O}(N^2N_A^2)$ [57].
- The product $\frac{1}{\gamma}\mathbf{D}^{-1}$ has a complexity in the order of $\mathcal{O}(N)$.
- The matrix subtraction $\frac{1}{\gamma}\mathbf{D}^{-1} - \mathbf{\Psi}$ has a complexity in the order of $\mathcal{O}(N^2)$.
- The matrix-vector product $(\frac{1}{\gamma}\mathbf{D}^{-1} - \mathbf{\Psi})\mathbf{p}$ has a complexity in the order of $\mathcal{O}(N^2)$.

In total, the order downlink power computation can be upper bounded by $\mathcal{O}(2N^2N_A^2)$ flops. The complexity of the μ-SC method can be summarized as follows:

- The vector times a matrix times a vector-vector product in (4.49) has a complexity in the order of $\mathcal{O}(NN_A^2)$.

- The computation normalization factor ζ has a complexity in the order of $\mathcal{O}(N + NN_A)$. The normalization of the real valued matrices in (4.49) has a complexity in the order of $\mathcal{O}(NN_A)$.

Thus, the scaling step (4.49) can be upper bounded by $\mathcal{O}(N^2 N_A^2)$. These two steps (DL power computation and the scaling step) can be jointly upper bounded by $\mathcal{O}(N^3 N_A^2)$. Assuming the inner loop needs K_I iterations, the order of the total complexity for one outer iteration is now given by $\mathcal{O}(K_I N^2(N_A^3 + N_A^2) + N^2 N_A^2)$. Assuming the outer loop needs K_O iterations, the the order of total complexity is then given by

$$\mathcal{O}(K_O K_I N^2(N_A^3 + N_A^2) + K_O N^2 N_A^2).$$

The SDP (4.17) requires interior point methods for solving it. The complexity of a fast interior point method [69] can be approximated by $\mathcal{O}(n^{3.5}\log(1/\epsilon))$, where n is the total variable size [109]. In [90], the authors estimate the order of the complexity of the convex solver based feasibility check problem to $\mathcal{O}(\log(1/\epsilon)\sqrt{NN_A}(N^3 N_A^6 + N^2 N_A^2))$. Assuming there are K_O outer iterations needed by the bisection algorithm, the total complexity is in the order of $\mathcal{O}(K_O \log(1/\epsilon)\sqrt{NN_A}(N^3 N_A^6 + N^2 N_A^2))$.

A.5 Proof of Proposition 22

Let $\boldsymbol{\omega}_c = \sqrt{p_c}\mathbf{v}_c$ with $\|\mathbf{v}_c\| = 1 \; \forall c \in \mathcal{S}$ and introducing additional implicit constraints $p_c \geq 0 \; \forall c \in \mathcal{S}$ with dual variables $\xi_c \geq 0 \; \forall c \in \mathcal{S}$ composed to the vector $\boldsymbol{\xi}$. The Lagrangian of The Lagrangian of the primal problem (7.8) is formed with the knowledge that the DL SINR γ is positive and with the non-negative Lagrange multipliers $\boldsymbol{\lambda} = [\lambda_1, \ldots, \lambda_M]$ and β:

$$\begin{aligned} L(\gamma, \mathbf{V}, \mathbf{p}, \boldsymbol{\lambda}, \beta, \boldsymbol{\xi}) &= \gamma - \beta\Big(\sum_{c\in\mathcal{S}} p_c \mathbf{v}_c^H \mathbf{M}_c \mathbf{v}_c - P\Big) + \sum_{c\in\mathcal{S}} \xi_c p_c \\ &- \sum_{i\in\mathcal{U}} \lambda_i\Big(-\frac{p_{c(i)}\mathbf{v}_{c(i)}^H \mathbf{R}_{c(i),i}\mathbf{v}_{c(i)}}{\gamma} + \sum_{c\neq c(i)} p_c \mathbf{v}_c^H \mathbf{R}_{c,i}\mathbf{v}_c + 1\Big). \end{aligned} \tag{A.18}$$

This Lagrangian can be converted to:

$$\begin{aligned} L(\gamma, \mathbf{V}, \mathbf{p}, \boldsymbol{\lambda}, \beta, \boldsymbol{\xi}) &= \gamma - \beta\Big(\sum_{c\in\mathcal{S}} p_c \mathbf{v}_c^H \mathbf{M}_c \mathbf{v}_c - P\Big) + \sum_{c\in\mathcal{S}} \xi_c p_c \\ &+ \underbrace{\sum_{i\in\mathcal{U}} \frac{\lambda_i p_{c(i)}\mathbf{v}_{c(i)}^H \mathbf{R}_{c(i),i}\mathbf{v}_{c(i)}}{\gamma} - \sum_{c\neq c(i)} \lambda_i p_c \mathbf{v}_c^H \mathbf{R}_{c,i}\mathbf{v}_c}_{\Psi} - \sum_{i\in\mathcal{U}} \lambda_i. \end{aligned} \tag{A.19}$$

With

$$a_{c(i),i} = \frac{\lambda_i p_{c(i)}\mathbf{v}_{c(i)}^H \mathbf{R}_{c(i),i}\mathbf{v}_{c(i)}}{\gamma}, \tag{A.20}$$

$$b_{c,i} = -\lambda_i p_c \mathbf{v}_c^H \mathbf{R}_{c,i} \mathbf{v}_c, \tag{A.21}$$

the function Ψ is defined by:

$$\Psi = \sum_{i \in \mathcal{U}} a_{c(i),i} + \sum_{c \neq c(i)} b_{c,i} \tag{A.22}$$

This function can be rearranged as follows:

$$\Psi = \sum_{c \in \mathcal{S}} \sum_{i \in \mathcal{U}_c} a_{c,i} + \sum_{j \notin \mathcal{U}_c} b_{c,j}, \tag{A.23}$$

where $\mathcal{U}_c$ denotes the set of active users in cell c. With the definition of the set $\mathcal{U}_c$ of user served by BS c, the function Ψ can be rearranged to:

$$\Psi = \sum_{c \in \mathcal{S}} \sum_{i \in \mathcal{U}_c} \frac{\lambda_i p_c \mathbf{v}_c^H \mathbf{R}_{c,i} \mathbf{v}_c}{\gamma} - \sum_{j \notin \mathcal{U}_c} \lambda_j p_c \mathbf{v}_c^H \mathbf{R}_{c,j} \mathbf{v}_c. \tag{A.24}$$

With the rearranged Ψ, the Lagrangian is given by:

$$\begin{aligned} L(\gamma, \mathbf{V}, \mathbf{p}, \boldsymbol{\lambda}, \beta, \boldsymbol{\xi}) = \gamma - \beta\Big(\sum_{c \in \mathcal{S}} p_c \mathbf{v}_c^H \mathbf{M}_c \mathbf{v}_c - P\Big) + \sum_{c \in \mathcal{S}} \xi_c p_c \\ + \sum_{c \in \mathcal{S}} \sum_{i \in \mathcal{U}_c} \frac{\lambda_i p_c \mathbf{v}_c^H \mathbf{R}_{c,i} \mathbf{v}_c}{\gamma} - \sum_{j \notin \mathcal{U}_c} \lambda_j p_c \mathbf{v}_c^H \mathbf{R}_{c,j} \mathbf{v}_c - \sum_{i \in \mathcal{U}} \lambda_i \end{aligned} \tag{A.25}$$

and rearranged as follows:

$$\begin{aligned} L(\gamma, \mathbf{V}, \mathbf{p}, \boldsymbol{\lambda}, \beta, \boldsymbol{\xi}) = \gamma + \beta P - \sum_{i \in \mathcal{U}} \lambda_i - \beta \sum_{c \in \mathcal{S}} p_c \mathbf{v}_c^H \mathbf{M}_c \mathbf{v}_c + \sum_{c \in \mathcal{S}} \xi_c p_c \\ + \sum_{c \in \mathcal{S}} \sum_{i \in \mathcal{U}_c} \frac{\lambda_i p_c \mathbf{v}_c^H \mathbf{R}_{c,i} \mathbf{v}_c}{\gamma} - \sum_{j \notin \mathcal{U}_c} \lambda_j p_c \mathbf{v}_c^H \mathbf{R}_{c,j} \mathbf{v}_c. \end{aligned} \tag{A.26}$$

Now, there is a summation over c and a summation over fixed $\mathbf{v}_c$ and the beamforming vectors can be removed from the inner sums as follows:

$$\begin{aligned} L(\gamma, \mathbf{V}, \mathbf{p}, \boldsymbol{\lambda}, \beta, \boldsymbol{\xi}) = \gamma + \beta P - \sum_{i \in \mathcal{U}} \lambda_i \\ + \sum_{c \in \mathcal{S}} p_c \mathbf{v}_c^H \Big(-\beta \mathbf{M}_c + \sum_{i \in \mathcal{U}_c} \frac{\lambda_i \mathbf{R}_{c,i}}{\gamma} - \sum_{j \notin \mathcal{U}_c} \lambda_j \mathbf{R}_{c,j} + \xi_c\Big) \mathbf{v}_c. \end{aligned} \tag{A.27}$$

The dual function of this problem is:

$$l(\boldsymbol{\lambda}, \beta, \boldsymbol{\xi}) = \sup_{\gamma, \mathbf{V}, \mathbf{p}} L(\gamma, \mathbf{V}, \mathbf{p}, \boldsymbol{\lambda}, \beta). \tag{A.28}$$

As in [159], since $\partial L(\gamma, \mathbf{p}, \mathbf{V}, \boldsymbol{\lambda}, \beta, \boldsymbol{\xi})/\partial p_c = 0$ at the optimum implies that

$$\mathbf{v}_c^H(-\beta\mathbf{M}_c + \sum_{i\in\mathcal{U}_c}\frac{\lambda_i\mathbf{R}_{c,i}}{\gamma} - \sum_{j\notin\mathcal{U}_c}\lambda_j\mathbf{R}_{c,j})\mathbf{v}_c \leq 0 \tag{A.29}$$

which further implies the constraints of the dual function. Hence, the Lagrangian dual problem can be stated as:

$$\begin{aligned}\gamma_M^L = \min_{\boldsymbol{\lambda},\beta}\max_{\gamma,\mathbf{V}\in\mathcal{V}}\ & \gamma + \beta P - \sum_{i\in\mathcal{U}}\lambda_i \\ \text{s.t.}\ & \mathbf{v}_c^H(-\beta\mathbf{M}_c + \sum_{i\in\mathcal{U}_c}\frac{\lambda_i\mathbf{R}_{c,i}}{\gamma} - \sum_{j\notin\mathcal{U}_c}\lambda_j\mathbf{R}_{c,j})\mathbf{v}_c \leq 0, \\ & \beta \geq 0,\ \lambda_i \geq 0,\ \forall\, i\in\mathcal{U}.\end{aligned} \tag{A.30}$$

With the same mathematical reformulations as in Proof A.1, the problem can be simplified to:

$$\begin{aligned}\gamma_M^L = \min_{\boldsymbol{\lambda},\beta}\max_{\gamma,\mathbf{V}\in\mathcal{V}}\ & \gamma \\ \text{s.t.}\ & \gamma \geq \frac{\mathbf{v}_c^H(\sum_{i\in\mathcal{U}_c}\lambda_i\mathbf{R}_{c,i})\mathbf{v}_c}{\mathbf{v}_c^H(\beta\mathbf{M}_c + \sum_{j\notin\mathcal{U}_c}\lambda_j\mathbf{R}_{c,j})\mathbf{v}_c}, \\ & \lambda_i \geq 0,\ \forall\, i\in\mathcal{U}, \\ & \sum_{i\in\mathcal{U}}\lambda_i \leq P,\ 0\leq\beta\leq 1.\end{aligned} \tag{A.31}$$

Similar to [57], the optimal value of the dual variable β can be obtained by investigating the objective function of (A.31). The objective over β is the minimization over γ with regard to β. Therefore the optimal β should reach its upper bound, i.e., $\beta = 1$.

A.6 Proof of Theorem 9

Proof. This is a short outline of the proof presented in [119]. The technique is based on a factorization of the polynomial $X(z)$ based on its roots. The non-negative trigonometric polynomial $X(z) = \sum_{k=-n+1}^{n-1} x(k)z^{-k}$ is real valued. Hence, $x(-k) = x^*(k)$ and, therefore, $X^*(z) = X(\frac{1}{z^*})$ holds. If $X^*(z_k) = 0$, then also $X(\frac{1}{z_k^*}) = X^*(z_k) = 0$ holds. The polynomial $P(z) = z^{n-1}\, X(z)$ is of degree $2(n-1)$ and can be factorized as follows:

$$P(z) = A\prod_{k=1}^{n-1}(z - z_k)\prod_{k=1}^{n-1}(z\,z_k^* - 1)$$

where A is a constant. The original polynomial is then

$$X(z) = z^{-(n-1)} P(z) = A \prod_{k=1}^{n-1} (1 - z^{-1} z_k) \prod_{k=1}^{n-1} (z\, z_k^* - 1).$$

The equation $X(e^{j\phi}) = |W(e^{j\phi})|^2$ is satisfied due to

$$|1 - e^{j\phi} z_k| = |e^{j\phi} - z_k|$$

and

$$|e^{j\phi} z_k^* - 1| = |z_k^* - e^{-j\phi}| = |e^{j\phi} - z_k|.$$

□

List of Symbols

a	antenna index of an antenna array of a BS array
$\mathcal{B}_k^t$	set of active BSs in hop t of slot k
$b(r(i))$	index or a BS serving RS $r(i)$ serving user i
$\mathcal{B}_i$	set of BSs serving user i
c	cell or BS array index
$c(i)$	BS array $c(i)$ serving user i
ϵ	precision of an iterative algorithm
G	N-partite graph
$\mathbf{h}_{c,i}^H$	MISO channel vector
$\mathbf{h}_{l,i}^H$	channel vector between BS array serving user l and user i
i	user index
K	number of slots in the regarded scheduling interval
k	index of the slot (Chapters 6, 5, otherwise general index (integer value))
LCM	lowest common multiple
$l(\boldsymbol{\mu})$	Lagrangian dual function
M	number of users
$\mathbf{M}_i$	diagonal matrix with dual variables for user i
$\boldsymbol{\mu}$	dual variables
N	number of BS antenna arrays
N_A	number of antenna elements at each BS array

N_B	number of BS arrays
N_c	number of users in cell c
n_i	additive noise
N_R	number of RSs
$\mathbf{n}_{r(i)}$	noise vector the RS $r(i)$ serving user i receives
N_S	number of stations (BSs and RSs)
$\mathbf{\Omega}$	beamforming matrix consisting of all beamforming vectors
$\mathbf{\Omega}_k$	beamforming matrix consisting of all beamforming vectors in slot k
$\mathbf{\Omega}_k^t$	set of beamforming vectors in hop t of slot k
$\boldsymbol{\omega}_l$	beamforming vector from BS array serving user l
$\boldsymbol{\omega}_s^t$	beamforming vector of station s in hop t
P	sum power constraint
$\mathbf{P}_i$	diagonal matrix with power constraints on its main diagonal
P_l	per-BS antenna array power constraint of the array serving user l
$P_{l,a}$	per-antenna power constraint of antenna a at the array serving user l
$\mathcal{P}$	convex domain given by power constraints
$\mathbf{R}_{c,i}$	spatial correlation matrix
$\hat{\mathbf{R}}_{c,i}$	normalized spatial correlation matrix
$r(i)$	index or a RS serving user i
$\mathcal{R}_k$	set of active RSs in slot k
$s^D(\boldsymbol{\mu})$	surrogate dual function of the MBP in the DL domain
$\mathcal{S}$	set of BSs
σ_i^2	noise variance
$\mathcal{S}_k^t$	set of active stations (RSs and BSs) in hop t of slot k

$\mathbf{S}$	scheduling matrix containing the assignments of users to BS arrays and slots
$s(\boldsymbol{\mu})$	surrogate dual function
$s^{\mathrm{U}}(\boldsymbol{\mu})$	surrogate dual function of the MBP in the UL domain
t	index of the hop
$\mathcal{U}$	set of users
$\mathcal{U}_c$	set of currently active users distributed in cell c
$\mathcal{U}_{c,0}$	initial set of active users distributed in cell c
$\mathcal{U}_k$	set of active users in slot k
$\mathbf{W}$	cost matrix of assignment problems
$\mathcal{W}$	set of all beamforming matrices $\boldsymbol{\Omega}_k$, $\forall k = 1, \ldots, K$

List of Abbreviations

AMC	adaptive modulation and coding
BS	base station
BTSP	bottleneck traveling salesman problem
CAS	channel aware scheduling
CDF	cumulative distribution function
CDP	column-wise delay optimization problem
CoMP	cooperative multipoint
CQI	channel quality information
CSI	instantaneous channel state information
DAB	digital audio broadcasting
DL	downlink
DVB	digital video broadcasting
FAS	finite autocorrelation sequence
FDD	frequency division duplex
FDMA	frequency division multiple access
FFT	fast Fourier transformation
GPS	global positioning system
GS	greedy scheduling
GSM	Global System for Mobile Communications
HC	Hamiltonian cycle
LOS	line of sight
LP	linear program
LSAP	linear sum assignment problem
LTE	Long-Term Evolution
MAP	multidimensional assignment problem
MB	max–min beamforming
MBP	max–min beamforming problem

MISO	multiple input single output
MRC	maximum ratio combining
MS	mobile station
NLOS	non-LOS
OFDM	orthogonal frequency division multiplexing
ORRS	opportunistic Round Robin scheduling
PFS	proportional fair scheduling
PMP	power minimization problem
QCQP	quadratically constrained quadratic program
QFS	quasi fair scheduling
QoS	quality-of-service
RRS	random Round-Robin scheduling
RS	relay station
SDP	semidefinite program
SDR	semidefinite relaxation
SINR	signal-to-interference-plus-noise ratio
SNR	signal-to-noise ratio
SOCP	second order cone problem
SPA	sector pattern adaptation
TDD	time division duplex
TSP	traveling salesman problem
UL	uplink
ULA	uniform linear array
UMTS	Universal Mobile Telecommunications System

Index

Bibliography

[1] Y. I. Abramovich, N. K. Spencer, and A. Y. Gorokhov, "Detection-estimation of more uncorrelated Gaussian sources than sensors in nonuniform linear antenna arrays. Part II. partially augmentable arrays," *IEEE Transactions on Signal Processing*, vol. 51, no. 6, pp. 1492–1507, Jun. 2003.

[2] T. Ahmad, R. Gohary, H. Yanikomeroglu, S. Al-Ahmadi, and G. Boudreau, "Coordinated port selection and beam steering optimization in a multi-cell distributed antenna system using semidefinite relaxation," *IEEE Transactions on Wireless Communications*, vol. 11, no. 5, pp. 1861 –1871, May 2012.

[3] I. F. Akyildiz, D. M. Gutierrez-Estevez, and E. C. Reyes, "The evolution to 4G cellular systems: LTE-advanced," *Physical Communication*, Aug. 2010.

[4] B. Alkire and L. Vandenberghe, "Convex optimization problems involving finite autocorrelation sequences," *Mathematical Programming*, vol. 93, no. 3, pp. 331–359, Dec. 2002.

[5] A. Aspremont and S. Boyd. (2003) Relaxations and randomized methods for nonconvex QCQPs. [Online]. Available: www.stanford.edu/class/ee392o/relaxations.pdf

[6] H. K. Bang and T. Ekman, "Opportunistic round Robin with extended window for time correlated channels," in *65th IEEE Vehicular Technology Conference, (VTC Spring)*, Dublin, Irland, Apr. 2007, pp. 2860–2863.

[7] P. Bello, "Characterization of randomly time-variant linear channels," *IEEE Transactions on Signal Processing*, vol. 11, no. 4, pp. 360–393, Dec. 1963.

[8] M. Bengtsson, "Jointly optimal downlink beamforming and base station assignment," in *IEEE International Conference on Acoustics, Speech, and Signal Processing*, vol. 5, 2001, pp. 2961–2964.

[9] M. Bengtsson and B. Ottersten, "Optimum and suboptimum transmit beamforming," in *Handbook of Antennas in Wireless Communications*. Boca Raton, USA: CRC Press, 2002.

[10] H. Boche and M. Schubert, "A general duality theory for uplink and downlink beamforming," in *56th IEEE Vehicular Technology Conference, (VTC Fall)*, vol. 1, Vancouver, Canada, Sep. 2002, pp. 87–91.

[11] ——, "Optimal multi-user interference balancing using transmit beamforming," *Wireless Personal Communications*, vol. 26, no. 4, Sep. 2003.

[12] ——, *Duality theory for uplink downlink multiuser beamforming*, Smart Antennas-State of the Art ed., ser. EURASIP Book Series on Signal Processing and Communications. Hindawi Publishing Corporation, 2006.

[13] A. Bou Saleh, S. Redana, B. Raaf, T. Riihonen, J. Hamalainen, and R. Wichman, "Performance of amplify-and-forward and decode-and-forward relays in LTE-advanced," in *IEEE 70th Vehicular Technology Conference Fall (VTC-Fall)*, Anchorage, USA, Sep. 2009, pp. 1–5.

[14] G. Bournaka, K. Cumanan, S. Lambotharan, and F. Lazarakis, "An iterative semidefinite and geometric programming technique for the SINR balancing in two-way relay network," in *IEEE Global Telecommunications Conference (GLOBECOM 2011)*, Dec. 2011.

[15] S. Boyd and L. Vandenberghe, *Convex optimization*. Cambridge University Press, 2004.

[16] M. Brookes. (2009) The matrix reference manual. [Online]. Available: http://www.ee.ic.ac.uk/hp/staff/dmb/matrix/intro.html

[17] S. Brueck, L. Zhao, J. Giese, and M. A. Amin, "Centralized scheduling for joint transmission coordinated multi-point in LTE-advanced," in *International ITG Workshop on Smart Antennas (WSA)*, Beremen, Germany, Feb. 2010.

[18] R. Brukard, M. Dell'Amico, and S. Martello, *Assignment problems*. SIAM, Society for Industrial and Applied Mathematics, 2009.

[19] D. W. H. Cai, T. Q. S. Quek, and C. W. Tan, "A unified analysis of max-min weighted SINR for MIMO downlink system," *IEEE Transactions on Signal Processing*, vol. 59, no. 8, pp. 3850–3862, Aug. 2011.

[20] ——, "Max-min SINR coordinated multipoint downlink transmission-duality and algorithms," *IEEE Transactions on Signal Processing*, vol. 60, no. 10, pp. 5384 –5395, Oct. 2012.

[21] D. W. H. Cai, T. Q. S. Quek, C. W. Tan, and S. H. Low, "Max-min weighted SINR in coordinated multicell MIMO downlink," in *IEEE International Symposium on Modeling and Optimization in Mobile, Ad Hoc and Wireless Networks (WiOpt)*, Princeton, USA, May 2011, pp. 286–293.

[22] Y. Cao. (2008) Munkres' assignment algorithm. [Online]. Available: http://www.mathworks.com/matlabcentral/fileexchange/20328-munkres-assignment-algorithm

[23] W. K. Celmons, D. A. Grundel, and D. E. Jaeffcoat, "Applying simulated annealing to the multidimensional assignment problem," in *Theory and Algorithms for Cooperative Systems*. Series on Computers and Operations Research, vol. 4, pp. 45–61.

[24] T.-H. Chang, Z.-Q. Luo, and C.-Y. Chi, "Approximation bounds for semidefinite relaxation of max-min-fair multicast transmit beamforming problem," *IEEE Transactions on Signal Processing*, vol. 56, no. 8, pp. 3932–3943, Aug. 2008.

[25] M. Chen and A. Yener, "Multiuser two-way relaying: detection and interference management strategies," *IEEE Transactions on Wireless Communications*, vol. 8, no. 8, Aug. 2009.

[26] J. Choi and R. Heath, "Interpolation based transmit beamforming for MIMO-OFDM with limited feedback," *IEEE Transactions on Signal Processing*, vol. 53, no. 11, pp. 4125–4135, Nov. 2005.

[27] T. Cover and A. E. Gamal, "Capacity theorems for the relay channel," *IEEE Transactions on Information Theory*, vol. 25, no. 5, pp. 572–584, Sep. 1979.

[28] J. P. Crouzeix and J. A. Ferland, "Algorithms for generalized fractional programming," *Mathematical Programming*, vol. 52, pp. 191–207, 1991.

[29] J. P. Crouzeix, J. A. Ferland, and S. Schaible, "An algorithm for generalized fractional programs," *Journal of Optimization Theory and Applications*, vol. 47, no. 1, pp. 35–49, Sep. 1985.

[30] ——, "A note on an algorithm for generalized fractional programs," *Journal of Optimization Theory and Applications*, vol. 50, no. 1, pp. 183–187, Jul. 1986.

[31] H. Dahrouj and W. Yu, "Coordinated beamforming for the multicell multi-antenna wireless system," *IEEE Transactions on Wireless Communications*, vol. 9, no. 5, pp. 1748–1759, May 2010.

[32] G. Dartmann, W. Afzal, X. Gong, and G. Ascheid, "Low complexity cooperative downlink beamforming in multiuser multicell networks," in *12th IEEE International Conference on Communication Technology, (ICCT)*, Nanjing, China, Nov. 2010.

[33] ——, "Joint optimization of beamforming, user scheduling, and multiple base station assignment in a multicell network," in *IEEE Wireless Communications and Networking Conference, (WCNC)*, Quintana Roo, Mexico, Mar. 2011, pp. 209–214.

[34] ——, "Low complexity cooperative multicast beamforming in multiuser multicell downlink networks," in *6th IEEE International ICST Conference on Cognitive Radio Oriented Wireless Networks*, Osaka, Japan, Jun. 2011, pp. 370–374.

[35] G. Dartmann and G. Ascheid, "Equivalent quasi-convex form of the multicast max–min beamforming problem," *IEEE Transactions on Vehicular Technology*, 2013, accepted for publication.

[36] G. Dartmann and X. Gong, "Dynamically scheduling connections of mobile stations in neighbouring cells in a mobile telecommunication network," *European Patent No. EP2337418*, Jun. 2011.

[37] G. Dartmann, X. Gong, W. Afzal, and G. Ascheid, "On the duality of the max-min beamforming problem with per antenna and per antenna array power constraints," *IEEE Transactions on Vehicular Technology*, vol. 62, no. 2, pp. 606 –619, Feb. 2013.

[38] G. Dartmann, X. Gong, and G. Ascheid, "Cooperative beamforming with multiple base station assignment based on correlation knowledge," in *72nd IEEE Vehicular Technology Conference, (VTC Fall)*, Ottawa, Canada, Sep. 2010.

[39] ——, "Jointly optimized transmit beamforming and temporal user scheduling in multiuser multicell scenarios based on correlation knowledge," in *IEEE Sarnoff Symposium*, Princeton, USA, Apr. 2010, pp. 1–5.

[40] ——, "Max-min beamforming with cooperative multipoint transmission," in *74th IEEE Vehicular Technology Conference, (VTC Fall)*, San Francisco, USA, Sep. 2011.

[41] ——, "On the pareto optimum of long-term max-min beamforming with general power constraints," in *IEEE Sarnoff Symposium*, Newark, USA, May 2012, pp. 1–5.

[42] ——, "Application of graph theory to the multicell beam scheduling problem," *IEEE Transactions on Vehicular Technology*, vol. 62, no. 4, May 2013.

[43] ——, “Low complexity cooperative multicast beamforming in heterogeneous networks,” in *77th IEEE Vehicular Technology Conference, (VTC Spring)*, Dresden, Germany, May 2013, accepted for publication.

[44] G. Dartmann, M. Jordan, X. Gong, and G. Ascheid, “Intercell interference mitigation with long-term beamforming and low SINR feedback rate in a multiuser multicell unicast scenario,” in *69th IEEE Vehicular Technology Conference, (VTC Spring)*, Barcelona, Spain, Apr. 2009.

[45] ——, “Jointly optimized beamforming in multicell scenarios based on correlation knowledge,” in *ITG-Fachtagung Mobilkommunikation*, Osnabrück, Germany, May 2009.

[46] G. Dartmann, D. K. Shah, X. Gong, and G. Ascheid, “Beamforming with relays in multicell networks based on correlation knowledge,” in *IEEE GLOBECOM Workshops (GC Workshops)*, Houston, USA, Dec. 2011, pp. 470–474.

[47] ——, “Beamforming with relays in heterogeneous networks based on correlation knowledge,” in *14th IEEE International Conference on Communication Technology, (ICCT)*, Chengdu, China, Nov. 2012.

[48] G. Dartmann, E. Zandi, and G. Ascheid, “A modified levenberg-marquardt method for the bidirectional relay channel,” *IEEE Transactions on Vehicular Technology*, 2013, submitted.

[49] ETSI, “Radio broadcast systems; digital audio broadcasting (DAB) to mobile, portable and fxed receivers, ETSI document draft prevision ets 300 401,” Mar. 1994.

[50] ——, “Digital video broadcasting (DVB); framing structure channel coding and modulation for digital terrestrial television, ETSI document final draft for ets 300 744,” Nov. 1996.

[51] D. V. P. Figueiredo, M. I. Rahman, N. Marchetti, F. H. P. Fitzek, M. D. Katz, Y. Cho, and R. Prasad, “Transmit diversity vs beamforming for multi-user OFDM systems,” in *7th International Symposium on Wireless Personal Multimedia Communications*, Abano Terme, Italy, Sep. 2004.

[52] A. Forenza and R. W. Heath Jr., “Impact of antenna geometry on MIMO communication in indoor clustered channels,” in *IEEE Antennas and Propagation Society International Symposium, 2004*, vol. 2, Monterey, USA, Jun. 2004, pp. 1700–1703.

[53] B. Friedlander and A. J. Weiss, “Direction finding in the presence of mutual coupling,” *IEEE Transactions on Antennas and Propagation*, vol. 39, no. 3, pp. 273–284, Mar. 1991.

[54] A. B. Gershman, N. D. Sidiropoulos, S. Shahbazpanahi, M. Bengtsson, and B. Ottersten, “Convex optimization-based beamforming,” *IEEE Signal Processing Magazine*, vol. 27, no. 3, pp. 62–75, May 2010.

[55] A. J. Goldsmith and S. G. Chua, “Variable-rate variable-power MQAM for fading channels,” *IEEE Transactions on Communications*, vol. 45, no. 10, pp. 1218–1230, Oct. 1997.

[56] G. H. Golub and C. F. van Loan, *Matrix computations*. The Johns Hopkins University Press, 1996.

[57] X. Gong, M. Jordan, G. Dartmann, and G. Ascheid, "Max-min beamforming for multicell downlink systems using long-term channel statistics," in *20th IEEE International Symposium on Personal, Indoor and Mobile Radio Communications*, Tokio,Japan, Sep. 2009, pp. 803–807.

[58] S. Grandhi and J. Zander, "Constrained power control in cellular radio systems," in *44th IEEE Vehicular Technology Conference*, 1994, pp. 824–828.

[59] M. Grant and S. Boyd, "CVX: Matlab software for disciplined convex programming, version 2.0 beta," http://cvxr.com/cvx, Sep. 2013.

[60] H. J. Greenberg and W. P. Pierskalla, "Surrogate mathematical programming," *Operations Research*, vol. 18, no. 5, pp. 924–93, Sep. 1970.

[61] D. A. Grundel, P. A. Krokhmal, C. A. S. Oliveira, and P. M. Pardalos, "On the number of local minima for the multidimensional assignment problem," *Journal of Combinatorial Optimization, Springer*, vol. 13, no. 1, pp. 1–18, Jan. 2007.

[62] G. Gutin and D. Karapetyan, "Local search heuristics for the multidimensional assignment problem," *Graph Theory, Computational Intelligence and Thought, Springer*, vol. 5420/2009, pp. 100–115, 2009.

[63] G. Gutin and A. Punnen, *The traveling salesman problem and its variations*. Kluwer Academic Publishers, 2002.

[64] D. Hammarwall, M. Bengtsson, and B. Ottersten, "On downlink beamforming with indefinite shaping constraints," *IEEE Transactions on Signal Processing*, vol. 54, no. 9, pp. 3566–3580, Sep. 2006.

[65] Y. Han, S. H. Ting, C. K. Ho, and W. H. Chin, "Performance bounds for two-way amplify-and-forward relaying," *IEEE Transactions on Wireless Communications*, vol. 8, no. 1, pp. 432–439, Jan. 2009.

[66] Y. Hara, L. Brunel, and K. Oshima, "Spatial scheduling with interference cancellation in multiuser MIMO systems," *IEEE Transactions on Vehicular Technology*, vol. 57, no. 2, pp. 893 –905, Mar. 2008.

[67] V. Havary-Nassab, S. ShahbazPanahi, and A. Grami, "Optimal distributed beamforming for two-way relay networks," *IEEE Transactions on Signal Processing*, vol. 58, no. 3, pp. 1238 –1250, Mar. 2010.

[68] V. Havary-Nassab, S. Shahbazpanahi, A. Grami, and Z.-Q. Luo, "Distributed beamforming for relay networks based on second-order statistics of the channel state information," *IEEE Transactions on Signal Processing*, vol. 56, no. 9, pp. 4306–4316, Sep. 2008.

[69] C. Helmberg, F. Rendl, R. Vanderbei, and H. Wolkowicz, "An interior-point method for semidefinite programming,," *SIAM Journal on Optimization*, vol. 6, no. 2, pp. 342–361, May 1996.

[70] R. A. Horn and C. R. Johnson, *Matrix analysis*. Cambridge University Press, Feb. 1990.

[71] P. Hosein, "Cooperative scheduling of downlink beam transmissions in a cellular network," in *IEEE GLOBECOM Workshops (GC Workshops)*, New Orleans, USA, Dec. 2008, pp. 1–5.

[72] P. Hosein and C. van Rensburg, "On the performance of downlink beamforming with synchronized beam cycles," in *69th IEEE Vehicular Technology Conference, (VTC Spring)*, Barcelona, Spain, Apr. 2009.

[73] J. Hromkovic and W. M. Oliva, *Algorithmics for Hard Problems*, 2nd ed. Secaucus, NJ, USA: Springer-Verlag New York, Inc., 2002.

[74] K. Hugl, J. Laurila, and E. Bonek, "Downlink beamforming for frequency division duplex systems," in *IEEE Global Telecommunications Conference, (GLOBECOM)*, vol. 4, Rio de Janeiro, Brazil, Dec. 1999, pp. 2097–2101.

[75] R. Irmer, H. Droste, P. Marsch, M. Grieger, G. Fettweis, S. Brueck, H.-P. Mayer, L. Thiele, and V. Jungnickel, "Coordinated multipoint: Concepts, performance, and field trial results," *IEEE Communications Magazine*, vol. 49, no. 2, pp. 102–111, Feb. 2011.

[76] A. Ispas, C. Schneider, G. Dartmann, X. Gong, G. Ascheid, and R. Thoma, "Analysis of mismatched downlink beamforming over non-stationary channels with interference," in *General Assembly and Scientific Symposium, 2011 XXXth URSI*, Istanbul, Turkey, Aug. 2011, pp. 1–4.

[77] H. W. Je, H. Lee, K. Kwak, S. Choi, Y.-J. Hong, and B. Clerckx, "Long-term channel information-based CoMP beamforming in LTE-advanced systems," in *IEEE Global Telecommunications Conference, (GLOBECOM)*, Houston, USA, Dec. 2011, pp. 1–6.

[78] Y. Jing and S. ShahbazPanahi, "Max-min optimal joint power control and distributed beamforming for two-way relay networks under per-node power constraints," *IEEE Transactions on Signal Processing*, vol. 60, no. 12, pp. 6576 –6589, Dec. 2012.

[79] M. Jordan, "Downlink beamforming for multiuser systems with incomplete feedback," Ph.D. dissertation, Fak. für Elektrotechnik und Informationstechnik, Rheinisch-Westf. Technische Hochschule Aachen (RWTH), Apr. 2011.

[80] M. Jordan, A. Dimofte, X. Gong, and G. Ascheid, "Conversion from uplink to downlink spatio-temporal correlation with cubic splines," in *69th IEEE Vehicular Technology Conference, (VTC Spring)*, Barcelona, Spain, Apr. 2009, pp. 1–5.

[81] M. Jordan, X. Gong, and G. Ascheid, "Conversion of the spatio-temporal correlation from uplink to downlink in FDD systems," in *IEEE Wireless Communications and Networking Conference, (WCNC)*, Budapest, Hungary, Apr. 2009, pp. 1–6.

[82] ——, "Multicell multicast beamforming with delayed SNR feedback," in *IEEE Global Telecommunications Conference, (GLOBECOM)*, Dec. 2009, pp. 1–6.

[83] M. Jordan, M. Senst, G. Ascheid, and H. Meyr, "Long-term beamforming in single frequency networks using semidefinite relaxation," in *67th IEEE Vehicular Technology Conference, (VTC Spring)*, Marina Bay, Singapore, May 2008, pp. 275–279.

[84] E. Jorswieck, E. Larsson, and D. Danev, "Complete characterization of the pareto boundary for the MISO interference channel," vol. 56, no. 10, pp. 5292–5296, Oct. 2008.

[85] V. Jungnickel, L. Thiele, T. Wirth, T. Haustein, S. Schiffermuller, A. Forck, S. Wahls, S. Jaeckel, S. Schubert, H. Gabler, C. Juchems, F. Luhn, R. Zavrtak, H. Droste, G. Kadel, W. Kreher, J. Mueller, W. Stoermer, and G. Wannemacher, "Coordinated multipoint trials in the downlink," in *IEEE GLOBECOM Workshops (GC Workshops)*, Honolulu, USA, Dec. 2009, pp. 1–7.

[86] V. Jungnickel, T. Wirth, M. Schellmann, T. Haustein, and W. Zirwas, "Synchronization of cooperative base stations," in *5th IEEE International Symposium on Wireless Communication Systems (ISWCS)*, Reykjavik, Iceland, Oct. 2008, pp. 329–334.

[87] E. Karipidis, N. D. Sidiropoulos, and Z.-Q. Luo, "Transmit beamforming to multiple co-channel multicast groups," in *1st IEEE International Workshop on Computational Advances in Multi-Sensor Adaptive Processing*, Puerto Vallarta, Mexico, Dec. 2005, pp. 109–112.

[88] ——, "Convex transmit beamforming for downlink multicasting to multiple co-channel groups," in *IEEE International Conference on Acoustics, Speech and Signal Processing, ICASSP*, vol. 5, Toulouse, France, May 2006, pp. 973–976.

[89] ——, "Far-field multicast beamforming for uniform linear antenna arrays," *IEEE Transactions on Signal Processing*, vol. 55, no. 10, pp. 4916–4927, Oct. 2007.

[90] ——, "Quality of service and max-min fair transmit beamforming to multiple cochannel multicast groups," *IEEE Transactions on Signal Processing*, vol. 56, no. 3, pp. 1268–1279, 2008.

[91] R. M. Karp, "Reducibility among combinatorial problems," in *Complexity of Computer Computations*. Plenum Press, New York, 1972, pp. 85–103.

[92] B. Klinz and G. J. Woeginger, "A new efficiently solvable special case of the three-dimensional axial bottleneck assignment problem," ser. Lecture Notes in Computer Science. Springer, 1995, pp. 150–162.

[93] M. Kobayashi and G. Caire, "Joint beamforming and scheduling for a multi-antenna downlink with imperfect transmitter channel knowledge," *IEEE Journal on Selected Areas in Communications*, vol. 25, no. 7, pp. 1468 –1477, Sep. 2007.

[94] U. Krause, "Concave perron-frobenius theory and applications," *Nonlinear Analysis, (TMA)*, vol. 47, pp. 1457–1466, Aug. 2004.

[95] H. W. Kuhn, "The hungarian method for the assignment problem," *Naval Research Logistics Quaterly 20*, pp. 83–97, 1955.

[96] T. Kuze, "Analogue beamforming," *IEEE 802.16 Broadband Wireless Access Working Group, Contribution No. IEEE C802.16m-08/438*, May 2007.

[97] Kyösti, et al. (2007, Sep.) IST-WINNER D1.1.2 P., WINNER II channel models, ver 1.1. [Online]. Available: https://www.ist-winner.org/WINNER2-Deliverables/D1.1.2v1.1.pdf

[98] L. Hentilä, P. Kyösti, M. Käske, M. Narandzic , and M. Alatossava. (2007, Dec.) MATLAB implementation of the WINNER Phase II Channel Model ver 1.1 . [Online]. Available: http://www.ist-winner.org/phase_2_model.html

[99] J. N. Laneman, D. N. C. Tse, and G. W. Wornell, "Cooperative diversity in wireless networks: Efficient protocols and outage behavior," *IEEE Transactions on Information Theory*, vol. 50, no. 12, pp. 3062–3080, Dec. 2004.

[100] E. L. Lawler, "Combinatorical optimization: networks and matroids." Holt Rinehart and Winston, New York, 1976.

[101] D. Li and X. Sun, "Nonlinear integer programming," in *International Series in Operations Research & Management Science*. Springer, 2006, vol. 84.

[102] J. Li, H. Zhang, X. Xu, X. Tao, T. Svensson, C. Botella, and B. Liu, "A novel frequency reuse scheme for coordinated multi-point transmission," in *71nd IEEE Vehicular Technology Conference, (VTC Spring)*, Taipei, Taiwan, May 2010, pp. 1–5.

[103] J. Li, Y. Xie, P. Stoica, X. Zheng, and J. Ward, "Beampattern synthesis via a matrix approach for signal power estimation," *IEEE Transactions on Signal Processing*, vol. 55, no. 12, pp. 5643–5657, 2007.

[104] Y.-C. Liang and F. P. S. Chin, "Downlink channel covariance matrix (DCCM) estimation and its applications in wireless DS-CDMA systems," *IEEE Journal on Selected Areas in Communications*, vol. 19, no. 2, pp. 222–232, Feb. 2001.

[105] L. Liu and H. Jafarkhani, "Novel successive transmit beamforming algorithms for MISO-OFDM systems," in *IEEE International Conference on Communications (ICC)*, vol. 12, Istanbul, Turkey, Jun. 2006, pp. 5336–5341.

[106] M. J. Lopez, "Multiplexing, scheduling, and multicasting strategies for antenna arrays in wirelss networks," Ph.D. dissertation, Department of Electrical Engineering and Computer Science, MIT, Cambridge, MA, Aug. 2002.

[107] D. G. Luenberger, "Quasi-convex programming," *SIAM Journal of Applied Mathematics*, vol. 16, no. 5, pp. 1090–1095, Sep. 1968.

[108] ——, *Optimization by Vector Space Methods*, 1st ed. New York, NY, USA: John Wiley & Sons, Inc., 1997.

[109] Z.-Q. Luo, W.-K. Ma, A. M.-C. So, Y. Ye, and S. Zhang, "Semidefinite relaxation of quadratic optimization problems," *IEEE Signal Processing Magazine, IEEE*, vol. 27, no. 3, pp. 20–34, May 2010.

[110] P. Marsch and G. Fettweis, in *7th International ITG Conference on Source and Channel Coding (SCC)*.

[111] T. Marzetta, "Noncooperative cellular wireless with unlimited numbers of base station antennas," *IEEE Transactions on Wireless Communications*, vol. 9, no. 11, pp. 3590 –3600, Nov. 2010.

[112] R. Mathar and J. Mattfeldt, "Channel assignment in cellular radio networks," *IEEE Transactions on Vehicular Technology*, vol. 42, no. 4, pp. 647 –656, Nov. 1993.

[113] H. Matsuoka and H. Shoki, "Comparison of pre-FFT and post-FFT processing adaptive arrays for OFDM systems in the presence of co-channel interference," in *14th IEEE Proceedings on Personal, Indoor and Mobile Radio Communications (PIMRC) 2003*, Sep. 2003.

[114] A. Molisch, L. Greenstein, and M. Shafi, "Propagation issues for cognitive radio," *Proceedings of the IEEE*, vol. 97, no. 5, pp. 787–804, 2009.

[115] J. Munkres, "Algorithms for the assignment and transportation problems," *SIAM Journal of Applied Mathematics*, vol. 5, no. 1, pp. 105–113, 1957.

[116] F. Negro, M. Cardone, I. Ghauri, and D. T. M. Slock, "SINR balancing and beamforming for the MISO interference channel," in *22nd IEEE International Symposium on Personal, Indoor and Mobile Radio Communications*, Toronto, Canada, Sep. 2011, pp. 1552–1556.

[117] T. Nieuwenhuizen, "Johri's general dual, the lagrangian dual, and the surrogate dual," *European Journal of Operational Research*, vol. 117, no. 1, pp. 183–196, Aug. 1999.

[118] T. J. Oechtering, C. Schnurr, I. Bjelakovic, and H. Boche, "Broadcast capacity region of two-phase bidirectional relaying," *IEEE Transactions on Information Theory*, vol. 54, no. 1, pp. 454–458, Jan. 2008.

[119] A. Papoulis, *Signal Analysis*. McGraw-Hill, New York, May 1977.

[120] K. I. Pedersen, P. E. Mogensen, and B. H. Fleury, "Spatial channel characteristics in outdoor environments and their impact on BS antenna system performance," in *48th IEEE Vehicular Technology Conference, (VTC 98)*, vol. 2, Ottawa, Canada, May 1998, pp. 719–723.

[121] S. W. Peters, A. Y. Panah, K. T. Truong, and R. W. Heath, "Relay architectures for 3GPP LTE-advanced," *EURASIP Journal on Wireless Communications and Networking*, vol. 2009, Jul. 2009.

[122] W. Pierskalla, "The multidimensional assignment problem," *Opeartions Research*, vol. 16, pp. 422–431, 1968.

[123] PlanetMath.org. (2012) Isomorphism of rings of real and complex matrices. [Online]. Available: http://planetmath.org

[124] R. D. Preuss and D. R. Brown, "Two-way synchronization for coordinated multicell retrodirective downlink beamforming," *IEEE Transactions on Signal Processing*, vol. 59, no. 11, pp. 5415–5427, Nov. 2011.

[125] F. Rashid-Farrokhi, K. J. R. Liu, and L. Tassiulas, "Transmit beamforming and power control for cellular wireless systems," *IEEE Journal on Selected Areas in Communications*, vol. 16, no. 8, pp. 1437–1450, Oct. 1998.

[126] M. Sandell, "Design and analysis of estimators for multicarrier modulation and ultrasonic imaging," Ph.D. dissertation, Division of Signal Processing, Lulea University of Technology, Sep. 1996.

[127] A. Schad and M. Pesavento, "Multiuser bi-directional communications in cooperative relay networks," in *4th IEEE International Workshop on Computational Advances in Multi-Sensor Adaptive Processing (CAMSAP)*, 2011, pp. 217–220.

[128] M. Schubert and H. Boche, "Solution of the multiuser downlink beamforming problem with individual SINR constraints," *IEEE Transactions on Vehicular Technology*, vol. 53, no. 1, pp. 18–28, Jan. 2004.

[129] ——, "QoS-based resource allocation and transceiver optimization," *Foundations and Trends in Communications and Information Theory*, vol. 2, no. 6, 2005.

[130] M. Schubert, N. Vucic, and H. Boche, "SIR balancing for strongly connected interference networks-existence and uniqueness of a solution," in *7th IEEE International Symposium on Wireless Communication Systems (ISWCS)*, York, UK, Sep. 2010, pp. 184–188.

[131] S. Shahbazpanahi and M. Dong, "A semi-closed-form solution to optimal distributed beamforming for two-way relay networks," *IEEE Transactions on Signal Processing*, vol. 60, no. 3, pp. 1511 –1516, Mar. 2012.

[132] A. K. Shaw, S. Pokala, and R. Kumaresan, "Toeplitz and Hankel matrix approximation using structured approach," in *Proceedings of the 1998 IEEE International Conference on Acoustics, Speech and Signal Processing, ICASSP*, Seattle, USA, May 1998.

[133] N. D. Sidiropoulos and T. N. Davidson, "Broadcasting with channel state information," in *Sensor Array and Multichannel Signal Processing Workshop Proceedings*, Barcelona, Spain, Jul. 2004, pp. 489–493.

[134] N. D. Sidiropoulos, T. N. Davidson, and Z.-Q. Luo, "Transmit beamforming for physical-layer multicasting," *IEEE Transactions on Signal Processing*, vol. 54, no. 6, pp. 2239–2251, Jun. 2006.

[135] Y. C. B. Silva and A. Klein, "Downlink beamforming and sinr balancing for the simultaneous provision of unicast/multicast services," in *16th IEEE Mobile and Wireless Communications Summit, (IST)*, Budapest, Hungary, Jul. 2007, pp. 1–5.

[136] ——, "Linear transmit beamforming techniques for the multigroup multicast scenario," *IEEE Transactions on Vehicular Technology*, vol. 58, no. 8, pp. 4353–4367, Oct. 2009.

[137] B. Song, R. L. Cruz, and B. D. Rao, "Network duality and its application to multi-user mimo wireless networks with sinr constraints," in *IEEE International Conference on Communications, (ICC)*, Seoul, Korea, May 2005, pp. 2684–2689.

[138] G. L. Stuber, J. R. Barry, S. W. McLaughlin, Y. Li, M. A. Ingram, and T. G. Pratt, "Broadband MIMO-OFDM wireless communications," *Proceedings of the IEEE*, vol. 92, no. 2, pp. 271–294, Feb. 2004.

[139] J. F. Sturm. (2009) Using sedumi 1.21, a matlab toolbox for optimization over symmetric cones. [Online]. Available: http://sedumi.ie.lehigh.edu/

[140] Y. Sun and K. J. R. Liu, "Transmit diversity techniques for multicasting over wireless networks," in *IEEE Wireless Communications and Networking Conference, (WCNC)*, Atlanta, USA, Mar. 2004, pp. 593–598.

[141] A. Syropoulos, "Mathematics of multisets," in *In Multiset Processing*. Springer-Verlag, 2001, pp. 347–358.

[142] G. Szegö, *Orthogonal polynomials*. New York: American Mathematic Society, 1939.

[143] C. W. Tan, M. Chiang, and R. Srikant, "Fast algorithms and performance bounds for sum rate maximization in wireless networks," in *IEEE INFOCOM*, Rio de Janeiro, Brazil, Apr. 2009, pp. 1350–1358.

[144] ——, "Maximizing sum rate and minimizing MSE on multiuser downlink: Optimality, fast algorithms and equivalence via max-min SIR," in *IEEE International Symposium on Information Theory, (ISIT)*, Seoul, Korea, Jul. 2009.

[145] ——, "Maximizing sum rate and minimizing MSE on multiuser downlink: Optimality, fast algorithms and equivalence via max-min SINR," *IEEE Transactions on Signal Processing*, vol. 59, no. 12, pp. 6127–6143, Dec. 2011.

[146] M. Tao and R. Wang, "Linear precoding for multi-pair two-way mimo relay systems with max-min fairness," *IEEE Transactions on Signal Processing*, vol. 60, no. 10, pp. 5361 –5370, Oct. 2012.

[147] L. Thiele, T. Wirth, K. Börner, M. Olbrich, V. Jungnickel, J. Rumold, and S. Fritze, "Modeling of 3D Field Patterns of Downtilted Antennas and Their Impact on Cellular Systems," in *International ITG Workshop on Smart Antennas (WSA 2009)*, Berlin, Germany, Feb. 2009.

[148] A. Tölli, M. Codreanu, and M. Juntti, "Linear multiuser MIMO transceiver design with quality of service and per-antenna power constraints," *IEEE Transactions on Signal Processing*, vol. 56, no. 7, pp. 3049–3055, Jul. 2008.

[149] A. Tölli, H. Pennanen, and P. Komulainen, "On the value of coherent and coordinated multi-cell transmission," in *IEEE International Conference on Communications Workshops, ICC Workshops*, Dresden, Germany, Jun. 2009, pp. 1–5.

[150] ——, "SINR balancing with coordinated multi-cell transmission," in *IEEE Wireless Communications and Networking Conference, (WCNC)*, Budapest, Hungary, Apr. 2009.

[151] D. N. C. Tse and P. Viswanath, *Fundamentals of wireless communication*. Cambridge University Press, 2005.

[152] R. Vaze and R. Heath, "Optimal amplify and forward strategy for two-way relay channel with multiple relays," in *IEEE Information Theory Workshop on Networking and Information Theory, (ITW 2009)*, Jun. 2009, pp. 181–185.

[153] P. Viswanath, D. N. C. Tse, and R. Laroia, "Opportunistic beamforming using dumb antennas," *IEEE Transactions on Information Theory*, vol. 48, no. 6, pp. 1277–1294, Jun. 2002.

[154] R. Wang, M. Tao, and Y. Huang, "Linear precoding designs for amplify-and-forward multiuser two-way relay systems," *IEEE Transactions on Wireless Communications*, vol. 11, no. 12, pp. 4457 –4469, Dec. 2012.

[155] W. Wang, S. Jin, and F.-C. Zheng, "Maximin SNR beamforming strategies for two-way relay channels," *IEEE Communications Letters*, vol. 16, no. 7, pp. 1006 –1009, Jul. 2012.

[156] H. Weingarten, Y. Steinberg, and S. Shamai, "The capacity region of the gaussian multiple-input multiple-output broadcast channel," *IEEE Transactions on Information Theory*, vol. 52, no. 9, pp. 3936–3964, Sep. 2006.

[157] A. Wiesel, Y. C. Eldar, and S. Shamai, "Linear precoding via conic optimization for fixed MIMO receivers," *IEEE Transactions on Signal Processing*, vol. 54, no. 1, pp. 161–176, Jan. 2006.

[158] S.-P. Wu and S. Boyd, "FIR filter design via spectral factorization and convex optimization," in *Applied and Computational Control, Signals and Circuits*. B. Datta Ed. Boston, MA: Birkauser, 1998, vol. 1, pp. 215–245.

[159] J. Yang and D. K. Kim, "Multi-cell uplink-downlink beamforming throughput duality based on Lagrangian duality with per-base station power constraints," *IEEE Communications Letters*, vol. 12, no. 4, pp. 277–279, Apr. 2008.

[160] K. Yang, D. Calin, C.-B. Chae, and S. Yiu, "Distributed beam scheduling in multi-cell networks via auction over competitive markets," in *IEEE International Conference on Communications, (ICC)*, Kyoto, Japan, Jun. 2011, pp. 1–6.

[161] W. Yang and G. Xu, "Optimal downlink power assignment for smart antenna systems," in *IEEE International Conference on Acoustics, Speech and Signal Processing, ICASSP*, vol. 6, Seattle, USA, May 1998, pp. 3337–3340.

[162] K. Yu, M. Bengtsson, B. Ottersten, D. McNamara, P. Karlsson, and M. Beach, "Second order statistics of NLOS indoor MIMO channels based on 5.2 GHz measurements," in *IEEE Global Telecommunications Conference, (GLOBECOM)*, vol. 1.

[163] W. Yu and T. Lan, "Transmitter optimization for the multi-antenna downlink with per-antenna power constraints," *IEEE Transactions on Signal Processing*, vol. 55, no. 6, pp. 2646–2660, Jun. 2007.

[164] L. Zhang, R. Zhang, Y.-C. Liang, Y. Xin, and H. Poor, "On Gaussian MIMO BC-MAC duality with multiple transmit covariance constraints," *IEEE Transactions on Information Theory*, vol. 58, no. 4, pp. 2064–2078, 2012.

[165] R. Zhang and S. Cui, "Cooperative interference management with MISO beamforming," *IEEE Transactions on Signal Processing*, vol. 58, no. 10, pp. 5450–5458, Oct. 2010.

[166] R. Zhang, Y.-C. Liang, , and S. Shuguang Cui, "Optimal beamforming for two-way multi-antenna relay channel with analogue network coding," *IEEE Journal on Selected Areas in Communications*, vol. 27, no. 5, pp. 699–712, Jun. 2009.

[167] J. Zhao, M. Kuhn, A. Wittneben, and G. Bauch, "Cooperative transmission schemes for decode-and-forward relaying," in *18th IEEE International Symposium on Personal, Indoor and Mobile Radio Communications, (PIMRC)*, Athens, Greece, Sep. 2007, pp. 1–5.

Publication List

Journal Publications

Dartmann, G., Gong, X., Afzal, W., and Ascheid, G.: "On the Duality of the Max-Min Beamforming Problem with Per-Antenna and Per-Antenna Array Power Constraints", *IEEE Transactions on Vehicular Technology*, vol. 62, no. 2, pp. 606–619, Feb. 2013, 10.1109/TVT.2012.2222946.

Dartmann, G., Gong, X., and Ascheid, G.: "Application of Graph Theory to the Multicell Beam Scheduling Problem", *IEEE Transactions on Vehicular Technology*, vol. 62, no. 4, pp. 1435-1449, May 2013, 10.1109/TVT.2013.2242912.

Dartmann, G., and Ascheid, G.: "Equivalent Quasi-Convex Form of the Multicast Max–Min Beamforming Problem", *IEEE Transactions on Vehicular Technology*, May 2013, accepted for publication.

Gong, X., Ispas, A., Dartmann, G., and Ascheid, G.: "Power Allocation and Performance Analysis in Spectrum Sharing Systems with Statistical CSI", *IEEE Transactions on Wireless Communications*, 2013, accepted for publication.

Patent

Dartmann, G. and Gong, X.:"Dynamically scheduling connections of mobile stations in neighbouring cells in a mobile telecommunication network", *European Patent* EP 2 337 418 A1, ICE RWTH, Dec. 2009.

Conference Publications

Dartmann, G., Gong, X., and Ascheid, G.:"Low Complexity Cooperative Multicast Beamforming in Heterogeneous Networks", *in Proceedings of IEEE Vehicular Technology Conference (VTC-Spring)*, 2013, accepted for publication.

Dartmann, G., Gong, X., and Ascheid, G.:"Beamforming with Relays in Heterogeneous Networks Based on Correlation Knowledge", *in Proceedings of 14th IEEE International Conference on Communication Technology (ICCT 2012)*, Nov. 2012, accepted for publication,

Gong, X., Dartmann, G., Ispas, A., and Ascheid, G.:"Optimal power allocation in a spectrum sharing system with partial CSI", *in Proceedings of IEEE Vehicular Technology Conference (VTC-Spring)*, May 2012.

Dartmann, G., Gong, X., and Ascheid, G.:"On the Pareto Optimum of Long-Term Max-Min Beamforming with General Power Constraints", *in 35th IEEE Sarnoff Symposium*, May 2012.

Loellmann, H., Dartmann, G., and Vary, P.:"Constrained Design of Allpass Transformed DFT Filter-Banks by Quadratic Programming", *in Proceedings of the IEEE International Conference on Acoustics, Speech, and Signal Processing (ICASSP)*, Mar. 2012.

Dartmann, G., Shah, D. K., Gong, X., and Ascheid, G.:"Beamforming with Relays in Multicell Networks Based on Correlation Knowledge", *in IEEE International Workshop on Multicell Cooperation (GLOBECOM 2011)*, pp. 470–474, Dec. 2011.

Gong, X., Ishaque, A., Dartmann, G., and Ascheid, G.:"Duality-Based Robust Transceiver Design for Cognitive Downlink Systems, *in Proceedings of IEEE Vehicular Technology Conference (VTC-Fall)*", Sept. 2011.

Dartmann, G., Gong, X., and Ascheid, G.:"Max-Min Beamforming with Cooperative Multipoint Transmission", *in Proceedings of IEEE Vehicular Technology Conference (VTC-Fall)*, IEEE, Sept. 2011.

Ispas, A., Schneider, C., Dartmann, G., Gong, X., Ascheid, G., and Thomä, R.:"Analysis of Mismatched Downlink Beamforming over Non-Stationary Channels with Interference", *in Proc. XXX General Assembly Scientific Symp. Int. Union Radio Science (URSI)*, Aug. 2011.

Dartmann, G., Gong, X., and Ascheid, G.:"Low Complexity Cooperative Multicast Beamforming in Multiuser Multicell Downlink Networks", *in 6th International ICST Conference on Cognitive Radio Oriented Wireless Networks*, IEEE, June 2011.

Gong, X., Ishaque, A., Dartmann, G., and Ascheid, G.:"MSE-based stochastic transceiver optimization in downlink cognitive radio networks", *in IEEE Wireless Communications and Networking Conference (WCNC)*, pp. 1426–1431 , Mar. 2011.

Dartmann, G., Afzal, W., Gong, X., and Ascheid, G.:"Joint Optimization of Beamforming, User Scheduling, and Multiple Base Station Assignment in a Multicell Network", *in IEEE Wireless Communications and Networking Conference (WCNC)*, pp. 209–214, Mar. 2011.

Dartmann, G., Gong, X., Afzal, W., and Ascheid, G.:"Low Complexity Cooperative Downlink Beamforming in Multiuser Multicell Networks", *in Proceedings of the IEEE International Conference on Communications and Technology (ICCT)* (Nanjing), Nov. 2010.

Dartmann, G., Gong, X., and Ascheid, G.:"Cooperative Beamforming with Multiple Base Station Assignment Based on Correlation Knowledge", *in Proceedings of IEEE Vehicular Technology Conference (VTC-Fall)*, Sept. 2010

Gong, X., Ishaque, A., Dartmann, G., and Ascheid, G.:"MSE-based Linear Transceiver Optimization in MIMO Cognitive Radio Networks with Imperfect Channel Knowledge, *in IAPR Workshop on Cognitive Information Processing*, June 2010.

Dartmann, G., Gong, X., and Ascheid, G.:"Jointly Optimized Transmit Beamforming and Temporal User Scheduling in Multiuser Multicell Scenarios Based on Correlation Knowledge“, *in IEEE Sarnoff Symposium*, Apr. 2010.

Gong, X., Jordan, M., Ishaque, A., Dartmann, G., and Ascheid, G.:”Robust MSE-based Transceiver Optimization in MISO Downlink Cognitive Radio Network“, *in IEEE Wireless Communications and Networking Conference (WCNC)*, Apr. 2010.

Gong, X., Jordan, J., Dartmann, G., and Ascheid, G.:”Max-Min Beamforming for Multicell Downlink Systems Using Long-Term Channel Statistics“, *in Proceedings of the IEEE International Symposium on Personal, Indoor, and Mobile Radio Communications (PIMRC)*, Sept. 2009.

Dartmann, G., Gong, X., Jordan, M., and Ascheid, G.:”Jointly Optimized Beamforming in Multicell Scenarios based on Correlation Knowledge, in ITG-Fachtagung Mobile Kommunikation“, ITG, May 2009.

Dartmann, G., Jordan, M., Gong, X., and Ascheid, G.:”Intercell Interference Mitigation with Long-Term Beamforming and low SINR Feedback Rate in a Multiuser Multicell Unicast Scenario, *in Proceedings of IEEE Vehicular Technology Conference (VTC-Spring)*, IEEE, Apr. 2009.

Jordan, M., Dartmann, G., and Ascheid, G.:“Beamforming in Single Frequency Networks with Connection Control”, *in IEEE 69th Vehicular Technology Conference: (VTC Spring)*, Apr. 2009

Loellmann, H., Dartmann, G., and Vary, P.:“Design of Multiple Order Allpass Transformed DFT Filter-Banks with Aliasing-Free Signal Rekonstruction by Linear Programming”, *in ITG-Fachtagung Sprachkommunikation*, Oct. 2008.

Loellmann, H., Dartmann, G., and Vary, P.:“General Least-Squares Design of Allpass Transformed DFT Filter-Banks”, *in Proceedings of European Signal Processing Conference (EUSIPCO)*, Aug. 2008.

Loellmann, H., Dartmann, G., and Vary, P.:“Least-Squares Desgin of Subsampled Allpass Transformed DFT Filter-Banks with LTI Property”, *in Proceedings of the International Conference on Acoustics, Speech, and Signal Processing (ICASSP)*, Mar. 2008.

Curriculum Vitae

Name	Guido Dartmann
Date of birth	11. April 1980
Place of birth	Münster, Deutschland

Since 09/2012	Chief engineer at Institute for Communication Technologies and Embedded Systems (ICE)
09/2007–08/2012	Research assistant and PhD student at Institute for Communication Technologies and Embedded Systems (ICE)
07/2007–08/2007	Student research assistant (WiHi) at Institute of Communication Systems and Data Processing (IND): design of a quadrature mirror filterbank with non-uniform spectral resolution
10/2006–06/2007	Diploma Thesis at Institute of Communication Systems and Data Processing (IND): design of analysis-synthesis filterbanks with non-uniform spectral resolution
10/2001–06/2007	Graduate studies at RWTH Aachen in computer engineering. Graduated as German Dipl.-Ing.
09/2000–8/2001	Civil service
08/1997–06/2000	Berufskolleg Hans-Böckler-Schule (Abitur)